Durham E-Theses

Cross-coupling methodology in the synthesis of luminescent metal complexes and multimetallic assemblies

Arm, Kathryn J.

How to cite:

Arm, Kathryn J. (2005) *Cross-coupling methodology in the synthesis of luminescent metal complexes and multimetallic assemblies*, Durham theses, Durham University. Available at Durham E-Theses Online: http://etheses.dur.ac.uk/2806/

Use policy

Cross-Coupling Methodology in the Synthesis of Luminescent Metal Complexes and Multimetallic Assemblies

Kathryn J. Arm

Department of Chemistry
University of Durham

A thesis submitted in part-fulfilment for the degree of
Doctor of Philosophy

November 2005

0 5 MAY 2006

Abstract

Cross-Coupling Methodology in the Synthesis of Luminescent Metal Complexes and Multimetallic Assemblies

Kathryn J. Arm

The synthesis of a series of complexes of the type $[M(C^\wedge N)_2(N^\wedge N)]^+$ is reported, where M is either iridium or rhodium, $C^\wedge N$ is a cyclometalating ligand such as 2-phenylpyridine (ppy) and $N^\wedge N$ is 2,2'-bipyridine (bpy) or a substituted bpy ligand. Several complexes are produced via an *in situ* Suzuki cross-coupling reaction between a bromo-substituted metal complex and an organic boronic acid. The introduction of fluoro-substituents in the $C^\wedge N$ ligand is found to significantly perturb the excited state properties of such complexes, whilst species containing bpy ligands appended with dimethylamino, pyridyl or hydroxy functionalities display pH responsive photophysical properties.

The Suzuki cross-coupling reaction is further extended to the controlled synthesis of multimetallic arrays containing from two to eight metal centres. This is achieved via the coupling of bromo-substituted metal complexes with previously unreported ruthenium, iridium or rhodium complexes bearing bpy ligands with boronic acid substituents. The regioselective bromination of ppy ligands already bound to metal centres allows for the elaboration of dimeric systems to tetrameric systems, and tetrameric systems to octameric systems by exploiting the same coupling reaction. Access to well-defined mixed metal species is achieved, including a tetrameric species which incorporates rhodium, iridium and ruthenium moieties. Similarly, unsymmetrical bridging units are simply created and can contain either bpy, ppy or 2,2':6',2''-terpyridine (tpy) coordinating units.

Photophysical investigations reveal that the energy transfer properties of these multimetallic assemblies, which contain simple phenyl bridging units between the bpy, ppy or tpy ligands, can be reliably predicted from the properties of the constituent building blocks. That is to say that the bridging ligand does not alter the relative excited state energies of the complexes when they are incorporated as building blocks in extended systems. This allows for the design of energy-channelling multimetallic species, potentially applicable to solar energy conversion devices.

Declaration

The work described herein was carried out in the Department of Chemistry, University of Durham between October 2002 and November 2005. All the work is my own unless otherwise stated and no part of it has been submitted for a degree at this or any other university.

Statement of Copyright

Acknowledgements

Table of Contents

Abbreviations

B_2neo_2	bis(neopentylglycolato)diboron
B_2pin_2	bis(pinacolato)diboron
bpy	2,2'-bipyridine
BSA	bovine serum albumin
C^N	a bidentate ligand coordinating via one C and one N atom
COSY	correlation spectroscopy
DCM	dichloromethane
DFT	density functional theory
DME	dimethoxyethane
DMF	dimethylformamide
DMSO	dimethylsulfoxide
dpp	bis(2-pyridyl)pyrazine
dppf	1,1'-bis(diphenylphosphino)ferrocene
dpyb	1,3-di(2-pyridyl)benzene
DSC	dye sensitised solar cell
EI	electron ionisation
ES^+	positive ion electrospray ionisation
EtOH	ethanol
HOMO	highest occupied molecular orbital
HSA	human serum albumin
HSQC	heteronuclear single quantum correlation
IC	internal conversion
ISC	intersystem crossing
ISC'	back intersystem crossing
LC	ligand-centred
LEC	light emitting electrochemical cell
LLCT	ligand-to-ligand charge transfer
LMCT	ligand-to-metal charge transfer
LUMO	lowest unoccupied molecular orbital

MC	metal-centred
mcpba	*m*-chloroperoxybenzoic acid
Me	methyl
MeCN	acetonitrile
MeOH	methanol
MLCT	metal-to-ligand charge transfer
MS	mass spectrometry
NBS	N-bromosuccinimide
NMR	nuclear magnetic resonance
N^N	a bidentate ligand coordinating via two N atoms
NOESY	nuclear Overhauser effect spectroscopy
OAc	acetate
OLED	organic light emitting diode
pba	anionic form of 4-(2-pyridyl)benzaldehyde formed upon cyclometalation
pbaH	4-(2-pyridyl)benzaldehyde as a free ligand
PET	photoinduced electron transfer
phen	1,10-phenanthroline
ppy	anionic form of 2-phenylpyridine formed upon cyclometalation
ppyH	2-phenylpyridine as a free ligand
R_f	retention function
ROESY	rotational nuclear Overhauser effect spectroscopy
SBLCT	σ-bond-to-ligand charge transfer
S_0	ground singlet state
S_n	nth excited singlet state
T_n	nth excited triplet state
THF	tetrahydrofuran
TLC	thin layer chromatography
tpy	2,2':6',2''-terpyridine
UV	ultra violet

CHAPTER 1

INTRODUCTION

1 Introduction

Ruthenium(II) complexes containing 2,2′-bipyridine (bpy) ligands, originally studied in the 1960s,[1,2] have attracted enormous attention over the past thirty years.[3]   A combination of rich photophysical and electrochemical properties has prompted research into hundreds of derivatised complexes, providing potential candidates for applications such as photocatalysis, luminescent sensors, electroluminescence and electron transfer reagents for conversion of light to chemical energy.

However, related iridium(III) systems, which exhibit similarly attractive photophysical properties, are faced with synthetic challenges associated with the kinetic inertness of this third row d^6 metal ion with respect to substitution.[4] Iridium systems containing a combination of both bpy and anionic cyclometalating C^N ligands, such as 2-phenylpyridine (ppy), can be synthesised much more readily.[5] The synthesis of such complexes generally involves the pre-synthesis of the ligand followed by binding to the iridium centre. Whilst this is usually a reliable and high yielding approach for the incorporation of simple ligands, the complexation step may not always proceed smoothly if a sophisticated ligand with more than one potential binding site is used.[6] An astute way to avoid this problem is to adopt an *in situ* approach to the synthesis which involves carrying out chemistry on the complex.

Monometallic transition metal complexes of the type discussed above can be used as building blocks for the generation of multimetallic systems. The resulting arrays therefore contain moieties which may absorb light, luminesce or display redox active characteristics, leading to applications in molecular electronics and devices, solar energy conversion and information storage.[7] The synthesis of such systems would also benefit from an *in situ* type approach, in order to gain full control over the final assembly structure, without introducing prolonged synthetic procedures.

1.1 Introduction to luminescence

Luminescence arises when an energetic excited state relaxes and loses its energy via the emission of radiation. The initial excited state is generated via the absorption of radiation which has energy corresponding exactly to that of some electronic transition within the system. According to Kasha's rule,[8] relaxation to the lowest energy excited state via non-radiative processes occurs very rapidly and much faster than the emission process, so that any luminescence observed is normally deemed to arise from this lowest excited state.

Fluorescence can be described as a radiative transition between states of the same multiplicity, normally singlet to singlet transitions. Fluorescent emission occurs on a similar timescale to non-radiative decay processes such as intersystem crossing (ISC), which leads to short fluorescent lifetimes usually of the order of nanoseconds.

In contrast, phosphorescence involves a radiative transition between states of different multiplicities. As this is a formally forbidden process, phosphorescent emission lifetimes are longer than those seen for fluorescence, and are usually of the order of microseconds. Phosphorescence often involves relaxation from the lowest excited triplet state, populated from the lowest excited singlet state via intersystem crossing, to a typically singlet ground state. Under ambient conditions phosphorescence is rarely observed, as other competing processes occur on a faster timescale, providing alternative non-radiative relaxation pathways. The competing pathways are best displayed on a Jablonski diagram (Figure 1). In systems where spin-orbit coupling is significant, electric dipole transitions may readily occur where $\Delta S \neq 0$. In these situations the spin quantum number becomes an inadequate description of the system and so phosphorescence is enhanced. Transition metal complexes, especially those of second or third row transition metals, are examples of this type of system, with the presence of a heavy atom promoting spin-orbit coupling and hence phosphorescence.
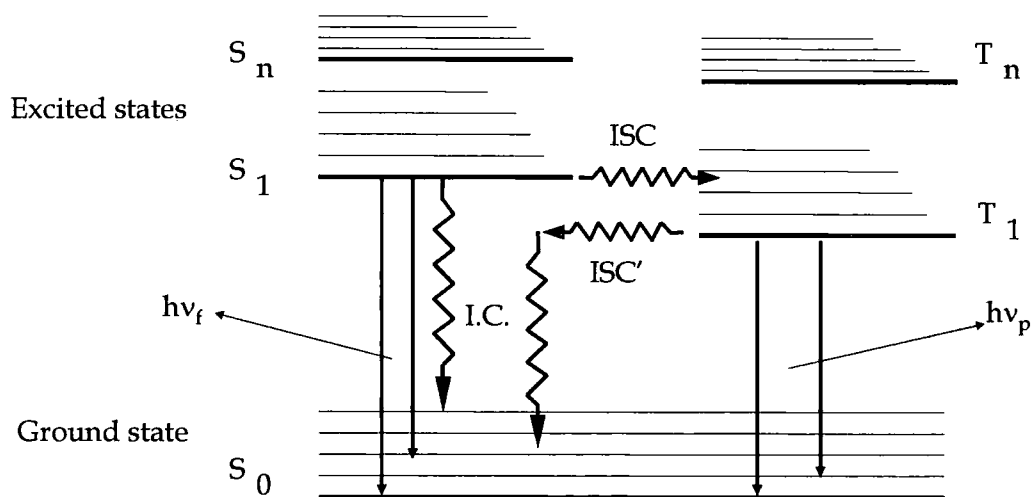
Figure 1 Jablonski Diagram: straight lines represent radiative processes whilst jagged lines represent non-radiative processes.

Transition metal complexes have a wide range of excited states available to them, arising from a complicated electronic structure generated by the combination of metal and ligand orbitals. A molecular orbital is comprised of two or more atomic orbitals and can be considered to receive greatest contribution from the atomic orbital of most

similar energy. As absorption of radiation brings about an electronic transition between two molecular orbitals, it is possible to characterise the resulting excited state in terms of the molecular orbitals involved. This gives rise to metal-centred (MC), ligand-centred (LC), metal-to-ligand charge transfer (MLCT) and ligand-to-metal charge transfer (LMCT) transitions and excited states.[9,10]

For polypyridyl transition metal complexes, LC π-π^* transitions are seen as intense absorptions in the UV region, whilst MC d-d transitions give rise to less intense absorptions in the same region, with the exact position being dependent on the ligand field strength. MLCT transitions are often observed as strong absorptions in the visible region due to the strong σ-donor and π-acceptor qualities of ligands such as 2,2'-bipyridine. In complexes where a 4d or 5d easily oxidisable transition metal is present, the energy level sequence is such that the lowest excited state is often an emissive MLCT state.[3] Intense emission may be observed from such systems with a lifetime in the region of a few hundred nanoseconds. Ruthenium complexes containing 2,2'-bipyridine type ligands remain the most thoroughly investigated complexes of this sort.[3]

1.1.1 Applications of long-lived luminescence

A luminescent sensor consists of an analyte binding site and a light emitting group which acts as a reporting group. A measurable change in some emission characteristic is brought about upon binding of a specific analyte. This could be observed as a change in the emission wavelength, intensity or lifetime and can, in turn, be related to the concentration of the analyte. The analyte involved can vary in complexity from a simple H^+ ion in pH sensitive systems, to more sophisticated biological molecules such as insulin.

However, biological samples often contain additional fluorescent species, emission from which may interfere with the signal returned from the luminescent sensor. Time-gated methods provide a way to combat this problem, by delaying measurements until a time after which the fluorescent background signals have decayed. Clearly, in order for this to work, the luminescent sensor must have a significantly longer lifetime of emission than the interfering species (Figure 2). Transition metal complexes which display long-lived phosphorescent emission under ambient conditions are ideally suited for this purpose. The use of ruthenium tris-bipyridine complexes in such responsive systems is discussed in section 1.2.2.2.
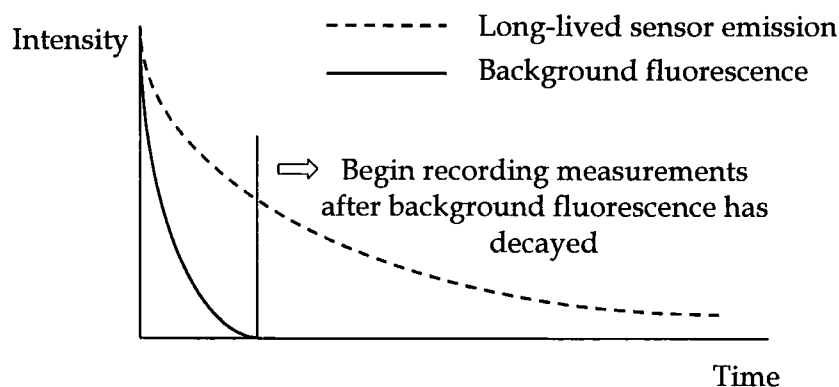
Figure 2 Time-gated discrimination of phosphorescence from background fluorescence

1.2 Ruthenium complexes containing 2,2'-bipyridine ligands

1.2.1 Ruthenium tris-2,2'-bipyridine

Ruthenium tris-2,2'-bipyridine (Figure 3) is among the most studied of metal complexes.[3,11] The ground D_{3h} state molecular structure, deduced in 1979, revealed the presence of a short Ru-N bond, indicating significant π-backbonding between Ru(II) and the π^* orbitals of 2,2'-bipyridine (bpy).[12]
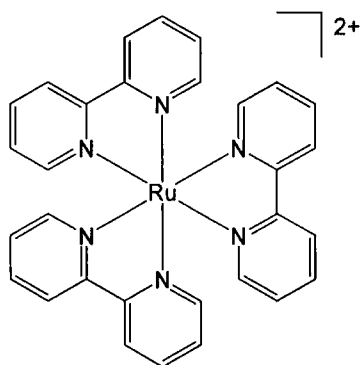
Figure 3 Ruthenium tris-2,2'-bipyridine

Initial reports suggested that luminescence from [Ru(bpy)$_3$]$^{2+}$ arose due to a charge transfer transition.[13] Since then, the absorption spectrum of [Ru(bpy)$_3$]$^{2+}$ has been confirmed to display both LC (π-π^*) bands at 285 nm and ^{1}MLCT bands at 240 nm and 450 nm, with a weak absorption at 550 nm corresponding to the creation of the lowest excited ^{3}MLCT state.[9,14] Efficient deactivation of upper lying excited states via radiationless decay has been reported, leading to the conclusion that emission from [Ru(bpy)$_3$]$^{2+}$ is phosphorescent,[14] rather than fluorescent which had previously been suggested.[15]

1.2.2 Ruthenium complexes with derivatised bipyridine ligands

1.2.2.1 Tuning photophysical properties using the acceptor ligand

The bipyridine ligand in [Ru(bpy)₃]²⁺ type complexes acts as an acceptor for the excited electron when an MLCT transition takes place. Therefore, the photophysical properties of the overall complex can be tuned by careful variation of this acceptor ligand. The steric bulk of groups attached to the bipyridine core can affect the planarity of the excited state and therefore the photophysical properties,[16] as can the overall delocalisation ability of the ligand and its rigidity.[17]

The effect of delocalisation is clearly exemplified by a series of ruthenium complexes which use 2,3-bis(2-pyridyl)pyrazine (dpp), 2,3-bis(2-pyridyl)quinoxaline (dpq) or 2,3-bis(2-pyridyl)benzoquinoxaline (dpb) as acceptor ligands (Figure 4). As the number of rings in the acceptor ligand is increased, the emission wavelength is increased due to stabilisation of the LC π*-acceptor levels and hence a reduction in the HOMO-LUMO energy gap.[17]

n = 0 : dpp
n = 1 : dpq
n = 2 : dpb
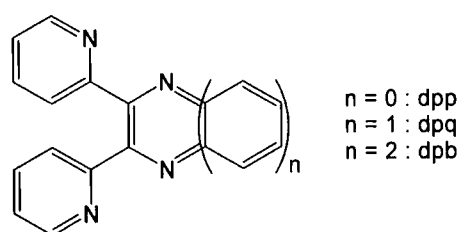
Figure 4 Structure of dpp, dpq and dpb ligands

The use of a pyrene moiety has been exploited in order to increase the triplet lifetime of a ruthenium tris-2,2'-bipyridine type complex.[18-20] A recent example of this achieves a substantial increase in the room temperature triplet lifetime through the binding of 5-pyrenyl-1,10-phenanthroline ligands to a ruthenium metal centre (Figure 5). The triplet lifetime reported of 148 μs is well beyond the range of any related system.[19,20]
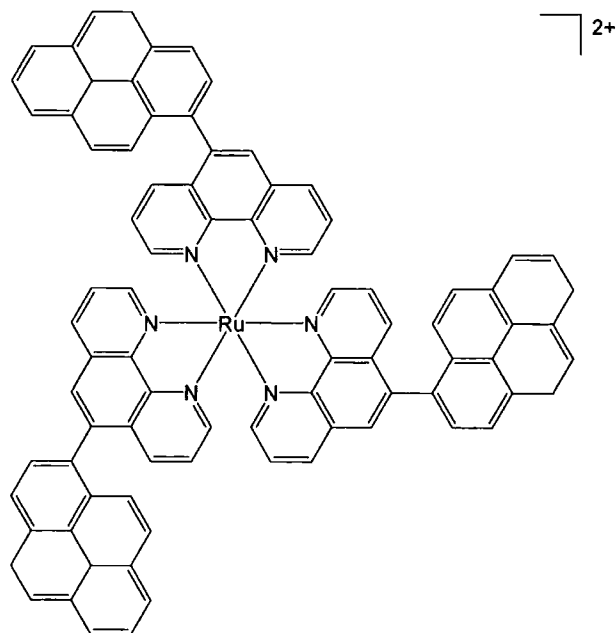
Figure 5 [Ru(5-pyrenyl-1,10-phenanthroline)₃][PF₆]₂[19,20]

1.2.2.2 Functionalisation of bipyridine ligands to create responsive systems

By incorporating functional groups onto the back of ruthenium polypyridyl complexes, luminescent sensor systems can be produced (see also section 1.1.1). The use of ruthenium bipyridine complexes as luminescent pH sensors has been widely investigated.[6,21-27] For instance, ruthenium bipyridine complexes containing pendent protonatable pyridyl groups (Figure 6a) have been reported to exhibit pH dependent emission characteristics.[6,27] Protonation of the pendent pyridyl groups is accompanied by a red shift in the position of the MLCT absorption due to the lowering in energy of the LC orbitals. Emission from these species is entirely quenched at pH values below 2, suggesting that rapid electron transfer from the excited ^{3}MLCT state to the pendent protonated pyridyl groups occurs. Alongside these studies, ruthenium complexes with deprotonatable pendent phenol groups were considered (Figure 6b).[27] Here it was found that the position of the hydroxyl group was crucial in determining the extent of luminescence quenching upon deprotonation, with the *para*-substituted system becoming completely quenched whilst the *meta* analogue was only partly quenched. This was attributed to a lack of internal charge transfer of the phenolate negative charge in the *meta* case.[27]
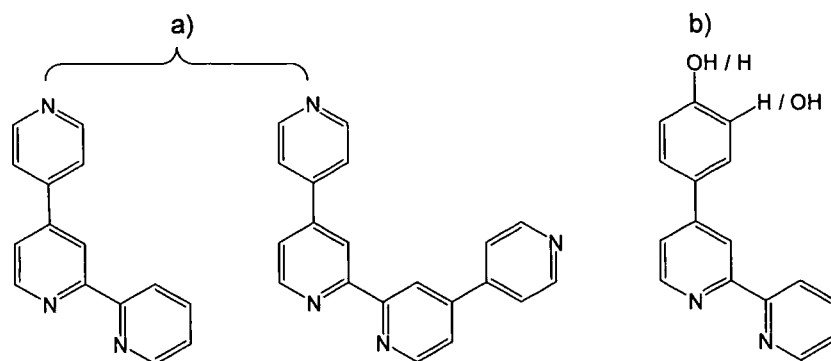
Figure 6 Ligands containing a) protonatable pendent pyridyl groups and b) deprotonatable hydroxyl groups[27]

The distinct photophysical properties of ruthenium polypyridyl complexes means that they are commonly employed as reversible DNA binding agents.[28] By binding to or intercalating into DNA some change in the photophysical properties of the complex may be observed. For example, the complex [Ru(bpy)$_2$(dppz)]$^{2+}$, where dppz is dipyrido[3,2-a:2′,3′-c]phenazine (Figure 7), can act as a luminescent probe for DNA.[29] Protonation at the pyrazine nitrogen atoms in protic solvents quenches the MLCT emission usually observed in aprotic solvents. However, the addition of DNA to the aqueous solution switches the emission back on due to intercalation of the dppz fragment into DNA, thus creating a responsive system. More recently, the related achiral complex [Ru(tpm)(py)(dppz)]$^{2+}$, where tpm is tris-(1-pyrazolyl)methane and py is pyridine, has been shown to exhibit sequence selectivity in DNA binding, with a binding constant of approximately an order of magnitude larger for GC base sequences than for AT sequences.[30] Subsequently, this complex has been adapted to form a bimetallic system which displays a similar DNA binding affinity.[31]
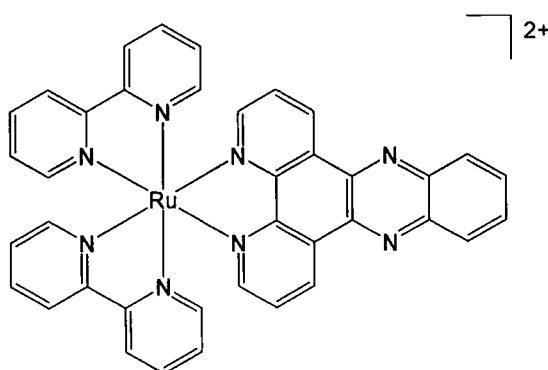
Figure 7 [Ru(bpy)$_2$(dppz)]$^{2+}$

Ruthenium complexes containing bipyridine ligands appended with a macrocyclic species are often able to sense for specific metal ions.[32-36] Rawle, Moore and Alcock[32] have prepared a ruthenium bipyridine complex containing a pendent

8

tetraazamacrocycle, and observe that MLCT emission is quenched upon the coordination of Cu^{2+} or Ni^{2+} within the macrocycle, and yet remains unchanged in the presence of Zn^{2+}. Similarly, complexes with pendent crown-ether groups have been noted to respond to binding of group IA and group IIA metal ions.[33] Lanthanide metal ions may also act as analytes, with Nd^{3+} having been seen to bind to ruthenium complexes containing modified calix[4]arene groups, bringing about a noticeable change in emission characteristics.[35] Macrocycles can also be created with groups that promote the coordination of anions. By creating a ruthenium complex bearing a macrocycle with carboxamide units, it is possible to either increase the emission intensity through the binding of dihydrogen phosphate, or completely quench emission through the binding of fluoride.[36]

1.2.2.3 Ruthenium complexes in light emitting electrochemical cells

Organic light emitting diodes (OLEDs) are being developed for applications in flat panel displays and lighting. The simplest configuration consists of a single layer of an organic semiconductor sandwiched between two electrodes. Under an applied voltage, holes are injected from the anode into the HOMO of the organic layer, whilst electrons are similarly injected from the cathode into the LUMO. As the two charge carrying species migrate towards the opposite electrode, they may combine and form an exciton. A fraction of these excitons recombine radiatively giving rise to light emission or electroluminescence. A light emitting electrochemical cell (LEC) consists of a sandwiched active polymer layer containing both electronic and ionic conductors (Figure 8). This can involve the presence of a transition metal complex which has the ability to transport both electrons and holes efficiently.[37,38]

Cathode (E.g. Ag)

Emissive layer
$[Ru(L_3)]^{2+}$

Indium Tin Oxide
(transparent)

Glass substrate
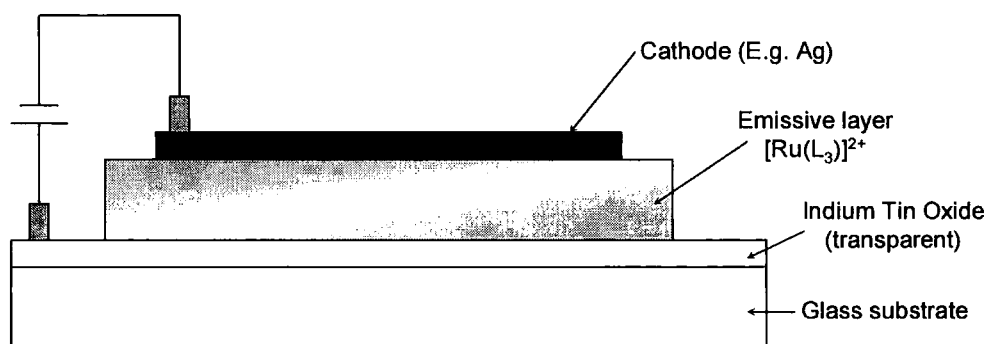
Figure 8 Device structure for a light emitting electrochemical cell

The first solid-state electroluminescent device from a transition metal complex was reported in 1996 and used a ruthenium polypyridyl complex with pendent sulfonate groups to aid solubility in water.[39] However, the quantum efficiency of this device was very low at 0.005%. Derivatised ruthenium polypyridyl complexes have played a key role in work carried out since this initial discovery in an attempt to optimise device characteristics. Work by Handy *et al* has employed a hydroxy methylated ruthenium tris-2,2'-bipyridine complex (Figure 9), producing efficiencies of up to 1%, proving that high efficiencies can be obtained from a single-layer spin-coated film of a low molecular weight ruthenium complex.[40]
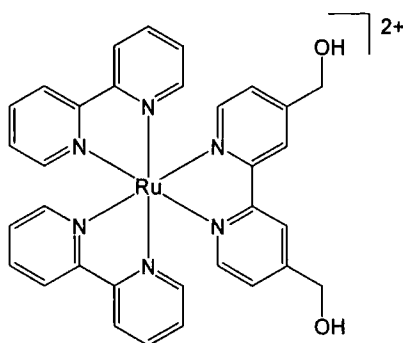
Figure 9 Hydroxy methylated ruthenium tris-bipyridine complex[40]

Alternatively, high molecular weight polymers with ruthenium complexes attached to the main chain can be used.[41-44] By introducing a layer-by-layer device structure and optimising layer concentration and thickness, efficiencies of up to 3% can be achieved.[44] A variation on this approach sees the blending of ruthenium polypyridyl complexes with organic polymeric species.[45-47] The blending of a dinonyl-substituted ruthenium complex with poly(methyl methacrylate) has produced a transition metal based device with an efficiency of 5.5%, the highest value reported for this type of device to date.[47]

Whilst steps have been taken to increase the quantum efficiency of LECs, long turn-on times and lack of colour tunability hamper their use in commercial application. However, the simple fabrication, low cost, low power consumption and attractive lifetime properties suggest that these devices could be used as monochromatic alphanumeric displays and backlights where turn-on time and colour is less important.[37]

1.2.2.4 Ruthenium complexes in dye sensitised solar cells

Photovoltaic devices take advantage of the fact that photons falling onto a semiconductor can create electron/hole pairs. This can generate a potential difference

10

across a junction between two materials. In a dye sensitised solar cell (DSC), a sensitiser is anchored to the surface of a wide band gap semiconductor of nanocrystalline morphology. The sensitiser, often a ruthenium polypyridyl complex, absorbs visible light and injects an electron into the conduction band of the semiconductor, which is most often TiO_2 due to its low cost, availability and non-toxicity. An electrolyte is able to donate an electron back to the sensitiser to return it to its original state. Electron migration through the external circuit will provide an electron at the counter electrode for regeneration of the electrolyte.[48-52] The first example of such a system containing a Ru based sensitiser was reported in 1991 with a light-to-electrical energy conversion of 7.1%.[53]

An ideal sensitiser will absorb all light below 920 nm, contain functional groups to allow attachment to the TiO_2 surface, efficiently inject electrons, have an excited state energy that is well matched with the energy of the TiO_2 conduction band, have a suitable redox potential to allow regeneration from an electrolyte and be stable under exposure to visible light.[51] The complex $[Ru(L)_2(X)_2]$, where L is 2,2'-bipyridyl-4,4'-dicarboxylic acid and X is NCS, was found to have excellent sensitising ability for TiO_2 films, with the presence of carboxylic acid groups allowing easy attachment to the semiconductor surface (Figure 10).[54] The optical transition involved was reported to have MLCT character with an electron being transferred from the metal to the functionalised bipyridine ligand attached to the TiO_2 surface.[55] This complex became known as the N3 dye and remained unmatched for 8 years despite a huge amount of research involving the synthesis of similar compounds.[48]
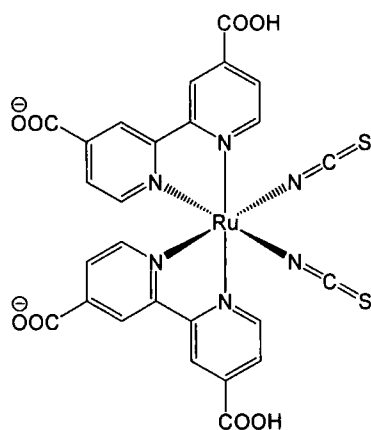
Figure 10 [Ru(2,2' bipyridyl-4,4' dicarboxylic acid)₂(NCS)₂], N3 dye[54]

However, in 2001 the "black dye" tri(cyanato)-(4,4',4"-tricarboxy-2,2':6',2"-terpyridine) ruthenium(II) achieved an improved efficiency for the conversion of light to electrical energy of 10.4%.[56] This is attributed to the better absorption in the near-IR when compared to N3. Further molecular engineering of the ruthenium dye structure

11

should allow for further increased light-harvesting in the region 700-900 nm. Studies on ruthenium complexes incorporating quarterpyridyl species,[57] and bipyridine ligands with vinyl linkages to carboxylic acid groups,[58,59] show promising conversion efficiencies, in the latter case from 8 – 10%.

1.3 Iridium tris-2,2'-bipyridine

Iridium is diagonally related to ruthenium in the periodic table, making iridium(III) essentially isoelectronic with ruthenium(II), both having a low spin d^6 configuration. Being a third row transition metal, iridium(III) is characterized by the great inertness of its coordination sphere with respect to substitution, requiring harsh reaction conditions in order to substitute the classical chlorine ligands of typical starting iridium salts.[4]

Iridium tris-2,2'-bipyridine was first reported[60] in 1958. Metal based oxidation of iridium(III) in this environment occurs at high potential (+2.17 V) resulting in an emissive state of primarily ligand-centred character,[61,62] rather than the MLCT emission seen for the ruthenium analogue.[14] This means that whilst $[Ru(bpy)_3]^{2+}$ is a strong photoreductant, $[Ir(bpy)_3]^{3+}$ acts as a strong photooxidant. An example of these properties can be seen when these two types of complexes are combined to create an electron shuttling system in an attempt to mimic the naturally occurring processes within photosynthesis.[63]

Following the initial studies on $[Ir(bpy)_3]^{3+}$, alternative binding modes for one of the 2,2'-bipyridine ligands were reported.[64-67] There was some debate over the exact nature of the binding involved, with monodentate binding of bpy accompanied by a water molecule in the sixth site being the first suggestion (Figure 11a).[64] A variation of this explanation involved the addition of water to the bipyridine ligand itself before binding to the iridium centre (Figure 11b).[65] Finally, after dismissing the earlier explanations based on experimental evidence, it was determined, partially from NMR data, that the bipyridine ligand was bound through one nitrogen atom and the carbon atom in the 3-position (Figure 11c).[66-68] This is an example of cyclometalation and, although rare for N^N bidentate ligands, it is very common in ligands which contain a benzene ring attached to a functional group containing a coordinating donor atom, usually nitrogen.
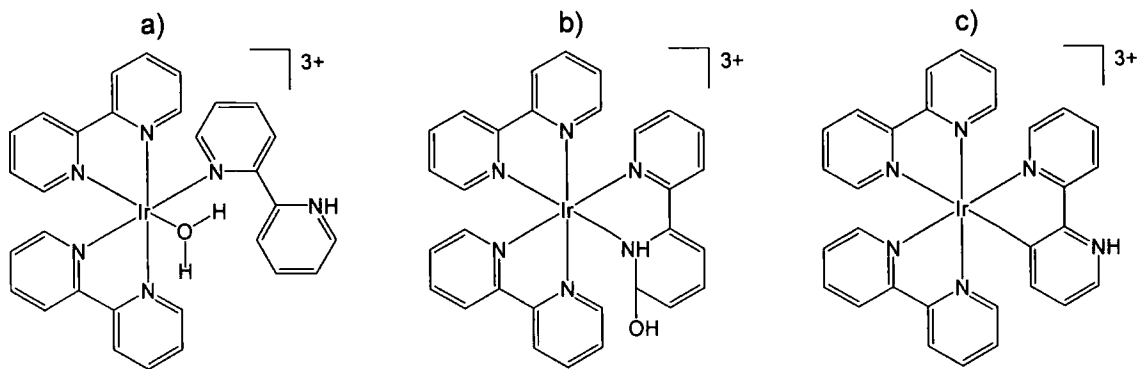
Figure 11 Alternative binding modes proposed for [Ir(bpy)₃]³⁺

1.4 Cyclometalation by 2-phenylpyridine ligands

2-Phenylpyridine (ppyH) is a ligand which is structurally similar to 2,2′-bipyridine but binds to the metal ion via the nitrogen atom and can cyclometalate through the carbon atom at the 2-position in the adjacent benzene ring. This ligand has a tendency to form binuclear dihalo-bridged metal complexes when reacted with metal chloride salts, such as those of iridium[69] and rhodium[70]. These dimeric species can be reacted on further to obtain complexes containing three ppy ligands (Figure 12). The excited state properties of the prototypical complex [Ir(ppy)₃] were first reported in 1985.[71] This is a charge neutral complex as the ppy ligand can be considered as binding to the central iridium atom via a carbanion: cyclometalation is accompanied by deprotonation of the cyclometalating carbon. The strong σ-donating effect of the metal-carbon bond increases electron density at the metal centre and hence makes iridium(III) more oxidisable, favouring MLCT transitions in complexes of this type.[69] At the time of discovery, [Ir(ppy)₃] was one of the strongest transition metal photoreductants reported.[71]
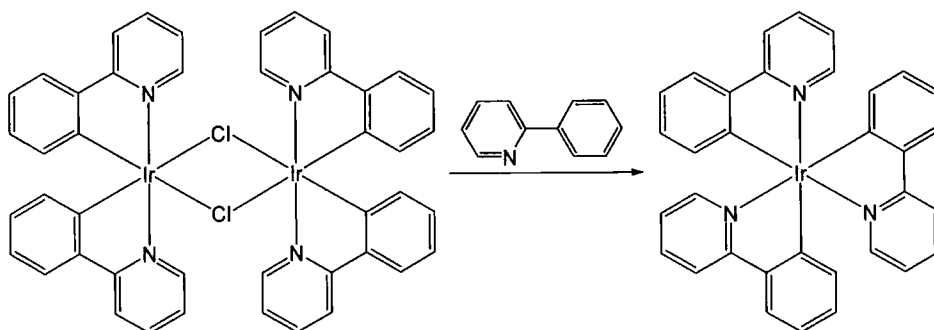
Figure 12 Synthesis of [Ir(ppy)₃] from dichloro-bridged dimer [Ir(ppy)₂Cl]₂

1.5 Iridium complexes with both 2-phenylpyridine and 2,2'-bipyridine ligands

We have seen that $[Ir(bpy)_3]^{3+}$ is a strong photooxidant with LC emission characteristics, whilst $[Ir(ppy)_3]$ is a powerful photoreductant with MLCT emission characteristics. By creating complexes with a combination of both ppy and bpy ligands it is possible to produce complexes with intermediate properties.

1.5.1 $[Ir(ppy)_2(bpy)]^+$

Watts et al[5,72-75] have investigated in detail the photophysical properties associated with the complex $[Ir(ppy)_2(bpy)]^+$ containing both cyclometalating and N^N coordinating ligands (Figure 13). Their initial synthesis[5] of this system was carried out by cleaving a dichloro-bridged diiridium cyclometalated precursor with 2,2'-bipyridine using a method previously used by Nonoyama for a similar rhodium complex.[76] Whilst there are two isomers that could possibly be produced, comparison with available structural data obtained for similar complexes pointed to the single isomeric form containing *cisoid* metal-carbon bonds.[72] Crystallographic data was later reported for the dichloro-bridged dimer[77] and subsequent literature on related compounds confirms that the *cisoid* relationship of the metal-carbon bonds is indeed retained upon the binding of an N^N coordinating ligand such as 2,2'-bipyridine.[78] The metal-carbon bonds exert a strong *trans* influence on the complex which results in the Ir-N(bpy) bonds being significantly longer than the Ir-N(ppy) bonds.
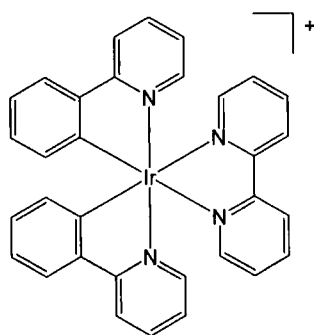
Figure 13 $[Ir(ppy)_2(bpy)]^+$

Preliminary results[5] on $[Ir(ppy)_2(bpy)]^+$ from Watts et al showed that oxidation at the iridium centre occurred much more readily in $[Ir(ppy)_2(bpy)]^+$ than in $[Ir(bpy)_3]^{3+}$, with the bpy ligand being more easily reduced than the ppy ligand. At 77K, a broad structureless emission was observed which was thought to arise from two unequilibrated MLCT states with very similar lifetimes. It was postulated that the lower energy MLCT transition would involve electron transfer to the π^* orbital of the

bpy ligand, whilst the higher energy MLCT state would involve the ppy ligand. Whilst the non-equilibration of these states could have been attributed to a lack of electronic coupling, this was deemed unlikely and instead nuclear distortions were identified as the cause.[5,72] The MLCT nature of the transition was supported by the investigation of solvatochroism,[74] whilst excited state absorption spectroscopy[73] and experiments involving direct excitation using a dye laser[75] confirmed that the lowest energy transition involved the bpy ligand and allowed resolution of the two emissive components that were initially suggested. At room temperature, it was found that emission from the lowest bpy based MLCT state dominated.[75]

Throughout the investigation into the photophysical properties of [Ir(ppy)$_2$(bpy)]$^+$, comparison has been made with the rhodium analogue [Rh(ppy)$_2$(bpy)]$^+$. Rhodium(III) is also a d^6 transition metal and is hence able to form similar complexes to iridium when combined with cyclometalating ligands.[70] However, the photophysical properties observed for the rhodium analogue are distinctly different.[5,79,80] Whilst the presence of two ppy ligands does allow for easier oxidation of the overall complex, unlike the iridium analogue, low temperature emission for rhodium has largely LC characteristics rather than being of MLCT origin. The single emission observed arises from a π-π^* excited state associated with the ppy ligand, but it is suggested that there may be a small extent of mixing with MLCT state also involving the ppy ligands.[79,80] At room temperature however, only very weak and short lived emission is observed, reportedly due to deactivation of the LC excited state via a low lying MC state.[79]

1.6 Iridium and rhodium complexes containing functionalised N^N and C^N coordinating ligands

By varying or functionalising the N^N and/or C^N coordinating ligands in complexes with the general formula [M(C^N)$_2$(N^N)]$^+$ where M is iridium(III) or rhodium(III), tailoring of the photophysical properties can be achieved. This enhances the possibility of these complexes finding practical application. A good example of this is a recent report by Slinker et al who, by attaching two tert-butyl groups to a 2,2'-bipyridine ligand, have created an emissive iridium complex which displays attractive properties when tested in a single layer organic light emitting device.[81]

Preliminary investigations by Watts et al[82] saw the introduction of electron donating methyl groups to the ppy ligand (Figure 14). When either of these ligands was combined in an iridium complex with bpy as the third ligand, an increase in electron density was found at the metal centre, which should facilitate MLCT transitions.

However, the poorer π-accepting ability of the methylated ppy ligand counteracts this, with the overall effect being one of very little change in the energy of MLCT transitions when compared to the unsubstituted parent complex. However, the presence of the methyl groups does enhance the photoreducing power of the complex.
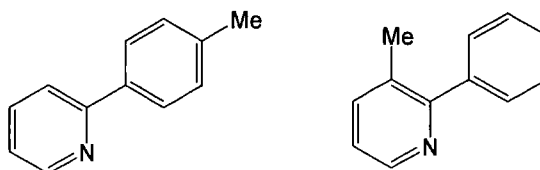
Figure 14 Methylated ppy ligands

An early rhodium example[83] exchanges the bpy ligand for either 1,10-phenanthroline (phen) or 2,2'-biquinoline (biq) (Figure 15). Emission was still reported to arise from a predominantly LC state, but whilst the lowest excited state for the phen complex involved the ppy ligands, as is the case for the bpy analogue, for the biq-containing complex this state involved the biq ligand itself. This arises due to the existence of several closely spaced levels of different orbital nature.

phen   biq
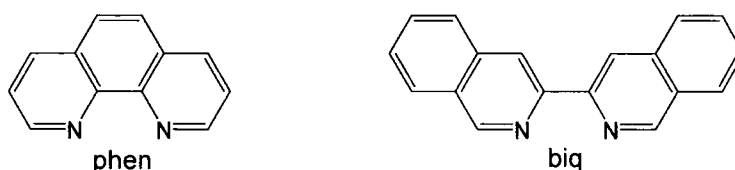
Figure 15 N^N binding ligands 1,10-phenanthroline (phen) and 2,2'-biquinoline (biq)

1.6.1 Iridium complexes with functionalised 2,2'-bipyridine based ligands

An alternative way to functionalise 2,2'-bipyridine based ligands for this type of iridium complex is to attach a phenyl group to the 6-position of either one[78,84-86] or both[86] of the pyridyl rings. When combined with two C^N coordinating ligands these N^N^C ligands are still found to bind to the central iridium atom in a bidentate manner via the two nitrogen atoms present. Additional functional groups can then be incorporated at other positions around the 2,2'-bipyridine structure. Examples of these ligands are summarised in Table 1.

Complexes containing this N^N-phenyl ligand with hydroxyl, chloro, methyl and carboxylate substituents at the para-position of an intermediate phenyl ring (Table 1 (i)-(iv) respectively) show how substitution can be used to fine tune the position of the emission maximum from these complexes.[78] However, a more dramatic effect can be seen if the three complexes containing carboxylate groups are considered (Table 1 (iv)-(vi)). By attaching the carboxylate group directly to one of the pyridyl rings in the

16

N^N-phenyl ligand, the electron withdrawing effect is markedly increased, with a red shift of the MLCT emission band to 735 nm.[84] By making the carboxylate more remote, the emission maxima becomes blue shifted to 606 nm.[84]
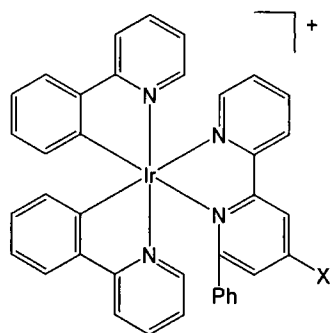
Entry	Substituent X	λ_{em} / nm	Ref.
(i)	OH (para-phenol)	620 (a)	78
(ii)	Cl (para-chlorophenyl)	645 (a)	78
(iii)	Me (para-methylphenyl)	630 (a)	78
(iv)	COOH (para-benzoic acid)	660 (a)/640 (b)	78,84
(v)	COOH	735 (b)	84
(vi)	O~~~~~COOH (phenyl ether chain acid)	606 (b)	84

Table 1 Emission Maxima of [Ir(C^N)₂(N^N)]+ complexes with 6-phenyl-substituted 2,2'-bipyridine ligands: (a) degassed MeCN 298K, (b) degassed CH₂Cl₂ 298K.

All of these iridium complexes containing N^N-phenyl ligands were initially reported to exhibit MLCT emission characteristics. However, more recent work has identified that the presence of the phenyl group may promote charge transfer transitions taking place from the ppy ligand to the bipyridine ligand.[87] This would be classed as a ligand-to-ligand charge transfer (LLCT) transition and may account for the difference in emission maxima seen for complexes such as those discussed here and those

containing bpy ligands without the extra phenyl ring (for example, [Ir(ppy)₂ (4'-(4''-bromo-phenyl)-2,2'-bipyridine)]⁺ which emits with MLCT characteristics at 611 nm in degassed acetonitrile at 298K[88]).

Alternatively, it is possible to attach two phenyl groups at the 6- and 6'-position of 2,2'-bipyridine to produce symmetrical ligands (Figure 16). These complexes, [Ir(ppy)₂(ph-N^N-ph)]⁺, are reported to emit from MLCT states of increased energy compared to the complexes previously discussed (Table 1). This is attributed to a reduction in planarity and hence destabilisation of the MLCT state.[86]
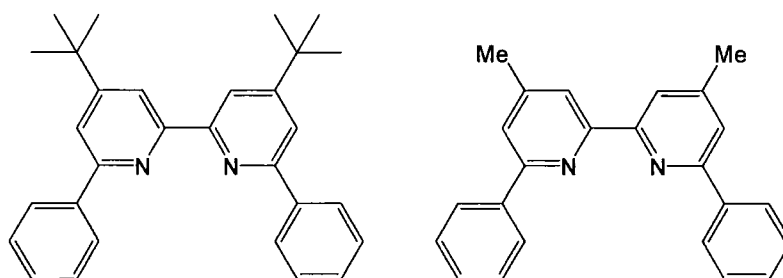
Figure 16 6,6'-Diphenyl-substituted 2,2'-bipyridine ligands

1.6.2 Complexes with N^N coordinating ligands other than 2,2'-bipyridine

The dichloro-bridged dimeric iridium and rhodium species discussed can be cleaved to form monometallic complexes using a number of different N^N coordinating species, not just 2,2'-bipyridine. For instance, the ligands 1,4,5,8-tetraazaphenanthrene (TAP) (Figure 17a) and 1,4,5,8,9,12-hexaazatriphenylene (HAT) (Figure 17b) have been used, with reports of [Ir(ppy)₂(HAT)]⁺ displaying dual emission similar to [Ir(ppy)₂(bpy)]⁺ at low temperature, and [Rh(ppy)₂(HAT)]⁺ and [Rh(ppy)₂(TAP)]⁺ displaying single emission. Unlike the bpy analogue however, emission from these rhodium complexes is of charge transfer nature, with donation from the Rh-C σ-bond to the HAT or TAP ligand (SBLCT).[89]
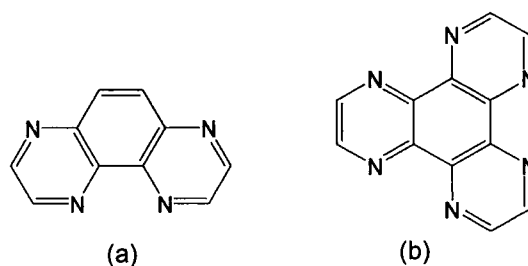
Figure 17 Structure of (a) 1,4,5,8-tetraazaphenanthrene (TAP) and (b) 1,4,5,8,9,12-hexaazatriphenylene (HAT)

Recent work by De Cola *et al*[90,91] makes use of a negatively charged phenyl-substituted pyridyl-1,2,4-triazole ligand (Figure 18) as the N^N coordinating species to create overall charge neutral iridium complexes which emit in the "almost blue" region.[90]
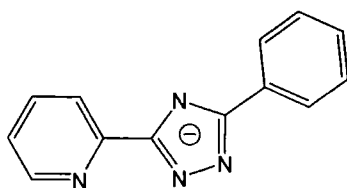
Figure 18 2-(5-Phenyl-4H-[1,2,4]triazol-3-yl)-pyridine

Included within this work is a discussion of the electron withdrawing effect of fluorine and trifluoromethyl groups on the phenyl ring of the ppy ligand.[90] They report that the iridium complex with fluorine substituents at the 3- and 5-position of the phenyl ring of ppy (Table 2 (b)) displays a considerable blue shift in emission compared to the non-fluorinated complex (Table 2 (a)), whilst barely any change is noted for 2,4-fluorine substituted complex (Table 2 (c)). This is attributed to the double electron withdrawing nature of the fluorine atom. Combining both the inductive and mesomeric electron withdrawing effects of fluorine results in an electron deficiency at sites which are *meta* to the fluorine atom. In the case of the 3,5-substitution pattern, this means that the site of cyclometalation becomes electron deficient and thus the σ-donating ability of the ppy ligand is reduced. This is seen as an increase in the energy of the MLCT state and a blue shift in the emission maxima. For the 2,4-substitution pattern there is little change in the electron density at the site of cyclometalation meaning that emission characteristics remain unchanged.
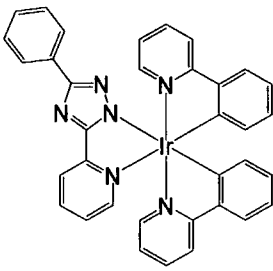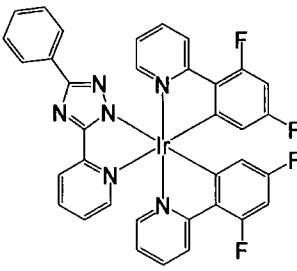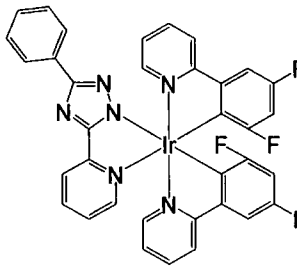
(a)	(b)	(c)
489 nm and 517 nm	461 nm and 491 nm	484 nm and 518 nm

Table 2 Fluorinated iridium complexes investigated by De Cola *et al*[90] and emission maxima given for solutions in CH_2Cl_2 at 293K.

Examples using trifluoromethyl groups in the same substitution patterns reveal very different results, with the 3,5-substitution pattern inducing a red shift in emission and the 2,4-substitution pattern delivering the blue shift this time. This is due to the

trifluoromethyl group only withdrawing electron density via an inductive effect.[90]

The high energy MLCT state for the iridium complex with fluorine substituents at the 3- and 5-position of the phenyl ring of ppy (Table 2 (b)) has led to its use as a sensitiser for europium in a d-f-d trimetallic assembly.[91] A pyridyl-1,2,4-triazole ligand with a pendent carboxylate group is pre-synthesised and bound to iridium, facilitating the linkage to a europium terpyridine based complex. Upon photoexcitation, emission of white light is observed due to partial energy transfer from the excited iridium moiety to the europium complex.

1.6.3 Development of [M(C^N)₂(N^N)]⁺ complexes for use in biological labelling studies

By functionalising [M(C^N)₂(N^N)]⁺ type complexes with isothiocyanate, iodoacetamide, amine or aldehyde groups, it is possible to create linkages to biological substrates and thus create luminescent bioconjugates.[92-97] As previously discussed, the intense long lived luminescence from such systems is attractive as it allows discrimination from background fluorescence via time resolved detection techniques. This can be used as a method of labelling and has found use in a number of heterogeneous assays.[93,94,97]

1.6.3.1 Isothiocyanate, iodoacetamide and amine functionalisation

Initial examples involve the functionalisation of a bpy or phen ligand with isothiocyanate, iodoacetamide and primary amine groups.[92,93] Combining these ligands in iridium complexes with two ppy ligands (Figure 19) produces MLCT emission from a state involving the N^N coordinated ligand. The electron-withdrawing effect of the isothiocyanate and iodoacetamide groups results in emission at lower energy than for the amine example. The presence of isocyanate and iodoacetamide groups allows for reaction with primary amine and sulfhydryl groups of biological substrates respectively. The phen complexes were reportedly coupled to human serum albumin (HSA) in this manner and provide the first examples of iridium polypyridyl complexes as labelling molecules for biological molecules.[92]

Figure 19 Iridium complexes with isothiocyanate, iodoacetamide and primary amine substituents for coupling to biological molecules

Further investigations into the effect of varying the C^N coordinating ligand have been carried out.[93] The C^N ligands investigated (Figure 20) were combined with the bpy and phen substituted ligands previously discussed to create a large series of new luminescent iridium complexes.

Figure 20 C^N coordinating ligands investigated by Lo *et al*[93]: (a) 2-(4-methylphenyl)-pyridine (mppy), (b) 3-methyl-1-phenylpyrazole (mppz), (c) 7,8-benzoquinoline (bzq) and (d) 2-phenylquinoline (pq)

Particular attention was drawn to complexes containing the 2-phenylquinoline (pq) ligand (Figure 20d) where emission characteristics were independent of the nature of the N^N coordinating ligand. This suggests that some LC or MLCT transitions involving the pq ligand are involved in creating the emissive excited state. Also of interest was the 7,8-benzoquinoline (bzq) (Figure 20c) series of complexes, where excited states of the bpy-NH₂ complex involved the bzq ligand, whilst for bpy-NCS it was the bpy ligand that was implicated. This was attributed to the increased π-acceptor qualities of bpy-NCS lowering the energy of MLCT involving the bpy ligand.

Complexes containing ppy or pq ligands and isothiocyanate-substituted bpy or phen ligands were used to label proteins HSA and avidin. Having successfully created these luminescent bioconjugates, the [Ir(pq)₂(phen)]-avidin conjugate was used in a competitive heterogeneous assay for digoxin, a potent cardiac glycoside commonly

prescribed for the treatment of patients suffering from congestive heart failure. In the assay the digoxin analyte competes with an immobilised digoxin derivative for the binding of a biotinylated anti-digoxin. The labelled avidin conjugate is used to recognise the immobilised biotinylated anti-digoxin.[93]

1.6.3.2 Aldehyde functionalisation

Creating similar complexes with aldehyde substituents provides an alternative way of labelling biomolecules. The first report of this sort involves the use of the cyclometalating ligand 4-(2-pyridyl)benzaldehyde (pba) in iridium complexes containing a bpy or phen type ligand (Figure 21).[94] Complexes of this type all give structured emission profiles at room temperature with a higher emission energy than is seen for the ppy analogue. A long-lived single exponential lifetime of emission is also observed. This suggests that emission arises predominantly from the LC π-π^* state associated with the pba ligand. The electron-withdrawing effect of the aldehyde group makes the iridium centre less electron rich thus making oxidation of iridium more difficult than in analogous ppy complexes.
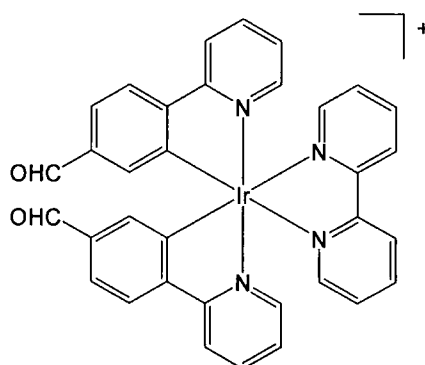
Figure 21 [Ir(pba)₂(bpy)]⁺

Bioconjugates incorporating these complexes are created via the coupling of the aldehyde group with a primary amine, followed by reductive amination to yield a secondary amine linkage. This has allowed the successful labelling of L-alanine and avidin. Again, an avidin labelled conjugate has been used in a heterogeneous competitive assay involving the recognition of biotin.[94]

Rhodium analogues containing pba ligands in conjunction with bpy or phen type ligands have been investigated[95] and also exhibit structured emission profiles associated with a pba LC state. Unusually long-lived emission is reported with lifetimes of 4.2 - 8.7 µs at room temperature compared to < 10 ns for the related ppy complex. Again the electron-withdrawing effect of the aldehyde group is reportedly

responsible for these results. Successful coupling to bovine serum albumin (BSA) has been carried out[95] but although the long luminescent lifetime is a very attractive property, the rather poor quantum yield of emission associated with these complexes may limit their use as labels with respect to iridium analogues.

The examples discussed so far have incorporated the aldehyde group in the ppy ligand. However, recent work has also studied related complexes containing an aldehyde group in the 2,2'-bipyridine ligand.[96] This can then allow for linkage to biomolecules[97] via the same coupling procedure as for the ppy cases above.

The N^N coordinating ligand 4-formyl-4'-methyl-2,2'-bipyridine (Figure 22) has been used in conjunction with a series of different C^N coordinating ligands to create strongly luminescent iridium complexes.[96] In the majority of cases emission was reported to arise from an MLCT state involving the bpy ligand. Complexes containing methyl-substituted ppy ligands displayed lower energy emission due to stabilisation of the MLCT state from the electron-donating effect of the methyl groups. However, as was the case for similar complexes which have been previously discussed[93], the presence of 2-phenylquinoline (pq) ligands gave emission with a substantial contribution from a pq LC state.
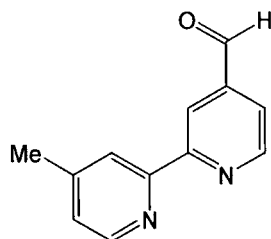
Figure 22 4-Formyl-4'-methyl-2,2'-bipyridine

These complexes have been successfully coupled via the aldehyde group to allow both luminescent labelling of BSA,[96] and direct linkage to a biotin moiety.[97] In the latter case a number of assays and luminescence titrations have been carried out.

1.7 Synthesis of C^N and N^N coordinating ligands

It is apparent from the examples discussed in the preceeding sections that it is necessary to elaborate on the basic bpy and ppy ligands in order to tailor the photophysical properties of their transition metal complexes and hence create candidates for practical applications. Attention will now turn to methods for the synthesis of such ligands, beginning with well established classical routes and moving

on to more recent metal catalysed cross-coupling approaches.

1.7.1 Classical Syntheses

1.7.1.1 Ring closing reactions

The Hantzsch synthesis of pyridines involves the condensation of two keto-ester molecules with an aldehyde in the presence of ammonia. The reaction proceeds via an aldol reaction between the enol or enolate form of the keto-ester and the aldehyde. The resulting adduct undergoes a conjugate Michael addition with another keto-ester molecule, which is followed by cyclisation with ammonia to yield a dihydropyridine. Oxidation, saponification and decarboxylation of this intermediate compound leads to the production of a substituted pyridyl ring (Figure 23). The Tschitschibabin synthesis[98] follows a similar route but requires harsh conditions to promote the one pot reaction of two ketones with an aldehyde in aqueous ammonia.
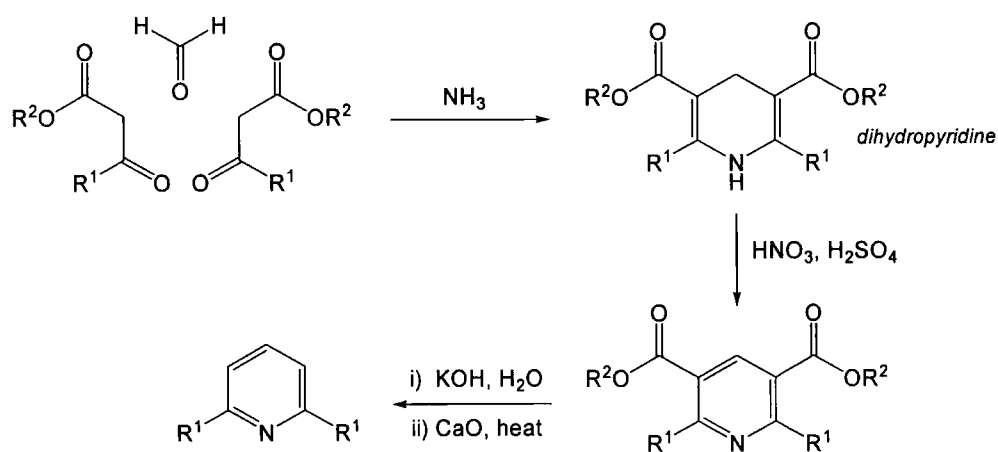
Figure 23 Hantzsch synthesis of pyridines

The Kröhnke synthesis[99,100] is an adaptation of the above syntheses with considerable advantages. In this case a pyridinium salt is treated with ammonium acetate in glacial acetic acid and an unsaturated ketone to give a 1,5-diketone via a Michael addition. The diketone is rarely isolated and instead undergoes ring closure with the ammonium acetate to give a substituted pyridine (Figure 24).
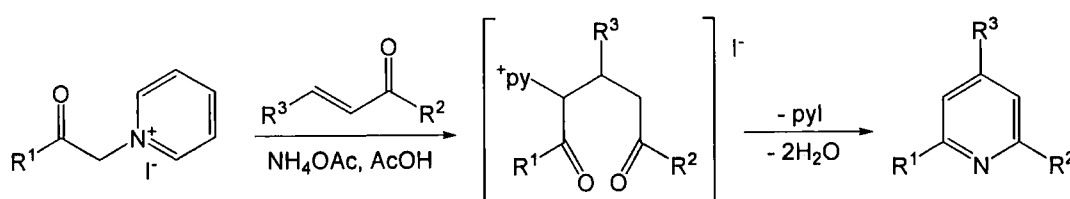
Figure 24 Kröhnke synthesis[99]

A significant advantage over the Hantzsch synthesis is the removal of the need for any dehydrogenation steps. In addition, much milder conditions can be employed than are required for the Tschitschibabin synthesis, which also demands that R^1 and R^2 are equivalent. This is not the case for the Kröhnke synthesis where R^1, R^2 and R^3 can be varied enormously and are not restricted to being equivalent. It can be seen that by allowing either of the R^1 or R^2 groups to be either a phenyl or pyridyl group, we have access to ppy and bpy type ligands respectively. In order to produce 2,4-disubstituted pyridine rings it is possible to use R^2 as a carboxylate group which may be thermally removed following ring closure. This type of reaction allows for the synthesis of a huge series of substituted pyridyl based species.[99]

1.7.1.2 N-oxide chemistry

An alternative approach, particularly for the synthesis of 4-substituted 2,2'-bipyridine ligands, involves building directly onto the back of 2,2'-bipyridine, which is a readily available starting material. However, pyridine is known to be resistant to electrophilic attack due to the electron-withdrawing nature of the nitrogen atom, so direct substitution reactions with bpy do not provide a useful route to the desired ligands. Instead N-oxide chemistry is applied.

In 1940, it was reported[101] that the dipole moment of pyridine-1-oxide was substantially lower than was expected and was attributed to the resonance structures shown in Figure 25. This led to the belief that pyridine-1-oxide should be more susceptible to electrophilic substitution at the 2 and 4 positions than pyridine itself. Indeed this was proved to be the case by performing a simple nitration reaction, with the 4-nitro-pyridine-1-oxide product being found to be very reactive at the nitro group.[102] As the nitro group was easy to reduce and readily displaced by nucleophilic reagents, a series of substituted pyridine-1-oxides was produced.
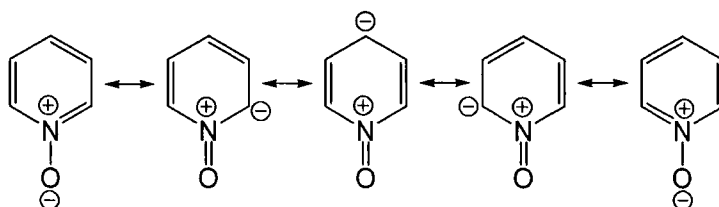
Figure 25 Resonance structures of pyridine-1-oxide

This methodology was applied to 2,2'-bipyridine to create an N,N-oxide (Figure 26a) which subsequently allowed the synthesis of a number of disubstituted bipyridine-1,1'-dioxides, incorporating amino, methoxy, ethoxy, phenoxy, carbethoxy and

carboxamido substituents by again taking advantage of a reactive 4-nitro group. It was reported that the N-oxide group could be selectively reduced using phosphorous trichloride yielding the appropriately substituted 2,2′-bipyridine.[103]

(a) **(b)**

* = sites activated towards substitution
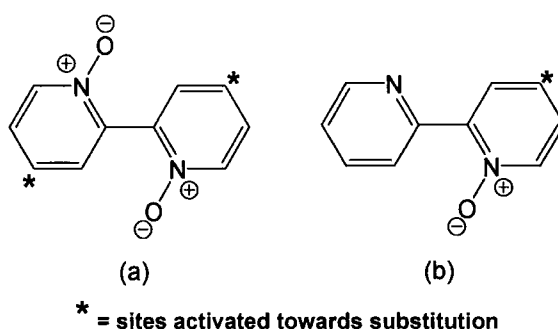
Figure 26 (a) 2,2'-Bipyridine-N,N'-oxide and (b) 2,2'-bipyridine-N-oxide

In order to create singly substituted 2,2′-bipyridyl species by this approach it is necessary to first generate a 2,2-bipyridine-1-oxide (Figure 26b) in which only one of the two pyridine rings is activated. This was originally attempted via reaction with hydrogen peroxide[104] but was found to lead to a mixture of N-oxide products. In 1970 it was reported that N-oxides of a series of amines could be produced in excellent yields via a simple reaction with m-chloroperoxybenzoic acid (mcpba).[105] The similar use of mcpba with 2,2′-bipyridine was subsequently found to provide a superior route to 2,2′-bipyridine-1-oxide.[106] Having produced this species, analogous nitration reactions to those reported for the N,N-dioxide systems are possible and allow the introduction of a number of functional groups.[106-109]

1.7.2 Synthesis via metal catalysed cross-coupling reactions

Metal catalysed cross-coupling reactions are among the most straightforward and general of methods now available for the formation of carbon-carbon bonds. However, this has not always been the case. For instance, the synthesis of biaryl species via the condensation of two molecules of an aromatic halide in the presence of copper, known as the Ullmann reaction,[110,111] requires extremely severe reaction conditions, leading to functional group intolerance. In particular, this reaction produces low yields when used for the synthesis of bipyridines.[112] More recently, metal catalysed cross-coupling reactions employing milder conditions and improved yields have been reported: examples using palladium-based catalysts are discussed here.

1.7.2.1 Palladium catalysed cross-coupling reactions

In the mid-1970's several groups reported independent yet simultaneous studies of a series of palladium catalysed cross-coupling reactions for C-C bond formation.[113] Most of these reports adopt a three-step catalytic cycle as the mechanism for the coupling, involving oxidative addition, transmetalation and reductive elimination steps (Figure 27).
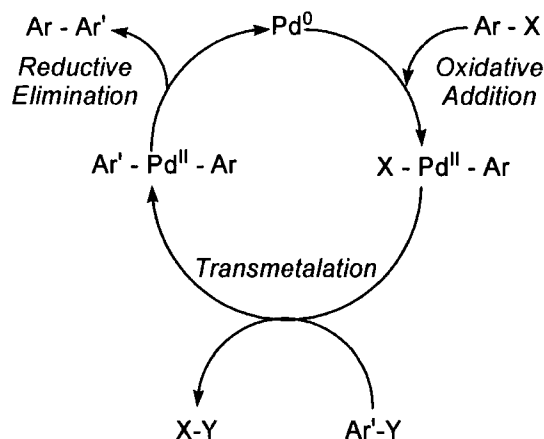
Figure 27 General palladium(0) catalysed cross-coupling cycle

1.7.2.1.1 Negishi cross-coupling reaction

The Negishi cross-coupling reaction involves the coupling of an organozinc compound with an aryl halide or triflate catalysed by palladium(0). This provides a general and mild procedure for the preparation of unsymmetrical biaryl systems.[114] Hetero-couplings of this type involving phenylzinc chloride have been reported to produce less of the unwanted homocoupled biphenyl side product than in systems using magnesium and aluminium. A further advantage is the tolerance of functional groups such as nitrile and ester groups. The cross-coupling reaction proceeds readily at room temperature in the presence of phosphine-containing palladium catalysts to produce numerous mixed biaryl products.[114]

This reaction has been extended to include the synthesis of polypyridyl species capable of chelating to a central metal ion. For instance, conversion of 2-bromopyridine into the appropriate organozinc compound, followed by coupling with a substituted pyridyl triflate in the presence of a palladium catalyst yields a substituted 2,2'-bipyridine (Figure 28).[115] Additionally, reaction of the same organozinc species with dibrominated bipyridyl species can lead to the production of terpyridyl and tetrapyridyl products (Figure 28).[116]
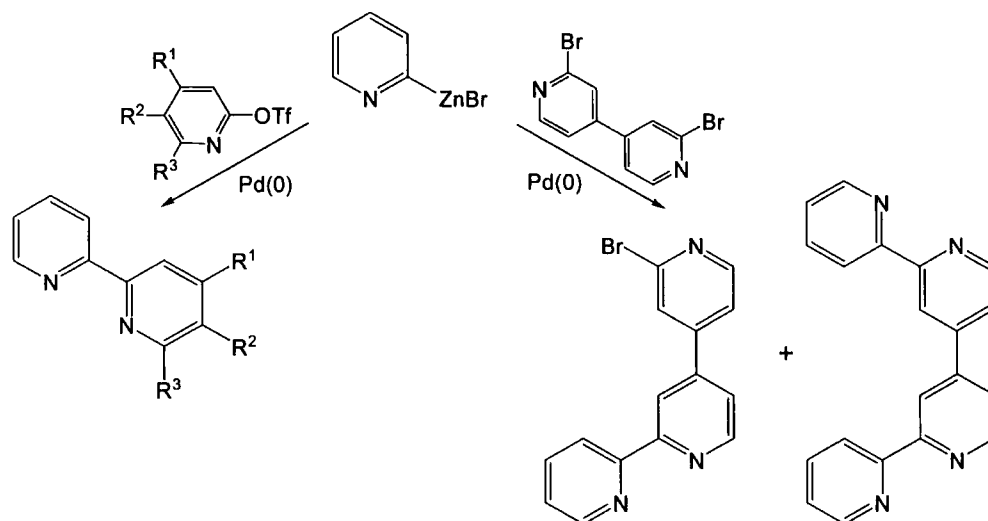
Figure 28 Negishi cross-coupling reactions to synthesise polypyridyls[115,116]

1.7.2.1.2 Stille cross-coupling reaction

In the Stille cross-coupling reaction, a palladium complex is used to catalyse the coupling of a tetraorganotin compound with a benzyl- or arylhalide.[117] Whilst this can also be a high yielding and functional group-tolerant preparation of biaryl systems, it is worth noting the toxic nature of the tin compounds involved.[118]

Mono-pyridyl rings containing complementary trimethylstannyl- and bromo-groups can be coupled in the presence of catalysts such as $Pd(PPh_3)_2Cl_2$ to generate 2,2':6',2"-terpyridine products,[119] whilst bipyridyl species with similar substituents couple to give rise to larger oligopyridines.[119,120] These reactions provide short and direct routes to polypyridyl species in good yields.

A series of work[121-123] carried out by Sauer *et al* documents the use of a [4+2] cycloaddition reaction between a series of triazines and tributylethynyl tin to generate polypyridyl species containing pendent tin substituents (Figure 29). These products are used as reagents in the Stille reaction to introduce substituents such as pyrimidine or thiophene to the polypyridyl backbone.[121] This'LEGO' system has been extended to the synthesis of branched oligopyridines containing up to 14 pyridine units.[122,123]
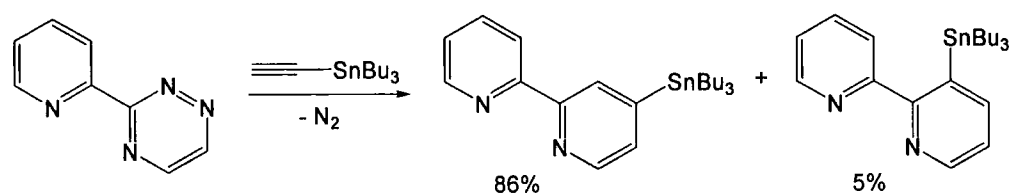
Figure 29 [4+2] Cycloaddition to create tin-substituted bipyridyl species[121-123]

1.7.2.1.3 Sonogashira cross-coupling reaction

The palladium catalysed cross-coupling of an arylhalide or aryltriflate with an ethynylated aryl compound forms the basis of the Sonogashira reaction.[124] The active catalyst can be generated *in situ* by combining the palladium complex with a copper species such as CuI. This can lower the temperature required for the coupling reaction to proceed.

The Sonogashira reaction can be used for the elaboration of pyridyl based compounds. Ethynyl-substituted bipyridines can be coupled with bromo- or triflate-functionalised bipyridyl or terpyridyl subunits using a Pd(PPh$_3$)$_4$ catalyst to create systems where two polypyridyl units are linked via an acetylenic bridge (Figure 30).[125] By reacting a bis-substituted ethynylbipyridine with similar reagents, three chelating units can be bridged in the same manner.[126] Indeed, this procedure has been adopted for the synthesis of a variety of pyridyl-based pre-organised polytopic ligands suitable for the chelation of a number of metal centres.[127] In addition, Sonogashira couplings involving 1,10-phenathroline and 2,2'-bipyrimidine ligands have given rise to sophisticated bridging ligands allowing for the construction of multimetallic systems.[128,129]
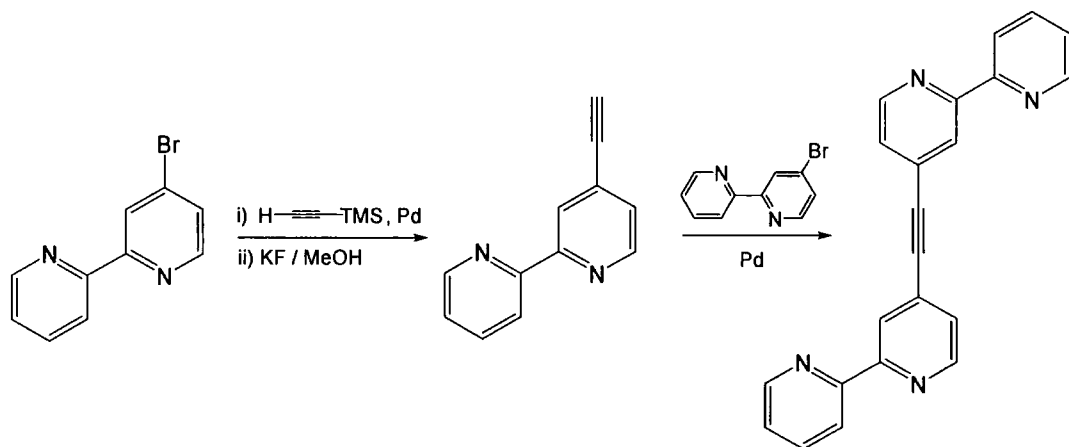
Figure 30 Sonogashira coupling on bipyridyl species[125]

1.7.2.1.4 Suzuki-Miyaura cross-coupling reaction

The Suzuki-Miyaura cross-coupling reaction[130] involves the palladium catalysed coupling of an organoboron compound with an organic halide or triflate. This reaction proceeds via the aforementioned catalytic cycle (Figure 31), with oxidative addition often being the rate limiting step. The mechanism involved in the transmetalation step is not completely understood but it is thought that it is accelerated by the presence of a base such as sodium or potassium carbonate, phosphate, hydroxide or alkoxide in one of two ways. In the first, the base interacts with the boron compound making it more

nucleophilic; in the second the base acts directly upon the palladium(II) species present. Advantages of the Suzuki-Miyaura reaction include functional group tolerance, low toxicity and the ease with which starting materials can be handled.[131]
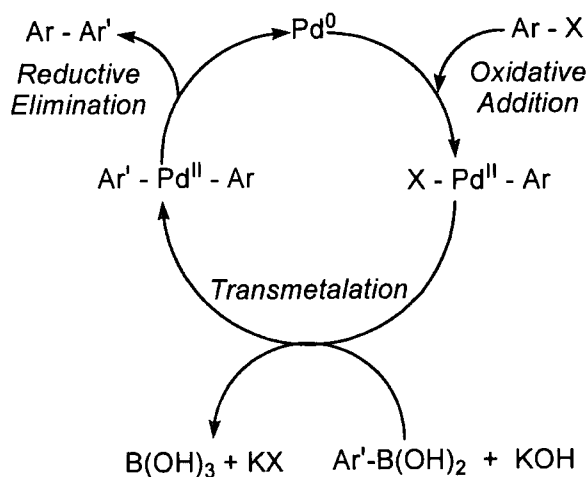
Figure 31 Catalytic cycle for the Suzuki-Miyaura cross-coupling reaction

Substituted bipyridines and 2-phenylpyridines have been produced using this reaction. The catalyst Pd(dppf)(OAc)$_2$, where dppf = 1,1'-bis(diphenylphosphino)ferrocene, is able to catalyse the production of 3,3'- and 3,4'-bipyridines using the relevant pyridineboronic acid.[132] Chloropyridines can be coupled with benzeneboronic acid in the presence of potassium carbonate and Pd(PPh$_3$)$_4$ to yield 2-phenylpyridine in excellent yields, a method that can be adapted to allow the incorporation of trifluoromethyl, nitro, methyl and methoxy substituents in the final ligand (Figure 32).[133] This is an attractive result as chloropyridines are more widely available and cheaper than their bromo- or iodo- counterparts, which are usually more successful in Suzuki reactions with conventional catalysts.
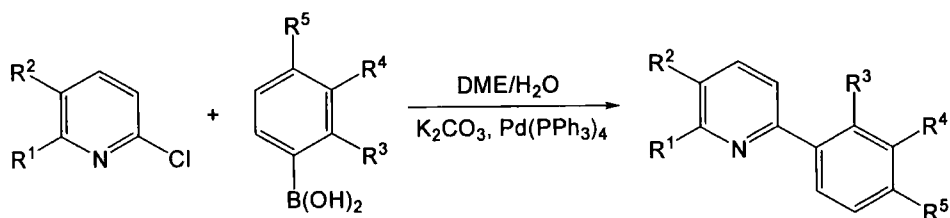
Figure 32 Suzuki-Miyaura reaction for the synthesis of substituted 2-phenylpyridines[133]

Alternatively, it is possible to take an already formed polypyridyl ligand with an attached bromo-substituent and perform a Suzuki-Miyaura reaction to elaborate on the ligand and introduce new functionality. This approach has provided a route for the development of 2,2':6',2"-terpyridine ligands appended with diphenylamino, dimethylamino, amino, cyano, nitro and aldehyde substituents.[134,135] In these instances

a Pd(PPh₃)₄ catalyst was employed in the presence of sodium carbonate base in either THF or DME solvent (Figure 33).
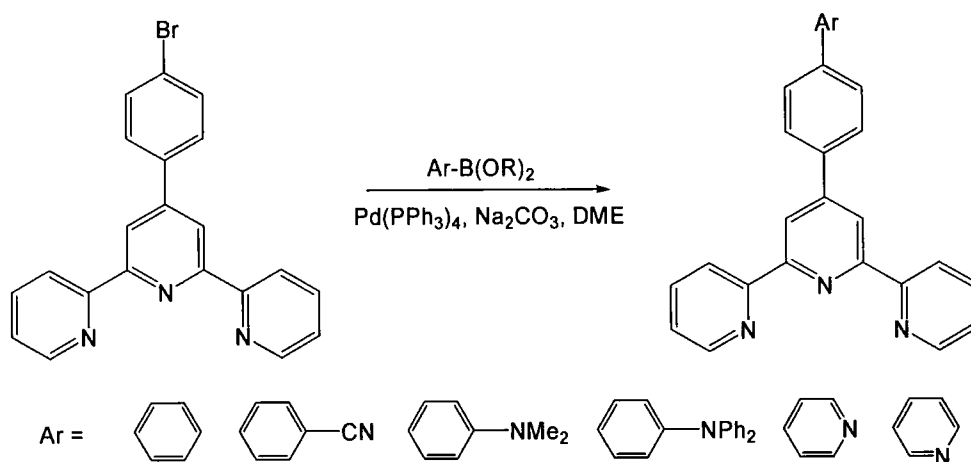
Figure 33 Suzuki-Miyaura cross-coupling reaction for the elaboration of terpyridine ligands[134,135]

1.7.2.2 Cross-coupling reactions on ligands once bound to a metal centre

Whilst the mild conditions and functional group tolerance of metal catalysed cross-coupling reactions have certainly proven useful for the synthesis of elaborate polypyridyl and cyclometalating ligands, all examples discussed so far have involved the pre-synthesis of the ligand which would then require binding to a metal centre. However, the incorporation of additional functional groups into these ligands may complicate the complexation procedure; if an alternative metal binding site is available, for instance. There is some evidence for this type of behaviour when the synthesis of a ruthenium complex of 2,2':4',4"-terpyridine is attempted.[6] It is suggested that at low temperatures, the poor yield of desired complex is due to the formation of a kinetic product involving coordination to the ruthenium via the pendent pyridyl group (Figure 34).
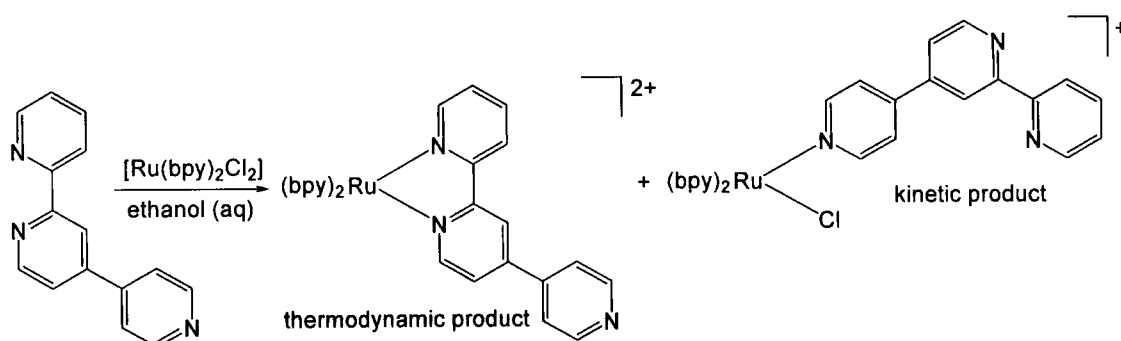
Figure 34 Thermodynamic vs kinetic binding of 2,2':4',4"-terpyridine[6]

One method which can be used to avoid this situation is to use cross-coupling reactions to elaborate upon ligands after they have been bound to a metal centre. This involves carrying out cross-coupling reactions on appropriately substituted metal complexes.

Work carried out by Tor *et al* looks at the use of the Sonogashira reaction for this purpose. It is possible to cross-couple a pre-complexed bromo-substituted 1,10-phenanthroline ligand with phenylacetylene in the presence of a palladium catalyst (Figure 35).[136] In fact, the author reports that it is easier to work with the ligand after it has been bound to ruthenium as the nitrogen atoms are effectively protected from reacting. Additionally, the electron-withdrawing nature of the metal facilitates the oxidative addition of palladium across the phenanthroline-bromine bond.[137] This method has been extended to allow the incorporation of metal complexes into oligonucleotides.[138,139]
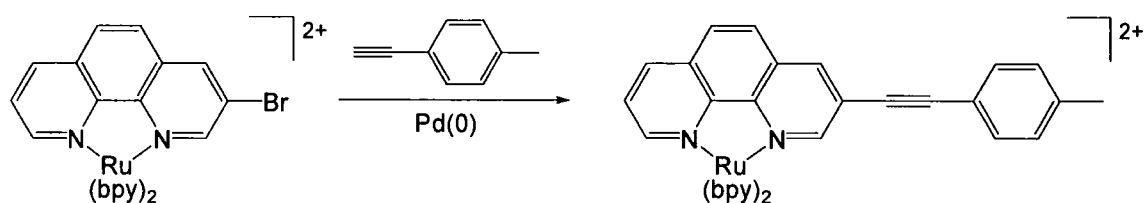
Figure 35 Sonogashira reaction to elaborate on ligands after complexation[136]

Boronic ester or acid compounds for use in the previously described Suzuki-Miyaura reaction can be synthesised via the Miyaura reaction,[140] which couples an aryl halide with a diboronic ester such as bis(neopentylglycolato)diboron (Figure 36) in the presence of a palladium catalyst and base via the usual catalytic cycle.
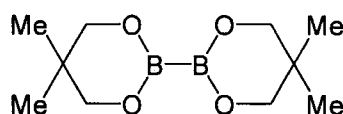
Figure 36 Bis(neopentylglycolato)diboron [B2neo2]

This reaction has not only been used to produce boronic ester substituted 2,2':6'2"-terpyridine ligands, but also to create analogous metal complexes by carrying out the cross-coupling reaction on the back of the ligand after it has been coordinated to ruthenium.[141] This then provides the opportunity to investigate the use of the Suzuki-Miyaura reaction for the coupling of aryl halides with boronic ester/acid substituted metal complexes (Figure 37), alongside the opposite situation where a bromo- or triflate-substituted metal complex can be reacted with an aryl boronic acid (Figure 38). Both of these routes utilise standard Suzuki-Miyaura conditions and are successful in providing a way to elaborate upon the ligand *in situ*. The latter method

has also been applied to the elaboration of iridium 2,2':6',2"-terpyridine complexes and has been used for the introduction of cyano and dimethylamino functional groups.[142]
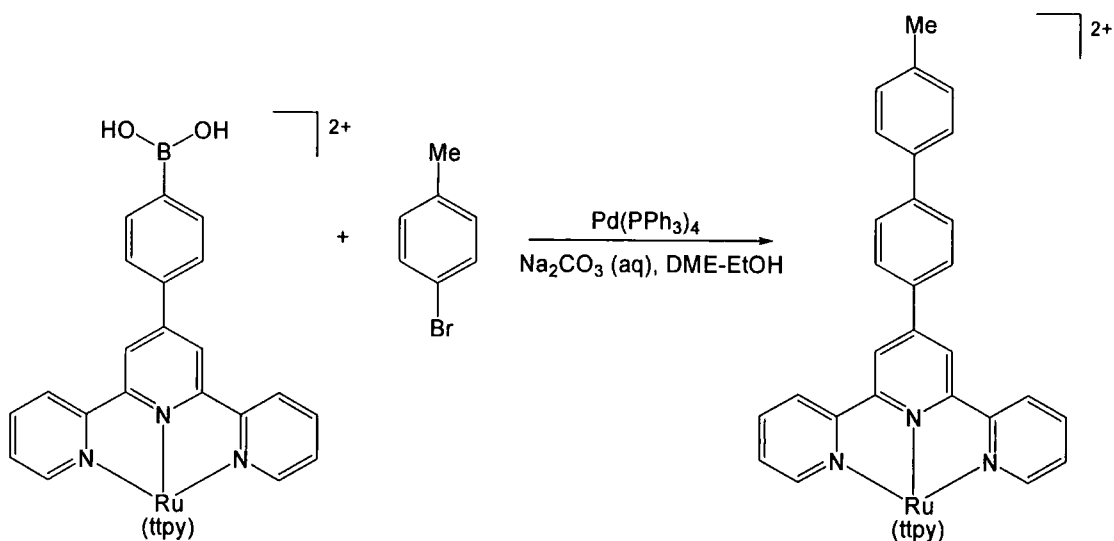
Figure 37 Suzuki-Miyaura reaction using a boronic acid substituted ruthenium complex[141]
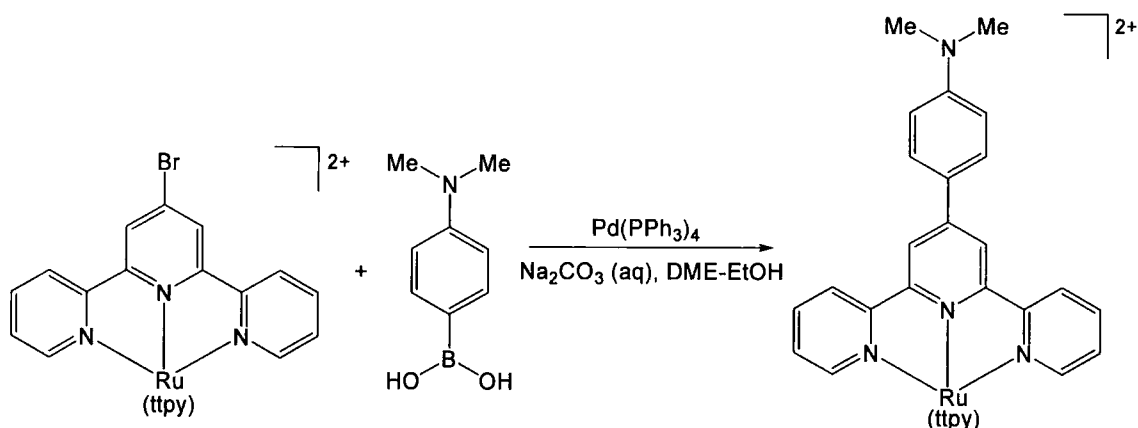
Figure 38 Suzuki-Miyaura reaction using a bromo-substituted ruthenium complex[141]

1.8 Multimetallic assemblies

It is possible to use molecular building blocks for the generation of large supramolecular arrays. If transition metal complexes are used as the building blocks, polynuclear complexes can be created via metal-ligand coordination bond formation. This allows the design of dendrimer systems consisting of sections which can absorb light, luminesce and/or display redox active characteristics. Careful consideration when designing such systems can lead to directional control of energy and electron transfer, and thus to applications in molecular electronics, photochemical molecular devices, solar energy conversion and information storage.[7]

1.8.1 'Complexes as metals, complexes as ligands' approach

The 'complexes as metals, complexes as ligands' approach provides a powerful synthetic route for the synthesis of both homo- and heteronuclear multimetallic systems. In this method, metal complexes with easily replaceable ligands are used as synthetic equivalents to 'metals', whilst complexes containing ligands with free chelating sites are used as 'complex ligands'.[7]

1.8.1.1 Bis(2-pyridyl)pyrazine (dpp) bridging ligands

Much work has focused upon the use of this approach to generate ruthenium and/or osmium containing assemblies with either 2,3-bis(2-pyridyl)pyrazine or 2,5-bis(2-pyridyl)pyrazine (Figure 39) or both as bridging ligands.[143-153]

(a)   (b)
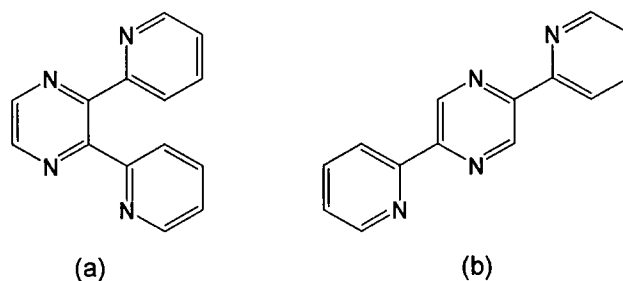
Figure 39 (a) 2,3-bis(2-pyridyl)pyrazine, (b) 2,5-bis(2-pyridyl)pyrazine

The simplest example takes a ruthenium complex containing one dpp type ligand as the 'complex ligand' and a Ru(N^N)₂Cl₂ complex as the 'complex metal', where N^N can be 2,2'-bipyridine or 2,2'-biquinoline.[143] Reaction of these components gives rise to a dinuclear ruthenium complex bridged by the dpp ligand and which can contain dissimilar N^N ligands if so desired.

The species [(bpy)₂Ru(dpp)]₂RuCl₂ (I) (where dpp can be 2,3-dpp or 2,5-dpp) can be produced from the reaction of RuCl₃.3H₂O and Ru(bpy)₂(dpp)(PF₆)₂ and subsequently acts as a 'complex metal' itself (Figure 40). When reacted with further quantities of a dpp ligand, the triruthenium species dimerises to form a hexanuclear ruthenium complex (II)[144] unless more controlled experimental conditions are used, whereupon the two chlorine atoms can be replaced by a dpp ligand and a new 'complex ligand' can be isolated instead.[145]

Alternatively, the reaction of RuCl₃.3H₂O with Ru(bpy)(dpp)₂²⁺ in the presence of acid generates a tetraruthenium 'complex ligand' (III).[146] This can be further reacted with a Ru(N^N)₂Cl₂ species to create a heptanuclear complex (IV),[146] or with the previously

mentioned complex [(bpy)$_2$Ru(dpp)]$_2$RuCl$_2$ (I), giving rise to a complex containing 13 ruthenium centres (V) (Figure 40).[147]
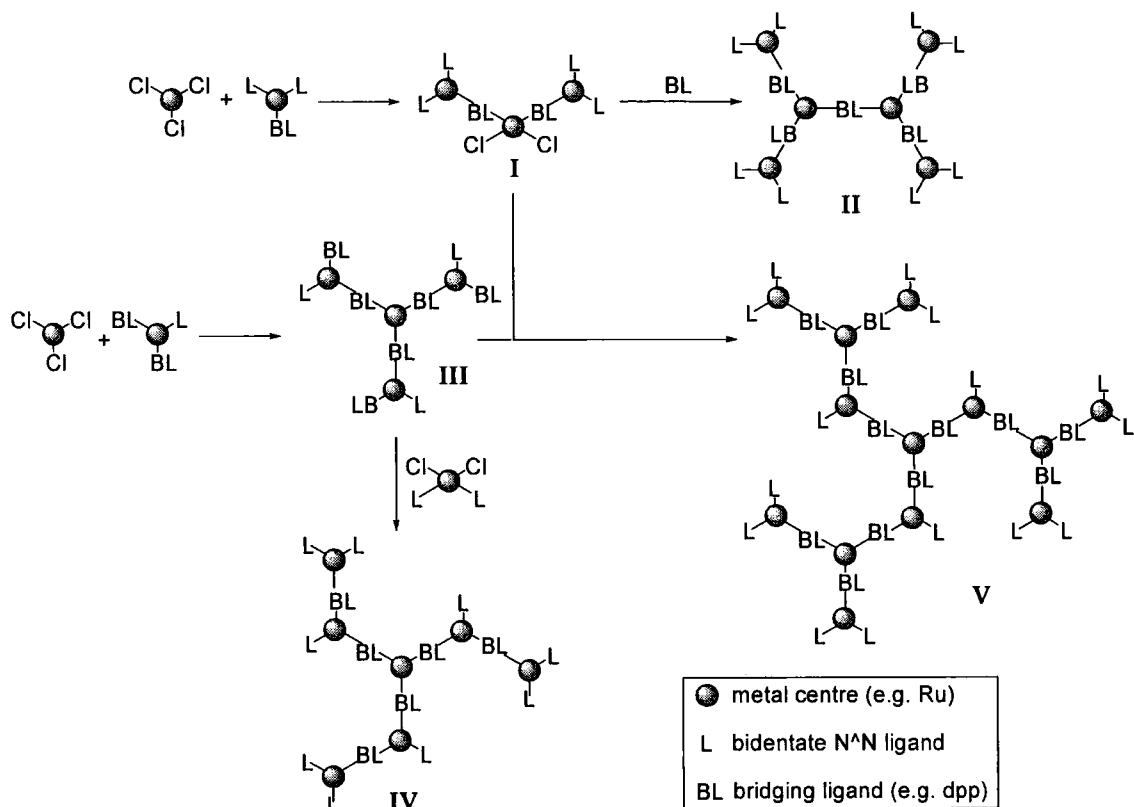
Figure 40 'Complexes as metals, complexes as ligands' approach using dpp bridging ligands

Ru(dpp)$_3$$^{2+}$ is another popular 'complex ligand'[148] as it can easily form the central core in a dendritic system. Reaction with Ru(N^N)$_2$Cl$_2$ yields a tetraruthenium product where the N^N species can be 2,2'-bipyridine, 1,10-phenathroline or 2,2':6',2"-terpyridine.[149] A similar reaction has been carried out starting from an osmium dpp core allowing the production of a heterometallic system.[150] Alternatively, reaction of Ru(dpp)$_3$$^{2+}$ with the triruthenium species [(bpy)$_2$Ru(dpp)]$_2$RuCl$_2$ generates a decaruthenium complex,[151] which as well as having been attempted with osmium analogues to generate heterometallic species,[152] has also been successful in producing a complex containing both 2,3-bis(2-pyridyl)pyrazine and 2,5-bis(2-pyridyl)pyrazine as bridging ligands.[153]

1.8.1.1.1 Control over the final composition of polynuclear systems

In order to introduce control over the structure of the final multimetallic assembly, a protection/deprotection procedure can be adopted using a singly methylated dpp ligand, 2-[2-(1-methylpyridiniumyl)]-3-(2-pyridyl)pyrazine (2,3-Medpp).[154] The process is outlined in Figure 41 and shows a tri-ruthenium species reacting with 2,3-

Medpp, which only has one available bidentate binding site, to produce a single product. Subsequent deprotection via demethylation yields the desired 'complex ligand' [Ru(dpp)(bpy)₂]₂Ru(dpp) (VI) which may then be used in further reactions with suitable 'complex metals'. This has allowed the production of well defined hexameric species (VII) containing more than one type of metal and/or bridging ligand.[155]
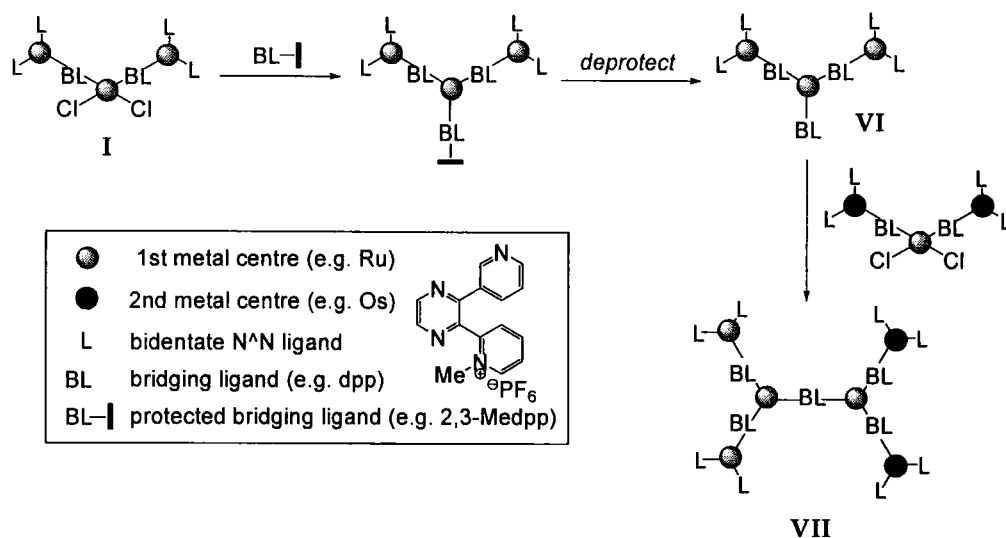
Figure 41 Protection/deprotection strategy using 2,3-Medpp for controlled synthesis of multimetallics

Methylated dpp ligands also find use in the divergent synthesis of dendrimer type systems. The required bifunctional species, such as Ru(dpp)₂Cl₂, undergo unavoidable self reaction and can produce dispersed and uncontrolled nuclearities.[7] By temporarily blocking the sites of chelation, a controlled and stepwise synthesis can be achieved. This is best shown pictorially in Figure 42 and has allowed the generation of systems containing up to 22 metal centres (VIII) with osmium or ruthenium metal centres.[156,157]
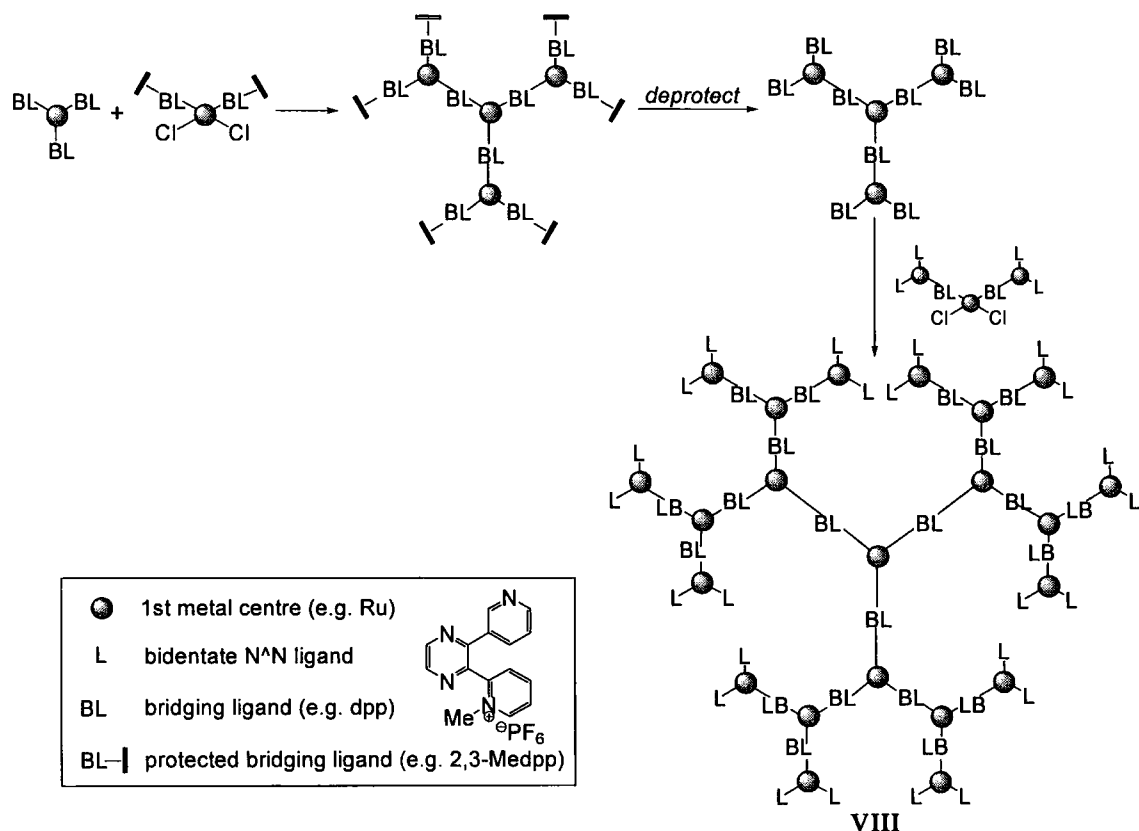
Figure 42 Divergent synthesis of dendritic species using the 'complexes as metals, complexes as ligands' approach

1.8.1.2 Extension to bridging ligands other than dpp with a variety of metal centres

The use of dpp type bridging ligands has shown how useful the 'complexes as ligands, complexes as metals' approach is for the generation of large osmium- and/or ruthenium-containing multimetallic species. Such bridges have also found use in the creation of polynuclear systems combining either ruthenium or osmium complexes with iridium or rhodium cyclometalated complexes.[158] Further examples of ruthenium- and rhodium- or iridium- containing systems have been produced using bridging ligands such as pyrazole-3,5-bis(benzimidazole),[159] 3,5-bis(pyridine-2-yl)-1,2,4-triazole[160] and 1,4,5,8,9,12-hexaazatriphenylene (HAT)[161]. These are generally synthesised via the reaction of a ruthenium complex containing the bridging ligand as the 'complex ligand' and an iridium or rhodium chloride containing species as the 'complex metal'. Additionally, ruthenium-rhodium systems have been created with simple alkyl groups being used to bridge between two 2,2'-bipyridine ligands.[162,163] Further extension of this method sees the incorporation of rhenium,[164-166] iron[167] and platinum[166] into multimetallic arrays.

37

1.8.2 Creating new binding sites by reactions 'in situ'

An alternative way to produce well-defined multinuclear metal complexes in a controlled manner is to create a new site capable of coordinating to another metal centre on the back of the ligand after it has been coordinated to a metal. This involves carrying out chemistry on the complex itself in order to convert it into a 'complex ligand' and avoids the presence of more than one binding site in the initial stages of synthesis.

1.8.2.1 Simple 'organic-type' reactions

Condensation reactions have been used as a method to elaborate upon ligands *in situ*. In one instance, iridium complexes containing bidentate ligands appended with hydroxyl groups have been reacted with similar bidentate ligands containing –COCl groups to produce a 'complex ligand' via an ester linkage.[168] This in turn can be used to generate bimetallic species. Another example makes use of a condensation reaction between a ruthenium complex of 1,10-phenanthroline-5,6-dione and 9,10-diamino-1,4,5,8-tetraazaphenanthrene. This creates the bridging ligand 1,10-phenanthrolino-[5,6-b]-1,4,5,8,9,12-hexaazatriphenylene *in situ*.[169]

Coordination of 4-bromo-2,2'-bipyridine to a metal such as ruthenium enhances its reactivity with species containing hydroxyl groups to generate ligands containing ether linkages. Ruthenium complexes containing one or more chloro-substituted terpyridine or bipyridine ligand have been reacted with 2,6-bis(2-pyridyl)-4-pyridone in order to create 'complex ligands' with at least one vacant terpyridine coordination site (Figure 43).[170] In some cases, further reaction with appropriate 'complex metals' has led to the production of tetra-, hexa- and nonanuclear complexes.[171]
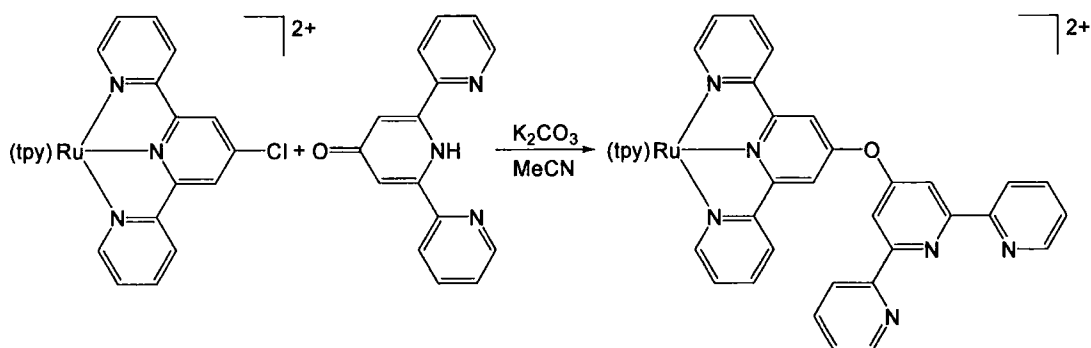
Figure 43 Elaboration *in situ* to generate new binding site

1.8.2.2 Cross-coupling reactions

Alternatively, metal catalysed cross-coupling reactions can be used to generate new binding sites via an *in situ* approach. For instance, the palladium catalysed Negishi cross-coupling reaction between a ruthenium complex containing a 2-bromo-substituted pyridyl ring and 2-pyridylzinc bromide gives rise to a new bidentate coordination site which can bind to an osmium centre under suitable reaction conditions.[116] Similarly, the Stille cross-coupling reaction has been used to couple a bromo-substituted ruthenium complex with an aryl stannyl compound to provide a free binding site.[172]

A particularly astute example along these lines makes use of a nickel catalysed self coupling reaction involving a ruthenium *ortho*-chloroimine complex to form a binuclear species, whilst simultaneously producing a third bidentate binding site also capable of binding to a ruthenium centre (Figure 44).[173]
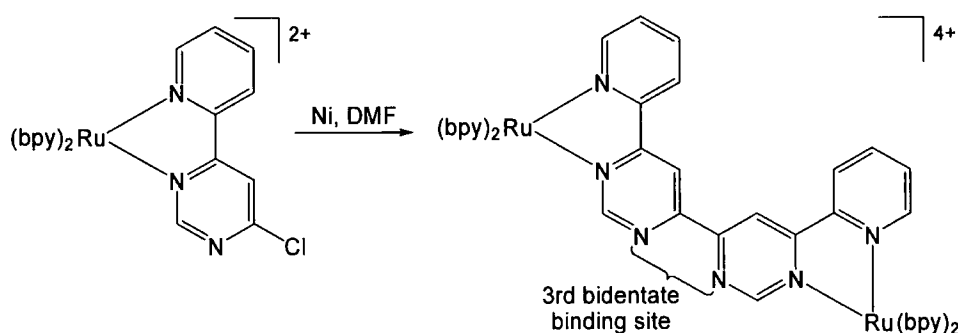
Figure 44 Nickel coupling of a ruthenium *ortho*-chloroimine to create a third bidentate binding site

1.8.3 Joining metal complexes together using cross-coupling reactions

The main drawback of the 'complexes as metals, complexes as ligands' approach is the need for time- and material-consuming protection/deprotection steps in order to gain full control over the final assembly structure. In an attempt to combat these drawbacks, metal catalysed cross-coupling reactions have been used for the direct linkage of metal complexes. As will be demonstrated in the examples below, this can be done by reacting substituted metal complexes with an appropriately-substituted entirely organic species as an indirect linking unit, or via the direct reaction of two complementarily-substituted metal complexes.

The Sonogashira cross-coupling reaction has been used for the synthesis of multimetallic systems, with Tor *et al*[137,174] having studied reactions involving complexes

39

with 1,10-phenanthroline ligands with bromo- or ethynyl-substituents in the 3-position. Initially, bromo-substituted complexes were reacted with di- or tri-ethynylated aryl compounds in the presence of $Pd(PPh_3)_2Cl_2$ and CuI in order to create multinuclear species in excellent yields.[136] Later work reports the successful direct reaction between bromo- and ethynyl-substituted complexes (Figure 45), allowing the controlled generation of mixed metal systems in good yields.[175,176]
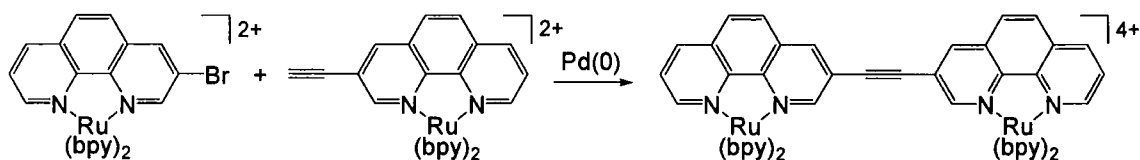
Figure 45 Use of the Sonogashira cross-coupling reaction for the direct linkage of metal complexes by Tor *et al*[175]

Additionally, in work by another group, the report that a cyclometalated ruthenium complex can be selectively brominated at the site opposite to cyclometalation using NBS in acetonitrile at room temperature,[177] has led to the production of a series of diethynylarene linked diruthenium complexes via the Sonogashira cross-coupling reaction.[178]

The Suzuki-Miyaura cross-coupling reaction has likewise been investigated for the direct joining together of metal complexes. Metal containing conjugated polymers[179,180] have been produced via the reaction of ruthenium complexes containing dibromo-substituted ligands with aryl diboronic acid species. The metal content of the resulting polymers can be controlled via the ratio of starting materials.

A similar approach has been taken for the generation of homo-dinuclear ruthenium and iridium species. A ruthenium complex containing a bromo-substituted dipyridylbenzene ligand can be reacted with a diboronic ester in the presence of $Pd(PPh_3)_4$ and base in order to generate a biruthenium system bridged by a series of phenylene groups.[181,182] Likewise, iridium complexes of the type $[Ir(ppy)_2(bpy-\phi-Br)]^+$ can be coupled using similar boronic acid species to give rise to analogous products (Figure 46).[88,183] This has been demonstrated for complexes with unsubstituted ppy ligands[88] and also for those with difluoro-substituted cyclometalating ligands.[183] It is worth noting that no examples of Suzuki reactions between a bromo-substituted metal complex and boronic acid substituted metal complex are previously reported.
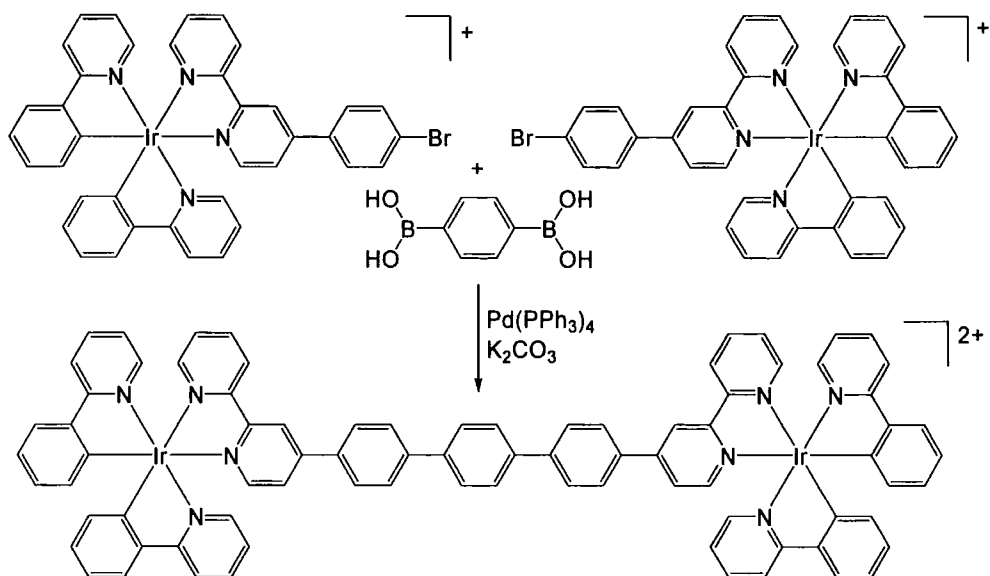
Figure 46 Suzuki cross-coupling reaction for the synthesis of diiridium complexes

1.9 Scope of the work presented here

The aims of this study were to investigate the use of the Suzuki-Miyaura cross-coupling reaction for:

(a) the synthesis of functionalised monometallic complexes of the type $[M(C^\wedge N)_2(N^\wedge N)]^+$ via an *in situ* approach, with an intention to create systems with pH responsive photophysical properties, and

(b) the controlled synthesis of well-defined multimetallic arrays via the direct coupling of appropriately functionalised metal complexes, giving rise to systems that possess directional energy transfer abilities, which may be reliably predicted from the properties of the constituent building blocks.

Following the generation of a series of variously substituted monometallic complexes, the photophysical properties discerned will allow for the careful design of energy funnelling multimetallic species. A fundamental challenge in the synthesis of such arrays lies in the development of previously unreported boronic acid appended metal complexes.

CHAPTER 2

SYNTHESIS OF MONOMETALLIC

COMPLEXES

2 Synthesis of Monometallic Complexes

This chapter discusses the synthesis of a series of d^6 monometallic transition metal complexes containing one or more ligands based on 2-phenylpyridine, 2,2'-bipyridine or 2,2':6',2"-terpyridine. Appropriate functional groups are incorporated into the complexes in an attempt to either introduce sensitive luminescence characteristics or to provide building blocks for use in the synthesis of multimetallic arrays (see Chapter 4). The *in situ* elaboration of complexes via a cross coupling methodology is also described.

2.1 [M(C^N)₂(N^N)]⁺ type complexes

As discussed in the introduction, the photophysical properties of complexes of the general formula [M(C^N)₂(N^N)]⁺, where M is Ir(III) or Rh(III), C^N is a cyclometalating ligand such as 2-phenylpyridine (ppy) and N^N is a bidentate nitrogen donating ligand such as 2,2'-bipyridine (bpy) (Figure 47), have been widely studied. The intense long lived emission observed, particularly from iridium examples, has led to applications in organic light emitting devices (OLEDs),[81] sensitising systems[91] and biological labelling studies.[92-97]
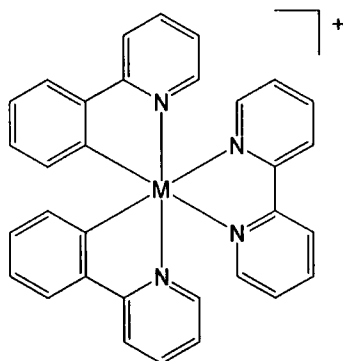
Figure 47 [M(C^N)₂(N^N)]⁺ type complex

In order to tailor the chemistry and fine tune the photophysical properties of such complexes, alterations are made to the periphery of the ligands. The synthesis of this type of system most often involves the pre-synthesis of the desired ligands followed by complexation to the metal centre, a method based on an early rhodium synthesis by Nonoyama.[76] Cyclometalating ligands such as 2-phenylpyridine (ppyH) have a tendency to form dichloro-bridged dimetallic species when allowed to react with either iridium[69] or rhodium[70] salts. These species can be cleaved (Figure 48) to generate two equivalents of a monometallic species by the further reaction with an N^N coordinating ligand such as 2,2'-bipyridine (bpy).[5] The first section of work presented

43

here adopts this synthetic procedure and details its use for the production of a series of novel functionalised iridum and rhodium complexes.
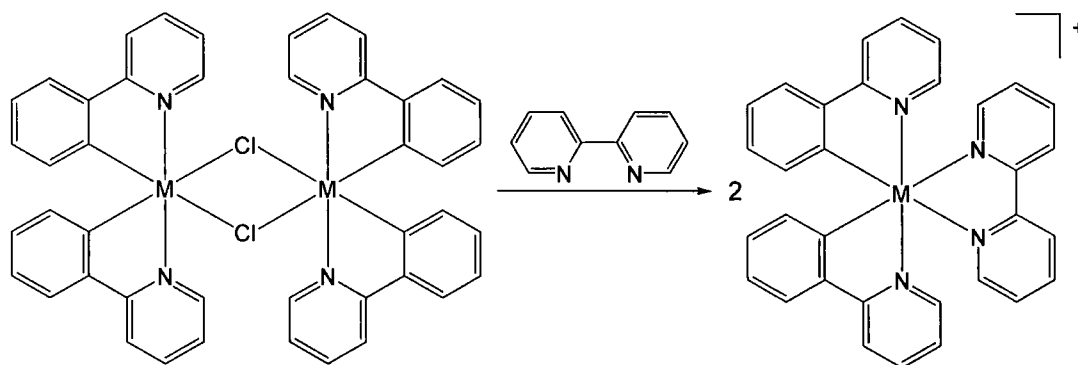
Figure 48 Reaction of a dichloro-bridged dimer with N^N species (M = Ir or Rh)

2.1.1 Synthesis of ligands

In order to prepare monometallic complexes of the type $[M(C^\wedge N)_2(N^\wedge N)]^+$, it is necessary to have access to a series of $C^\wedge N$ and $N^\wedge N$ coordinating ligands, the synthesis of which is described in this section.

2.1.1.1 Synthesis of C^N type ligands

Whilst cyclometalating ligands 2-phenylpyridine (ppyH) and 4-(2-pyridyl)-benzaldehyde (pbaH) are commercially available, three fluorinated 2-phenylpyridine based ligands (**1H** (ppyH-F), **2H** (ppyH-F₂) and **3H** (ppyH-F₃), Figure 49) were prepared via the Suzuki cross-coupling of 2-bromopyridine and the appropriately fluorinated phenylboronic acid. By using Pd(PPh₃)₄ as the catalyst in degassed dimethoxyethane (DME) in the presence of aqueous K₂CO₃ as the base, yields of 40 – 70% were obtained after purification via column chromatography. Whilst ligands **1H** and **2H** have been previously[133] and since[184] synthesised via this approach, this is the first reported preparation of the trifluorinated analogue **3H** by any route.

		X	Y	Z
1H	ppyH-F	H	H	F
2H	ppyH-F₂	F	H	F
3H	ppyH-F₃	F	F	F
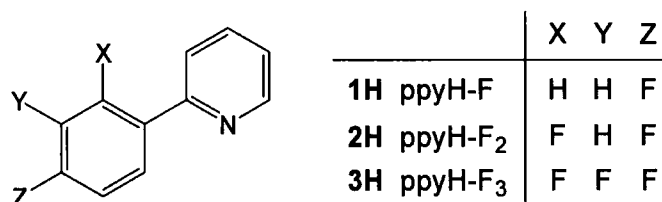
Figure 49 Fluorinated 2-phenylpyridine based ligands

2.1.1.2 Synthesis of N^N type ligands

2.1.1.2.1 N-oxide chemistry

Previously reported N-oxide chemistry[106,108] was exploited in order to produce 4-bromo-2,2'-bipyridine **7**. The reaction of 2,2'-bipyridine with *m*-chloroperoxybenzoic acid[106] produced 2,2'-bipyridine-N-oxide **4** in 45% yield. This is preferable to an alternative route employing hydrogen peroxide[104] which produces a mixture of mono and bis N-oxide products. The N-oxide ring of **4** is activated, particularly at the 4-position, towards substitution reactions, whereas the pyridyl ring remains relatively resistant. As such, a subsequent nitration reaction employing fuming nitric acid and concentrated sulphuric acid yielded 4-nitro-2,2'-bipyridine-N-oxide **5** upon basicification.[108] The nitro group was exchanged for a bromo group to give 4-bromo-2,2'-bipyridine-N-oxide **6** via reaction with acetyl bromide in glacial acetic acid.[108] Finally the N-oxide was reduced in the presence of phosphorous tribromide to give the desired ligand[108] **7** in 65% yield (Figure 50).
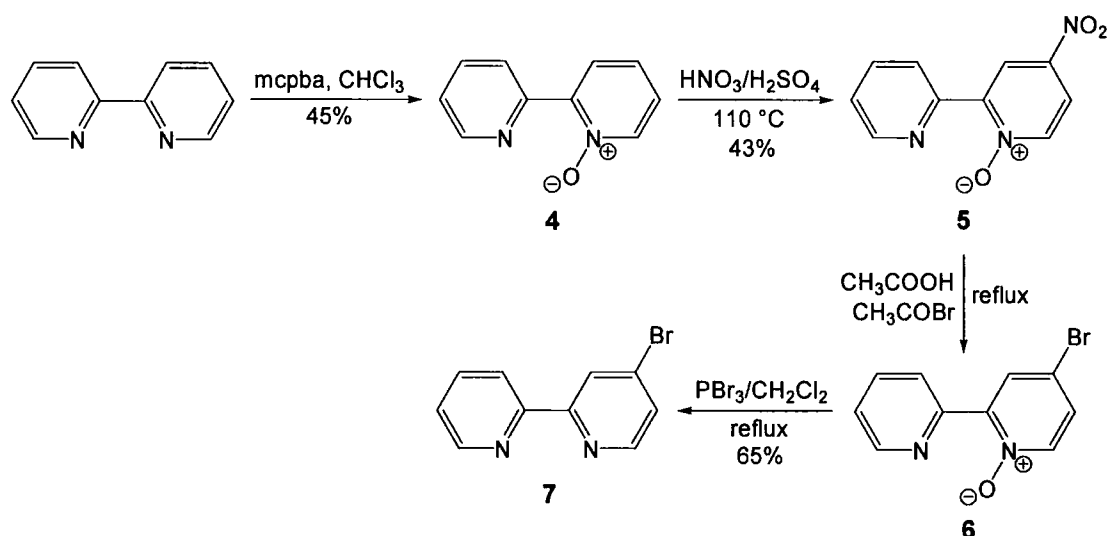
Figure 50 Synthesis of 4-bromo-2,2'-bipyridine

2.1.1.2.2 Hantzsch synthesis of pyridines

The synthesis of 4-(4-bromophenyl)-2,2'-bipyridine (bpy-φ-Br) **10** was achieved by using the Hantzsch synthesis of pyridines as described by Schmehl *et al*.[22] This multi-step procedure (Figure 51) begins with the synthesis of an intermediate enone **8**, which was achieved in excellent yield (86%) via the condensation of 4-bromobenzaldehyde with sodium pyruvate. Reaction of **8** with 1-(2-oxo-2-pyridin-2-yl-ethyl)-pyridinium iodide **9**, itself synthesised via an established methodology[100] using 2-acetylpyridine, pyridine and iodine, produced a 6-carboxy-substituted 2,2'-bipyridine. Thermal decarboxylation followed by purification via either recrystallisation from ethanol or

column chromatography using aluminium oxide, where the carboxy-species remained bound to the column whilst the desired product was eluted using dichloromethane, yielded the desired ligand **10** in good yield. The *p*-methoxy substituted analogue (bpy-φ-OMe) had been prepared previously within the group in a similar manner from anisaldehyde.
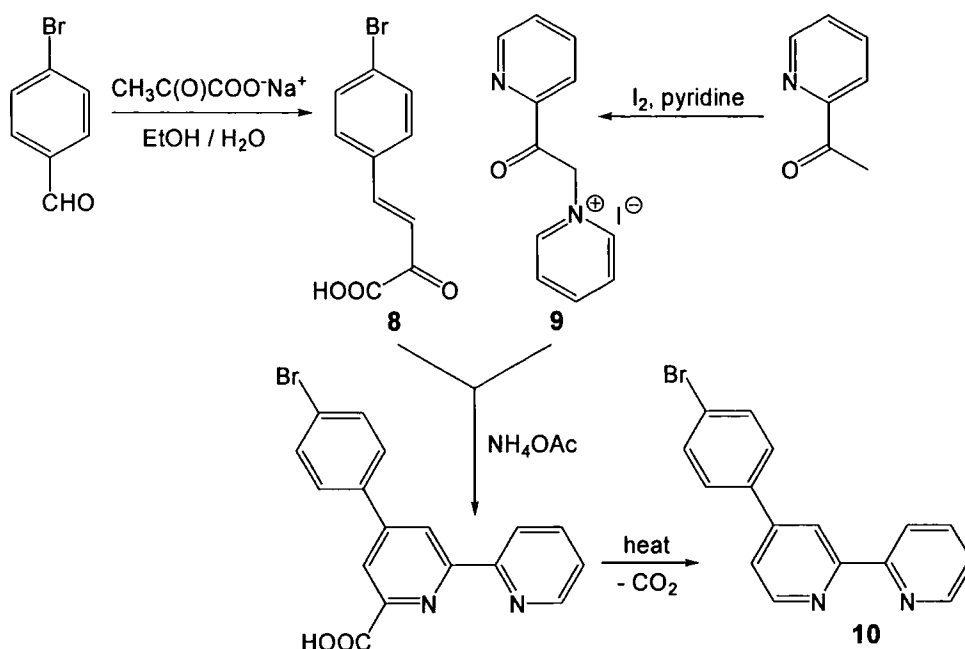
Figure 51 Synthesis of 4-(4-bromophenyl)-2,2'-bipyridine via Hantzsch condensation

A similar Hantzsh type synthesis (Figure 52) was attempted for the generation of the pyridyl-substituted ligand, 4-(4-pyridyl)-2,2'-bipyridine (bpy-py) **11**. This synthesis requires that the pyridinium iodide described above is reacted with a pyridyl-substituted enone. However, upon employing the same conditions and procedures as previously described for the synthesis of this enone, no product was precipitated. This is probably due to the presence of both acidic and basic functionalities in the molecule with similar pK$_a$ values. It is likely that precipitation would have only occurred over a narrow pH range where only one of these two functionalities was protonated; any other conditions will lead to a cationic or anionic species of higher water solubility. The reaction with 1-(2-oxo-2-pyridin-2-yl-ethyl)-pyridinium iodide was attempted without prior isolation of the enone but no further tractable product could be obtained. Furthermore, the addition of Mohr's salt (ammonium iron(II) sulfate) to this reaction mixture did not produce a positive test for a bipyridyl species.
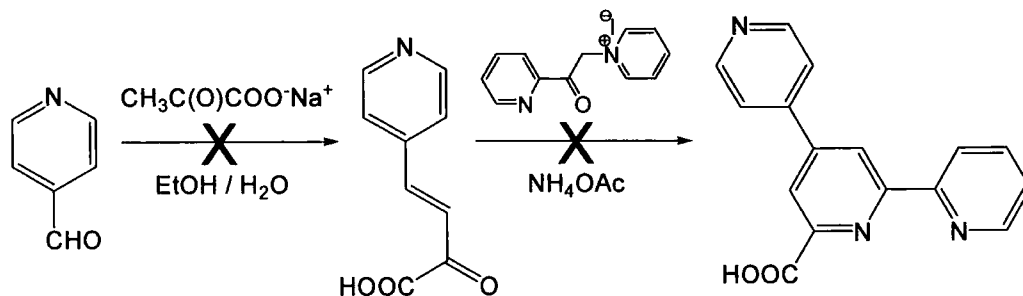
Figure 52 Failed synthesis of 4-(4-pyridyl)-2,2'-bipyridine via Hantzsch type synthesis

2.1.1.2.3 Suzuki cross-coupling reaction

The use of the Suzuki cross-coupling reaction for the synthesis of bpy-py **11** was investigated (Figure 53). Previous work within our group has reported the use of this reaction for the synthesis of a series of 4'-aryl substituted 2,2':6',2"-terpyridine ligands. In particular, the writer demonstrated during an MChem project (2001-02) that pyridyl-phenyl groups could be introduced into terpyridines in this way.[135] The reaction of 4-bromo-2,2'-bipyridine **7** with pyridine boronic acid in degassed DME solvent in the presence of an aqueous sodium carbonate base and Pd(PPh₃)₄ catalyst gave rise to **11** in 39% yield after purification via column chromatography. Additional amounts of boronic acid and catalyst were added after 24 hours to ensure that the reaction proceeded to completion.

7: n=0
10: n=1

11: n=0
12: n=1
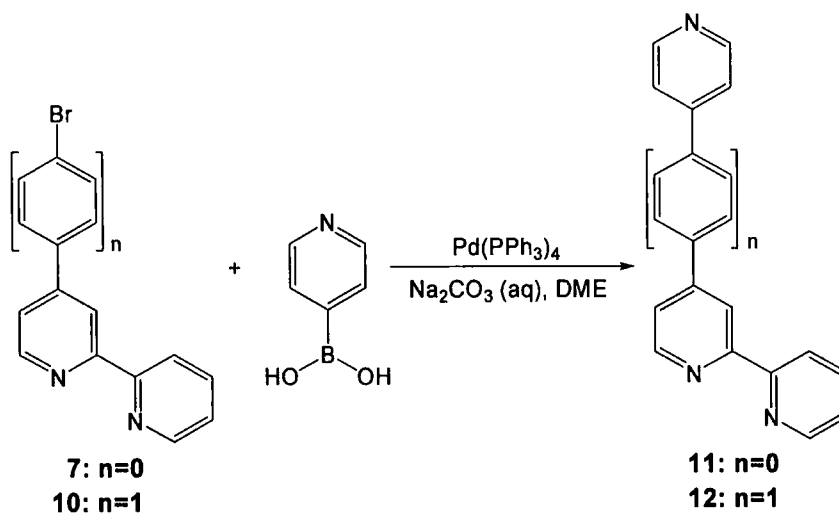
Figure 53 Successful synthesis of 4-(4-pyridyl)-2,2'-bipyridine and

4-(4-(4-pyridyl)phenyl)-2,2'-bipyridine via the Suzuki reaction

The previously unreported ligand 4-(4-(4-pyridyl)phenyl)-2,2'-bipyridine (bpy-ϕ-py) **12** was prepared in a similar manner via the cross coupling of 4-(4-bromophenyl)-2,2'-bipyridine **10** with pyridine boronic acid (Figure 53). Recrystallisation from ethanol produced crystals suitable for characterisation via X-ray

diffraction (Figure 54 and Appendix I). The structure reveals that the ligand is not planar, with the intermediate phenyl ring being displaced by 34.6° from the plane of the bipyridine rings, a value which is intermediate between those reported for 4-(3-hydroxyphenyl)-2,2′-bipyridine[27] (41.5°) and 1,4-bis(2,2′-bipyrid-4-yl)benzene[185] (24.3°).
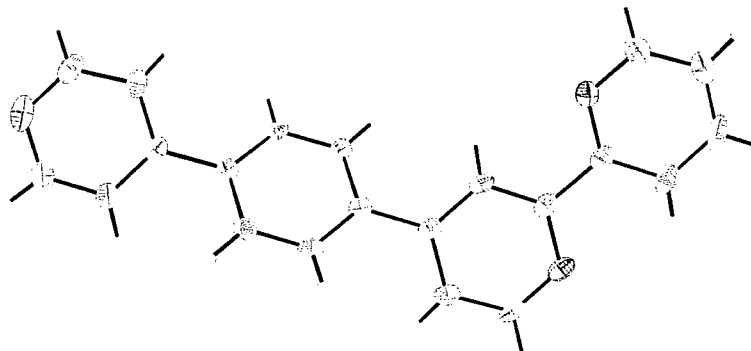
Figure 54 Crystal structure of bpy-φ-py 12, T = 120K with anisotropic displacement parameters shown at the 50% probability level.

2.1.1.2.4 Miyaura cross-coupling reaction for boronic acid substituted ligands

One of the initial aims of the work presented in this thesis was to investigate the use of the Suzuki cross coupling reaction for the generation of multimetallic systems. In order to achieve this in a controlled and direct manner it is necessary to have access to boronic acid appended complexes. The first step towards this goal is the generation of a boronic acid substituted ligand.
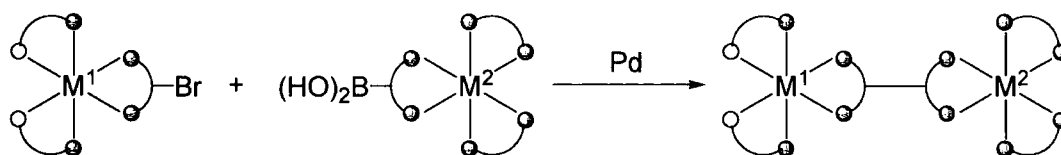
Figure 55 General scheme for the synthesis of multimetallic systems using the Suzuki cross-coupling reaction, highlighting the requirement for boronic acid substituted complexes

The conventional route to arylboronic acids involves the reaction of an aryllithium compound with trimethylborate to generate the dimethylester of the boronic acid, which readily hydrolyses to the acid during work up. During the course of the work described in this thesis, this route was reported for the synthesis of 4-(4-phenylboronic acid)-2,2′-bipyridine (bpy-φ-B(OH)₂) **13** but only in 20% yield.[186] We had chosen instead to employ a cross-coupling reaction for the introduction of the boronic acid group, owing to unsatisfactory results when conventional chemistry was applied to bromo-substituted terpyridine systems.[141]

The Miyaura reaction[140] synthesises arylboronates via a palladium catalysed cross-coupling reaction between an aryl halide and a diboron species such as bis(pinacolato)diboron (B_2pin_2) or bis(neopentylglycolato)diboron (B_2neo_2) (Figure 56). $Pd(dppf)Cl_2$ was found to be one of the most efficient catalysts for this conversion, in conjunction with a weak base such as potassium acetate. Reactions with either one of the aforementioned diboron species has successfully produced the appropriate boronic ester substituted terpyridine ligand, with the neopentylglycolato analogue being found to hydrolyse to the acid more readily.[141]

(a)   (b)
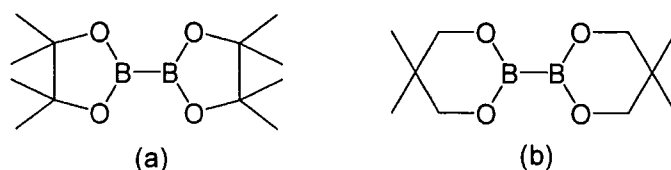
Figure 56 Diboron compounds for use in the Miyaura cross-coupling reaction:

(a) bis(pinacolato)diboron (B_2pin_2), (b) bis(neopentylglycolato)diboron (B_2neo_2)

This procedure was used here for the synthesis of 4-(4-neopentyl glycolatoboron-phenyl)-2,2'-bipyridine (bpy-φ-Bneo) **14**. The reaction was achieved by applying the same conditions as reported for the terpyridine example to couple 4-(4-bromophenyl)-2,2'-bipyridine **10** with B_2neo_2 (Figure 57). The crude product was usually found to be contaminated with triphenylphosphine oxide and B_2neo_2. Attempts to purify by extracting the desired product into aqueous basic solution followed by subsequent acidification to reprecipitate the product were unsuccessful in producing any appreciable amount of either boronic ester or acid substituted ligand. Instead, dissolution in ethanol at reflux followed by hot filtration was used to significantly reduce the amount of B_2neo_2 present, and the product was used for subsequent complexation to metals without further purification.

10   14
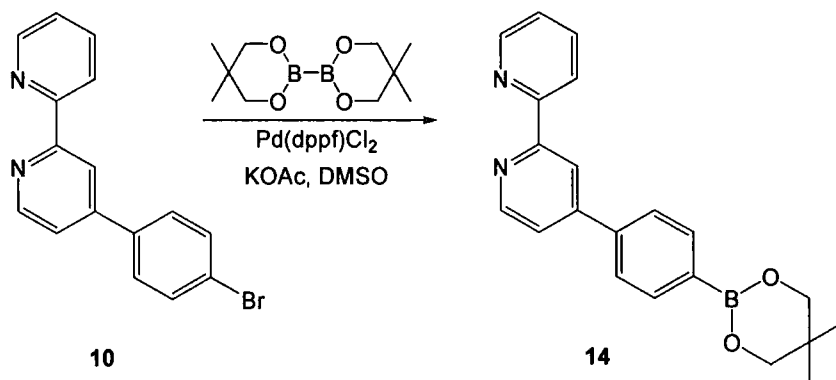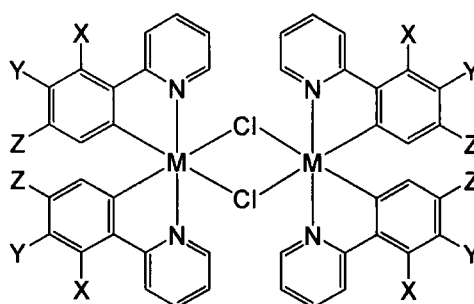
Figure 57 Synthesis of 4-(4-neopentyl glycolatoboron-phenyl)-2,2'-bipyridine via the Miyaura cross-coupling reaction

2.1.2 Synthesis of dichloro-bridged dimers [M(C^N)₂Cl]₂

Dichloro-bridged dimers containing the cyclometalating ligands ppyH, 4-(2-pyridyl)benzaldehyde (pbaH), ppyH-F **1H**, ppyH-F₂ **2H** and ppyH-F₃ **3H** were synthesised.

The syntheses of [Ir(ppy)₂Cl]₂ **15**[69], [Ir(pba)₂Cl]₂ **16**[94], [Ir(ppy-F₂)₂Cl]₂ **17** (during the course of this work)[187] and [Rh(ppy)₂Cl]₂ **18**[70] have been reported in the literature, with all (except **18**) being based upon the original synthesis by Nonoyama[188] using a 3:1 mixture of 2-ethoxyethanol and water as the solvent. These conditions were employed, with the exception that where the use of a large excess of cyclometalating ligand had been reported (4 equivalents[69,94]) only 2 - 2.2 equivalents were used in order to avoid the production of any unwanted tris-product. [Rh(pba)₂Cl]₂ **19**[95] has also been reported previously but using a 3:1 mixture of ethanol and water. The synthesis of this dimer was successfully achieved in similar yields by using either 2-ethoxyethanol or ethanol with water, although repetition of the reaction using 2-ethoxyethanol proved unsuccessful.

The 2-ethoxyethanol/water procedure was also used for the synthesis of the previously unreported dichlorobridged dimers [Ir(ppy-F)₂Cl]₂ **20**, [Rh(ppy-F)₂Cl]₂ **21**, [Rh(ppy-F₂)₂Cl]₂ **22** and [Ir(ppy-F₃)₂Cl]₂ **23**. The yields obtained are summarised in Figure 58.

No.	M	X	Y	Z	Yield
15	Ir	H	H	H	62%
16	Ir	H	H	CHO	82%
17	Ir	F	H	F	75%
18	Rh	H	H	H	88%
19	Rh	H	H	CHO	76%
20	Ir	H	H	F	62%
21	Rh	H	H	F	84%
22	Rh	F	H	F	88%
23	Ir	F	F	F	76%

Figure 58 Yields obtained for the synthesis of dichloro-bridged dimers

Crystallographic data has been published for both iridium[77] and rhodium[95] containing dichloro-bridged dimers of this type. In both cases, the metal-carbon bonds show a mutual *cis* orientation around both metal centres. This is attributed to the strong *trans* influence of the metal-carbon bonds and is generally accepted to be the case for all

50

systems of this sort.

2.1.3 Reaction of [M(C^N)₂Cl]₂ species with 2,2'-bipyridine ligands

2.1.3.1 Synthetic conditions and purification procedures

In order to generate monometallic species, the dichloro-bridged dimers mentioned above can be reacted with two equivalents of a 2,2'-bipyridine ligand, as first reported by Nonoyama[76]. The original synthesis of [Rh(bhq)₂(bpy)]Cl, where bhq = benzo-[h]-quinoline, involved the reaction of [Rh(bhq)₂Cl]₂ with one equivalent of 2,2'-bipyridine in ethanol at elevated temperature. Since this report, a variety of conditions have been investigated in order to generate similar rhodium and iridium complexes. Work carried out by Neve *et al* describes the high yielding synthesis of [Ir(ppy)₂(bpy-X)]⁺ species via the reaction of the dichloro-bridged dimer and appropriate bpy ligand in a 1:2 ratio in a refluxing dichloromethane-methanol (4:5) solvent mixture.[78] These relatively mild conditions have been adopted for the syntheses presented here. The [M(ppy-X)₂(bpy-Y)]⁺ type complexes prepared are summarised in Table 3 with the basic structure for this type of complex being displayed in Figure 47.

In order to successfully isolate the hexafluorophosphate salt of these complexes, ion exchange was carried out by the addition of the complex dissolved in the minimum volume of acetonitrile to a saturated aqueous solution of potassium hexafluorophosphate. Column chromatography using dichloromethane and methanol eluant (up to 5% methanol) was used for the purification of the complexes.

Table 3 shows that the reaction of any of the dichloro-bridged dimers with unsubstituted 2,2'-bipyridine proceeds in excellent yields ranging from 73% - 93% yield. Of this series, only complexes **24, 25** and **26** have been reported previously.[5,95] The reactions also proceed relatively cleanly, with three of the rhodium examples, **25, 28** and **30**, requiring no further purification after ion exchange according to both mass spectrometry and elemental analysis. It is worth noting, however, that reactions involving [Rh(pba)₂Cl]₂ **19** proceeded more successfully in cases when the dimer was first purified via filtration through celite in dichloromethane as reported by Lo.[95] Reactions of the dichloro-bridged dimers with bromo-substituted bipyridines also proceed in good yields and, as these complexes were primarily prepared to provide building blocks for larger assemblies, in most cases further purification was not considered necessary.

No.	Metal	C^N Ligand	N^N Ligand	% Yield
24	Ir	ppy	bpy	93%
25	Rh	ppy	bpy	93%
26	Rh	bpa	bpy	92%
27	Ir	ppy-F 1	bpy	92%
28	Rh	ppy-F 1	bpy	93%
29	Ir	ppy-F_2 2	bpy	73%
30	Rh	ppy-F_2 2	bpy	94%
31	Ir	ppy-F_3 3	bpy	81%
32	Ir	ppy	bpy-Br 7	98%
33	Ir	pba	bpy-Br 7	*
34	Rh	pba	bpy-Br 7	94%
35	Ir	ppy-F 1	bpy-Br 7	97%
36	Ir	ppy-F_2 2	bpy-Br 7	78%
37	Ir	ppy	bpy-φ-Br 10	69%
38	Ir	pba	bpy-φ-Br 10	*
39	Rh	pba	bpy-φ-Br 10	74%
40	Ir	ppy	bpy-φ-OMe	58%
41	Ir	pba	bpy-φ-OMe	31%
42	Ir	ppy	bpy-py 11	22%
43	Ir	pba	bpy-py 11	19%
44	Ir	ppy	bpy-φ-py 12	21%

Table 3 Summary of [M(ppy-X)2(bpy-Y)]+ type complexes prepared.

* These complexes were used without further purification.

Previously unreported methoxy- and pyridyl-substituted iridium complexes **40 - 44** were prepared from [Ir(ppy)$_2$Cl]$_2$ or [Ir(pba)$_2$Cl]$_2$, albeit in lower yields than those obtained when using bromo- or unsubstituted bpy ligands. In particular, those complexes containing both aldehyde and pendent pyridyl functionalities proved difficult to purify. Multiple attempts at column chromatography were necessary to prepare a pure sample of complex **43**, whilst purification of the analogue containing the bpy-φ-py ligand **12** was not achieved despite initial indications from electrospray mass spectrometry that the desired complex had at least partly formed. It is worth remembering that both the bipyridyl group and the pendent pyridyl groups of ligands **11** and **12** are capable of coordinating to transition metals. Whilst it is expected that bidentate binding should be favoured thermodynamically, it is possible that a kinetic

product could involve binding of the single pyridyl group thus giving rise to a mixture of products. As discussed in the introduction, this phenomenon has been seen in the literature[6] when mild reaction conditions are used for the synthesis of ruthenium complexes containing a pyridyl-substituted bipyridine ligand.

2.1.3.2 Characterisation and confirmation of purity

All of the complexes included in Table 3 have been characterised via a combination of ^{1}H NMR, ^{19}F NMR (where appropriate), electrospray mass spectrometry, elemental analysis and thin layer chromatography. Full assignment of the ^{1}H NMR spectra was achieved using ^{1}H-^{1}H COSY and NOESY two-dimensional spectra. Assignment is also assisted by the characteristic low frequency peak at between 5.8 ppm and 6.9 ppm (in either d[6]-acetone or CD$_3$CN) corresponding to the proton adjacent to the site of cyclometalation (ppy-H$^{6'}$) which experiences the largest shielding effect out of all of the protons (see Figure 59 for the H atom numbering scheme used). Additionally, the peaks with the highest shifts, usually between 8.5 ppm and 9.5 ppm (again in either d[6]-acetone or CD$_3$CN) tend to correspond to bpy-H^3 and bpy-H$^{3'}$, unless an aldehyde is present, in which case the CHO proton is responsible for the peak with the highest shift.
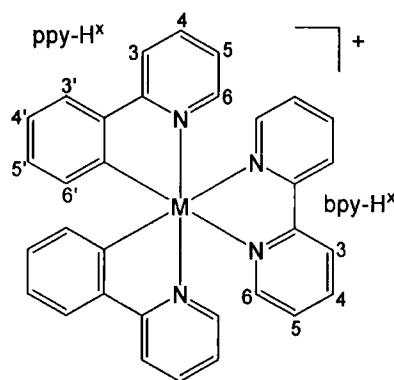
Figure 59 H atom numbering scheme used in assignment of NMR data

However, assignment of splitting patterns and coupling constants for the ^{1}H NMR is somewhat complicated by the presence of inequivalent ppy ligands in complexes containing unsymmetrically substituted bipyridine ligands. This is exemplified by comparing the NMR spectra of the unsubstituted complex **24** with the spectra for complex **37**, which contains an unsymmetrical bpy-ϕ-Br ligand.

For complex **24**, a doublet can be seen at 6.35 ppm corresponding to ppy-H$^{6'}$. This splitting pattern is as expected due to vicinal coupling with ppy-H$^{5'}$. However, the same peak in the spectrum for complex **37** appears as two overlapping doublets,

indicating that the two ppy ligands contained in this complex are inequivalent due to the unsymmetrical nature of the neighbouring bipyridine ligand. In some cases, as for this example peak, it is possible to resolve the splitting patterns to some extent, but in other cases, where splitting patterns are more complicated (see the region 6.8 ppm – 7.2 ppm of the spectra below as an example) multiplets are assigned to single proton environments. For simplification, protons belonging to the ppy ligands are assigned as if equivalent; a realistic approach when considering the minimal difference observed only in the fine structure of some of the resonances measured at 500 MHz.
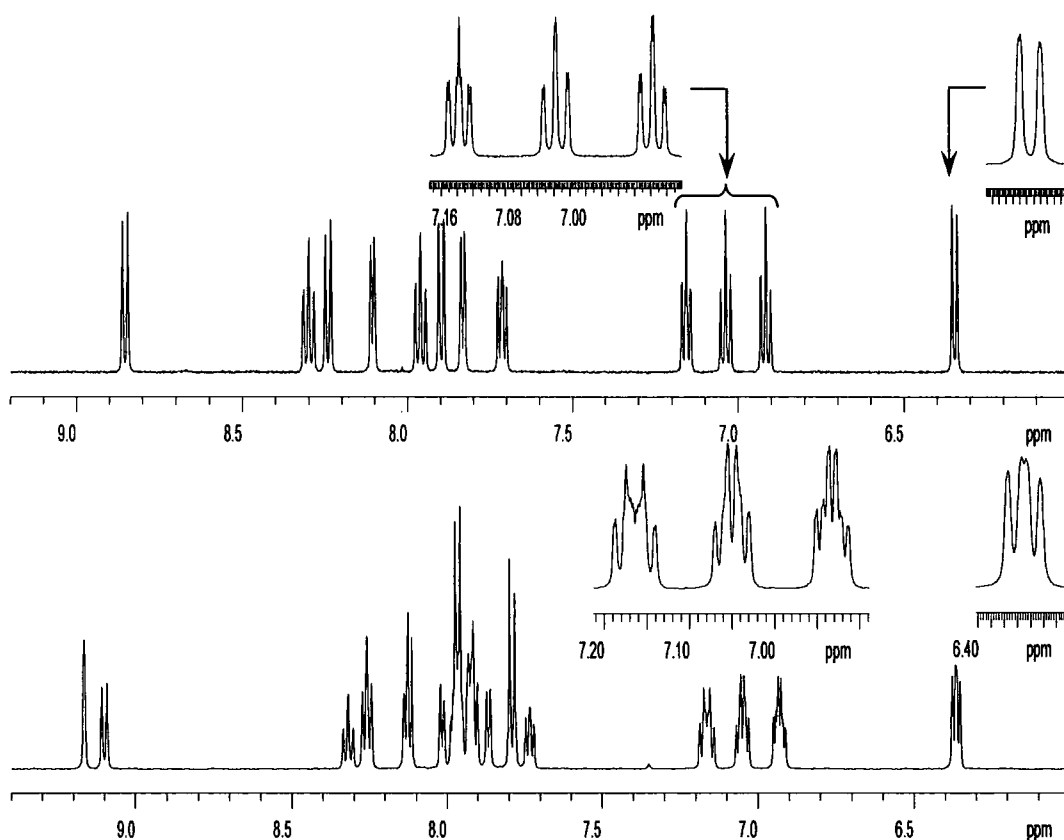
Figure 60 ^{1}H NMR spectra for [Ir(ppy)$_2$(bpy)]$^+$ 24 (upper) and [Ir(ppy)$_2$(bpy-ϕ-Br)]$^+$ 37 (lower) measured at 500 MHz.

2.1.3.3 Isomers

As previously discussed, the ppy ligands contained within dichloro-bridged dimers adopt a conformation where the two carbon-metal bonds are arranged in a *cis* fashion. This is retained upon the reaction with a 2,2'-bipyridine ligand, giving rise to complexes with *cisoid* metal-carbon bonds alongside a *trans* arrangement of the nitrogen donors of the ppy ligands. Strictly, this leads to a mixture of diastereomers when an unsymmetrical bpy is used, but this is not considered to have any appreciable influence on the photophysical properties of such complexes.[189]

2.2 Chemistry on the complex

Whilst the synthetic route involving dichloro-bridged dimers and bipyridine ligands has allowed the preparation of a series of monometallic iridium and rhodium complexes, complications arise when using ligands with more than one potential binding site. This can lead to a mixture of products and also render purification a long and tedious process which may eventually yield only a small amount of desired product. A potential way of avoiding this is to create straightforward complexes which, as seen in the previous section, can be produced in good yields, and then to carry out chemistry on the ligands *in situ*. In this way, further functionality can be introduced which might otherwise have affected the reliability of the complexation step. Additionally, time and effort are saved in a divergent strategy in which a simple functional group conversion can be carried out cleanly on a complex, rather than having to synthesise new starting materials in order to generate a new ligand which must then be reliably complexed to a metal.

2.2.1 Conversion of methoxy to hydroxyl *in situ*

Ward *et al* report the interconversion of a methoxy group into a hydroxyl group by performing chemistry on the back of a 2,2'-bipyridine ligand whilst it is complexed to a ruthenium metal centre.[6] Based upon this preparation, the generation of the hydroxy-substituted iridium complex [Ir(ppy)₂(bpy-φ-OH)][PF₆] **45** was achieved (Figure 61) via reaction of methoxy-substituted complex **40** with an excess of BBr₃ under an inert atmosphere in dichloromethane at room temperature. This provides a quick, easy and high yielding synthesis of **45** and removes any complications that could arise due to the monodentate binding of the phenol group to the metal centre – a problem that may otherwise occur if the hydroxyl group had been present in the uncomplexed ligand.
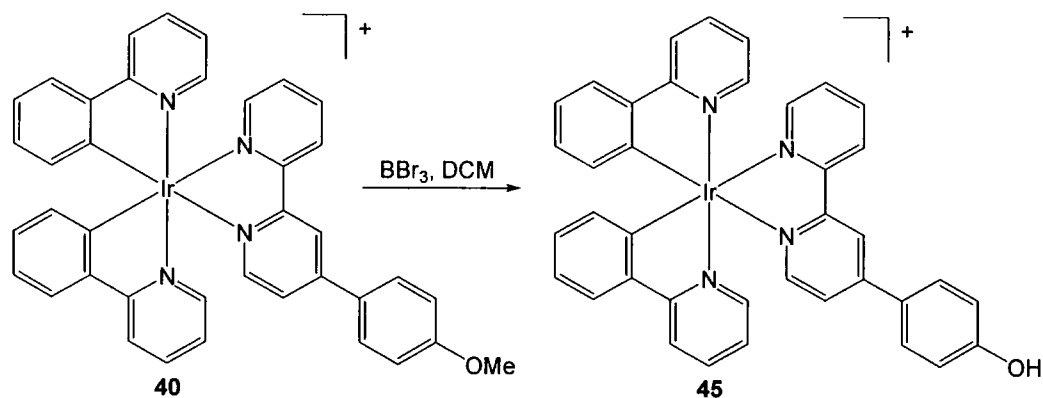
Figure 61 Conversion of -OMe to -OH whilst ligand is bound to iridium

However, this reaction was unsuccessful when attempted for the methoxy-substituted iridium complex containing pba ligands **41**, with no sign of the desired hydroxy-substituted product being formed. A reduced integral for the ^{1}H NMR peak associated with the CHO proton suggests that the boron species may coordinate to the aldehyde group, making it susceptible to nucleophilic attack rather than bringing about the desired demethylation at the methoxy site.

2.2.2 *In situ* bromination of monometallic complexes

Work by Coudret *et al*[177] reports a procedure for the regiospecific halogenation of the ruthenium complex [Ru(bpy)$_2$(ppy)][PF$_6$] upon treatment with N-bromosuccinimide in acetonitrile at room temperature (Figure 62). Bromination occurs exclusively at the position on the ppy ligand *para* to the position of cyclometalation to ruthenium. It was concluded therefore that the carbon-ruthenium bond not only activates the metalated ring towards electrophilic substitution but also controls its regioselectivity.
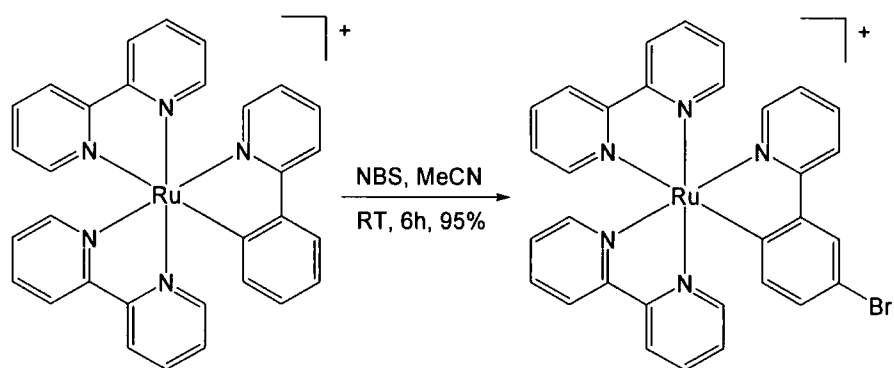
Figure 62 Regioselective bromination of ppy ring using NBS

We reasoned that a carbon-iridium bond should have similar activating properties to a carbon-ruthenium bond, and hence that treatment of [Ir(ppy)$_2$(bpy)]$^+$ **24** with *two* equivalents of NBS should lead to a regiospecifically dibrominated complex **46**. In

56

practice this proved successful, with the reaction proceeding at room temperature, although an excess of NBS was required (Figure 63). This provides a reliable *in situ* route to species that can be used in subsequent Suzuki reactions for either the elaboration of a simple ligand or the synthesis of multimetallic systems.
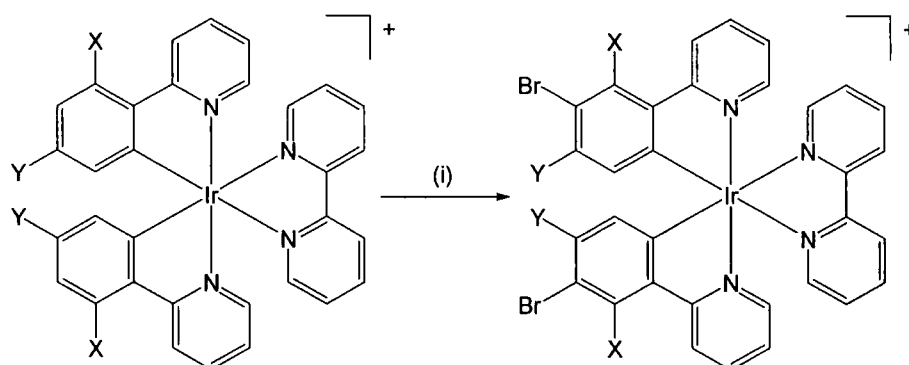
For X = H and Y = H, (i) = NBS, MeCN, 20°C, 36h to give complex **46** in 86% yield.

For X = H and Y = F, (i) = NBS, MeCN, 50°C, 5 days to give complex **47** in 84% yield.

For X = F and Y = F, no successful reaction conditions were found.

Figure 63 Bromination of iridium complexes using N-bromosuccinimide

The possibility of brominating only one of the ppy ligands was investigated as this could be a powerful intermediate, allowing access to unsymmetrically substituted monometallic complexes. This seemed unlikely as bromination at one ppy ligand should not have any great effect on an electrophilic substitution reaction at another ppy ligand contained within the same complex. Indeed this was found to be the case and, upon the addition of only one equivalent of NBS to **24**, electrospray mass spectrometry implied that the product contained a statistical mixture of non-brominated, singly brominated and doubly brominated products.

Dibromination was also attempted for the fluorinated iridium complexes **27** and **29**, but no bromination took place at room temperature, with 100% starting material being recovered in both cases. Upon heating to 50°C, complex **27**, containing two singly fluorinated ppy ligands, was found to brominate selectively at the expected position to give complex **47**. A single pure product was obtained after 5 days, with an additional equivalent of NBS being added to the reaction after 4 days (Figure 63). Unfortunately, even at this elevated temperature, bromination between the two fluorine atoms in complex **29** did not prove possible. This could be due to electronic effects imposed by the two fluorine atoms affecting the electrophilic substitution reaction. It is possible that the inductive electron withdrawing effect of the two fluorine atoms is sufficient to counterbalance any increased electron density arising from cyclometalation.

2.2.3 Metal catalysed cross-couplings for elaborating ligands *in situ*

An alternative and recent approach, which avoids the pre-synthesis of complicated ligands, has made use of metal catalysed cross-coupling reactions for the elaboration of ligands *in situ*. In particular, the mild conditions employed and functional group tolerance observed make the Sonogashira and Suzuki-Miyaura palladium catalysed cross-coupling reactions attractive for this purpose.

As discussed in the introduction, metal complexes containing appropriately functionalised ligands can be elaborated *in situ* by coupling with either acetylene compounds in the Sonogashira reaction,[136,137] or with haloaromatics or arylboronic acids in the Suzuki reaction.[141,142] In particular, iridium complexes containing bromo-substituted 2,2':6',2"-terpyridines can be coupled with arylboronic acids (Figure 64) by employing conditions similar to those used for 'organic' type reactions; Pd(PPh₃)₄ catalyst, aqueous sodium carbonate base but with DMSO solvent in order to solubilise the complex.[142]
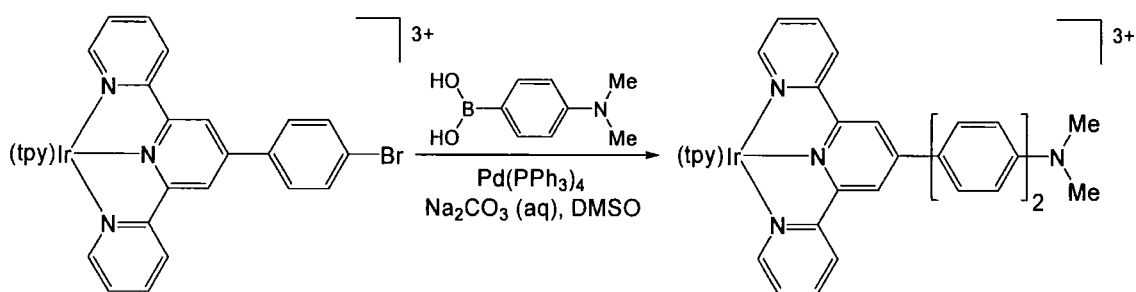
Figure 64 Suzuki cross-coupling for elaboration of ligands *in situ*

The work presented here investigates the use of the Suzuki cross-coupling reaction for the *in situ* elaboration of ligands contained within [M(C^N)₂(N^N)]⁺ type complexes. There are no literature reports of such cross-coupling reactions having been attempted on this type of system.

2.2.3.1 Suzuki couplings for elaboration in situ

A series of successful *in situ* Suzuki cross-coupling reactions were carried out between a number of [M(C^N)₂(N^N)]⁺ type complexes, containing either bpy-Br **7** or bpy-ϕ-Br **10** as the N^N coordinating ligand, and either benzeneboronic acid or dimethylaminophenyl-4-boronic acid. The conditions reported for similar terpyridine systems were adopted, namely Pd(PPh₃)₄ catalyst and aqueous sodium carbonate base in degassed DMSO solvent.[142] The resulting complexes are listed in Table 4.

No.	Metal	C^N ligand	N^N starting ligand	N^N product ligand	% Yield
48	Ir	ppy	bpy-Br 7	bpy-φ-NMe$_2$	*
49	Ir	ppy	bpy-φ-Br 10	bpy-φ-φ-NMe$_2$	*
50	Ir	pba	bpy-Br 7	bpy-φ-NMe$_2$	50%
51	Ir	pba	bpy-φ-Br 10	bpy-φ-φ-NMe$_2$	28%
52	Ir	ppy	bpy-Br 7	bpy-ph	80%
53	Ir	ppy-F 1	bpy-Br 7	bpy-ph	78%
54	Ir	ppy-F$_2$ 2	bpy-Br 7	bpy-ph	72%
55	Rh	pba	bpy-Br 7	bpy-ph	84%

Table 4 Summary of complexes synthesised via *in situ* elaboration using the Suzuki reaction bpy-φ-NMe$_2$ = 4-(4-dimethylaminophenyl)-2,2′-bipyridine, bpy-φ-φ-NMe$_2$ = 4-(4-(4-dimethylaminophenyl)phenyl)-2,2′-bipyridine and bpy-ph = 4-phenyl-2,2′-bipyridine. * these complexes were initially prepared by Paul Atkinson during an MChem project (2002) but purification and photophysical study were carried out as part of this work.

Dimethylamino-appended iridium complexes **48 – 51** were successfully synthesised via the cross-coupling of iridium complexes containing either bpy-Br **7** or bpy-φ-Br **10** and dimethylaminophenyl-4-boronic acid (Figure 65).

48: X = H, n = 0, 49: X = H, n = 1
50: X = CHO, n = 0, 51: X = CHO, n = 1

Figure 65 Synthesis of dimethylamino-substituted complexes using the Suzuki reaction

Attempts to synthesise the pyridyl-substituted complex [Ir(pba)$_2$(bpy-φ-py)]$^+$ in a similar manner failed to produce the desired complex. Previous work on organic-based Suzuki reactions[135] involving pyridine-4-boronic acid have required that additional boronic acid be added partway through the reaction in order to reach completion, suggesting that thermal decomposition of the boronic acid may be occurring under the Suzuki reaction conditions. The thermal stability, or lack thereof, of pyridine boronic acids has been mentioned in the literature,[190] and whilst pyridine-4-

boronic acid is reportedly more stable than pyridine-2-boronic acid, it is still possible that decomposition is occurring under the reaction conditions used here.

Complexes **52** – **55**, which contain phenyl-substituted bipyridine ligands, were synthesised via the cross-coupling reaction of the appropriate iridium or rhodium complexes containing bpy-Br with phenylboronic acid. In all of these cases excellent yields were obtained (72% - 80%) and purification was achieved via column chromatography. The use of a rhodium parent complex provides reassurance that this chemistry is not restricted to iridium systems.

In addition to the complexes described in Table 4, a Suzuki reaction was carried out between iridium complex **46**, which contains two brominated ppy ligands and benzeneboronic acid in order to generate complex **56** (Figure 66). This synthesis shows that successful *in situ* Suzuki cross-coupling reactions are not confined to starting materials with the bromo-substituent appended to the bpy ligand and that two Suzuki couplings can be carried out simultaneously and still produce an excellent yield (84%) of desired product.

46   **56**
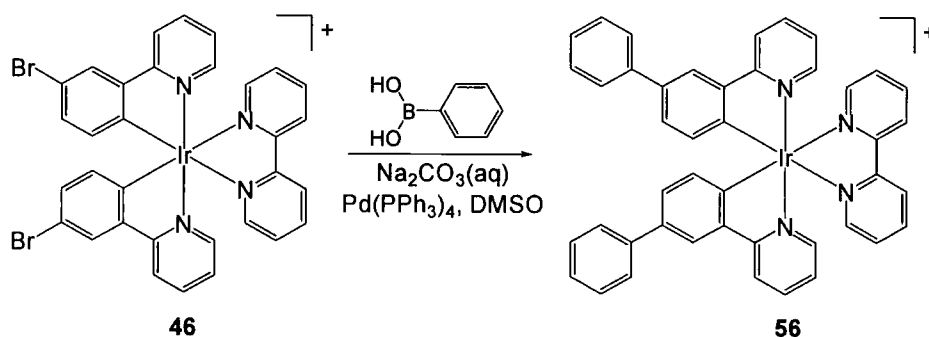
Figure 66 Simultaneous *in situ* Suzuki reactions for elaborating ligands

2.3 Boronic acid substituted iridium and ruthenium complexes

So far, this work has demonstrated how the Suzuki reaction can be used successfully to cross-couple complexes containing bromo-substituted ligands with aryl boronic acids. In principle, this procedure could be extended to allow the synthesis of multimetallic species, but, as mentioned in section 2.1.1.2.4, in order to do so in a controlled single step reaction, a boronic acid appended complex would be required (Figure 55). At the outset of this work, there were no reported examples of second or third row transition metal complexes containing boronic acid substituted bipyridyl ligands.

2.3.1 *Synthesis of boronic acid appended complexes*

The first boronic acid substituted metal complex to be investigated here was [Ru(bpy)$_2$(bpy-ϕ-B(OH)$_2$)]$^{2+}$ **57**. In order to prevent deboronation of the ligand, a mild synthesis was required. The chosen synthesis (Figure 67) was based on a preparation reported by Meyer *et al*[191], which produces a [Ru(bpy)$_2$(CH$_3$C(O)CH$_3$)]$^{2+}$ intermediate via the reaction of Ru(bpy)$_2$Cl$_2$ in acetone in the presence of a silver salt. By adopting the more mild conditions subsequently reported by Hammarström *et al*[192], the boronate substituted ligand **14** was successfully bound to the ruthenium centre without raising the temperature of the reaction mixture above room temperature. The small amount of complex containing the deboronated ligand produced was separated from the desired complex via column chromatography, yielding complex **57** in 55% yield and allowing the isolation of side-product [Ru(bpy)$_2$(4-phenyl-2,2'-bipyridine)][PF$_6$]$_2$ **58**. By this stage any boronic ester that may have been present had been hydrolysed completely to the acid.
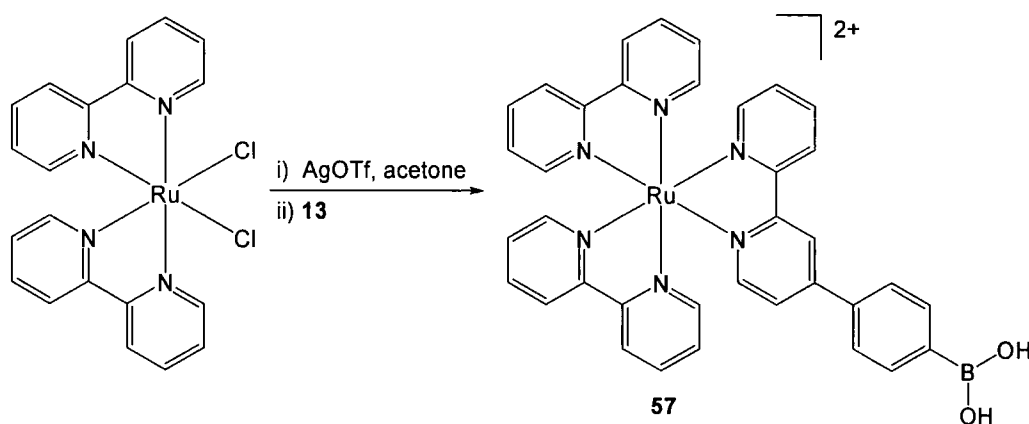
Figure 67 Synthesis of boronic acid appended ruthenium complex 57

The stability of complex **57** is not completely understood. Occasionally, some degree of decomposition appeared to occur overnight, whilst in other instances the complex was stored for a number of weeks without any problem. Whilst electrospray mass spectrometry suggested that the decomposition product could be deboronated complex **58**, it is worth noting that deboronation of complex **57** may well occur under the conditions present in the mass spectrometer itself. Indeed, it proved quite difficult to obtain mass spectra for samples which had been otherwise proved to contain purely the boronic acid complex **57**. In an effort to overcome decomposition problems, subsequent reactions were carried out promptly after the purification of complex **57**.

The synthesis of a series of boronic acid substituted cyclometalated iridium and rhodium complexes was achieved via treatment of the appropriate [M(C^N)$_2$Cl]$_2$ dimer

61

with the boronate substituted ligand. The resulting complexes are summarised in Table 5. Purification attempts via column chromatography using DCM/methanol eluant were unsuccessful in providing a pure sample, perhaps due to encouraged deboronation by the presence of methanol. Whilst some degree of purification was achieved by using an eluant of acetonitrile, water and saturated aqueous KNO_3, this additional step was usually omitted and complexes **59 – 62** used in subsequent reactions without any further purification. Where a mixture of boronate and boronic acid substituted complexes were evident from the ^1H NMR spectrum, integrals were used to estimate the ratio of the two products and this was taken into consideration when calculating masses.

No.	Metal	C^N ligand
59	Ir	ppy
60	Ir	ppy-F **1**
61	Ir	ppy-F$_2$ **2**
62	Rh	pba
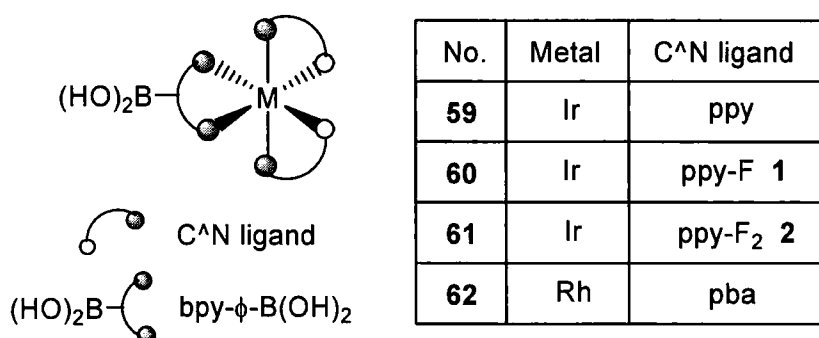
Table 5 Boronic acid substituted iridium and rhodium complexes prepared

2.4 Complexes containing 2,2':6',2"-terpyridine ligands

The synthesis mentioned so far has involved the use of the bidentate ligands 2,2'-bipyridine and 2-phenylpyridine. Iridium and ruthenium complexes containing 2,2':6',2"-terpyridine (tpy) ligands have also been reported in the literature to display interesting photophysical properties.[4,193] The synthesis of such complexes generally employs more harsh reaction conditions than those seen in previous sections.

As the focus was again to produce building blocks which could potentially be used in a Suzuki cross-coupling reaction to generate multimetallic arrays, bromo-substituted ruthenium and iridium terpyridine complexes were produced. It was hoped that this would allow access to multimetallic systems incorporating not only bidentate ligands but also 2,2':6',2"-terpyridine as a terdentate ligand.

Intermediate species Ir(tpy)Cl$_3$ **63** and Ru(tpy)Cl$_3$ **64** were synthesised according to established literature procedures,[194,195] with the iridium analogue requiring more harsh reaction conditions. The 4'-(4-bromophenyl)-2,2':6',2"-terpyridine ligand was coordinated to the iridium precursor **63** at high temperature in refluxing ethylene glycol to produce [Ir(tpy)(4-(4-bromophenyl)-2,2':6',2"-terpyridine)][PF$_6$]$_3$ **65** as

described previously by our group.[142] The ruthenium example required less harsh conditions and made use of an acetone intermediate as described in Section 2.3.1, but involved heating to 80°C in ethanol for 3.5 hours for coordination of the bromo-substituted ligand to form [Ru(tpy)(4-(4-bromophenyl)-2,2':6',2''-terpyridine)][PF₆]₂ **66**.

M = Ir **63**, Ru **64**

M = Ir   (i)   tpy-φ-Br, ethylene glycol, 220°C,
                15 mins
M = Ru, (i)   AgOTf, acetone/ethanol
           (ii) tpy-φ-Br, ethanol, 80°C, 3.5 h

M = Ir **65**, Ru **66**
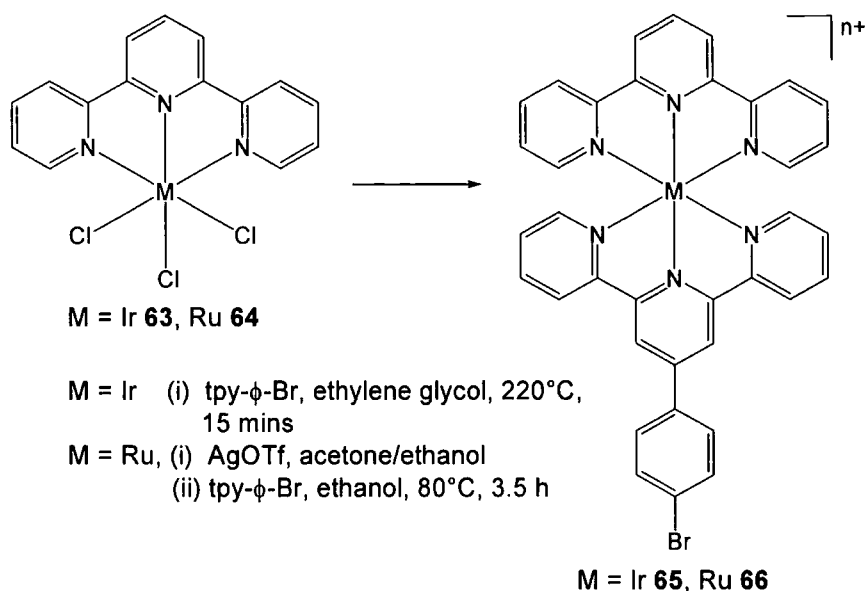
Figure 68 Synthesis of complexes containing 4'-bromophenyl-2,2':6',2''-terpyridine ligands

2.5 Concluding remarks

This chapter has discussed the synthesis of monometallic transition metal complexes of the type [M(C^N)₂(N^N)]⁺ from the appropriate [M(C^N)₂Cl]₂ dimers and N^N coordinating ligands, including, where necessary, the synthesis of the C^N and N^N coordinating ligands. The *in situ* elaboration of ligands once bound in this type of complex has been investigated, with the Suzuki cross-coupling reaction successfully introducing phenyl and dimethylaminophenyl substituents. Complexes containing bromo- and boronic acid substituents have been prepared in order to investigate the use of the Suzuki reaction for the generation of multimetallic arrays. Terdentate ligands bearing bromo-substituents have also been coordinated to transition metal centres to potentially allow access to mixed ligand higher order systems.

CHAPTER 3

PHOTOPHYSICAL AND COMPUTATIONAL STUDY OF MONOMETALLIC COMPLEXES

3 Photophysical and Computational Study of Monometallic Complexes

3.1 Photophysical properties of [Ir(C^N)₂(N^N)]⁺ complexes

3.1.1 Photophysics of [Ir(ppy)₂(bpy)]⁺

Previous photophysical studies on [Ir(ppy)₂(bpy)]⁺ have determined that the two lowest energy excited states arise from MLCT transitions, whilst electrochemical investigation indicates that the bpy ligand is more easily reduced than the ppy ligand. This suggests that the lowest of the two MLCT states involves charge transfer to the bpy ligand, whilst the ppy ligand is involved in a higher energy MLCT state. Dual emission has been reportedly observed from these two excited states during low temperature experiments, but at room temperature, emission from the bpy based state predominates.[5]

The photophysical properties of [Ir(ppy)₂(bpy)]⁺ were investigated under the conditions used for the other complexes as part of this work, to serve as a model. Results are summarised in Table 6 and the absorption and emission spectra are shown in Figure 69. The absorption spectrum observed here in acetonitrile matches closely the spectrum reported in methanol.[5] In line with this previous work, peaks at 256 nm and 265 nm are attributed to π-π* ligand centred transitions, whilst peaks between 300 nm and 470 nm correspond to MLCT transitions. The emission wavelength of 610 nm recorded in acetonitrile is also similar to the value reported for methanolic solutions (606 nm) and the lifetime measured in degassed acetonitrile matches that previously reported to within experimental error.[5]

Complex	[Ir(ppy)₂(bpy)]⁺ 24
Absorption Maxima /nm (Extinction Coefficient (ε) /M⁻¹ cm⁻¹)	465 (724) 405 (3710) 370 (6160) 334 (9210) 303 (22400) 265 (44100) 256 (45800)
Emission Maximum[a] /nm	610
Quantum Yield x 10² degassed (aerated)	9.7 (1.8)
Lifetime /ns degassed (aerated)	370 (66)

Table 6 Photophysical properties of [Ir(ppy)₂(bpy)][PF₆] 24 in CH₃CN at 298K. [a] λ_{ex} = 400 nm.
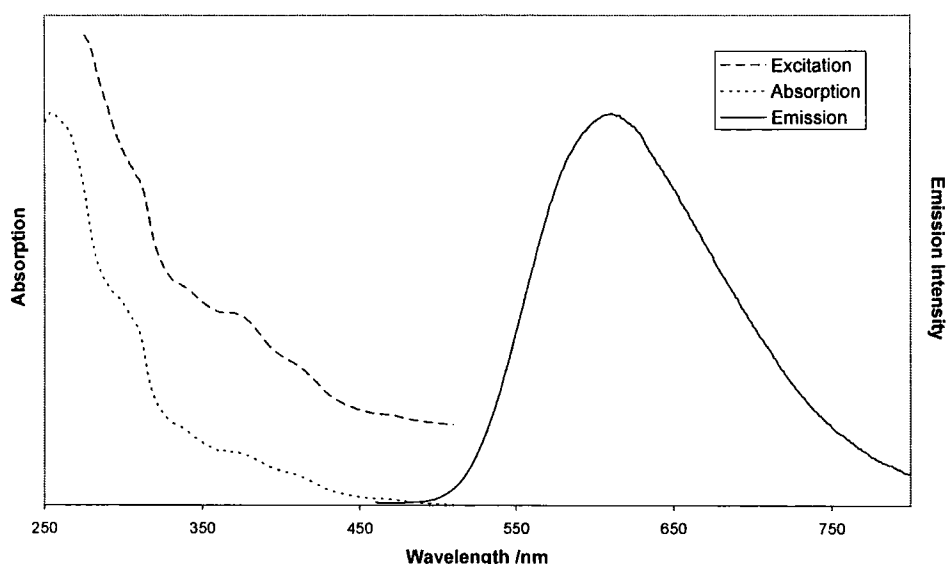
Figure 69 Normalised absorption and emission spectra (λ_{ex} = 400 nm) for [Ir(ppy)$_2$(bpy)]$^+$ 24 with overlaid excitation spectrum (λ_{em} = 610 nm) offset for clarity. Spectra recorded in acetonitrile at 298K.

3.1.2 Effect of substituents in the ppy ligand

A series of [Ir(C^N)$_2$(bpy)]$^+$ complexes were prepared where the C^N coordinating ligand was a substituted ppy ligand. The effect of these substituents on the photophysical properties of the resulting complexes was investigated and results are summarised in Table 7.

Complex	27	29	31	56
Absorption Maxima /nm (ε /M^{-1} cm^{-1})	455 (506) 408 (1820) 362 (7070) 309 (20800) 298 (24800) 265 (46600) 252 (48500)	446 (364) 418 (883) 355 (5560) 308 (20300) 300 (22500) 257 (41300) 248 (43700)	450 (344) 418 (1180) 388 (3750) 368 (5460) 322 (10700) 309 (20600) 298 (24400) 257 (42300) 248 (44900)	410 (4410) 330 (13700) 310 (34000) 274 (83000) 267 (81000)
Emission Maximum[a] /nm	570	538	547	628
Quantum Yield x 10^2 degassed (aerated)	39 (3.3)	53 (3.9)	44 (3.3)	5.3 (2.0)
Lifetime /ns degassed (aerated)	1040 (92)	1490 (115)	1360 (106)	147 (52)

Table 7 Photophysical properties of [Ir(ppy-F)$_2$(bpy)]$^+$ 27, [Ir(ppy-F$_2$)$_2$(bpy)]$^+$ 29, [Ir(ppy-F$_3$)$_2$(bpy)]$^+$ 31 and [Ir(ppy-ph)$_2$(bpy)]$^+$ 56, in CH$_3$CN at 298K. [a] λ_{ex} = 400 nm.

3.1.2.1 Fluoro substituents

The introduction of fluorine substituents into the ppy ligand brings about a dramatic change in the emission characteristics of the complexes **27, 29** and **31**. The position of the emission maximum is blue shifted in the order :

$$[Ir(ppy)_2(bpy)]^+ \; \textbf{24} < [Ir(ppy\text{-}F)_2(bpy)]^+ \; \textbf{27} < [Ir(ppy\text{-}F_3)_2(bpy)]^+ \; \textbf{31} < [Ir(ppy\text{-}F_2)_2(bpy)]^+ \; \textbf{29}$$
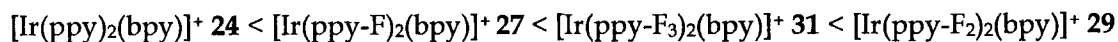
with $[Ir(ppy\text{-}F_3)_2(bpy)]^+$ **31** seemingly falling out of sequence between complexes **27** and **29**. The emission profiles for these complexes are shown in Figure 70.
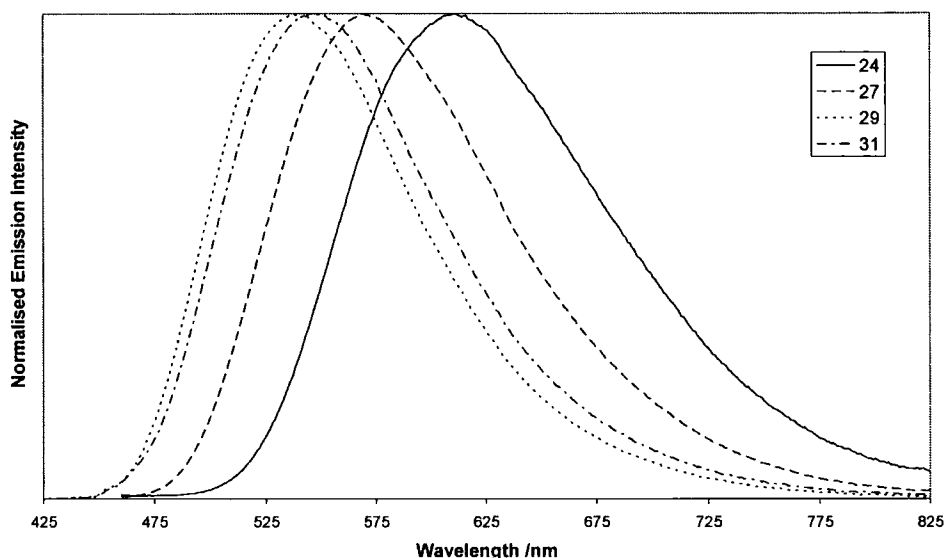
Figure 70 Normalised emission spectra (λ_{ex} = 400 nm) of $[Ir(ppy)_2(bpy)]^+$ 24, $[Ir(ppy\text{-}F)_2(bpy)]^+$ 27, $[Ir(ppy\text{-}F_2)_2(bpy)]^+$ 29 and $[Ir(ppy\text{-}F_3)_2(bpy)]^+$ 31. Spectra recorded in acetonitrile at 298K.

De Cola *et al*[90] have discussed the effect of fluoro substituents on the emission characteristics of complexes similar to these. The combined mesomeric and inductive electron-withdrawing effect of the fluoro substituents creates electron deficiency at sites *meta* to the fluorine atom (Figure 71). In complexes **27** and **29**, the positioning of the fluorine atoms results in electron deficiency at the site of cyclometalation. This reduces the σ-donor capabilities of the ppy ligand and reduces electron density at the metal centre, rendering the HOMO lower in energy. As a result, the emissive MLCT state is increased in energy, which is observed as a blue shift in the emission maximum. The effect is greater for complex **29** than **27** due to the presence of two appropriately positioned fluorine atoms creating twice the electron-withdrawing effect. However, the introduction of a third fluorine substituent in complex **31** would not be expected to affect the electron density at the site of cyclometalation and so no further

blue shift should be observed. Indeed, this complex has a similar but slightly red shifted emission maximum when compared to the difluoro-substituted complex **29**, possibly because the accumulation of electron density at the two carbons neighbouring the cyclometalating carbon seen for complexes **27** and **29** is disfavoured in the presence of the third fluorine substituent.

* sites of electron deficiency due to electron-withdrawing fluorine atoms
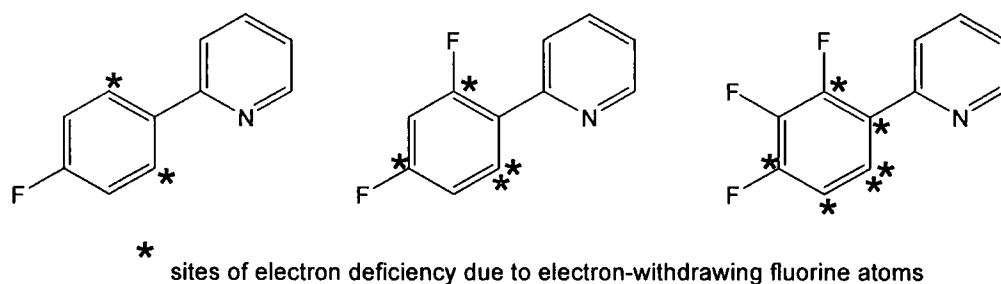
Figure 71 Electron-withdrawing effect in fluoro-substituted ppy ligands

A blue shift in emission maximum had been reported for the tris-cyclometalated complex [Ir(ppy-F)$_3$] which emits at 468 nm compared to 494 nm for the unsubstituted parent complex [Ir(ppy)$_3$] under the same conditions.[196] Additionally, during the course of this work, [Ir(ppy-F$_2$)$_3$] was prepared and photophysical investigation revealed a blue shift of 42 nm at 298K relative to [Ir(ppy)$_3$] which is associated with stabilisation of the HOMO as discussed here.[187]

As the quantum yield (Φ) and observed lifetime (τ_{obs}) of emission are also increased upon the incorporation of fluoro substituents, the increase in energy of the emissive MLCT state must be accompanied by a reduction in the overall rate constant associated with the relaxation process. The quantum yield and lifetime increase by similar factors, suggesting a significant decrease in the rate of non-radiative processes (Σk_{nr}) according to the equations: $\tau_{obs} = (k_r + \Sigma k_{nr})^{-1}$ and $\Phi = k_r . \tau_{obs}$

Values for the radiative and non-radiative rate constants (k_r and Σk_{nr} respectively) of fluoro-substituted complexes **27**, **29** and **31** have been calculated from these equations and are compared to values for unsubstituted parent complex **24** in Table 8. This shows that the rate constant for non-radiative processes is decreased by approximately an order of magnitude upon introduction of fluoro substituents into the ppy ligand. This is in accordance with the energy gap law, as increasing the energy of the MLCT emissive state through the introduction of fluoro substituents removes the extent to which deactivation via a non-emissive state can occur, hence decreasing the rate of decay attributed to non-radiative processes.

Complex	**24**	**27**	**29**	**31**
τ_{obs} / ns	370	1040	1490	1360
$\Phi \times 10^2$	9.7	38	53	44
$k_r \times 10^{-5}$ / s^{-1}	2.6	3.7	3.6	3.2
$\Sigma k_{nr} \times 10^{-6}$ / s^{-1}	2.4	0.60	0.32	0.41

Table 8 Calculated radiative and non-radiative rate constants for [Ir(ppy)₂(bpy)]⁺ 24,

[Ir(ppy-F)₂(bpy)]⁺ 27, [Ir(ppy-F₂)₂(bpy)]⁺ 29 and [Ir(ppy-F₃)₂(bpy)]⁺ 31.

3.1.2.2 Phenyl substituents

Conversely, the introduction of a phenyl substituent into the ppy ligand in [Ir(ppy-ph)₂(bpy)]⁺ **56** causes a red shift in the emission maximum compared to the unsubstituted parent complex, along with a decrease in quantum yield and lifetime of emission. This could be attributed to the reverse effect of that seen for the fluoro substituted complexes, with the phenyl group acting as a mesomeric electron donor (Figure 72) and thus increasing the σ-donor ability of the ppy ligand. This would lower the energy of the emissive MLCT state and produce a red shift in the emission maximum. No work has previously been published on the effect of phenyl-substituted ppy ligands on the photophysical properties of either complexes of this sort or for similar [Ir(ppy)₃] type complexes.
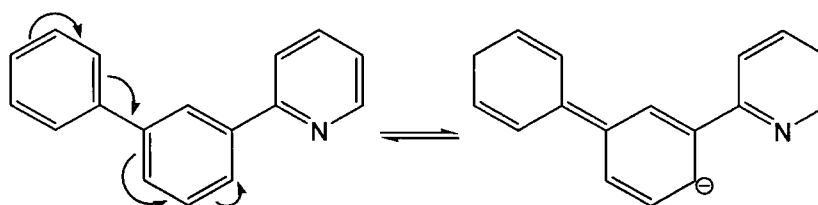
Figure 72 Mesomeric electron donation by phenyl substituent

3.1.3 Effect of substituents in the bpy ligand

A series of [Ir(C^N)₂(N^N)]⁺ type complexes was produced with the bipyridine ligand carrying substituents at the 4-position of one ring. Substituents investigated include phenyl, methoxy, hydroxy, pyridyl and dimethylamino groups. The photophysical properties of these complexes are discussed in the following sections.

3.1.3.1 Phenyl substituents on the bpy ligand

The photophysical properties of complexes **52** – **54**, which each contain a 4-phenyl-2,2'-bipyridine ligand, are summarised in Table 9.

Complex	52	53	54
Absorption Maxima / nm (ε / M^{-1} cm^{-1})	466 (997) 403 (4040) 374 (8150) 337 (12000) 312 (23600) 267 (54800) 256 (54100)	455 (807) 425 (1370) 338 (12300) 309 (25300) 268 (56700) 254 (54200)	446 (598) 417 (1300) 359 (7860) 333 (12100) 313 (23500) 300 (28100) 262 (49100) 250 (49200)
Emission Maximum[a] / nm	613	572	539
Quantum Yield x 10^2 degassed (aerated)	13 (2.5)	38 (3.8)	66 (5.8)
Lifetime / ns degassed (aerated)	406 (79)	1040 (100)	1390 (142)

Table 9 Photophysical properties of [Ir(ppy)₂(bpy-ph)]⁺ 52, [Ir(ppy-F)₂(bpy-ph)]⁺ 53 and [Ir(ppy-F₂)₂(bpy-ph)]⁺ 54 measured in acetonitrile at 298K. [a] λ_{ex} = 400 nm.

In contrast to the previous example where a phenyl substituent on the ppy ligand induced a red shift in emission wavelength, the introduction of such substituents at the 4-position of the 2,2'-bipyridine ligand in [Ir(C^N)₂(N^N)]⁺ complexes does not produce a significant change in the emission properties when compared to the unsubstituted parent complex (Figure 73).
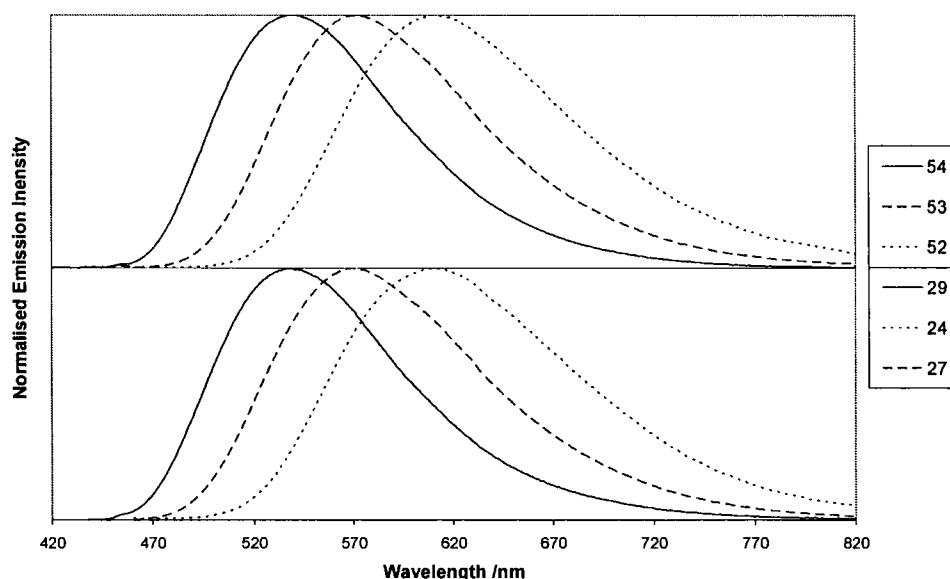
Figure 73 Normalised emission spectra of [Ir(ppy)₂(bpy-ph)]⁺ 52, [Ir(ppy-F)₂(bpy-ph)]⁺ 53 and [Ir(ppy-F₂)₂(bpy-ph)]⁺ 54 (upper spectra), and [Ir(ppy)₂(bpy)]⁺ 24, [Ir(ppy-F)₂(bpy)]⁺ 27, and [Ir(ppy-F₂)₂(bpy)]⁺ 29 (lower spectra). Recorded in acetonitrile at 298K using λ_{ex} = 400 nm.

The emission profiles obtained via excitation at the same wavelength have very similar maxima to those of the relevant unsubstituted parent complex. Similar observations have been made by de Cola *et al* who deduced that the lowest excited state is very little perturbed by the incorporation of phenyl linking units attached to the bipyridine ligand in multimetallic species.[88]

3.1.3.2 *[Ir(ppy)$_2$(N^N)]$^+$ where N^N contains pyridyl, amino, methoxy or hydroxy functionality*

Photophysical data collected for [Ir(C^N)$_2$(N^N)]$^+$ complexes bearing methoxy, hydroxy, pyridyl, and dimethylamino functionality at the 4-position of the bipyridine ligand, either with or without phenyl spacer groups, are summarised in Table 10.

For complexes **40**, **42**, **44** and **45**, the absorption spectrum remains very similar to that seen for the unsubstituted parent complex [Ir(ppy)$_2$(bpy)]$^+$ **24**, with the lowest energy excited state involving charge transfer from iridium to the substituted bpy ligand. However, for complexes **48** and **49** an increase in molar absorptivity is observed at low energy, around 400 nm. This implies that the MLCT absorption usually found in this region may be accompanied by another transition of similar energy, leading to an overall increase in the observed extinction coefficient.

For the methoxy- and hydroxy-substituted complexes **40** and **45**, no significant change in the emission characteristics is observed, presumably indicating that such pendent groups have little effect on the energy of the HOMO and LUMO levels in these complexes.

Complex	40	42	44	45
Absorption Maxima /nm (ε /M^{-1} cm^{-1})	465 (1110) 410 (3650) 379 (8740) 352 (12600) 310 (25700) 271 (39100) 256 (36800)	465 (1220) 402 (4020) 378 (7080) 314 (16300) 263 (40500) 252 (44900)	465 (3410) 404 (4730) 381 (9230) 350 (14200) 293 (43000) 269 (48200) 254 (43300)	465 (1380) 402 (4580) 375 (9460) 353 (12400) 306 (25400) 271 (37800) 257 (36600)
Emission Maximum[a] /nm	608	637	619	606
Quantum Yield x 10^2 degassed (aerated)	15 (2.8)	7.9 (2.4)	14 (3.0)	10 (2.0)
Lifetime /ns degassed (aerated)	457 (76)	292 (81)	407 (81)	443 (79)

Complex	48	49
Absorption Maxima /nm (ε /M^{-1} cm^{-1})	402 (19300) 346 (17700) 300 (27000) 254 (43400)	382 (24300) 310 (34900) 264 (52200) 256 (53800)
Emission Maximum[a] /nm	610	611
Quantum Yield x 10^2 degassed (aerated)	0.90 (0.20)	1.0 (0.20)
Lifetime /ns degassed (aerated)	433 (81)	420 (81)

Table 10 Photophysical properties of complexes [Ir(ppy)₂(bpy-ϕ-OMe)]⁺ 40, [Ir(ppy)₂(bpy-py)]⁺ 42, [Ir(ppy)₂(bpy-ϕ-py)]⁺ 44, [Ir(ppy)₂(bpy-ϕ-OH)]⁺ 45, [Ir(ppy)₂(bpy-ϕ-NMe₂)]⁺ 48 and [Ir(ppy)₂(bpy-ϕ-ϕ-NMe₂)]⁺ 49 measured in acetonitrile at 298K. [a] λ_{ex} = 415 nm.

However, for pyridyl-substituted complexes [Ir(ppy)₂(bpy-py)]⁺ **42** and [Ir(ppy)₂(bpy-ϕ-py)]⁺ **44**, a red shift in the emission maximum is observed compared to parent complex **24**, with a larger effect seen for complex **42** whick lacks an intermediate phenyl ring (Figure 74). This is attributed to the electron withdrawing nature of the pendent pyridyl ring, which facilitates MLCT from iridium to the bpy ligand. The electronic effect of the pyridyl ring on the bound bipyridine unit is presumably reduced upon the insertion of an intermediate phenyl spacer group.
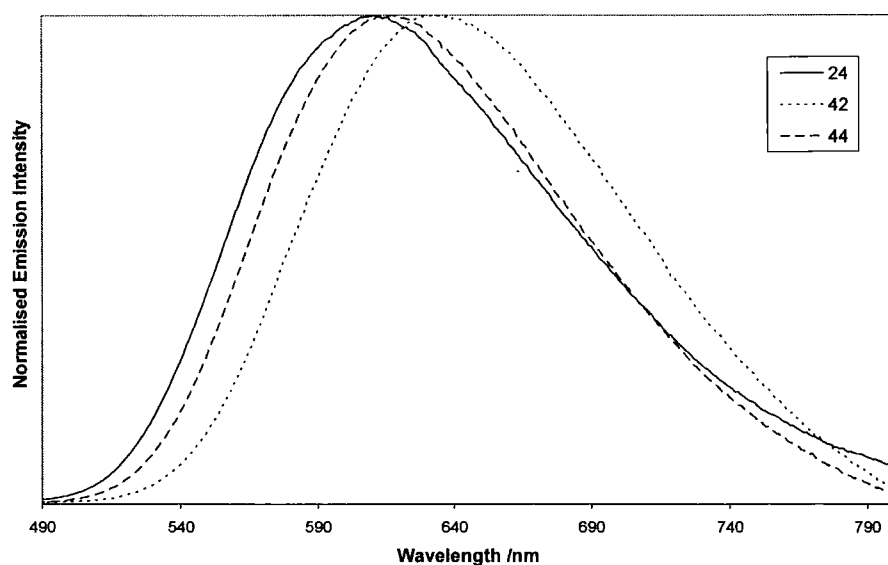
Figure 74 Normalised emission spectra (λ_{ex} = 415 nm) for [Ir(ppy)$_2$(bpy-py)]$^+$ 42, [Ir(ppy)$_2$(bpy-ϕ-py)]$^+$ 44 and the parent complex [Ir(ppy)$_2$(bpy)]$^+$ 24 (λ_{ex} = 400 nm). Spectra recorded in acetonitrile at 298K.

Dimethylamino-substituted complexes **48** and **49** display an emission wavelength almost identical to unsubstituted complex **24** but the quantum yield of emission is markedly reduced to the order of 1%. Two possible explanations for this behaviour are as follows.

As the pendent amine group contains a lone pair of electrons on the nitrogen atom, it is possible that photoinduced electron transfer (PET) could be deactivating the excited state. As displayed in Figure 75, PET from the lone pair to the HOMO of the complex followed by back electron transfer would allow re-creation of the ground state without the generation of radiation.[197] This phenomenon has been widely studied for use in luminescent sensing,[197,198] and has included examples of organic amine containing molecules such as those featured in Figure 76.[199,200] However, this process is usually associated with systems containing a donor and acceptor separated by an insulating spacer group. As this is not the case for the complexes studied here, this explanation may not be appropriate. Moreover, the emissive lifetimes of complexes **48** and **49** are not significantly lower than for the other complexes presented. This suggests that an additional pathway of deactivation of the emitting state is not the cause of the low quantum yield, but rather energy losses prior to its formation, or a smaller fraction of excitation energy reaching the emissive state.
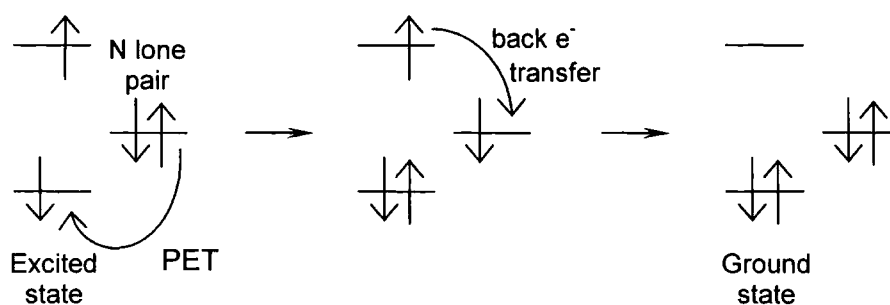
Figure 75 Photoinduced electron transfer (PET) and back electron transfer to deactivate an excited state
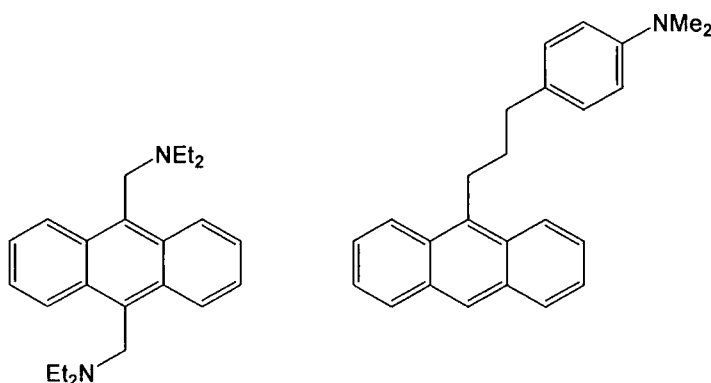
Figure 76 Organic amine containing molecules which can undergo PET

An alternative explanation is that a low energy intra-ligand charge transfer (ILCT) state may be responsible. Density functional theory calculations carried out as part of this work support the existence of such a state (see section 3.2). The calculations show that the HOMO of the dimethylamino-substituted complex is localised primarily on the dimethylamino group, whilst the LUMO is delocalised over the two chelating pyridyl rings of the bpy ligand. An ILCT transition localised on this ligand could occur at a similar energy to the MLCT transition, which may account for the increased molar absorptivity observed at ~ 400 nm in the absorption spectrum. If this is the case, upon excitation at 400 nm it is possible that two excited states are generated: the usual emissive MLCT state and an ILCT state. As the lifetime of emission of the dimethylamino-substituted complexes remains similar to the others discussed in this section, it is possible that the reduced quantum yield is arising because the excitation energy is split between the two low energy excited states generated. If these states are not efficiently coupled and the ILCT is only weakly or perhaps even non-emissive, this would account not only for the reduced quantum yield but also for the unchanged lifetime of emission.

3.1.3.3 Exchanging ppy for pba

As discussed previously, by substituting at the ppy ligand the photophysical properties of [Ir(C^N)₂(N^N)]⁺ complexes can be varied. A series of complexes based on those described in the preceeding section was produced with 4-(2-pyridyl)benzaldehyde as the C^N coordinating ligand. The photophysical properties of these complexes are summarised in Table 11.

Complex	41	43	50	51
Absorption Maxima /nm (ε /M⁻¹ cm⁻¹)	414 (5030) 345 (18000) 314 (39000) 294 (46400) 276 (50800) 252 (35900)	407 (3760) 339 (10600) 309 (24700) 291 (30900) 271 (38200) 252 (35400)	412 (15800) 299 (38300) 272 (38700) 255 (35500)	417 (12400) 366 (19200 312 (37800) 298 (42100) 275 (44000)
Emission Maximum[a]/nm	539, 571	544, 577	539, 573	539, 571
Quantum Yield x 10² degassed (aerated)	27 (1.5)	44 (2.1)	6.5 (0.40)	3.0 (0.20)
Lifetime /ns degassed (aerated)	5160, 1160 (188)	2890, 730 (171)	4470, 576 (324, 90)	5050, 1230 (203)

Table 11 Photophysical properties of complexes [Ir(pba)₂(bpy-φ-OMe)]⁺ 41, [Ir(pba)₂(bpy-py)]⁺ 43, [Ir(pba)₂(bpy-φ-NMe₂)]⁺ 50 and [Ir(pba)₂(bpy-φ-φ-NMe₂)]⁺ 51 measured in acetonitrile at 298K. [a] λ_{ex} = 415 nm.

The absorption spectra recorded for these complexes are similar to the ppy analogues. In particular, enhanced absorption is observed at low energy (~ 400 nm) for the dimethylamino-substituted complexes. As was discussed previously for ppy containing complexes 48 and 49, this could be attributed to a low lying ILCT state associated with the dimethylamino group. The lower quantum yields combined with similar emissive lifetimes of complexes 50 and 51 when compared to the other pba containing complexes may further support this explanation (see earlier discussion relating to complexes 48 and 49 for further details).

The emission characterstics of the pba containing complexes are distinctly different from those of analogous complexes containing ppy as the C^N coordinating ligands. The emission spectra for all of the pba complexes display a structured profile with a significant blue shift in the maximum compared to that seen for the ppy equivalent. A comparison of a pba vs ppy complex emission spectrum is shown in Figure 77 for a dimethylamino-substituted complex. Additionally, the emission from the pba containing complexes is found to decay in a biexponential fashion, whilst the quantum

yield and lifetime are both increased in comparison to analogous ppy complexes, the latter by around an order of magnitude.
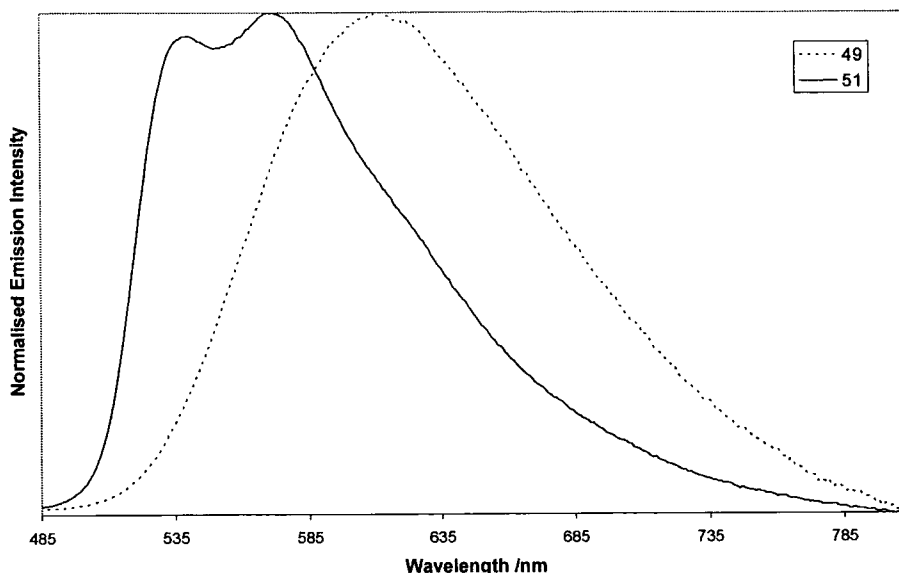
Figure 77 Comparison of emission spectra (λ_{ex} = 415 nm) of [Ir(ppy)2(bpy-ϕ-ϕ-NMe2)]+ 49 and [Ir(pba)2(bpy-ϕ-ϕ-NMe2)]+ 51. Spectra recorded in acetonitrile at 298K.

Similar results to these have been discussed by Lo et al[94] for [Ir(pba)2(N^N)]+ complexes where N^N is either 2,2′-bipyridine or a methylated 1,10-phenanthroline ligand, although monoexponential decay of emission is reported in those cases. Following these examples by Lo, emission from this series of pba complexes is deduced to arise from an LC state on the pba ligand, which probably mixes to some extent with an MLCT state also involving the pba ligand. The change in excited state character arises due to the electron-withdrawing nature of the aldehyde functionality, which lowers the energy of the metal orbitals to such an extent that a new HOMO of ligand character is generated (Figure 78). Structured emission is typical of LC emission as the potential energy curves belonging to the ground and excited states are both of ligand character and, hence, less shifted with respect to each other than for ground and excited states of different character (e.g. for MLCT transitions).

The biexponential decay of emission noted here under degassed conditions is independent of emission wavelength and therefore suggests that emission may originate from two excited states which are poorly coupled at room temperature. For complex 50, biexponential decay is also observed in aerated acetonitrile which implies that for the other pba containing complexes, the shorter component is too short to measure under aerated conditions.
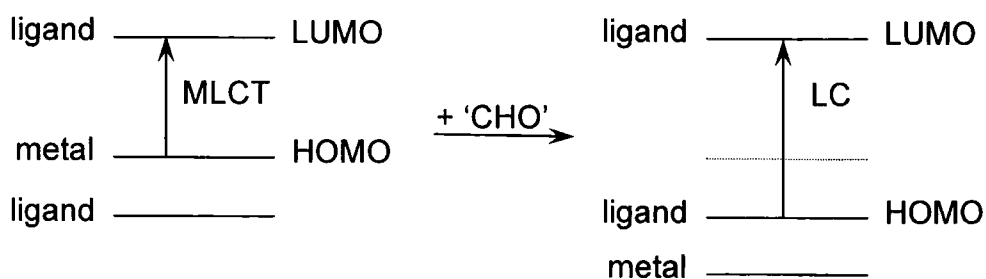
Figure 78 Change in excited state upon introduction of pba ligands

3.1.4 Effect of pH on the photophysical properties of appropriately functionalised [Ir(C^N)$_2$(N^N)]$^+$ complexes

Of the complexes discussed so far, a number contain protonatable or deprotonatable functional groups and may, therefore, exhibit pH dependent photophysical properties. This was investigated for complexes bearing pendent dimethylamino, pyridyl or hydroxy functionality.

3.1.4.1 Amino-substituted complexes

The effect of acid on the photophysical properties of dimethylamino-substituted complexes **48 – 51** is summaried in Table 12.

Complex	48	49	50	51
Emission Maximum /nm in neutral solution	610	611	539, 573	539, 571
Emission Maximum /nm in acidic solution	614	613	536, 564[a]	538, 561[a]
Relative Emission Intensity I^{H+}/I	5.5	4.7	1.0	0.3
Lifetime /ns in acidic solution degassed (aerated)	360 (81)	386 (81)	653, 63 (88)	760, 109 (113)

Table 12 Effect of acid of the photophysical properties of amino-substituted complexes [Ir(ppy)$_2$(bpy-φ-NMe$_2$)]$^+$ **48**, [Ir(ppy)$_2$(bpy-φ-φ-NMe$_2$)]$^+$ **49**, [Ir(pba)$_2$(bpy-φ-NMe$_2$)]$^+$ **50** and [Ir(pba)$_2$(bpy-φ-φ-NMe$_2$)]$^+$ **51** measured in acetonitrile at 298K using λ$_{ex}$ = 415 nm.

[a] approximate values as weak emission profiles made position of maxima unclear.

An increase in emission intensity by a factor of approximately five is observed for [Ir(ppy)$_2$(bpy-φ-NMe$_2$)]$^+$ **48** and [Ir(ppy)$_2$(bpy-φ-φ-NMe$_2$)]$^+$ **49** in the presence of acid (Figure 79). As the emission maximum and lifetime are essentially unaffected by pH, it

can be assumed that emission is arising from the same MLCT state whether the amino group is protonated or unprotonated.
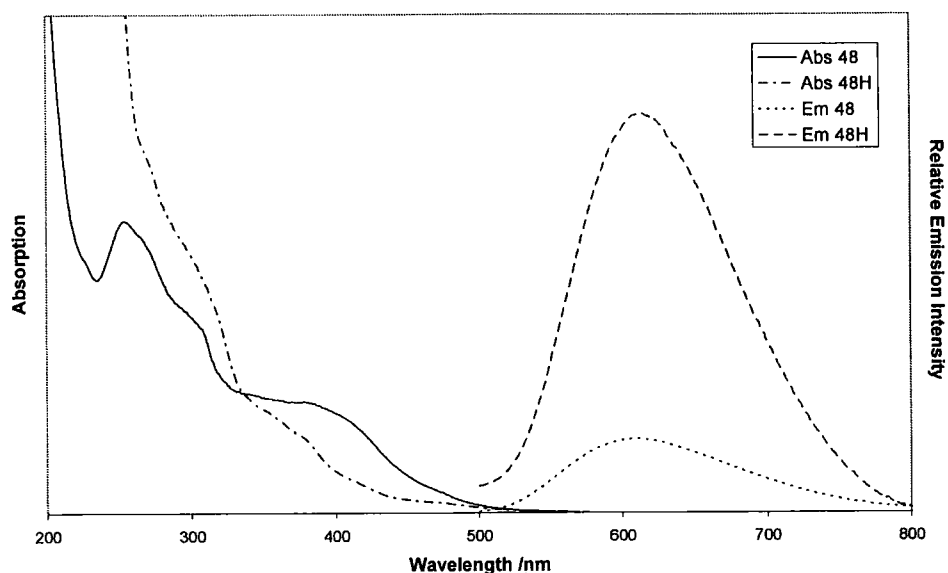
Figure 79 Absorption and emission (λ_{ex} = 415 nm) spectra of [Ir(ppy)₂(bpy-φ-NMe₂)]⁺ 48 with (48H) and without (48) acid. Spectra recorded in acetonitrile at 298K.

The increase in emission intensity can be explained using either of the explanations previously discussed to account for the low quantum yields of these complexes in the unprotonated form (see section 3.1.3.2). Both of these revolve around the removal of the nitrogen lone pair of electrons upon protonation at the amine site. In the case of PET, there is simply no free pair of electrons to participate and so PET can no longer provide a competitive decay mechanism. For the ILCT case, protonation increases the energy of the ligand-centred charge transfer transition to such an extent that interference with the radiative decay process is no longer possible. The net result in both cases is an increase in the observed emission intensity.

Further evidence supporting the ILCT explanation can be found from studying the absorption spectrum measured in acidic solution (Figure 79). Upon addition of acid there is clearly a reduction in absorption at low energy, particularly around 400 nm. This would concur with the above explanation that protonation removes the low energy ILCT state and hence reduces absorption in this region of the spectrum.

The effect of acid on the absorption spectrum of complexes [Ir(pba)₂(bpy-φ-NMe₂)]⁺ 50 and [Ir(pba)₂(bpy-φ-φ-NMe₂)]⁺ 51 is similar to that seen for the ppy analogues 48 and 49, with a decrease in absorption at around 400 nm suggesting the possible removal of an ILCT state through protonation at the amine site. However, in section 3.1.3.3 it was

apparent that pba-containing complexes display very different emission properties to their ppy analogues. As such, the removal of such a state may not affect the photophysical properties of complexes **50** and **51** in the same manner as for complexes **48** and **49**.

Indeed, the effect of acid on the emission spectra of complexes **50** and **51** is quite different to that seen for **48** and **49**. Upon acidification, the structured emission profile is retained but accompanied by a blue shift of the lower energy maximum by ~ 10 nm, with either no change (**50**) or a decrease (**51**) in emission intensity. The lifetime of emission is also reduced by around one order of magnitude. These results suggest that emission remains primarily LC upon acidification with the further blue shift perhaps resulting from the interaction of acid at the aldehyde group of the pba ligand.

3.1.4.2 Hydroxy-substituted complexes

The effect of base on hydroxy complex $[Ir(ppy)_2(bpy-\phi-OH)]^+$ **45** is the reverse of that found for acid upon analogous dimethylamino complexes **48** and **49**. No change in emission maximum is observed, indicating that the same excited state is emitting, but in this instance the emission intensity is markedly reduced upon deprotonation of the hydroxy site (Figure 80).
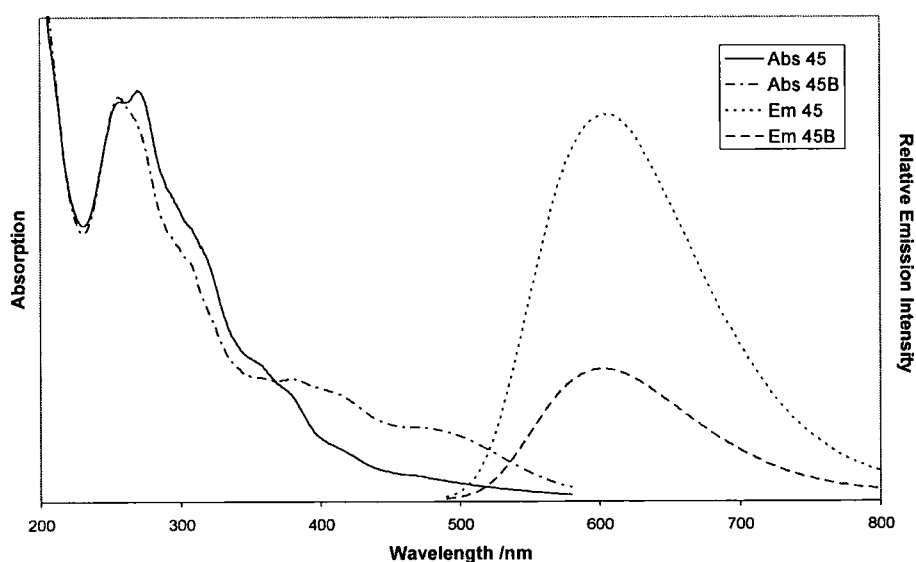
Figure 80 Comparison of absorption and emission spectra for $[Ir(ppy)_2(bpy-\phi-OH)]^+$ 45 with (45B) and without (45) base, measured in acetonitrile at 298K.

This could be explained in a manner similar to that used to explain the increase in emission intensity observed upon acidification of $[Ir(ppy)_2(bpy-\phi-NMe_2)]^+$ **48** and

79

[Ir(ppy)$_2$(bpy-ϕ-ϕ-NMe$_2$)]$^+$ **49**, with the -O$^-$ form being analogous to -NMe$_2$, and -OH to -N$^+$(H)Me$_2$. Deprotonation of the -OH group generates a free pair of electrons which are capable of deactivating the emissive state via either of the PET or ILCT mechanisms previously discussed. Study of the absorption spectrum upon deprotonation of hydroxy complex **45** reveals an increased absorption at wavelengths > 400 nm, which could be attributed to the creation of a low energy ILCT state upon deprotonation, supporting the proposal of deactivation via this mechanism.

Alternatively, it is possible that emission becomes quenched due to the introduction of quinonoidal character upon deprotonation. This has been previously reported for iridium complexes bearing hydroxy-substituted terpyridine ligands[201], and for ruthenium complexes containing the same bpy ligand as studied here.[27] In the latter work, emission from [Ru(bpy)$_2$(bpy-ϕ-OH)]$^{2+}$ was seen to be almost entirely quenched upon deprotonation of the -OH group. This was explained by delocalisation of the negative charge generated over the entire ligand bringing the negative charge closer to the metal centre and creating a strong π donor ligand (Figure 81). This has the effect of lowering the metal orbitals to a similar energy to the ligand π^* level. Thermal equilibration of the emissive MLCT state with the MC state, which offers a radiationless decay pathway, results in the quenching of emission. This could also be the case here, with perhaps a reduced extent of quenching attributed to the presence of cyclometalating ligands which increase the electron density at the metal centre and reduce the delocalisation effect to some extent. The establishment of a low energy band in the absorption spectrum upon addition of base could be attributed to a ligand centred state associated with the quinonoidal type ligand resulting from delocalisation of the negative charge.
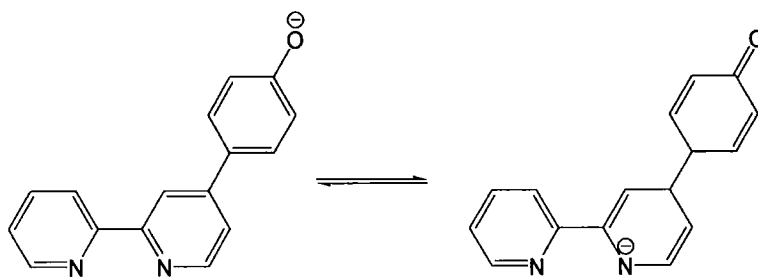
Figure 81 Creation of quinonoidal character upon deprotonation of hydroxy group

Regardless of which of these two explanations is correct, the net result remains the same: a proportion of the excitation energy is consumed in the generation of an additional excited state, which, if not equilibrated with the emissive MLCT state, could account for the reduction in emission intensity upon the addition of base to **45**.

3.1.4.3 Pyridyl-substituted complexes

The addition of acid to any of the pyridyl-substituted iridium complexes causes a quenching of emission to such an extent that a maximum can no longer be detected (Table 13).

Complex	42	43	44
Emission Maximum /nm in acidic solution	- (a)	- (a)	- (a)
Relative Emission Intensity I^{H+}/I	0.04	0.1	0.03

Table 13 Effect of acid on the photophysical properties of [Ir(ppy)₂(bpy-py)]⁺ 42, [Ir(pba)₂(bpy-py)]⁺ 43 and [Ir(ppy)₂(bpy-φ-py)]⁺ 44 in CH₃CN at 298K (λex = 415 nm). (a) emission from acidified solutions was so weak that no maximum could be determined, relative emission intensity was calculated at emission maximum measured for non-acidic sample.

A similar effect has been reported for ruthenium complexes containing the bpy-py ligand.[27] This was explained by considering that protonation of the pyridyl group creates an effective electron acceptor, which can receive an electron from the MLCT excited state and hence quench emission. This could also be the case for ppy complexes [Ir(ppy)₂(bpy-py)]⁺ 42 and [Ir(ppy)₂(bpy-φ-py)]⁺ 44, although in the ruthenium example this was accompanied by a red shift in the lowest MLCT absorption band upon protonation which is not observed here (Figure 82).
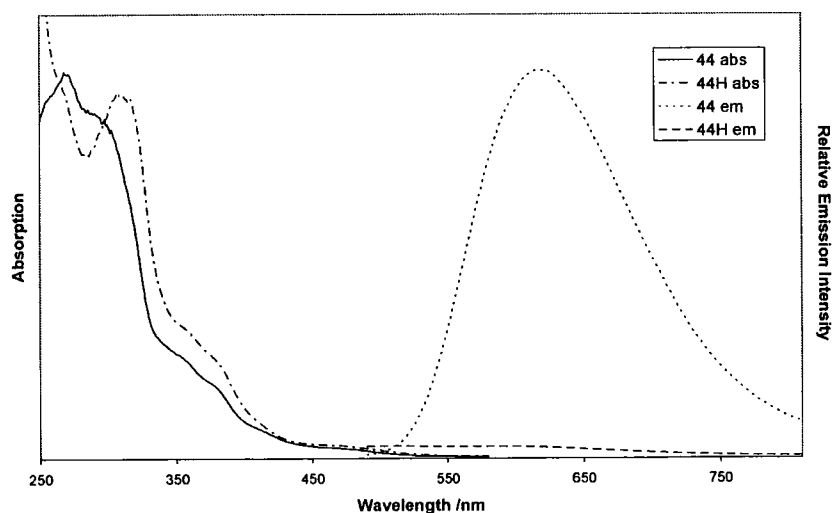
Figure 82 Absorption and emission (λex = 415 nm) spectra of [Ir(ppy)₂(bpy-φ-py)]⁺ 44 with (44H) and without (44) acid. Spectra recorded in acetonitrile at 298K.

Emission is also reduced upon acidification of pba complex [Ir(pba)₂(bpy-py)]⁺ **43**, but by a factor of ten less than that from the ppy complexes **42** and **44**. This could be associated with the fact that complex **43** is most likely a less powerful photoreductant than the ppy analogue, resulting in reduced electron transfer to the pyridyl group upon protonation and hence less quenching of emission.

3.2 Computational studies of [Ir(C^N)₂(N^N)]⁺ complexes

In conjunction with photophysical studies of [Ir(C^N)₂(N^N)]⁺ complexes, a number of structures were also investigated via density functional theory (DFT) calculations. Calculated orbital characteristics for the two highest occupied molecular orbitals (HOMO and HOMO - 1) and the two lowest unoccupied molecular orbitals (LUMO and LUMO +1) are summarised in Table 14.

Complex	HOMO - 1	HOMO	LUMO	LUMO + 1
[Ir(ppy)₂(bpy)]⁺ **24**	ppy (88%)	Ir (53%) + ppy (43%)	bpy (93%)	bpy (90%)
[Ir(pba)₂(bpy)]⁺	pba (78%)	Ir (57%) + pba (39%)	bpy (94%)	pba (94%)
[Ir(ppy)₂(bpy-py)]⁺ **42**	ppy (85%)	Ir (48%) + ppy (47%)	bpy (93%)	bpy (96%)
[Ir(pba)₂(bpy-py)]⁺ **43**	pba (74%)	Ir (51%) + pba (45%)	bpy (94%)	pba (77%)
[Ir(ppy)₂(bpy-φ-py)]⁺ **44**	bpy (100%)	Ir (48%) + ppy (47%)	bpy (93%)	bpy (95%)
[Ir(ppy)₂(bpy-φ-NMe₂)]⁺ **48**	Ir (48%) + ppy (46%)	bpy (94%) (47% NMe₂)	bpy (94%) (1% NMe₂)	bpy (87%)
[Ir(ppy)₂(bpy-φ-φ-NMe₂)]⁺ **49**	Ir (49%) + ppy (47%)	bpy (99%) (48% NMe₂)	bpy (94%) (0.4% NMe₂)	bpy (90%)
[Ir(pba)₂(bpy-φ-NMe₂)]⁺ **50**	Ir (51%) + ppy (44%)	bpy (96%) (48% NMe₂)	bpy (94%) (1% NMe₂)	pba (95%)
[Ir(pba)₂(bpy-φ-φ-NMe₂)]⁺ **51**	Ir (51%) + ppy (45%)	bpy (100%) (48% NMe₂)	bpy (94%) (0.4% NMe₂)	pba (94%)

Table 14 Summary of calculated molecular orbital characterstics according to DFT calculations. Percentages in parenthesis denote the proportion of entire electron density localised at a particular site. Orbitals with ≥ 75% of electron density at one ligand are classified as being characteristic of that ligand, but some small percentage of electron density will reside at either the other ligand or at the metal centre.

The B3LYP density functional was used throughout, with the 6-31G basis set being employed for all ligand atoms and LANL2DZ for the iridium atom. An effective core potential (ECP) was used to replace the inert inner core electrons of iridium(III) which are not involved in bonding, thus allowing a substantial reduction in calculation time. Outer core $[(5s)^2(5p)^6]$ electrons were still included along with valence $(5d)^6$ electrons. It is worth noting that when orbitals are designated as 'metal-based' there is usually also a significant amount of C^N ligand character. This is attributed to the effective covalent nature of the cyclometalating Ir-C bond.

Calculations for parent complex $[Ir(ppy)_2(bpy)]^+$ **24** confirm that the lowest excited state is generated from a charge transfer transition between a metal-based orbital and a bpy-based orbital (Figure 83).
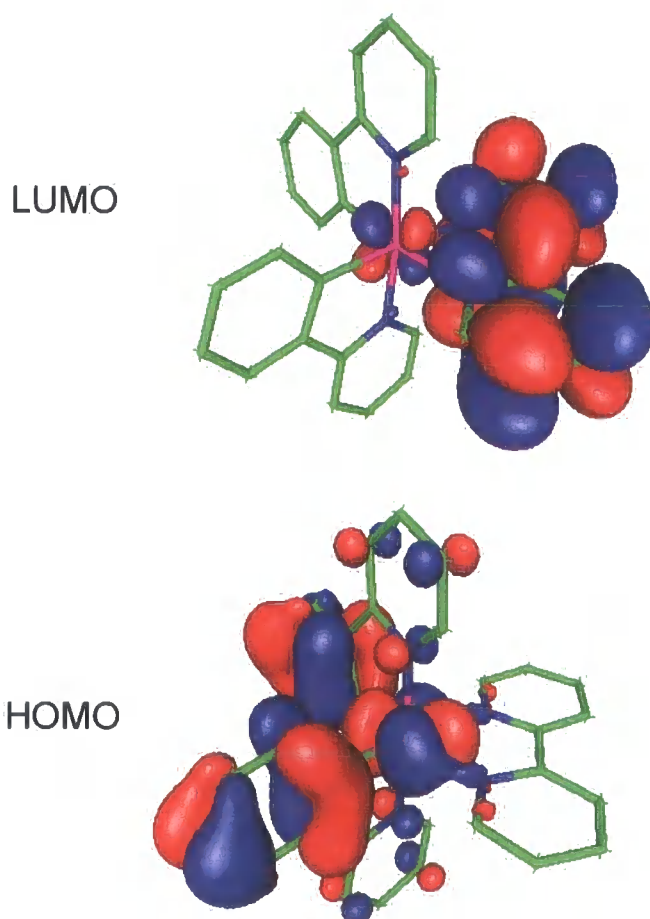
Figure 83 Contour plots of the HOMO and LUMO of $[Ir(ppy)_2(bpy)]^+$ 24

The same result is seen for pyridyl-substituted complexes $[Ir(ppy)_2(bpy-py)]^+$ **42** and $[Ir(ppy)_2(bpy-\phi-py)]^+$ **44**. However, the second lowest unoccupied orbital is calculated to be of bpy character also, which conflicts with reported photophysical results which suggest that the next lowest excited state is generated via a MLCT transition to the ppy

ligand. This implies that theoretical calculations should not be relied upon too heavily for these complexes, where the relative energies of molecular orbitals may be very similar.

According to these calculations, upon exchange of ppy for pba the character of the HOMO and LUMO remain unchanged, whilst the LUMO+1 orbital switches to pba character rather than bpy character. Photophysical measurements imply that emission is primarily pba-LC, possibly with some MLCT mixing. This suggests that the pba-based orbital calculated as the LUMO+1 orbital here may actually be lower in energy, enabling it to become the LUMO. Additionally, it is likely that the HOMO-1 orbital, calculated here of pba character, is of very similar energy to the metal-based HOMO, thus giving rise to a mixture of LC and MLCT characteristic emission.

The orbital character of dimethylamino-substituted complexes **48 - 51** is of particular interest, with the calculated HOMO and LUMO both being localised on the bpy ligand. When comparing the electron density distribution over the bpy ligand it is found that almost half of the electron density is located on the NMe$_2$ group in the HOMO, whilst almost none is found at the same site in the LUMO (Figure 84). This suggests that an ILCT transition originating from the NMe$_2$ group could be responsible for a low energy state. This provides evidence to support the ILCT rationalisation used to explain the low quantum yield associated with complexes **48** and **49** (see section 3.1.3.2) and the increased emission intensity upon acidification (see section 3.1.4.1).
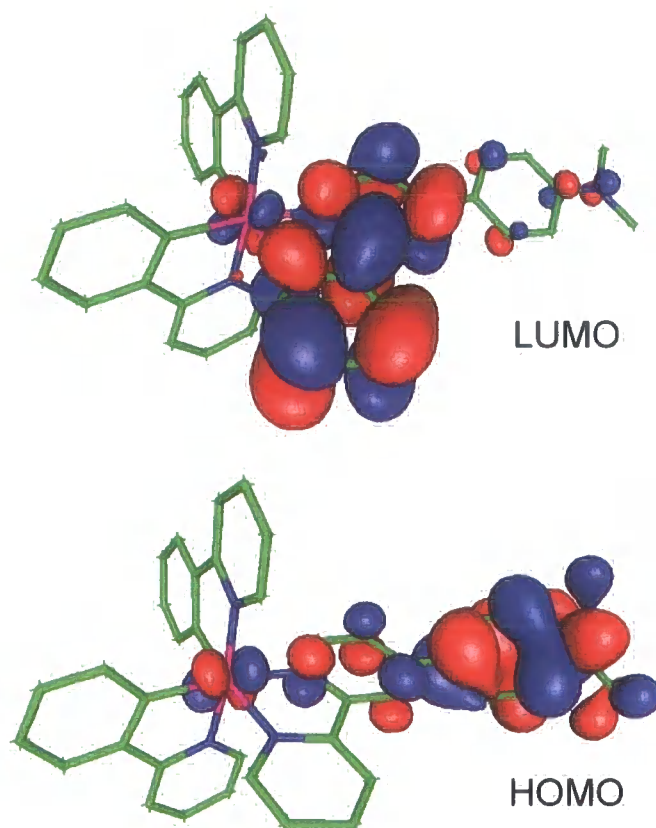
Figure 84 Contour plots of the HOMO and LUMO of [Ir(ppy)₂(bpy-φ-NMe₂)]⁺ 48

In an extension to this work, further calculations were carried out on similar complexes also carrying pendent dimethylamino functionality, and on an iridium complex with a pendent electron donating pyrene substituent. The results obtained for Pt(dpyb-φ-NMe₂)Cl, [Ir(tpy-φ-NMe₂)₂]³⁺ and [Ir(tpy)(tpy-φ-pyr)]³⁺, where dpyb-φ-NMe₂ is 1,3-di(2-pyridyl)-5-(*p*-Me₂N-C₆H₄)-benzene, tpy-φ-NMe₂ is 4′-(*p*-Me₂N-C₆H₄)-2,2′:6′,2″-terpyridine and tpy-φ-pyr is 4′-(1-pyrenyl)-2,2′:6′,2″-terpyridine, are summarised in Table 15.

Complex	HOMO - 1	HOMO	LUMO	LUMO + 1
Pt(dpyb-φ-NMe₂)Cl	Cl (39%) + dpyb (38%) + Pt (23%)	dpyb (33% NMe₂)	dpyb (0.1% NMe₂)	dpyb (5% NMe₂)
[Ir(tpy-φ-NMe₂)₂]³⁺	tpy (21% NMe₂)	tpy (21% NMe₂)	tpy (2.2% NMe₂)	tpy (2.1% NMe₂)
[Ir(tpy)(tpy-φ-pyr)]³⁺	tpy-φ-pyr (94% pyr)	tpy-φ-pyr (74% pyr)	tpy (90%)	tpy (97%)

Table 15 Summary of DFT calculated molecular orbital characterstics for complexes carrying amine or other electron donating substituents. Percentages in parenthesis denote the proportion of entire electron density localised at a particular site.

The HOMO and LUMO of [Pt(dpyb-φ-NMe₂)Cl] are both calculated to be localised on the dimethylamino appended ligand (Figure 85), with the same electron density distribution as noted for complexes **48 – 51**. This suggests that for this platinum complex, a low energy ILCT excited state may exist. The photophysical properties of this complex have been reported[202] and indicate that the lowest energy excited state does indeed possess ILCT character, unlike related complexes without strongly electron donating substituents which tend to exhibit LC emission characteristics.
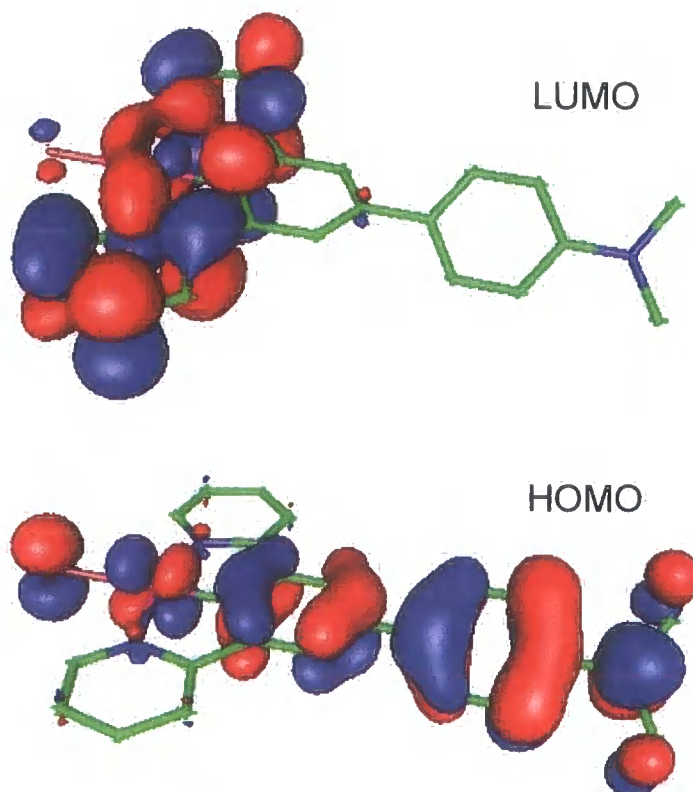
Figure 85 Contour plots of the HOMO and LUMO of [Pt(dpyb-φ-NMe₂)Cl]

For the two iridium-terpyridine complexes investigated, calculations suggest that both the HOMO and LUMO are of ligand character (Figure 86). In particular, electron density within the HOMO is localised on either the dimethylamino or pyrene group, whilst in the LUMO the electron density at these sites is essentially reduced to zero. This implies that low energy ILCT transitions can occur, with the electron rich dimethylamino or pyrene groups acting as donors. The photophysical properties of these complexes have been reported and, indeed, a low energy ILCT state is deduced as responsible for emission in the near IR.[203] The similar results obtained from computational and photophysical methods in this instance are encouraging, and demonstrate that DFT calculations do provide some degree of reliable interpretation of molecular orbitals. However, other results do imply that it is wise to treat them with

some caution, especially where close lying energy levels may exist.
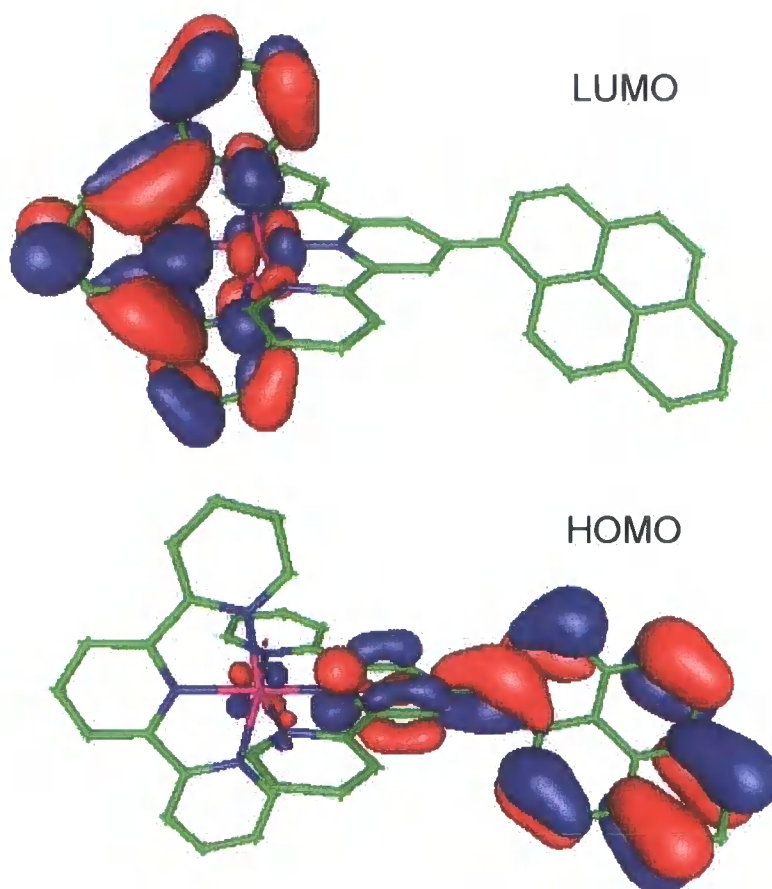
Figure 86 Contour plots of the HOMO and LUMO of [Ir(tpy)(tpy-φ-pyr)]³⁺

3.3 Photophysical properties of [Rh(C^N)₂(N^N)]⁺ complexes

The photophysical properties of [Rh(ppy)₂(bpy)]⁺ **25** have been reported previously and differ substantially from those discussed for the analogous iridium complex [Ir(ppy)₂(bpy)]⁺ **24**. Investigation of these properties was carried out as part of this work in order to obtain directly comparable data in the same solvent and under the same conditions, and results are summarised as part of Table 16.

The absorption spectrum obtained for **25** in acetonitrile almost exactly matches that recorded in methanol.[5] However, using our equipment, no measurable emission was observed at room temperature in aerated or degassed acetonitrile solutions. Indeed, reports state that only very weak emission has been observed for this complex at ambient temperature with the lifetime being < 10 ns.[5] At 77K, an intense and structured emission is reported to arise from an LC state associated with the cyclometalating ligand, although some mixing with an MLCT state has been suggested.[5,79] It has been postulated that this LC emissive state can be deactivated at

room temperature by a low lying MC state.[79]

Complex	**25**	**28**	**30**
Absorption Maxima /nm (ε /M^{-1} cm^{-1})	367 (4260) 308 (17200) 298 (18600) 257 (29000) 240 (28600)	355 (6840) 308 (23700) 296 (26700) 255 (43100) 240 (43200)	350 (4960) 308 (23800) 297 (24100) 255 (38700) 232 (41500)
Emission Maximum /nm	none observed	none observed	none observed

Table 16 Photophysical properties of [Rh(ppy)$_2$(bpy)]$^+$ 25, [Rh(ppy-F)$_2$(bpy)]$^+$ 28 and [Rh(ppy-F$_2$)$_2$(bpy)]$^+$ 30 measured in acetonitrile at 298K.

It could be imagined that the introduction of electron-withdrawing substituents into the ppy ligands in [Rh(C^N)$_2$(bpy)]$^+$ type complexes could perturb the resulting photophysical properties. By withdrawing electron density from the metal centre, the relative energies of the emissive and deactivating excited states will change, perhaps to such an extent that thermal equilibration between the non-emissive MC state and the emissive state is no longer possible at room temperature. This could potentially bring about observable emission at room temperature. For complexes **28** and **30**, which contain one or two fluorine substituents per ppy ligand respectively, this was found not to be the case. The electron-withdrawing effect of the fluorine substituents is apparently not sufficient to prevent deactivation of the emissive state at room temperature.

However, work done by Lo *et al*[95] uses the aldehyde-containing ligand pba in place of ppy and reports a moderately intense emission at room temperature from [Rh(pba)$_2$(bpy)]$^+$ **26**. Clearly, the electron-withdrawing nature of this substituent is sufficient to alter the relative energies of the emissive and deactivating states. This complex was studied as part of this work alongside the related complex **55** containing a phenyl substituent at the 4-position of the bpy ligand (Table 17).

Complex	26	55
Absorption Maxima /nm (ε /M^{-1} cm^{-1})	392 (6260) 317 (24100) 308 (36400) 297 (38400) 273 (32600) 255 (35000) 243 (35400)	393 (4810) 317 (27300) 310 (32100) 295 (34000) 272 (41600) 254 (34600) 243 (32300)
Emission Maximum[a] /nm	508, 546, 584(sh)	508, 546, 584(sh)
Quantum Yield x 10^2 degassed (aerated)	0.90 (0.10)	0.90 (0.10)
Lifetime /ns degassed (aerated)	7475, 1072 (598, 20)	7896, 1210 (620, 30)

Table 17 Photophysical properties of [Rh(pba)$_2$(bpy)]$^+$ 26 and [Rh(pba)$_2$(bpy-ϕ)]$^+$ 55 measured in acetonitrile at 298K. [a] λ_{ex} = 400 nm.

Photophysical data collected for [Rh(pba)$_2$(bpy)]$^+$ **26** compares favourably with that reported by Lo *et al*[95]. Emission is deduced to arise from an LC state associated with the pba ligand based on the structured emission observed (Figure 87), remarkably long emissive lifetime and independence of emission energy on the N^N ligand (as investigated in Lo's work[95]). As expected, the introduction of a phenyl substituent to the bpy ligand in complex **55** does not affect the photophysical properties of the complex, as this ligand is not involved in generation of the emissive excited state.
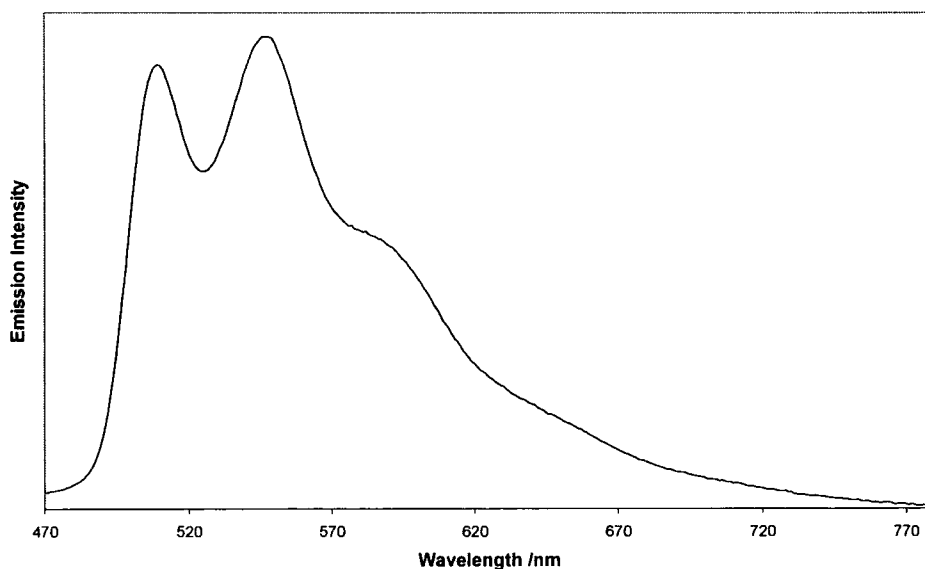
Figure 87 Emission spectrum of [Rh(pba)$_2$(bpy-ϕ)]$^+$ 55 recorded in acetonitrile at 298K.

3.4 Photophysical properties of [Ru(N^N)₃]²⁺ complexes

The photophysical properties of ruthenium tris-bipyridine complexes have been extensively studied.[3] The prototypical complex [Ru(bpy)₃]²⁺ is reported to display relatively long-lived emission at room temperature, which is attributed to an MLCT excited state. This is in stark contrast to ruthenium bis-terpyridine complexes, in which distortion from an ideal octahedral geometry brings about quenching of the emissive excited state via a low lying MC state.[193]

In this work, the effect of adding a phenyl substituent to the 4-position of one of the bpy ligands in [Ru(bpy)₃]²⁺ was investigated. Results are summarised in Table 18 with comparison to both the unsubstituted parent complex and [Ru(bpy)₂(φ-bpy-φ)]²⁺ where φ-bpy-φ is 4,4'-biphenyl-2,2'-bipyridine.

Complex	[Ru(bpy)₃]²⁺ (b)	58	[Ru(bpy)₂(φ-bpy-φ)]²⁺ (b)
Absorption Maxima/nm (ε /M⁻¹ cm⁻¹)	450 (lowest energy absorption)	454 (16900) 430 (14000) 399 (7030) 288 (84100) 253 (35000) 246 (36300)	458 (lowest energy absorption)
Emission Maximum /nm	611 - 620	627 (a)	628
Quantum Yield x 10² degassed (aerated)	5.9 - 8.6	9.0 (1.5)	-
Lifetime /ns degassed (aerated)	860 - 890	1291 (196)	-

Table 18 Photophysical properties of [Ru(bpy)₂(bpy-φ)]²⁺ 58 in comparison with [Ru(bpy)₃]²⁺ and [Ru(bpy)₂(φ-bpy-φ)]²⁺ where φ-bpy-φ is 4,4'-biphenyl-2,2'-bipyridine measured in acetonitrile at 298K. (a) λ_{ex} = 455 nm. (b) taken from reference[3]

The introduction of a phenyl-substituent into one of the bpy ligands in complex 58 results in a red shift in the emission intensity when compared to the parent unsubstituted complex. This has also been observed for related complex [Ru(bpy)₂(φ-bpy-φ)]²⁺ in the same solvent.[204] Photophysical studies on [Ru(bpy)₂(φ-bpy-φ)]²⁺ in other solvents and at low temperature have revealed that emission remains MLCT in character but may involve three equilibrated states.[205,206] It is possible that the electron donating ability of the phenyl-substituent is responsible for either lowering the energy of the ligand orbitals or increasing the metal orbitals, thus reducing the energy of the resulting MLCT state.

3.5 Concluding remarks

The photophysical properties of a number of monometallic complexes are reported. The effect of substituents in both the C^N and N^N coordinating ligands of [Ir(C^N)$_2$(N^N)]$^+$ complexes has been investigated, with the pH dependence of emission being determined for those complexes bearing either protonatable pyridyl or dimethylamino groups, or deprotonatable hydroxy substituents. Computational studies support the suggested existence of a low energy ILCT state, which may be responsible for some of the pH responsive emission characteristics observed. The attempted use of electron-withdrawing fluorine substituents to bring about emission from analogous rhodium complexes has proved unsuccessful, although the use of pba leads to emissive complexes. The photophysical properties found for these monometallic complexes will be exploited for the design of multimetallic systems in which the channelling of energy is desired.

CHAPTER 4

SYNTHESIS OF MULTIMETALLIC COMPLEXES

4 Synthesis of Multimetallic Complexes

The synthesis of heterometallic systems has most often involved the pre-synthesis of ligands followed by stepwise complexation procedures. The 'complexes as metals, complexes as ligands' approach is an example of this where complexes containing labile ligands are used as synthetic equivalents to 'metals', whilst complexes with ligands containing free chelating sites act as 'complex ligands'.[7,9] However, in order to gain control over the final assembly structure using this technique, it is necessary to introduce protection and deprotection steps, for example by using methylation to block a potential binding site.[154-157]

More recently, the use of metal catalysed cross-coupling reactions has been investigated for the generation of multimetallic systems. There are two angles from which this type of synthesis can be approached. The first involves *in situ* reactions on the back of a metal complex in order to produce a new chelating site, which can in turn be complexed to a second metal centre. Both nickel[173] and palladium[116,172] catalysed reactions have been used for this purpose. Alternatively, cross-coupling reactions can be used for the direct joining of two or more metal complexes.

The Sonogashira reaction has been studied for this purpose.[137,174,178] Initially multimetallic systems were generated via the coupling of bromo-substituted complexes with organic multi-ethynylated compounds,[136] but this technique can only ever form homonuclear and symmetrical systems. Subsequent reports by the same group[175,176] detail the direct cross coupling of bromo- and ethynyl-substituted complexes for the controlled synthesis of multimetallic systems in good yields (Figure 88).
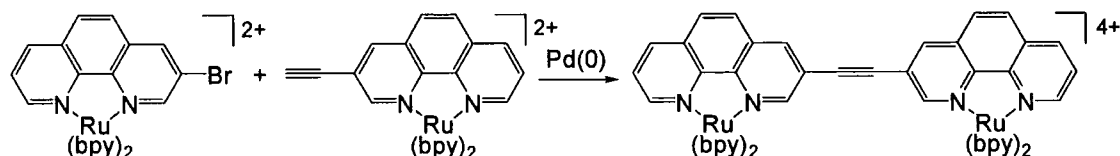
Figure 88 Sonogashira coupling of metal complexes to generate bimetallic systems[175]

The Suzuki cross-coupling reaction has also been used for the generation of multimetallic species, with successful couplings between bromo-substituted metal complexes and purely organic aryl boronic acids (Figure 89) having been described.[181,182] Some further papers have been published on this topic during the course of this work,[88,183] however, no reports of direct couplings between bromo- and

boronic acid functionalised metal complexes have been reported to date.
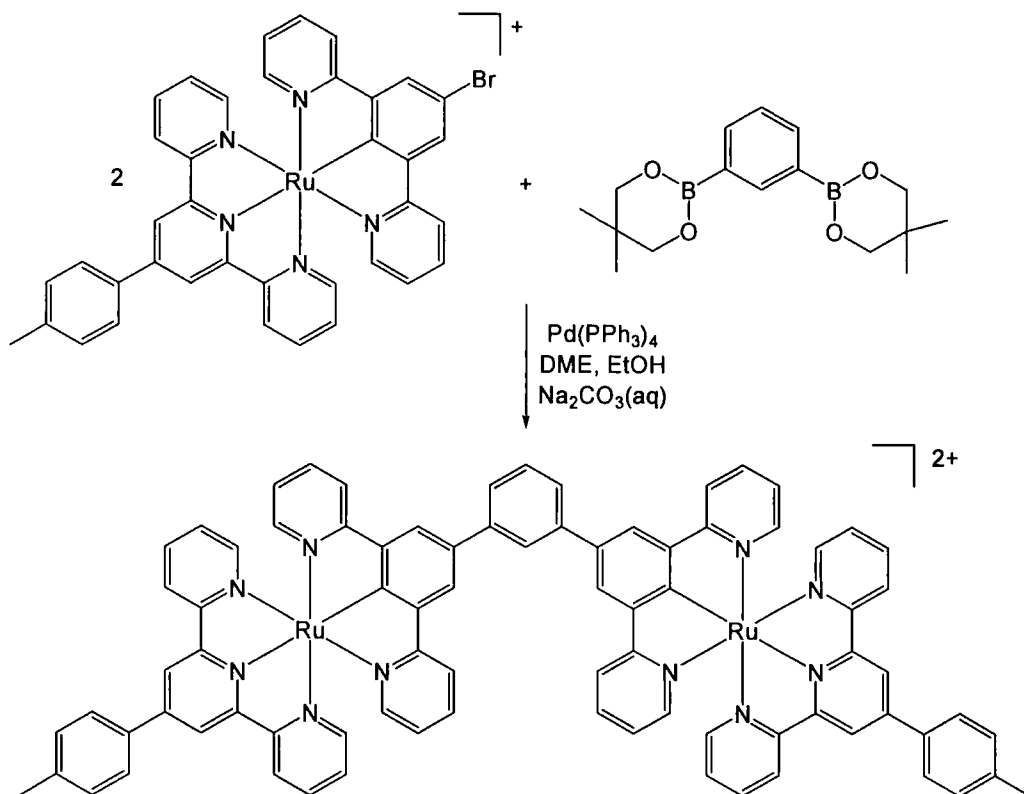
Figure 89 Suzuki cross-coupling to generate multimetallic species[181]

The work presented in this chapter addresses this area and investigates the use of the Suzuki cross-coupling reaction for the direct coupling of appropriately functionalised metal complexes, in order to provide a simple, reliable, versatile and controlled synthesis of multimetallic systems (Figure 90). Chapter 2 details the synthesis of monometallic metal complexes which incorporate the necessary pendent bromo- or boronic acid functionalities. Within the current chapter, the cross-coupling of these building blocks to generate bi- and trinuclear complexes is discussed, followed by the *in situ* elaboration of these multimetallic species to allow access to higher order systems.
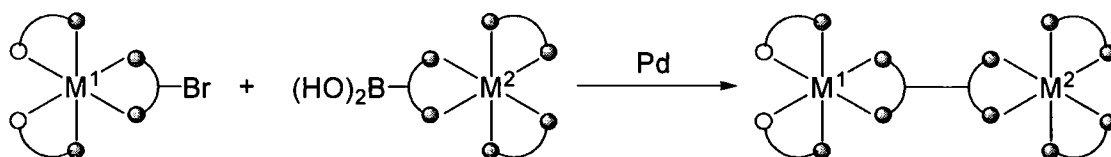
Figure 90 Schematic representation of the Suzuki reaction for the direct coupling of appropriately substituted metal complexes

4.1 Suzuki couplings between monometallic building blocks

In the first instance, Suzuki cross-coupling reactions were studied between appropriately functionalised monometallic building blocks. At the start of this work, there were a few isolated reports showing that metal complexes containing bromo-substituted polypyridyl ligands can undergo successful Suzuki cross-coupling reactions with aryl boronic acid species,[141,181,182] and indeed some of the earlier work presented in Chapter 2 demonstrates this. The electron withdrawing effect of coordinating the ligand to a metal centre is believed to facilitate the oxidative addition step involved in the catalytic cycle. However, the reactivity and general behaviour of unreported boronic acid substituted metal complexes were unknown.

It was of interest to use this synthetic technique to produce multimetallic arrays capable of funnelling energy to one specific terminus. In order to create this channelling effect, the building blocks involved are required to have excited state energies within a particular range. For instance, monometallic complex [Ir(ppy)$_2$(bpy-ph)]$^+$ 52 has an emission wavelength of 613 nm, rendering it higher in energy than [Ru(bpy)$_2$(bpy-ph)]$^{2+}$ 58 which emits at 627 nm. By combining these two building blocks to form a single molecule, it is expected that energy transfer would take place in the iridium to ruthenium direction (Figure 91) if the bridging ligand does not greatly affect the excited state properties of the multimetallic species. This allows the design of multimetallic arrays in which it may be possible to predict reliably the direction of energy transfer.
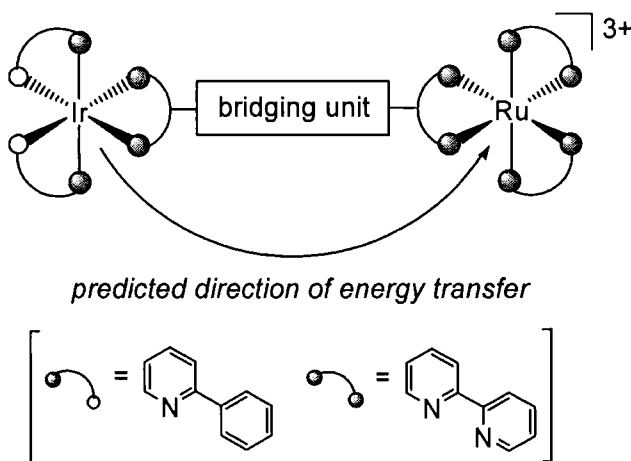
Figure 91 Predicted energy transfer direction for bimetallic species containing
[Ir(C^N)$_2$(N^N)]$^+$ and [Ru(bpy)$_3$]$^{2+}$ building blocks

4.1.1 [Ir(C^N)₂(N^N)]⁺ and [Ru(bpy)₃]²⁺ building blocks

Suzuki reactions were carried out in an attempt to cross-couple iridium complexes of the type [Ir(C^N)₂(N^N)]⁺, containing a bromo-substituent on either the N^N or C^N coordinating ligand, with a boronic acid substituted complex. In all cases the conditions employed were based on those previously reported for the Suzuki coupling of bromo-substituted iridium 2,2':6',2''-terpyridine complexes with aryl boronic acids:[142] a Pd(PPh₃)₄ catalyst and aqueous sodium carbonate base in degassed DMSO solvent. Complexes prepared via this route are summarised in Table 19.

No.	Bromo Reagent [Ir(C^N)₂(N^N)]⁺		Boronic Acid Reagent [M(L)₂(bpy-φ-B(OH)₂)]ⁿ⁺		Product
	C^N ligand	N^N ligand	C^N/N^N ligand (L)	Metal	
67	ppy	bpy-Br	bpy	Ru	Ir-φ-Ru
68	ppy	bpy-φ-Br	bpy	Ru	Ir-φ-φ-Ru
69	ppy-Br	bpy	bpy	Ru	[Ru-φ]₂-Ir
70	ppy-Br	bpy	ppy-F₂	Ir	[Ir^F2-φ]₂-Ir

Table 19 Multimetallic species obtained via direct coupling of monometallic building blocks using the Suzuki reaction

Bromo-substituted iridium complexes [Ir(ppy)₂(bpy-Br)][PF₆] **32** and [Ir(ppy)₂(bpy-φ-Br)][PF₆] **37** were independently reacted with [Ru(bpy)₂(bpy-φ-B(OH)₂)][PF₆]₂ **57** to generate the heteronuclear iridium-ruthenium bimetallic species Ir-φ-Ru **67** and Ir-φ-φ-Ru **68** respectively, both in 66% yield. In fact, the successful syntheses of **67** and **68** proceeded remarkably cleanly, with the main side product being identified as deboronated ruthenium complex **58**, which was removed via column chromatography.

Figure 92 Synthesis of Ir-φ-Ru 67 and Ir-φ-φ-Ru 68 using the Suzuki reaction

In order to investigate the possibility of carrying out simultaneous Suzuki couplings to create trimetallic species, the dibrominated iridium complex **46**, containing two brominated ppy ligands, was reacted on separate occasions with [Ru(bpy)$_2$(bpy-ϕ-B(OH)$_2$)][PF$_6$]$_2$ **57** and [Ir(ppy-F$_2$)$_2$(bpy-ϕ-B(OH)$_2$)][PF$_6$] **61** (Figure 93). By employing the same Suzuki reaction conditions, trimetallic species [Ru-ϕ]$_2$-Ir **69** and [Ir^{F2}-ϕ]$_2$-Ir **70** were isolated and purified via column chromatography. Although [Ir^{F2}-ϕ]$_2$-Ir **70** carries an overall +3 charge, as this is spread over what is essentially equivalent to three monometallic complexes, the R$_f$ of this complex is very similar to that of the starting materials, rendering purification more difficult in this case.

Figure 93 Synthesis of [Ru-ϕ]$_2$-Ir 69 and [Ir^{F2}-ϕ]$_2$-Ir 70 using the Suzuki reaction

4.1.2 Building blocks containing 2,2':6',2"-terpyridine ligands

The examples considered so far involve a combination of ppy and bpy based ligands with iridium and ruthenium metal centres. The synthesis of iridium and ruthenium complexes containing bromo-substituted 2,2':6',2"-terpyridine ligands was carried out in order to investigate the use of the Suzuki cross-coupling reaction for the generation of mixed ligand multimetallic species with unsymmetrical bridging ligands, which may otherwise be time consuming and complicated to pre-synthesise.

By applying the same Suzuki reaction conditions, successful cross couplings were achieved between [Ir(tpy)(tpy-ϕ-Br][PF$_6$]$_3$ **65** and [Ru(bpy)$_2$(bpy-ϕ-B(OH)$_2$)][PF$_6$]$_2$ **57**, and between [Ru(tpy)(tpy-ϕ-Br)][PF$_6$]$_2$ **66** and [Ir(ppy)$_2$(bpy-ϕ-B(OH)$_2$)][PF$_6$] **59** to give rise to heterometallic dimeric species ^{tpy}Ir-ϕ-ϕ-Ru^{bpy} **71** and ^{tpy}Ru-ϕ-ϕ-Ir^{ppy} **72** (Figure 94). Separation of complex **71** from unreacted [Ir(tpy)(tpy-ϕ-Br)]$^{3+}$ proved difficult due

97

to similar R_f values, but was achieved after multiple purifications via column chromatography.

Figure 94 Synthesis of ^{tpy}Ir-φ-φ-Ru^{bpy} 71 and ^{tpy}Ru-φ-φ-Ir^{ppy} 72 using the Suzuki reaction

4.2 Generation of larger multimetallic systems: in situ Suzuki couplings on multimetallic species

The work reported above shows that the Suzuki cross-coupling reaction can be used as a powerful tool for the controlled synthesis of multimetallic systems. However, the examples given so far involve coupling reactions between monometallic building blocks, and as such the number of metal centres involved has been limited to two or three. As an extension to this work, the use of the Suzuki reaction for the elaboration of multimetallic species *in situ* has been investigated, in an effort to develop a divergent and controlled method for the generation of larger multimetallic systems.

4.2.1 Bromination of dimeric species

In Chapter 2, the regiospecific bromination of monometallic complexes of the type [Ir(C^N)₂(N^N)]⁺ was discussed. Providing that the phenyl ring of the C^N ligand was not fluoro-substituted, bromination at the site *para* to cyclometalation was found to proceed smoothly at room temperature in the presence of N-bromosuccinimide in acetonitrile. The application of this reaction to multimetallic complexes containing [Ir(C^N)₂(N^N)]⁺ moieties would allow access to brominated species which could be used in further cross-coupling reactions to create higher order systems (Figure 95).
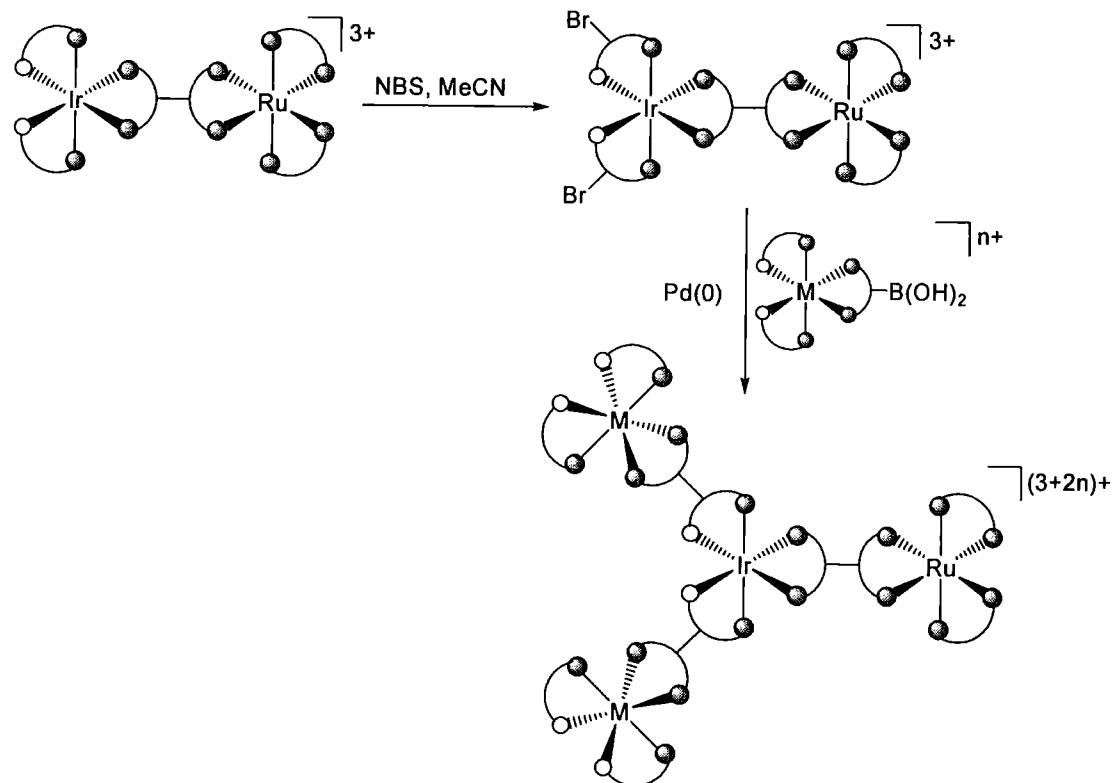
Figure 95 General scheme for the *in situ* elaboration of multimetallic species to generate higher order systems

Reaction of the bimetallic complexes Ir-φ-Ru **67** and Ir-φ-φ-Ru **68** with NBS in acetonitrile at room temperature was successful in producing the dibrominated species Ir^{Br2}-φ-Ru **73** and Ir^{Br2}-φ-φ-Ru **74** respectively (Figure 96). Excellent yields were obtained following ion exchange to isolate the hexafluorophosphate salt and no further purification was required before using these species in subsequent cross-coupling reactions.
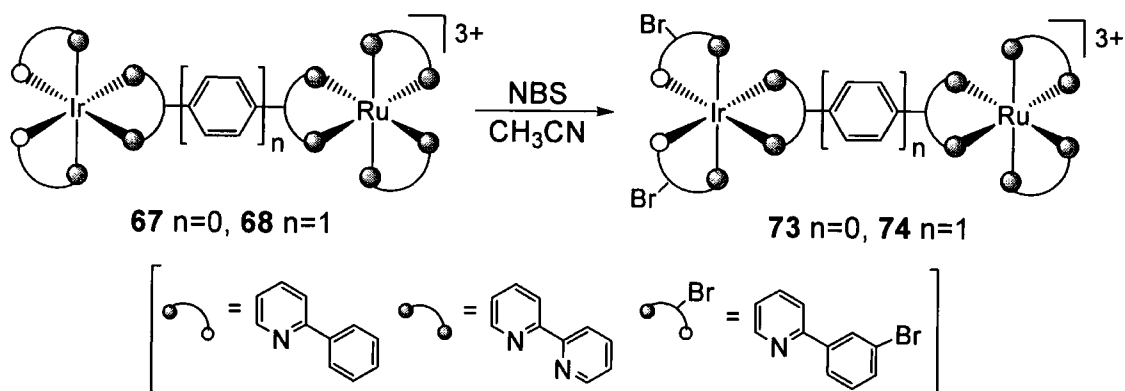
Figure 96 Dibromination of dimeric species to produce Ir^{Br2}-φ-Ru 73 and Ir^{Br2}-φ-φ-Ru 74

4.2.2 Suzuki couplings to generate tetrameric species

Having the ability to exert some control over the direction of energy transfer in multimetallic species by careful selection of the peripheral building blocks is an attractive prospect. In order to extend brominated complexes **73** and **74** to tetrameric species possessing this energy-channelling ability, the boronic acid appended complexes chosen for the Suzuki reaction must provide a building block of at least equal, but preferably higher energy than those already incorporated. [Ir(ppy)$_2$(bpy-ϕ-B(OH)$_2$)]$^+$ **59**, [Ir(ppy-F)$_2$(bpy-ϕ-B(OH)$_2$)]$^+$ **60**, [Ir(ppy-F$_2$)$_2$(bpy-ϕ-B(OH)$_2$)]$^+$ **61** and [Rh(pba)$_2$(bpy-ϕ-B(OH)$_2$)]$^+$ **62** were selected as candidates to fulfil this role based on the emission energies for the respective [M(C^N)$_2$(bpy-ϕ)]$^+$ units as reported in Chapter 3. An example structure indicating the predicted direction of energy transfer is shown in Figure 97.
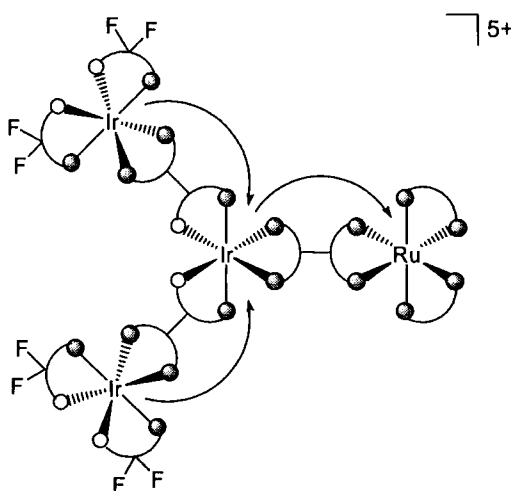
Figure 97 Predicted direction of energy transfer for an example tetrameric species

Investigation into the use of the Suzuki reaction to couple the dibrominated binuclear complexes Ir^{Br2}-ϕ-Ru **73** and Ir^{Br2}-ϕ-ϕ-Ru **74** with these boronic acid substituted metal complexes was carried out. Successful reactions of this type require that two simultaneous Suzuki couplings take place, as seen for the synthesis of trinuclear complexes **69** and **70**. Tetranuclear complexes produced via cross-couplings carried out in degassed DMSO in the presence of aqueous sodium carbonate base and Pd(PPh$_3$)$_4$ catalyst are summarised in Table 20 with the general scheme outline in the accompanying figure (Figure 98). These reactions were observed to proceed relatively cleanly, with excess boronic acid substituted complexes being removed via column chromatography. The synthesis of mixed metal species [Rh-ϕ]$_2$-Ir-ϕ-Ru **78** demonstrates that the Suzuki coupling can be extended to include rhodium based building blocks as well as those containing iridium and ruthenium.
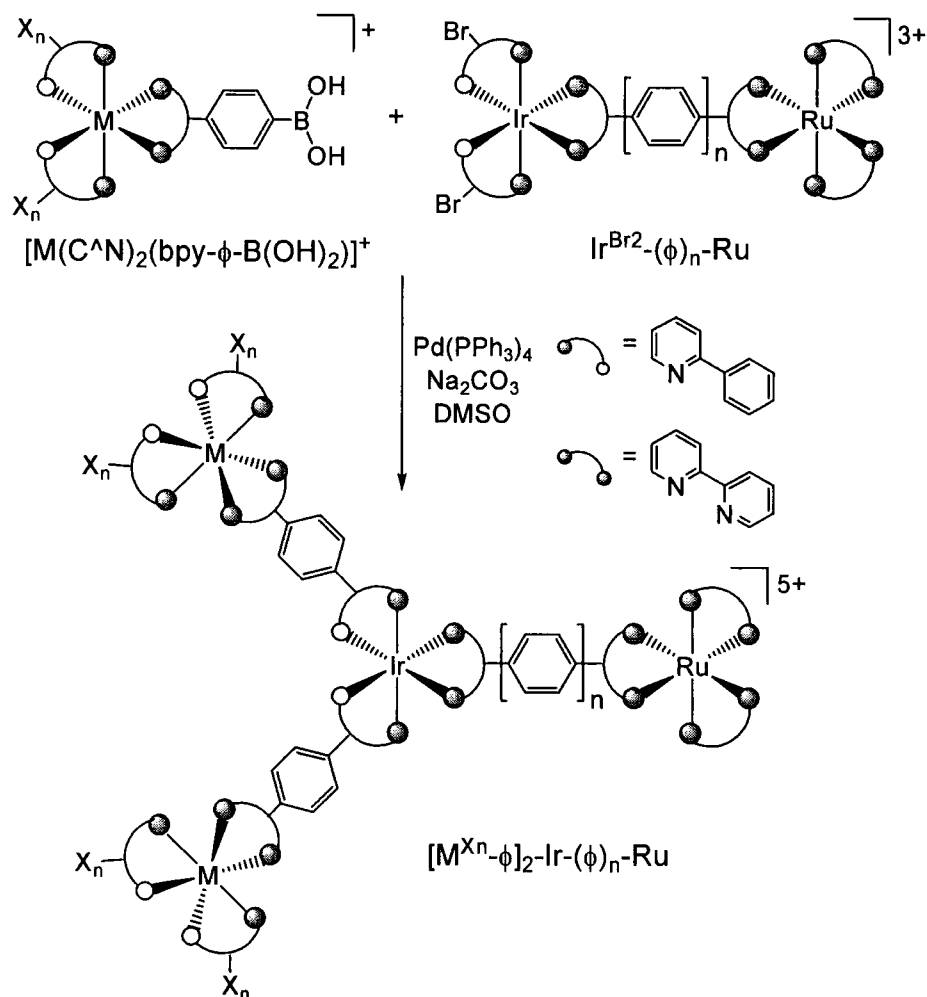
Figure 98 General scheme for the production of tetrameric species using the Suzuki reaction

No.	Bromo reagent	Boronic acid reagent	Product	Yield
75	Ir^{Br2}-ϕ-ϕ-Ru **74**	[Ir(ppy)$_2$(bpy-ϕ-B(OH)$_2$)]$^+$ **59**	[Ir-ϕ]$_2$-Ir-ϕ-ϕ-Ru	51%
76	Ir^{Br2}-ϕ-ϕ-Ru **74**	[Ir(ppy-F)$_2$(bpy-ϕ-B(OH)$_2$)]$^+$ **60**	[Ir^F-ϕ]$_2$-Ir-ϕ-ϕ-Ru	41%
77	Ir^{Br2}-ϕ-ϕ-Ru **74**	[Ir(ppy-F$_2$)$_2$(bpy-ϕ-B(OH)$_2$)]$^+$ **61**	[Ir^{F2}-ϕ]$_2$-Ir-ϕ-ϕ-Ru	41%
78	Ir^{Br2}-ϕ-Ru **73**	[Rh(pba)$_2$(bpy-ϕ-B(OH)$_2$)]$^+$ **62**	[Rh-ϕ]$_2$-Ir-ϕ-Ru	37%

Table 20 Tetrameric species synthesised using the Suzuki cross-coupling reaction

For all of the tetrameric species described, almost complete assignment of the ^{1}H NMR spectra was achieved with assistance from spectra of the relevant monometallic and bimetallic complexes in the same deuterated solvent, ^{1}H-^{1}H COSY spectra and ^{1}H-^{1}H ROESY spectra. These compounds were found to be too large for ^{1}H-^{1}H NOESY spectra to be obtained. An example of an assigned ^{1}H NMR spectrum is given for complex **77** in Figure 99.

101
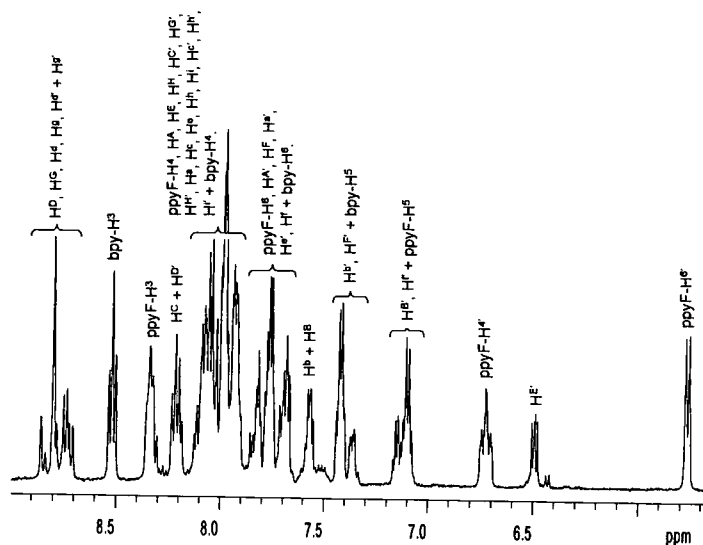
Figure 99 ^{1}H NMR spectrum for tetrameric complex 77 measured at 500 MHz

The large positive charge associated with the complexes makes them ideal for characterisation via electrospray mass spectrometry. A series of peaks can be reported for various combinations of the complex with different numbers of hexafluorophosphate anions. Whilst high resolution electrospray mass spectrometry produced excellent agreements between measured and calculated masses, the number of molecular formulae that matched the calculated mass within 5 ppm and involved only those atoms contained within the desired complex was rather high. As such, to support the mass measurements, it was found that isotope peak matching could be used and provides a definitive proof of identity of the complex. This is demonstrated in Figure 100 for complex 77.
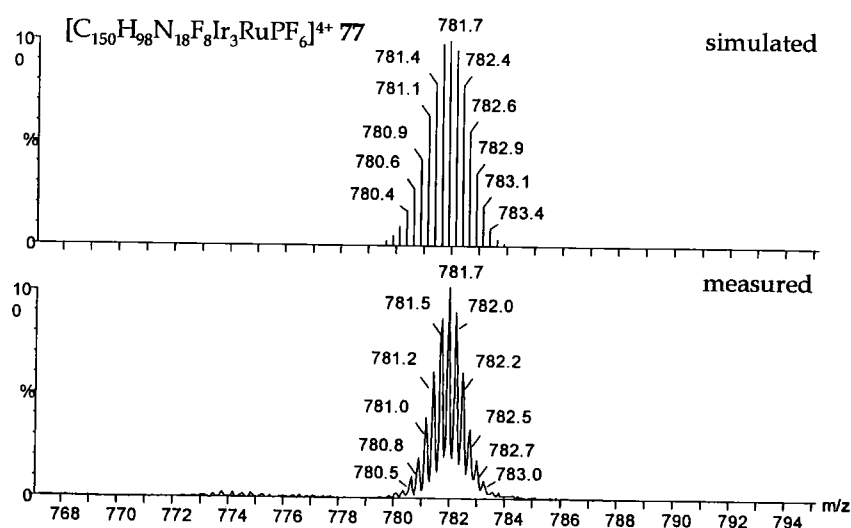
Figure 100 Isotope peak matching for tetrameric complex 77

102

4.2.3 Octanuclear species

To extend the use of the Suzuki cross-coupling reaction for the generation of multimetallic systems one step further, the synthesis of an octanuclear complex was attempted; the simplest way to achieve this being the *in situ* bromination of a terameric species containing four ppy type ligands. The cross-coupling of such a species with an appropriate boronic acid substituted complex would generate a complex containing eight metal centres.

Investigation of the regioselective NBS bromination reaction on monometallic complexes of the type [Ir(C^N)$_2$(N^N)]$^+$ had revealed that the complex containing ppy-F ligands could be brominated *trans* to the site of cyclometalation if the reaction mixture was gently heated. The analogous reaction was attempted for tetrameric species [Ir^F-φ]$_2$-Ir-φ-φ-Ru 76 also containing ppy-F ligands, but a single product could not be isolated (Figure 101). Electrospray mass spectrometry revealed the presence of a mixture of bromination products, including a species containing five bromine atoms. The complexity of the ^{1}H NMR spectrum rendered identification of the site of the 5th bromination impossible.
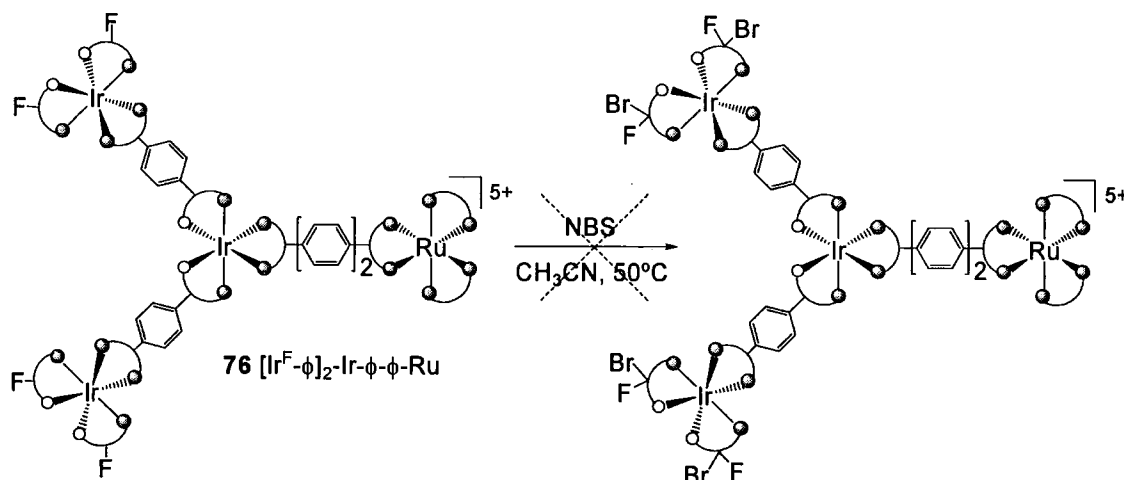
Figure 101 Failed attempt to brominate tetrameric species [Ir^F-φ]$_2$-Ir-φ-φ-Ru 76

Instead, bromination of the tetrameric species [Ir-φ]$_2$-Ir-φ-φ-Ru 75 with unsubstituted ppy ligands was attempted by reaction with NBS in acetonitrile at room temperature. This was successful in brominating tetramer 75 at the four expected positions giving [Ir^{Br2}-φ]$_2$-Ir-φ-φ-Ru 79 in quantitative yield. A subsequent Suzuki reaction between this multiply brominated species and [Ir(ppy-F$_2$)$_2$(bpy-φ-B(OH)$_2$)]$^+$ 61 was successful in producing octameric species [[Ir^{F2}-φ]$_2$-Ir-φ]$_2$-Ir-φ-φ-Ru 80 (Figure 102). Purification via column chromatography proved more difficult in this case, probably due to the increased charge and size of the molecule, which would perhaps make it more suitable

for purification via size exclusion methods or electrophoresis. Full assignment of the ^{1}H NMR was not achieved in this instance due to the large number (194!) of aromatic protons present, although characteristic peaks at either end of the spectrum were identified. Electrospray mass spectrometry and isotope peak matching confirmed the formation of the desired species **80** (Figure 103).
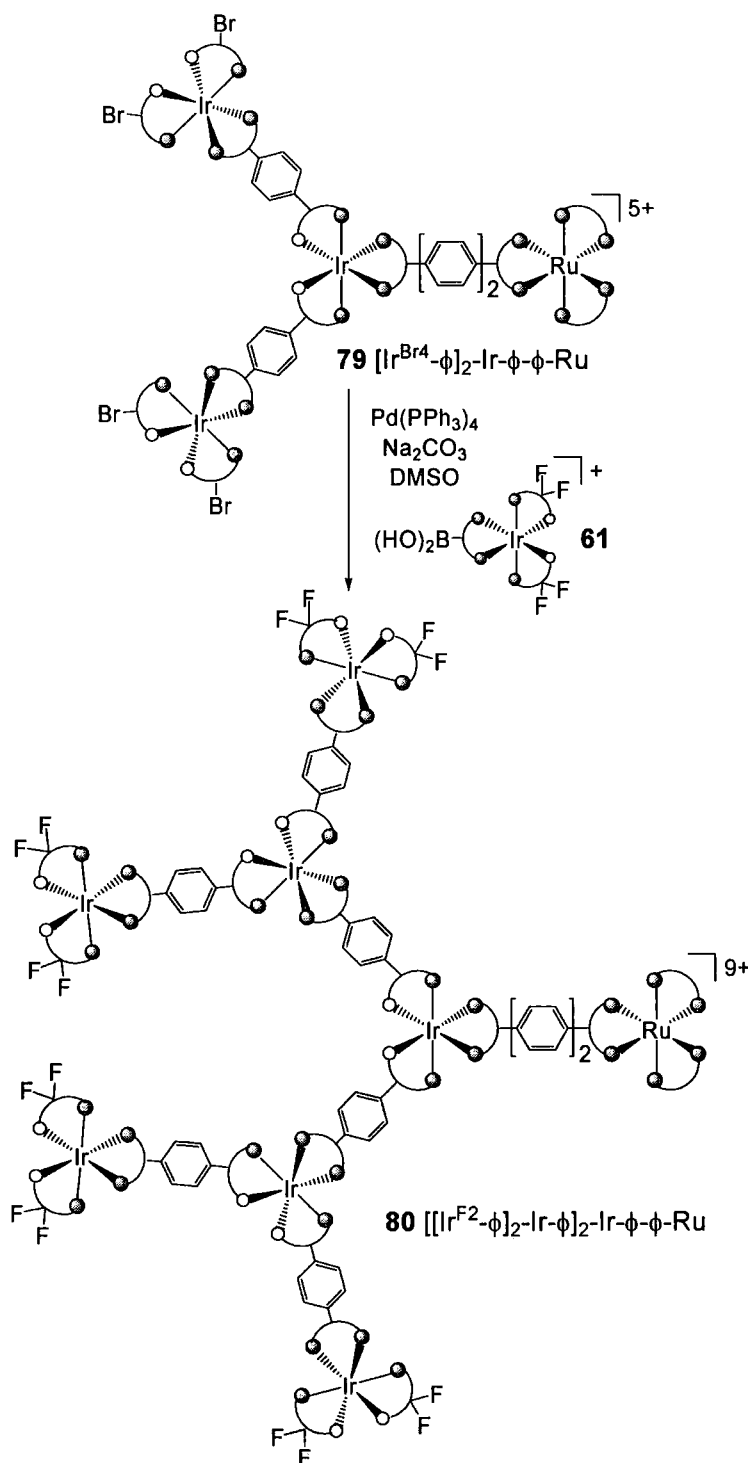
Figure 102 Synthesis of octameric species [[Ir^{F2}-φ]$_2$-Ir-φ]$_2$-Ir-φ-φ-Ru 80 via the Suzuki reaction

$[Ir_7RuC_{302}H_{194}F_{16}N_{34}]^{9+}$ **80**
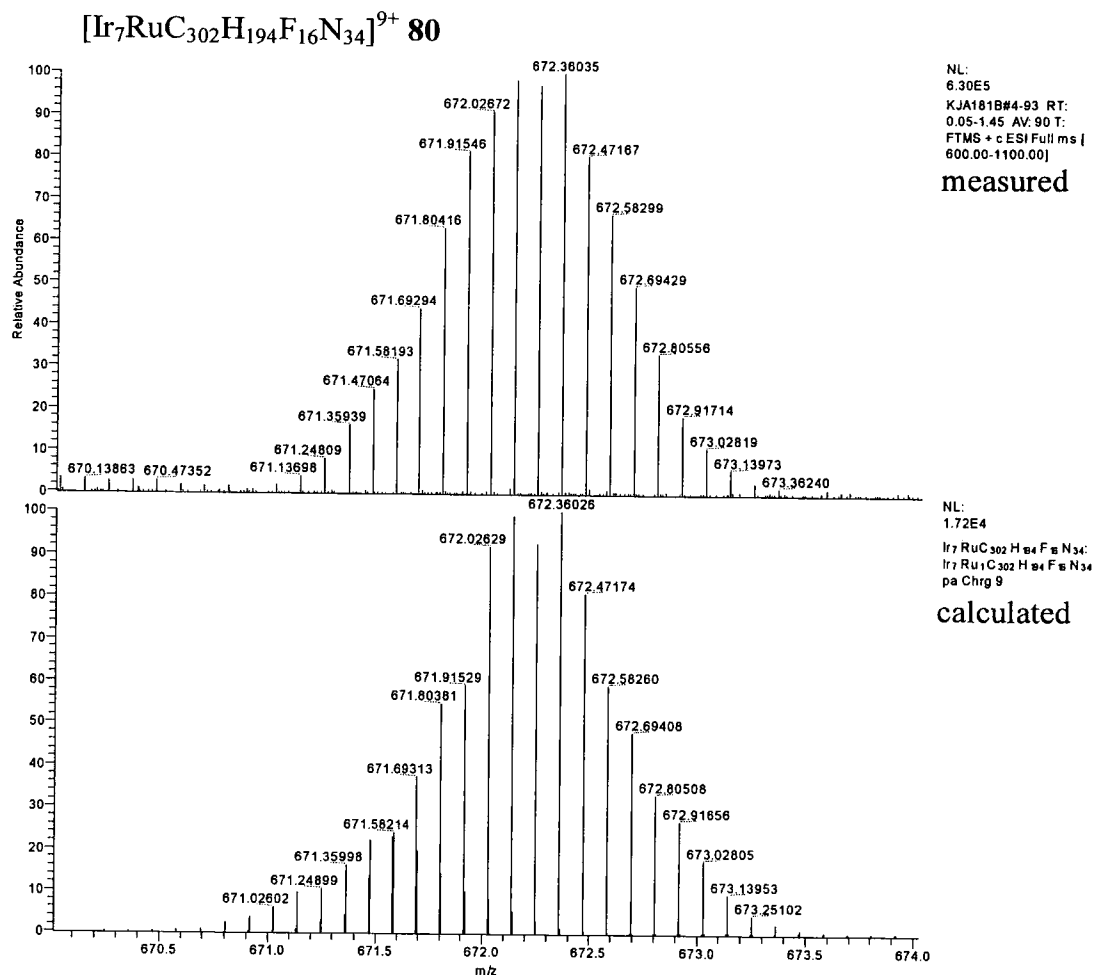
Figure 103 Isotope peak matching for octameric complex 80

4.3 Concluding remarks

The work presented in this chapter provides the first documentation of the successful use of the Suzuki cross-coupling reaction for the direct coupling of bromo- and boronic acid functionalised metal complexes. A series of multimetallic complexes has been synthesised containing from two to eight metal centres, with examples including a combination of ruthenium, iridium and rhodium. A number of coordinating ligands have been used within these complexes including 2,2'-bipyridine, 2-phenylpyridine and 2,2':6',2"-terpyridine type ligands. Whilst initial studies involved the coupling of appropriately functionalised monometallic complexes, the exploitation of a simple and mild *in situ* bromination reaction allows further coupling of multimetallic species in a stepwise divergent manner. The technique presented here avoids both the pre-synthesis of bridging ligands and the need for any protection or deprotection steps. The Suzuki cross-coupling reaction provides a simple, reliable and versatile synthesis for the controlled generation of multimetallic arrays.

CHAPTER 5

PHOTOPHYSICAL STUDY OF MULTIMETALLIC COMPLEXES

5 Photophysical Study of Multimetallic Complexes

The idea of producing multimetallic arrays with energy-channelling abilities, via the careful selection of components which have excited states within a particular energy range, was introduced in chapter 4. In this chapter, the photophysical properties of the new multimetallic complexes prepared by cross-coupling are discussed in an attempt to determine whether or not energy transfer can be reliably predicted based on the properties of monometallic building blocks.

5.1 Photophysical properties of bimetallic complexes

5.1.1 Complexes containing $[Ru(bpy)_3]^{2+}$ and $[Ir(C^\wedge N)_2(N^\wedge N)]^+$ building blocks

As reported in chapter 3, monometallic complex $[Ru(bpy)_2(bpy-ph)]^{2+}$ **58** has an emission maximum of 627 nm in aerated acetonitrile at room temperature, whilst $[Ir(ppy)_2(bpy)]^+$ **24** and $[Ir(ppy)_2(bpy-ph)]^+$ **52** emit at 610 nm and 613 nm respectively under the same conditions. If these two types of building block are combined within the same molecule, it is possible that the resulting bimetallic species may exhibit photophysical properties that are predictable from the properties of the individual components. That is, that energy transfer may take place from the higher energy iridium-based excited state to the lower energy ruthenium-based excited state, thus resulting in emission characteristic of the ruthenium tris-bipyridine moiety. However, this prediction relies entirely upon the bridging ligand having little or no effect upon the excited state energy of the bimetallic complex. If this is the case, then the bimetallic species would be expected to retain the properties previously identified for the individual building blocks.

Throughout this work, the bridging units that are generated via cross-coupling methodology are phenyl or biphenyl linkers, joined via substitution at the *para* position. In order to investigate the effect of these phenyl bridging units on the excited state energy of bimetallic species containing $[Ir(ppy)_2(bpy)]^+$ and $[Ru(bpy)_3]^{2+}$ building blocks, the photophysical properties of bimetallic complexes Ir-ϕ-Ru **67** and Ir-ϕ-ϕ-Ru **68** were studied. A summary of the results obtained is provided in Table 21.

The absorption spectra for both bimetallic complexes display peaks characteristic of the ruthenium and iridium building blocks, with the overall shape of the spectra being similar to those resulting from addition of the spectra belonging to the two relevant building blocks (Figure 104 and Figure 105). This suggests that the iridium and

ruthenium components are retaining the properties exhibited when isolated as monometallic complexes. For complex **68**, containing two phenyl bridging rings, an enhancement in molar absorptivity is observed between 320 and 400 nm attributed to extended conjugation in comparison to the building blocks. This is not observed for complex **67** which only contains one bridging phenyl ring.

Complex	Ir-φ-Ru **67**	Ir-φ-φ-Ru **68**
Absorption Maxima /nm (ε / M^{-1} cm^{-1})	460 (13700) 435 (12200) 365 (15500) 310 (38900) 288 (68700) 255 (44700) 250 (44000)	454 (22500) 430 (20100) 353 (43400) 324 (60200) 288 (112000) 253 (67900) 246 (66800)
Emission Maximum[a] /nm	638	629
Quantum Yield x 10^2 degassed (aerated)	16 (2.1)	11 (1.7)
Lifetime /ns degassed (aerated)	1830 (245)	1590 (225)

Table 21 Photophysical properties of Ir-φ-Ru **67** and Ir-φ-φ-Ru **68** measured in acetonitrile at 298K. [a] λ_{ex} = 455 nm.
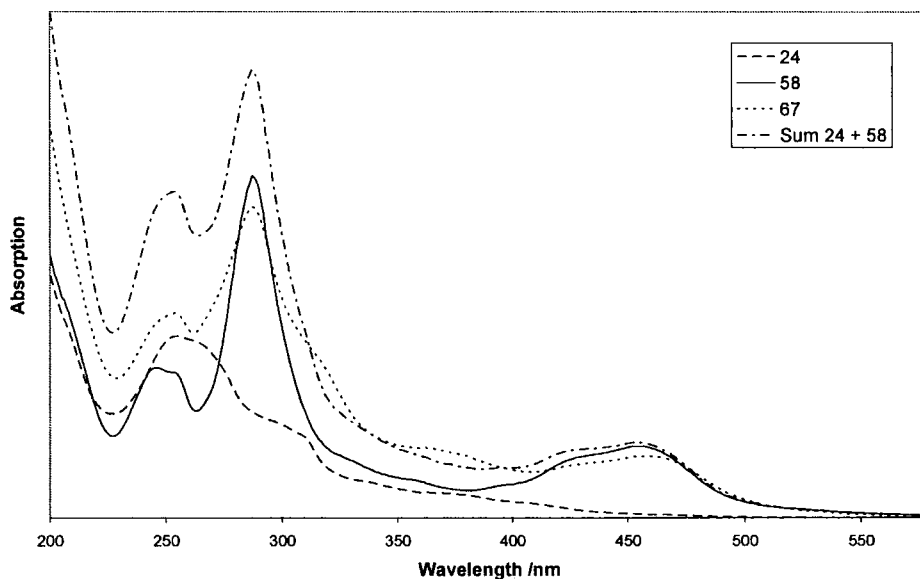
Figure 104 Absorption spectra of Ir-φ-Ru **67** and building blocks [Ir(ppy)$_2$(bpy)]$^+$ **24** and [Ru(bpy)$_2$(bpy-ph)]$^{2+}$ **58**, measured in acetonitrile at 298K.
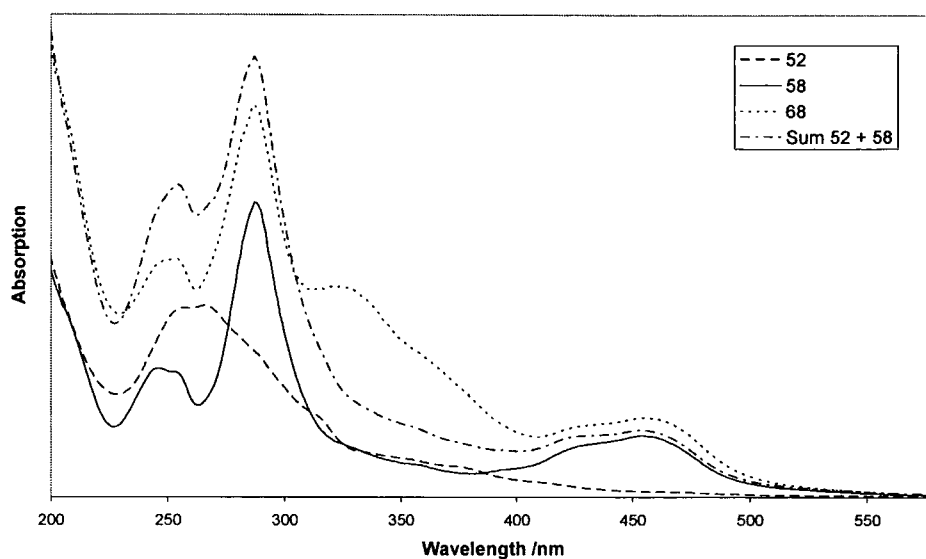
Figure 105 Absorption spectra of Ir-φ-φ-Ru 68 and building blocks [Ir(ppy)₂(bpy-ph)]⁺ 52 and [Ru(bpy)₂(bpy-ph)]²⁺ 58, measured in acetonitrile at 298K.

Upon excitation at any wavelength within the range 300 – 500 nm, a single emission band is observed at 638 nm and 629 nm for Ir-φ-Ru **67** and Ir-φ-φ-Ru **68** respectively, close to that observed for [Ru(bpy)₂(bpy-ph)]⁺ **58** at 627 nm. No emission band is observed at higher energy, in the region where the mononuclear units [Ir(ppy)(bpy)]⁺ or [Ir(ppy)₂(bpy-ph)]⁺ would be expected to emit (Figure 106).

The red shift of emission maximum observed for Ir-φ-Ru **67** may suggest that the ruthenium centre is somewhat perturbed by the iridium centre due to separation by only one phenyl ring. This implies that the iridium complex acts as a more strongly electron withdrawing substituent than a simple phenyl group. For both bimetallic complexes, the excitation spectrum registered at the emission maximum matches the profile of the absorption spectrum (Figure 106). These combined observations provide conclusive evidence that excitation is followed by rapid energy transfer to the ruthenium centre, as can be predicted from the relative energies of the building blocks involved.
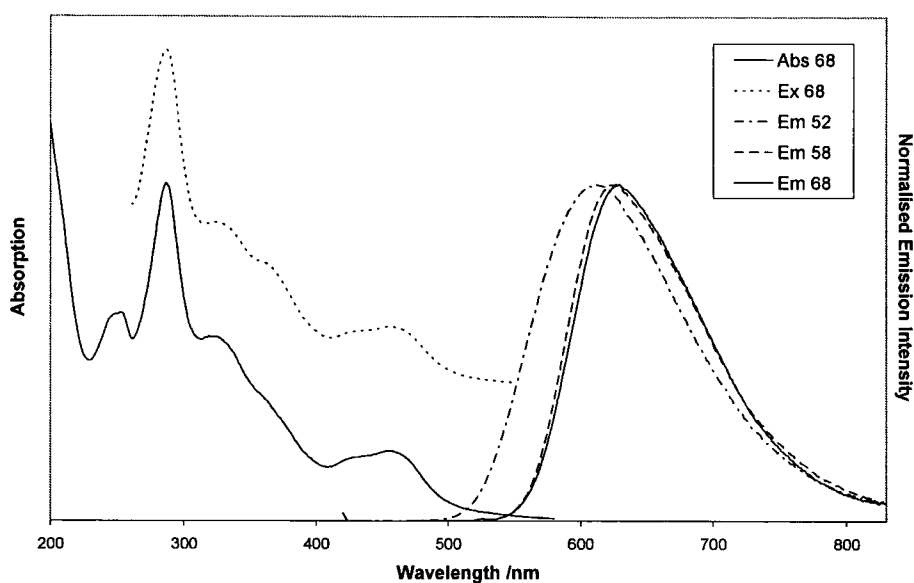
Figure 106 Normalised absorption and emission spectra (λ_{ex} = 455 nm) for Ir-φ-φ-Ru 68 in aerated CH₃CN at 298K, with overlaid excitation spectrum (λ_{em} = 630 nm) offset for clarity. Emission spectra for building blocks [Ir(ppy)₂(bpy-ph)]⁺ 52 and [Ru(bpy)₂(bpy-ph)]²⁺ 58 also given for comparison.

Previous work carried out on bimetallic species also containing [Ru(bpy)₂(N^N)]²⁺ and [Ir(ppy)₂(N^N)]⁺ building blocks clearly shows that the final photophysical properties observed are absolutely dependent upon the bridging ligand. For instance, whilst the 3,5-bis(pyridin-2-yl)-1,2,4-triazole (bpt) (Figure 107a) bridged complex [(bpy)₂Ru(bpt) Ir(ppy)₂]²⁺ also displays emission characteristic of the ruthenium centre,[160] the similar complex, bridged instead by 1,4,5,8,9,12-hezaazatriphenylene (HAT) (Figure 107b), exhibits iridum-based emission characteristics.[161] This implies that energy transfer occurs in the opposite direction in the HAT complex, meaning that this bridge must affect the excited state energy of the bimetallic complex.

(a) bpt   (b) HAT
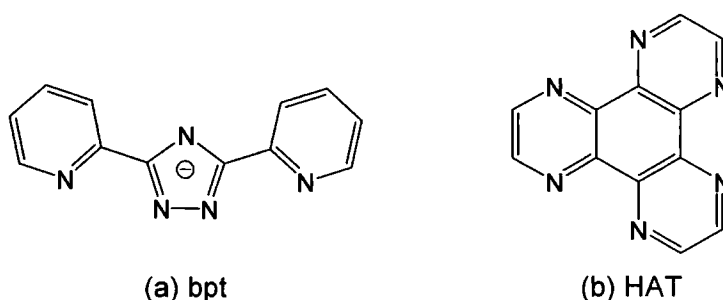
Figure 107 Bridging ligands (a) 3,5-bis(pyridin-2-yl)-1,2,4-triazole (bpt) and (b) 1,4,5,8,9,12-hezaazatriphenylene (HAT)

The results obtained for complexes **67** and **68** suggest that the phenyl or biphenyl bridging unit present has little or no effect on the excited state of the overall complex.

110

This allows for the reliable prediction of energy transfer in complexes of this nature, and hence the appropriate design of energy-channelling systems.

5.1.2 Complexes combining [Ru(bpy)₃]²⁺ or [Ir(ppy)₂(bpy)]⁺ building blocks with terpyridine-containing units

Complexes ᵗᵖʸIr-φ-φ-Ruᵇᵖʸ **71** and ᵗᵖʸRu-φ-φ-Irᵖᵖʸ **72** contain unsymmetrical bridging ligands, terminating with either a ppy or bpy ligand at one end and with the terdentate 2,2′:6′,2″-terpyridine (tpy) ligand at the other. The photophysical properties of these two complexes were investigated and results are summarised in Table 22.

The building blocks chosen for comparison in the case of **71** are [Ir(Me-tpy)(ttpy)]³⁺ (λ_{em} = 506 nm)[194], where Me-tpy is 4′-methyl-2,2′:6′,2″-terpyridine and ttpy is 4′-tolyl-2,2′:6′,2″-terpyridine, and [Ru(bpy)₂(bpy-ph)]²⁺ (λ_{em} = 627 nm). For complex **72**, the models are [Ru(ttpy)₂]²⁺ (non-emissive at 298 K)[207] and [Ir(ppy)₂(bpy-ph)]⁺ (λ_{em} = 613 nm).

Complex	ᵗᵖʸIr-φ-φ-Ruᵇᵖʸ **71**	ᵗᵖʸRu-φ-φ-Irᵖᵖʸ **72**
Absorption Maxima /nm (ε /M⁻¹ cm⁻¹)	457 (9060) 429 (8840) 373 (14600) 350 (18100) 320 (24900) 285 (43800) 251 (30200)	485 (26200) 458 (17000) 352 (42700) 324 (68200) 308 (86200) 271 (71100)
Emission Maximum(a) /nm	630	none observed at room temperature
Quantum Yield x 10² degassed (aerated)	0.27 (0.07)	-
Lifetime /ns degassed (aerated)	1550 (207)	-

Table 22 Photophysical properties of ᵗᵖʸIr-φ-φ-Ruᵇᵖʸ 71 and ᵗᵖʸRu-φ-φ-Irᵖᵖʸ 72 measured in acetonitrile at 298K. (a) λ_{ex} = 455 nm.

A single emission band at 630 nm arises from excitation of complex **71** at either 365 nm or 455 nm, indicative of emission from the ruthenium tris-bipyridine centre. No emission band is observed at 506 nm where the iridium bis-terpyridine unit would be expected to emit. As the excitation spectrum measured at the emission wavelength matches the absorption profile (Figure 108), it is confirmed that rapid energy transfer occurs to the ruthenium moiety followed by emission characteristic of this site. However, in this instance, a significantly reduced quantum yield is observed,

111

which when combined with the observed lifetime, corresponds to a radiative rate constant (k_r) of 1.7×10^3 s^{-1} and a non-radiative rate constant (Σk_{nr}) of 6.4×10^5, compared to respective values of 7.0×10^4 s^{-1} and 7.0×10^5 s^{-1} for $[Ru(bpy)_2(bpy\text{-}ph)]^{2+}$. Therefore, the reduced quantum yield is attributed to a reduction in k_r for complex **71**.
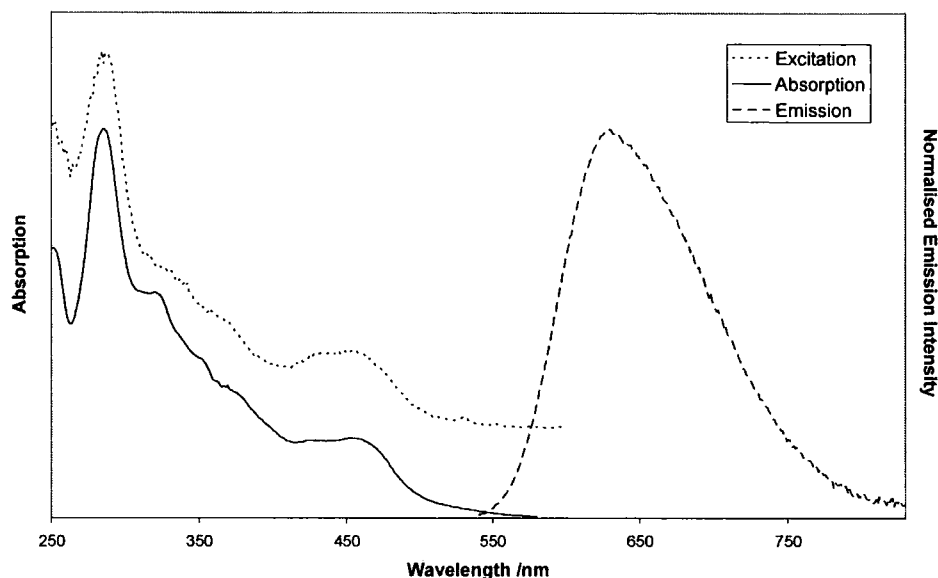
Figure 108 Normalised absorption and emission spectra (λ_{ex} = 455 nm) for $^{tpy}Ir\text{-}\phi\text{-}\phi\text{-}Ru^{bpy}$ 71 in aerated acetonitrile at room temperature, with overlaid excitation spectrum (λ_{em} = 630 nm) offset for clairty.

For complex **72**, no distinct emission maximum is observed at room temperature. A peak in the vicinity of 613 nm would be expected under these conditions if emission was arising from the iridium moiety, so the lack of emission implies that energy is being transferred to the ruthenium terpyridine part of the complex, which is then non-radiatively deactivated. This is a well known phenomenon for ruthenium bis-terpyridine complexes and is attributed to the distortion from ideal octahedral geometry enforced by the terpyridine ligand, which in turn lowers the energy of the metal-centred state and offers a competitive non-radiative decay pathway.[193]

In order to probe the photophysical properties of this complex further, low temperature measurements were carried out. At 165K in ethanol, complex **72** exhibited an emission band centred at around 660 nm regardless of excitation wavelength, whilst at 77K a blue shift of the maximum by approximately 20 nm was observed. This behaviour is similar to that reported for related complex $[Ru(ttpy)_2]^{2+}$, which has an emission maximum of 648 nm in butyronitrile solvent at 155K, and 628 nm at 90K.[195] As such, it can be concluded that in bimetallic complex **72**, energy is efficiently transferred to the ruthenium moiety, with the resulting emission being characteristic of

ruthenium bis-terpyridine complexes.
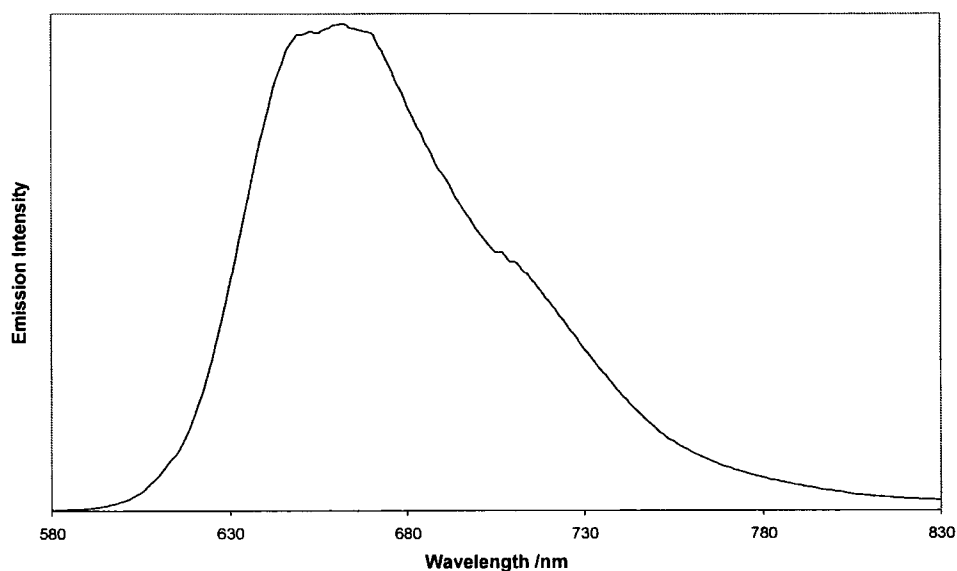
Figure 109 Emission profile of ᵗᵖʸRu-φ-φ-Irᴾᴾʸ 72 recorded in ethanol at 165K (λ_{ex} = 485 nm).

Whilst systems containing this type of unsymmetrical bridging ligand remain relatively unexplored, bridges between two terpyridine termini in ruthenium-iridium systems have received some attention. Work on $[(tpy)Ru(tpp)IrCl_3]^{2+}$ where tpp is the bridging ligand 2,3,5,6-tetrakis-(2-pyridyl)-pyrazine (Figure 110) reveals similar behaviour to the systems reported here, with emission arising from the lower energy ruthenium moiety, even though the lowest energy absorption is known to be irdium-based.[208]
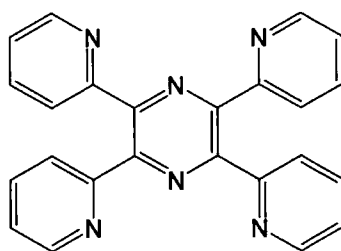
Figure 110 Bridging ligand 2,3,5,6-tetrakis-(2-pyridyl)-pyrazine (tpp)

However, very recently it has been reported that the introduction of rigidity into the bridging ligand (BL) of $[(tpy)M(tpy\text{-}BL\text{-}tpy)M(tpy)]^{n+}$ type complexes can prevent efficient energy transfer between the metal centres and hence result in multiple luminescence.[209] The photophysical results collected here indicate that both of the terpyridine-containing complexes studied exhibit efficient energy transfer and emission properties which can be predicted based upon the relative excited state energies of the component building blocks. This reinforces the previous statement that

113

the phenyl bridging units have little or no effect on the excited state properties of these dimeric systems.

5.2 Photophysical properties of trimetallic complexes

Trimetallic complexes [Ru-φ]$_2$-Ir **69** and [Ir^{F2}-φ]$_2$-Ir **70** also contain unsymmetrical bridging ligands, but in this case the phenyl groups link between a bpy ligand and a ppy ligand. The photophysical properties of these complexes were investigated and results are summarised in Table 23. For complex **69**, the building blocks involved can be considered to be [Ru(bpy)$_2$(bpy-ph)]$^{2+}$ **58** and [Ir(ppy)$_2$(bpy)]$^+$ **24**, whilst for complex **70** a combination of [Ir(ppy)$_2$(bpy)]$^+$ **24** and [Ir(ppy-F$_2$)$_2$(bpy-ph)]$^+$ **54** is used.

Complex	[Ru-φ]$_2$-Ir **69**	[Ir^{F2}-φ]$_2$-Ir **70**
Absorption Maxima / nm (ε / M^{-1} cm^{-1})	456 (45700) 433 (42100) 389 (41400) 365 (55300) 333 (64800) 307 (98200) 288 (190000) 255 (107000) 250 (103000)	367 (35300) 305 (65800) 259 (88800)
Emission Maximum[a] / nm	628	613
Quantum Yield x 10^2 degassed (aerated)	14 (1.9)	6.4 (1.6)
Lifetime / ns degassed (aerated)	1710 (198)	312 (85)

Table 23 Photophysical properties of [Ru-φ]$_2$-Ir **69** and [Ir^{F2}-φ]$_2$-Ir **70** measured in acetonitrile at 298K. [a] λ$_{ex}$ = 455 nm (**69**) or 400 nm (**70**).

The absorption spectrum of **69** is similar to the weighted sum of absorption spectra for building blocks [2[Ru(bpy)$_2$(bpy-ph)]$^+$ + [Ir(ppy)$_2$(bpy)]$^+$], with increased absorption between 320 - 400 nm (Figure 111) probably due to extended conjugation as observed for dimeric species **68**. This suggests that the trimetallic species is retaining the properties exhibited by the individual building blocks.

Upon excitation of **69** at any wavelength between 360 - 460 nm, a single emission band is observed at 628 nm, close to that associated with the ruthenium building block. However, this is also similar to the emission wavelength for [Ir(ppy-ph)$_2$(bpy)]$^+$ which could also be assumed as a good model for the iridium part of this system. Nevertheless, the lifetime and quantum yield of emission for complex **69** are

characteristic of emission arising from the ruthenium tris-bipyridine moiety. As the excitation spectrum obtained at the emission maximum matches the absorption spectrum, it is concluded that energy transfer to and subsequent emission from the ruthenium termini is occurring.
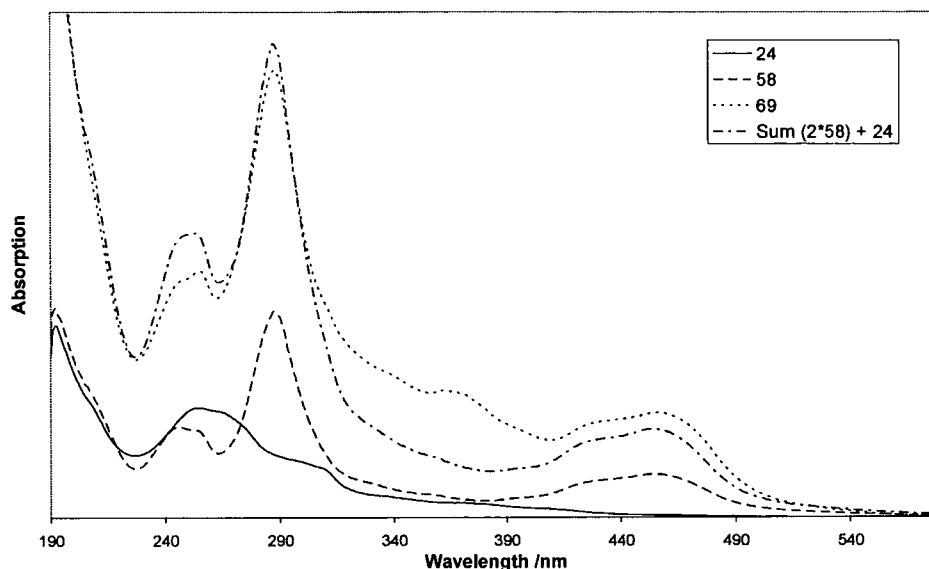
Figure 111 Comparison of absorption spectra of [Ru-φ]₂-Ir 69 and building blocks [Ir(ppy)₂(bpy)]⁺ 24 and [Ru(bpy)₂(bpy-ph)]²⁺ 58. Measured in acetonitrile at 298K.

The absorption spectrum of **70** has a similar profile to those seen for the iridium-based building blocks, but intensity of absorption is substantially lower in the region below 310 nm than would be expected from a sum of the appropriate absorption spectra (Figure 112). This could be attributed to the movement of LC transitions to lower energy due to increased conjugation, especially as increased absorption is again observed in the region 360 – 400 nm.

Upon excitation of **70** at 400 nm a single emission band is observed at 613 nm, which is very close to that observed for the unsubstituted complex [Ir(ppy)₂(bpy)]⁺ **24**. The lifetime and quantum yield of emission of **70** are of the same order of magnitude as those reported for complex **24** in Chapter 3. Again, the excitation spectrum recorded at the emission maximum matches the absorption profile, indicating that emission is arising from the non-fluorinated iridium centre after efficient energy transfer from the other iridum centres in the molecule.
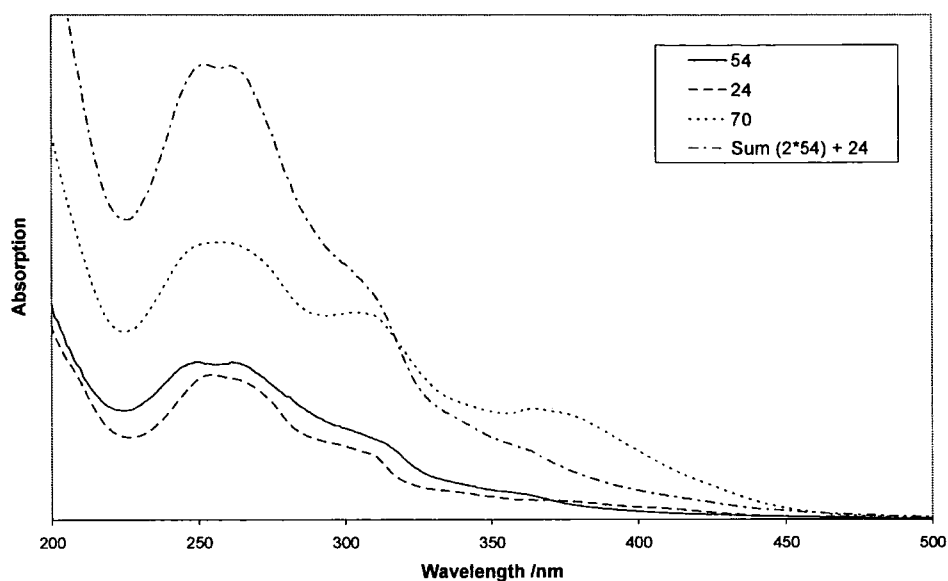
Figure 112 Comparison of absorption spectra of [Ir^{F2}-φ]$_2$-Ir 70 and building blocks [Ir(ppy)$_2$(bpy)]$^+$ 24 and [Ir(ppy-F$_2$)$_2$(bpy-ph)]$^+$ 54. Measured in acetonitrile at 298K.

The direction of energy transfer and emission characteristics from both of the trimetallic species studied here can be reliably predicted from the relevant monometallic building blocks. This indicates again that phenyl bridging units do not alter the excited state energy of the overall complex.

5.3 Photophysical studies of tetrametallic species

The photophysical properties of three tetrameric species involving ruthenium and iridium metal centres were investigated and results are summarised in Table 24. The following building blocks are chosen for comparison: [Ir(ppy)$_2$(bpy-ph)]$^+$ 52 and [Ru(bpy)$_2$(bpy-ph)]$^+$ 58 for [Ir-φ]$_2$-Ir-φ-φ-Ru 75; [Ir(ppy-F)$_2$(bpy-ph)]$^+$ 53, [Ir(ppy)$_2$(bpy-ph)]$^+$ 52 and [Ru(bpy)$_2$(bpy-ph)]$^+$ 58 for [Ir^F-φ]$_2$-Ir-φ-φ-Ru 76, and [Ir(ppy-F$_2$)$_2$(bpy-ph)]$^+$ 54, [Ir(ppy)$_2$(bpy-ph)]$^+$ 52 and [Ru(bpy)$_2$(bpy-ph)]$^+$ 58 for [Ir^{F2}-φ]$_2$-Ir-φ-φ-Ru 77. Figure 113 shows the absorption, excitation and emission spectra obtained for complex 77, along with emission spectra for the relevant monometallic building blocks.

Complex	[Ir-φ]₂-Ir-φ-φ-Ru 75	[Ir^F-φ]₂-Ir-φ-φ-Ru 76	[Ir^F2-φ]₂-Ir-φ-φ-Ru 77
Absorption Maxima /nm (ε /M⁻¹ cm⁻¹)	455 (28100) 365 (101000) 309 (137000) 287 (192000) 257 (161000)	454 (28500) 418 (39000) 367 (105000) 313 (141000) 286 (206000) 255 (178000)	450 (26300) 418 (35900) 356 (89000) 308 (135000) 286 (183000) 251 (154000)
Emission Maximum[a] /nm	630	630	630
Quantum Yield x 10² degassed (aerated)	14 (2.1)	14 (2.1)	13 (1.7)
Lifetime /ns degassed (aerated)	1710 (225)	1680 (219)	1660 (225)

Table 24 Photophysical properties of [Ir-φ]₂-Ir-φ-φ-Ru 75, [Ir^F-φ]₂-Ir-φ-φ-Ru 76 and [Ir^F2-φ]₂-Ir-φ-φ-Ru 77 measured in acetonitrile at 298K. [a] λ_{ex} = 455 nm.
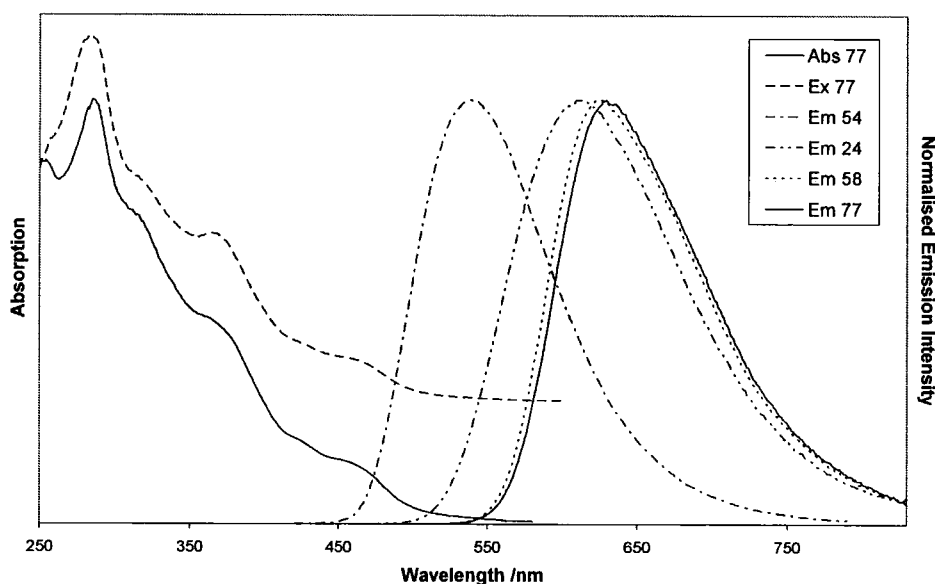
Figure 113 Normalised absorption and emission spectra (λ_{ex} = 455 nm) for [Ir^F2-φ]₂-Ir-φ-φ-Ru 77 in aerated acetonitrile at room temperature, with overlaid excitation spectrum (λ_{em} = 630 nm) offset for clarity. Emission spectra for building blocks [Ir(ppy-F₂)₂(bpy-ph)]⁺ 54, [Ir(ppy)₂(bpy-ph)]⁺ 52 and [Ru(bpy)₂(bpy-ph)]⁺ 58 also given for comparison.

The absorption spectra for complexes 75 - 77 are similar in shape to the sum of the spectra of the relevant building blocks with, in all cases, enhanced molar absorptivity in the 320 - 400 nm region attributed to increased conjugation in the multimetallic species.

All three tetrameric species exhibit a single emission band at 630 nm regardless of excitation wavelength, with the lifetime and quantum yield measurements typical of the [Ru(bpy)$_2$(bpy-ph)]$^+$ building block. The excitation spectrum recorded at the emission maximum matches the absorption profile closely for all three complexes (e.g. Figure 113 for complex 77). As for the analogous dimeric species **68**, this suggests that in all three tetrameric species, excitation is followed by rapid energy transfer to the ruthenium terminus, in line with the ordering of the energy levels of the three constituent units (e.g. Figure 114 for complex **77**). In addition, it seems that the incorporation of fluorine substituents to raise the energy of the excited state of peripheral units is not necessary for the cascade of energy to the ruthenium terminus to occur.
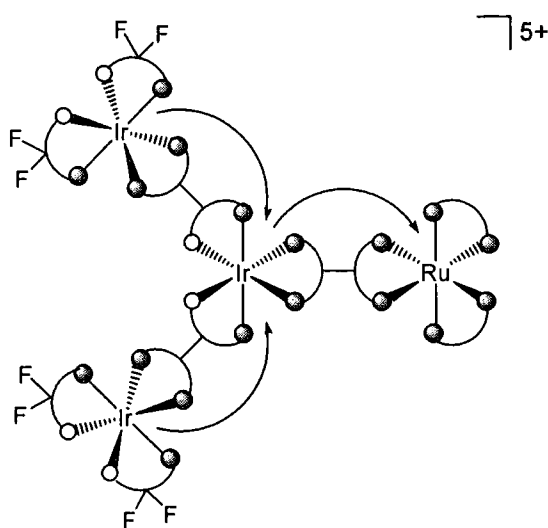
Figure 114 Direction of energy transfer in tetrameric complex 77

The direction of energy transfer occurring within these tetrameric species contrasts greatly to that observed for similar species containing the 2,3-bis(2-pyridyl)pyrazine (2,3-dpp) bridging ligand. The complex [Ru[(2,3-dpp)Ir(ppy)$_2$]$_3$]$^{5+}$ (Figure 115) displays iridium-based emission upon direct excitation of the ruthenium centre, indicating that energy is efficiently transferred in the ruthenium-to-iridium direction.[158] This implies that the dpp bridge is involved in perturbing the excited state of the tetranuclear complex, unlike the phenyl bridging units used in this work.
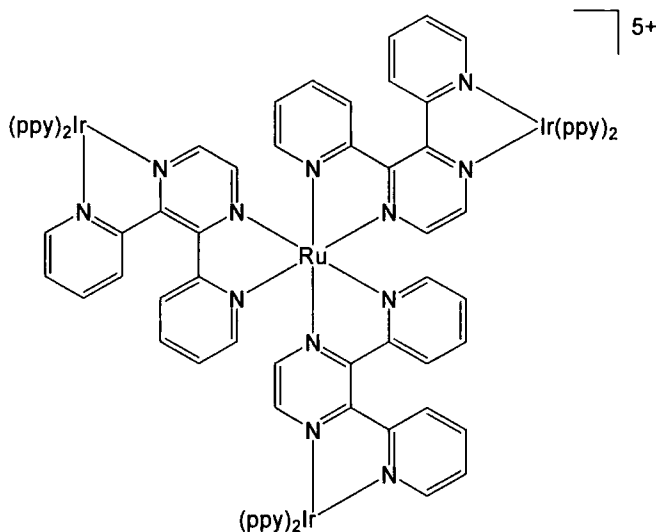
Figure 115 [Ru[(2,3-dpp)Ir(ppy)₂]₃]⁵⁺ where dpp is 2,3-bis(2-pyridyl)pyrazine

Further evidence for the lack of effect of the phenyl bridging units on the properties of tetranuclear complexes may be taken from electrochemical measurements on [Ir^{F2}-ϕ]$_2$-Ir-ϕ-ϕ-Ru **77**, which revealed that the oxidation of Ru^{2+} to Ru^{3+} occurs at 1.27 V, approximately the same potential as that recorded for both dimeric complex Ir-ϕ-ϕ-Ru **68** (1.28 V) and monometallic species [Ru(bpy)₂(bpy-ph)]⁺ **58** (1.26 V).

A tetrameric species involving peripheral rhodium units of the type [Rh(pba)₂(bpy)]⁺ in combination with the aforementioned ruthenium and iridium building blocks was also studied. The photophysical properties of [Rh-ϕ]$_2$-Ir-ϕ-Ru **78** are summarised in Table 25.

Complex	[Rh-ϕ]$_2$-Ir-ϕ-Ru **78**
Absorption Maxima /nm (ε /M^{-1} cm^{-1})	456 (20200) 369 (67000) 309 (146000) 289 (175000) 256 (128000) 249 (124000)
Emission Maximum[a] /nm	640
Quantum Yield x 10² degassed (aerated)	15 (2.1)
Lifetime /ns degassed (aerated)	1980 (256)

Table 25 Photophysical properties of [Rh-ϕ]$_2$-Ir-ϕ-Ru 78 in CH₃CN at 298K. [a] λ_{ex} = 455 nm.

In this instance there is only one bridging phenyl ring between the iridium and

119

ruthenium centres and so the building blocks for comparison are [Rh(pba)₂(bpy-ph)]⁺ 55, [Ir(ppy)₂(bpy)]⁺ 24 and [Ru(bpy)₂(bpy-ph)]²⁺ 58.

The absorption spectrum of **78** adopts a shape similar to the sum of the spectra of the individual building blocks, but again an increased absorption is noted between 310 - 400 nm due to extended conjugation. The single emission band with a maximum of 640 nm, obtained via excitation at wavelengths between 370 nm and 455 nm, is red shifted compared to the other tetrameric systems studied, but very similar to the analogous dimeric species Ir-φ-Ru **67** (λ_{em} = 638 nm) also with one bridging phenyl unit. This could be attributed to the electron withdrawing effect imposed by the iridium complex which is only separated by a single phenyl ring in this case.

Again, as the excitation spectrum obtained at the emission maximum closely matches the absorption profile (Figure 116), it is concluded that energy transfer to and emission from the ruthenium moiety is occurring. As the rhodium building block is only moderately emissive at room temperature, the energy transfer taking place throughout this tetrameric complex must be fast enough to compete with the other deactivating processes present.
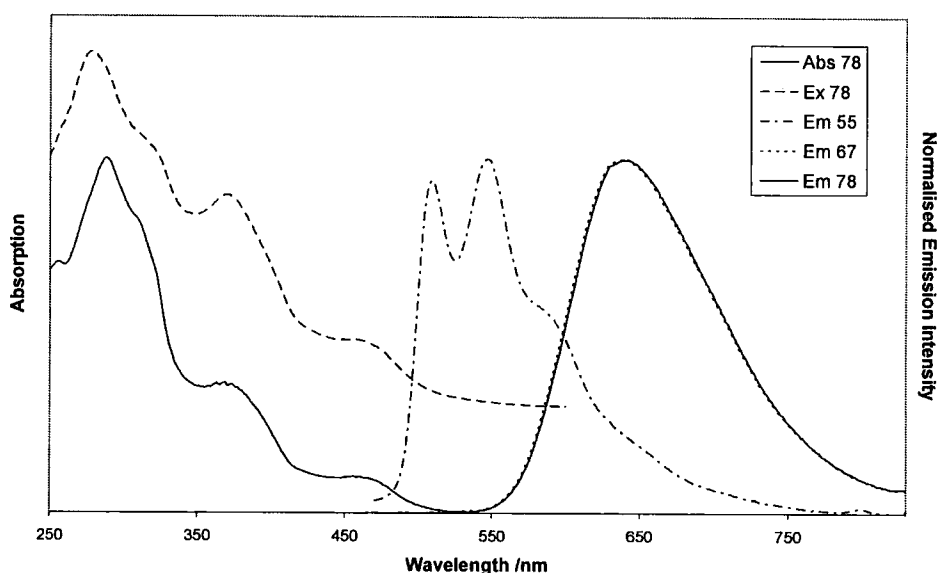
Figure 116 Normalised absorption and emission spectra (λ_{ex} = 455 nm) for [Rh-φ]₂-Ir-φ-Ru **78** in aerated acetonitrile at room temperature, with overlaid excitation spectrum (λ_{em} = 640 nm) offset for clarity. Emission spectra for building blocks [Rh(pba)₂(bpy-ph)]⁺ **55** and Ir-φ-Ru **67** also given for comparison.

5.4 Photophysical properties of an octametallic complex

The photophysical properties of octanuclear complex [[Ir^{F2}-ϕ]$_2$-Ir-ϕ]$_2$-Ir-ϕ-ϕ-Ru **80** have been investigated. For this complex, the same building blocks apply as for tetranuclear complex [Ir^{F2}-ϕ]$_2$-Ir-ϕ-ϕ-Ru **77** (i.e. [Ir(ppy-F$_2$)$_2$(bpy-ph)]$^+$ **54**, [Ir(ppy)$_2$(bpy-ph)]$^+$ **52** and [Ru(bpy)$_2$(bpy-ph)]$^+$ **58**).

Complex	[[Ir^{F2}-ϕ]$_2$-Ir-ϕ]$_2$-Ir-ϕ-ϕ-Ru **80**
Absorption Maxima /nm (ε /M^{-1} cm^{-1})	455 (25200) 368 (148000) 303 (224000) 280 (262000) 252 (260000)
Emission Maximum[a] /nm	630
Quantum Yield x 10^2 degassed (aerated)	12 (1.9)
Lifetime /ns degassed (aerated)	1590 (208)

Table 26 Photophysical properties of [[Ir^{F2}-ϕ]$_2$-Ir-ϕ]$_2$-Ir-ϕ-ϕ-Ru **80** measured in acetonitrile at 298K. [a] λ_{ex} = 455 nm.

As seen for a number of the multimetallic complexes previously discussed, the absorption spectrum of **80** is of similar shape to the sum of the spectra for the building blocks but with increased absorption between 330 - 410 nm, and decreased absorption between 240 - 300 nm (Figure 117). This is likely to correspond to the increased conjugation found in the octameric species in comparison to the building blocks, shifting some of the ligand centred transitions to lower energy.

A single emission band is observed at 630 nm regardless of excitation wavelength, with a lifetime of 1590 ns and quantum yield of 0.12 in degassed acetonitrile at room temperature. These emission parameters are characteristic of emission from the ruthenium building block. Overlaying the excitation spectrum obtained at the emission maximum with the absorption spectrum (Figure 118) confirms that rapid energy transfer is followed by emission from the ruthenium terminus of the molecule for this complex also. This confirms once again that the phenyl bridging units have little or no effect on the excited state properties of the overall multinuclear complex, even when large systems containing eight metal centres are studied.

121
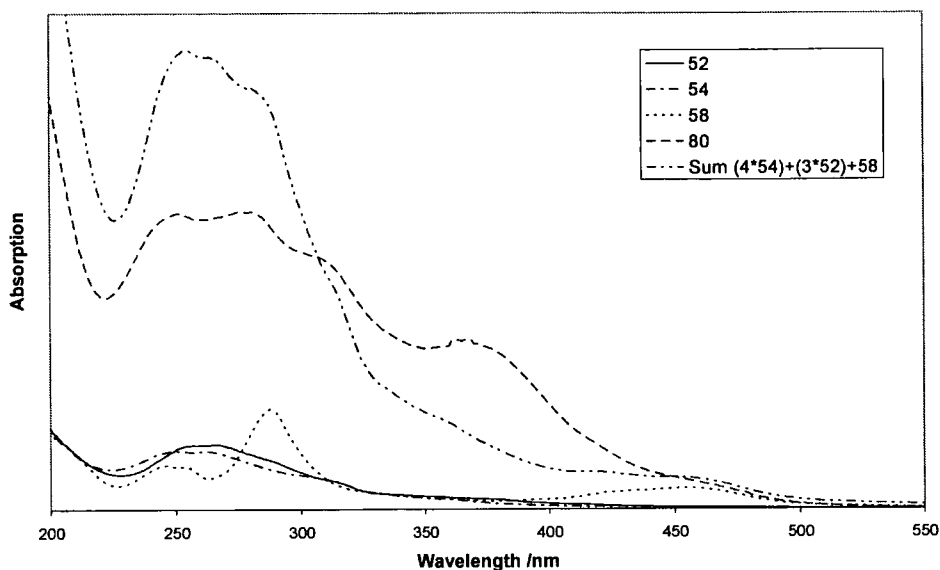
Figure 117 Comparison of absorption spectra of [[Ir^{F2}-φ]₂-Ir-φ]₂-Ir-φ-φ-Ru 80 and building blocks [Ir(ppy-F₂)₂(bpy-ph)]⁺ 54, [Ir(ppy)₂(bpy-ph)]⁺ 52 and [Ru(bpy)₂(bpy-ph)]²⁺ 58, measured in acetonitrile at 298K.
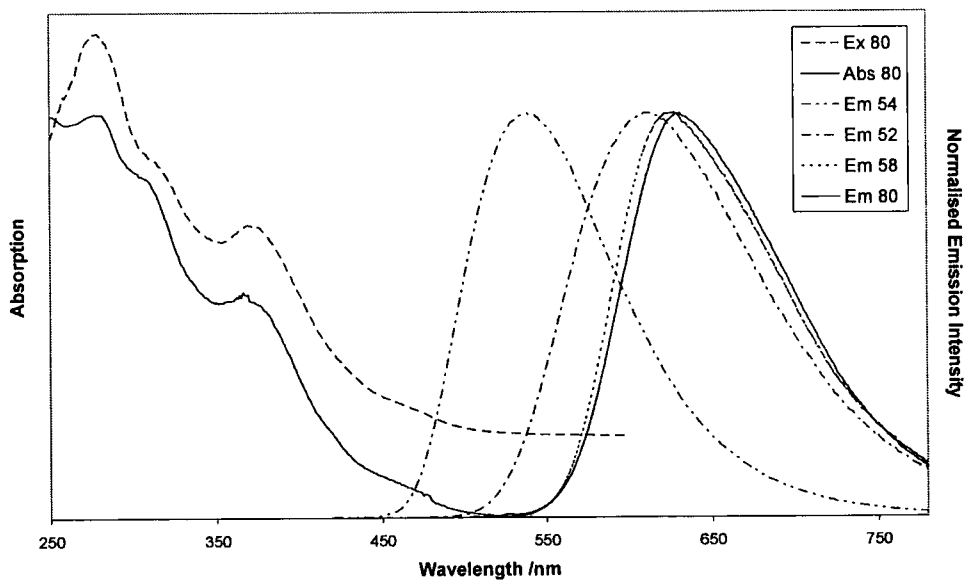
Figure 118 Normalised absorption and emission spectra for [[Ir^{F2}-φ]₂-Ir-φ]₂-Ir-φ-φ-Ru 80 in aerated acetonitrile at room temperature (λ_{ex} = 455 nm), with overlaid excitation spectrum (λ_{em} = 630 nm) offset for clarity. Emission spectra for building blocks [Ir(ppy-F₂)₂(bpy-ph)]⁺ 54, [Ir(ppy)₂(bpy-ph)]⁺ 52 and [Ru(bpy)₂(bpy-ph)]²⁺ 58 also given for comparison.

5.5 Concluding remarks

The photophysical properties of a series of multimetallic species have been investigated. In all cases, evidence for rapid energy transfer to the metal centre of lowest excited state energy is reported, with emission displaying characteristics of this terminal unit. The photophysical properties of the overall multinuclear complexes retain the properties displayed by individual monometallic building blocks, implying that the phenyl bridging units have little or no effect on the excited state energy of the overall system. This confirms that the photophysical properties of multimetallic complexes containing simple phenyl bridging units may be reliably predicted based on the properties of the individual building block complexes, allowing the design of such systems for the channelling of energy to a specific location. This idea could find use in systems using similar complexes for light harvesting, such as solar energy conversion.

CHAPTER 6

EXPERIMENTAL

6 Experimental

6.1 Synthetic procedures and characterisation

The solvents used throughout were of Analar® quality and used as supplied, with the exception of acetonitrile which was HPLC grade. Water was purified using the Purite™ system having conductivity of ≤ 0.04 µScm^{-1}. Reagents were used as supplied. Thin layer chromatography was carried out using neutral aluminium oxide plates (Merck Art 5550) or silica plates (Merck Art 5554), both types being fluorescent upon irradiation at 254 nm. Preparative column chromatography employed silica (Merck Silica Gel 60, 230 – 400 mesh) or neutral alumina (Merck Aluminium Oxide 90, Brockmann activity 2 - 3).

NMR spectra were recorded using either a Varian Mercury-200 spectrometer at 199.99 MHz (^{1}H), 50.29 MHz (^{13}C) and 188.18 MHz (^{19}F), a Varian Unity-300 spectrometer at 299.91 MHz (^{1}H), 75.41 MHz (^{13}C) and 188 MHz (^{19}F), a Bruker-400 spectrometer at 399.97 MHz (^{1}H), 50.58 MHz (^{13}C) or a Varian Inova-500 spectrometer at 499.87 MHz (^{1}H), 125.71 MHz (^{13}C) and 376.35 MHz (^{19}F) and referenced to residual protio solvent resonances. NMR data are reported with chemical shifts (δ) in ppm and coupling constants (J) in Hertz. ^{1}H NMR spectra were assigned with assistance from ^{1}H-^{1}H COSY (correlation spectroscopy, through-bond interactions) and ^{1}H-^{1}H NOESY (nuclear Overhauser effect spectroscopy, through-space interactions) spectra. ^{13}C NMR spectra were recorded with proton decoupling and were assigned with assistance from ^{1}H-^{13}C HSQC (heteronuclear single quantum correlation) and ^{13}C DEPT (distortionless enhancement by polarisation transfer) spectra. Numbering systems are outlined in molecular diagrams for each compound. Attention is drawn to the numbering system used for complexes containing 2-phenylpyridine ligands, which begins with (1) at the site of cyclometalation, (2) at the position of pyridyl-substitution and continues logically around the phenyl ring.

Electron ionisation mass spectra were recorded by the EPSRC National Mass Spectrometry Service at the University of Wales, Swansea. Electrospray ionisation mass spectra (ES$^+$ MS) were recorded at the University of Durham using a Micromass LCT spectrometer with methanol or acetonitrile as the carrier solvent. High resolution mass spectra were recorded either at the University of Durham using a Micromass LCT spectrometer at 5000 resolution using sodium iodide as the reference or a Thermo Finnigan LTQ FT at 100000 resolution with external calibration, or by the EPSRC Mass Spectrometry Service at the University of Wales, Swansea.

I.R. spectra were recorded on a Perkin-Elmer 1600 FTIR spectrometer operated using GRAMS software. C, H & N analysis was performed using an Exeter Analytical Inc CE-440 elemental analyser. Single crystal X-ray diffraction experiments were carried out using SMART CCD area detectors and graphite-monochromated MoK_α radiation. The structures were solved by direct methods and refined against F^2 of all data, using SHELXTL software.[210]

6.2 Photophysical and electrochemical measurements

UV-Vis absorption spectra were recorded using a Biotech Instruments XS spectrometer operating with LabPower software. Samples were contained in quartz cuvettes with a path length of 1 cm. All spectra were run against a reference of pure solvent contained within a matched cell. Extinction coefficients were determined by a dilution technique and graphical application of the Beer-Lambert law.

Steady-state luminescence spectra were recorded using an Instruments S.A. Fluoromax-2 spectrometer, equipped with a Hamamatsu R928 photomultiplier tube, operating with DataMax software. Quartz fluorescence cuvettes of path length 1 cm were employed and the absorbance of each solution at the excitation wavelength was below 0.1 to avoid inner filter effects. Emission was detected at right angles to the excitation source with appropriate filters used where required to remove second order peaks. All emission spectra were corrected after data acquisition for dark count and for the spectral response of the detector. Excitation spectra were automatically corrected for lamp output through use of a beam splitter, which directs 8% of the excitation light to a reference photodiode. Low temperature measurements were obtained from samples held in a 1 cm pathlength quartz cuvette in a liquid nitrogen cooled cryostat (Oxford Instruments Optical Cryostat, DN 1704).

Aerated luminescence quantum yields were recorded using a dilution technique with respect to a standard of ruthenium(II) tris(2,2'-bipyridine) chloride in aqueous solution (Φ_{st} = 0.028).[211] The quantum yield to be determined (Φ) may be calculated with respect to the standard by application of the following equation:

$$\Phi = \Phi_{st} \left[\frac{\left[\dfrac{dI}{dA}\right]}{\left[\dfrac{dI}{dA}\right]_{st}} \right] \left[\frac{\eta^2}{\eta_{st}^{\,2}} \right]$$

where (dI/dA) is the gradient from the plot of integrated emission intensity *vs.*

126

absorbance, η is the refractive index of the solvent and symbols with subscript 'st' are the respective values for the standard. Only the linear portion of the plot was used to determine the gradient. Degassed quantum yields were obtained from the ratio of integrated emission intensities from degassed and aerated solutions of the same sample. Trifluoroacetic acid was used in order to acidify solutions to pH <2, whilst tetramethylammonium hydroxide was used for basic solutions of pH >10. The effect of acid (or base) was deduced by taking the ratio of integrated emission intensities from acidified (or basicified) and neutral solutions of the same sample with correction for change in absorbance at excitation wavelength where necessary.

Excited state lifetime measurements were measured using a time-resolved fluorescence spectrometer. Samples were excited in 1 cm pathlength quartz fluorescence cuvettes by third harmonic radiation (355 nm, ~1-2 mJ per pulse, pulse length ~7 ns) from a Q-switched Nd:YAG laser (Spectra Physics GCE-150-10). Stray light at 1064 nm (fundamental) and 532 nm (second harmonic) was removed by the use of optical filters. Emission was detected at right angles to the excitation source with a photomultipler tube (Hamaatsu R298) and recorded using a digital storage oscilloscope (Tetronix TDS-340), before transfer to a PC for analysis. The raw data was deconvoluted to account for detector response by reference to a separate sample of 1,4-bis(5-phenyloxazol-2-yl)benzene (POPOP) or rhodamine, and fitted to an exponential decay by minimisation of the sum of squared residuals.

Cyclic voltammetry was carried out in a background electrolyte of tetrabutylammonium tetrafluoroborate (0.1 M) in acetonitrile controlled with Autolab PGSTAT30 potentiostat (Eco Chemie B.V.). Computer control and data storage were achieved using GPES Manager. A three electrode assembly was employed using platinum wire counter and reference electrodes and a platinum working electrode. The electrodes were placed in a cell which was filled with 10 mL of the desired solution and purged with nitrogen.

6.3 Density functional calculations

B3LYP density functional theory calculations were performed using the Gaussian98 software package,[212] employing the 6-31G basis set for ligand atoms and the LANL2DZ basis set for iridium. The inner core electrons of iridium were replaced with a relativistic effective core potential (ECP), leaving the outer core [$(5s)^2(5p)^6$] electrons and the $(5d)^6$ valence electrons of iridium(III). The geometries were fully optimised without symmetry constraints.

6.4 Synthesis of ligands

2-(4-Fluorophenyl)pyridine [ppyH-F] **1**
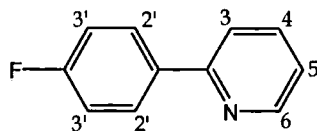
A Schlenk tube was charged with 2-bromopyridine (0.29 mL, 3.0 mmol), 4-fluorophenylboronic acid (462 mg, 3.3 mmol), aqueous K_2CO_3 (1.24 g, 9.0 mmol), water (0.2 mL) and DME (10 mL). The solution was thoroughly degassed via three freeze-pump-thaw cycles and placed under nitrogen. $Pd(PPh_3)_4$ (173 mg, 0.15 mmol) was added to the Schlenk tube under a positive pressure of nitrogen. A reflux condenser was attached to the Schlenk tube and the apparatus was evacuated and back filled with nitrogen. The solution was stirred at 80 – 85°C for 22 hours. After cooling to room temperature, DME was removed under reduced pressure and the resulting residue was dissolved in DCM and water. The DCM layer was washed with aqueous solutions of KOH (1M, 3 x 100 mL), dried over Na_2SO_4 and evaporated to yield an oil. Purification was achieved via column chromatography (SiO_2 gel) using gradient elution from 100% hexane to 10% diethyl ether and 90% hexane (274 mg, 1.60 mmol, 53%). ^1H NMR (500 MHz, $CDCl_3$): δ 8.69 (d, 1H, J = 4.4, H^6), 8.02 – 7.96 (2 overlapping d, 2H, H$^{2'}$), 7.77 (t, 1H, J = 7.8, H^4), 7.70 (d, 1H, J = 7.8, H^3), 7.27 – 7.23 (m, 1H, H^5), 7.16 (t, 2H, J = 8.7, H$^{3'}$). ^{13}C NMR (500 MHz, $CDCl_3$): δ 164.7 (C), 162.7 (C), 156.5 (C), 149.6 (CH^6), 137.3 (CH^4), 129.0 (d, J$_{C-F}$ = 35, CH$^{2'}$), 122.3 (CH^5), 120.5 (CH^3), 115.9 (d, J$_{C-F}$ =86, CH$^{3'}$). ^{19}F NMR (400 MHz, $CDCl_3$): δ -113.3. ES$^+$ MS: m/z = 174.1 [M + H$^+$]. HR ES$^+$ MS: 174.07135 measured, 174.07135 calculated for [$C_{11}H_9NF$]$^+$. TLC (SiO_2, 60% hexane, 40% ether): R$_f$ = 0.64.

2-(4,6-Difluorophenyl)pyridine [ppyH-F$_2$] **2**
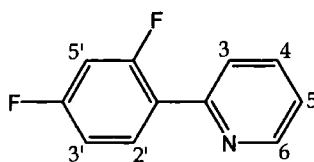
A Schlenk tube was charged with 2-bromopyridine (0.29 mL, 3.0 mmol), 2,4-difluorophenylboronic acid (525 mg, 3.3 mmol), aqueous K_2CO_3 (1.24 g, 9.0 mmol), water (0.2 mL) and DME (10 mL). The solution was thoroughly degassed via three freeze-pump-thaw cycles and placed under nitrogen. $Pd(PPh_3)_4$ (173 mg, 0.15 mmol) was added to the Schlenk tube under a positive pressure of nitrogen. A reflux

condenser was attached to the Schlenk tube and the apparatus was evacuated and back filled with nitrogen. The solution was stirred at 80 - 85°C for 22 hours. After cooling to room temperature, DME was removed under reduced pressure and the resulting residue was dissolved in DCM and water. The DCM layer was washed with aqueous solutions of KOH (1 M, 3 x 100 mL), dried over Na_2SO_4 and evaporated to yield an oil. Purification was achieved via column chromatography (SiO_2 gel) using gradient elution from 100% hexane to 2% diethyl ether and 98% hexane (405 mg, 2.12 mmol, 71%). ^{1}H NMR (400 MHz, $CDCl_3$): δ 8.71 (d, 1H, J = 4.5, H[6]), 8.00 (td, 1H, J = 8.8, 6.7, H[2']), 7.77 - 7.74 (m, 2H, H[3] and H[4]), 7.26 (ddd, 1H, J = 8.7, 4.8, 0.9, H[5]), 7.01 (dddt, 1H, J = 8.8, 8.0, 2.4, 1.2, H[3']), 6.92 (dddd, 1H, J = 11.2, 8.8, 2.4, 0.8, H[5']). ^{13}C NMR (400MHz, $CDCl_3$): δ 164.6 - 159.4 (2 overlapping dd, 2 CF), 152.6 (d, J_{C-F} = 9.2, C[2]), 149.9 (CH[6]), 136.6 (CH[4]), 132.2 (dd, J_{C-F} = 39, 18, CH[2']), 124.3 (d, J_{C-F} = 36, CH[3]), 123.8 (d, J_{C-F} = 47, C[1']), 122.6 (CH[5]), 112.0 (dd, J_{C-F} = 83, 15, CH[3']), 104.5 (t, J_{C-F} = 104, CH[5']). ^{19}F NMR (400 MHz, $CDCl_3$): δ -109.7, -113.4. ES[+] MS: m/z = 192.4 [M+H][+]. TLC (SiO_2, 60% hexane, 40% ether): R_f = 0.61.

2-(4,5,6-Trifluorophenyl)pyridine [ppyH-F₃] **3**
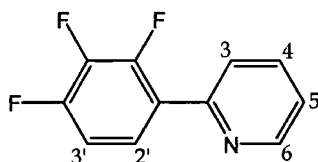
A Schlenk tube was charged with 2-bromopyridine (0.29 mL, 3.0 mmol), 2,3,4-trifluorophenylboronic acid (581 mg, 3.3 mmol), aqueous K_2CO_3 (1.24 g, 9.0 mmol), water (0.2 mL) and DME (15 mL). The solution was thoroughly degassed via three freeze-pump-thaw cycles and placed under nitrogen. $Pd(PPh_3)_4$ (173 mg, 0.15 mmol) was added to the Schlenk tube under a positive pressure of nitrogen. A reflux condenser was attached to the Schlenk tube and the apparatus was evacuated and back filled with nitrogen. The solution was stirred at 80 - 85°C for 84 hours. After cooling to room temperature, DME was removed under reduced pressure and the resulting residue was dissolved in DCM and water. The DCM layer was washed with aqueous KOH (1 M, 3 x 100 mL), dried over Na_2SO_4 and evaporated to yield an oil. Purification was achieved via column chromatography (SiO_2 gel) using gradient elution from 100% hexane to 10% diethyl ether and 90% hexane (245 mg, 1.17 mmol, 39%). ^{1}H NMR (500 MHz, $CDCl_3$): δ 8.72 (d, 1H, J = 4.5, H[6]), 7.82 - 7.73 (m, 3H, H[2'], H[3] and H[4]), 7.30 (ddd, 1H, J = 7.1, 4.9, 1.3, H[5]), 7.09 (dddd, 1H, J = 11.3, 9.2, 7.1, 2.1, H[3']). ^{13}C NMR (500 MHz, $CDCl_3$): δ 152.6 - 148.8 (2 dd, 2 C-F), 151.7 (q), 150.0 (CH[6]), 140.4 (dt, C-F), 137.0 (CH[2'], CH[3] or CH[4]), 125.1 (q), 124.5 (2 from CH[2'], CH[3] and CH[4]), 123.1

(CH^5), 112.6 (dd, J = 68.5, 15.0, CH$^{3'}$). ^{19}F NMR (200 MHz, CDCl$_3$): δ -133.8 - -133.9 (m, F$^{6'}$), -138.8 - -139.0 (m, F$^{5'}$), -160.7 (tdd, J = 20.4, 6.8, 2.5, F$^{4'}$). ES$^+$ MS: m/z = 210.0 [M + H]$^+$. HR ES$^+$ MS: m/z = 210.05250 measured, 210.05251 calculated for [C$_{11}$H$_7$NF$_3$]$^+$. TLC (SiO$_2$, 60% hexane, 40% ether): R$_f$ = 0.58.

2,2'-Bipyridine-N-oxide[106] **4**
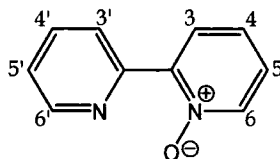
3-Chloroperoxybenzoic acid (13.8 g of 57% w/w, equivalent to 0.046 mol) was dissolved in chloroform (180 mL) and added slowly to a solution of 2,2'-bipyridine (7.14 g, 0.046 mol) in chloroform (25 mL) at 0°C. The resulting solution was stirred at room temperature for 18 hours, during which time a white precipitate developed. Thin layer chromatography revealed the presence of starting material at this point, so more 3-chloroperoxybenzoic acid (1 g) was added in chloroform (130 mL) and the solution stirred for a further 3 hours. The reaction mixture was washed with 5% Na$_2$CO$_3$ solution (3 x 150 mL), dried over MgSO$_4$ and evaporated to give an oily solid. Recrystallisation from hexane/ether yielded a white solid (2.68 g). The aqueous layers were re-extracted with chloroform (5 x 100 mL). The chloroform extractions were combined, dried over MgSO$_4$ and evaporated to yield a yellow oil and white solid. Ether was added and the solution filtered to separate the insoluble impurity. Removal of ether under reduced pressure yielded a white solid (0.85 g). This product was combined with that previously collected (3.53 g, 0.021 mol, 45%). ^{1}H NMR (400 MHz, CDCl$_3$): δ 8.90 (d, 1H, J = 8.1, H$^{3'}$), 8.73 (d, 1H, J = 4.8, H$^{6'}$), 8.32 (d, 1H, J = 6.6, H^6), 8.18 (dd, 1H, J = 8.0, 2.0, H^3), 7.82 (td, 1H, J = 8.0, 1.8, H$^{4'}$), 7.37 + 7.35 (2 x t, 2H, H^4, H^5), 7.26 (ddd (+ CHCl$_3$), 1H, H$^{5'}$).

4-Nitro-2,2'-bipyridine-N-oxide[108] **5**
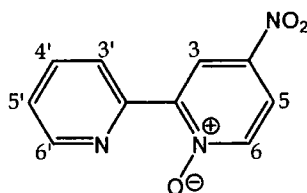
Fuming nitric acid (16 mL) was carefully added to a solution of 2,2'-bipyridine-N-oxide **4** (3.44 g, 0.02 mol) in concentrated sulfuric acid (25 mL) to give a clear orange/yellow solution. The mixture was heated to 110°C for 4 hours, during which time some white

solid was formed. After cooling to 0°C, the solution and solid were slowly added to ice giving a pale green solution, which turned blue as the ice melted, and white solid. Filtration to remove the white solid produced a clear yellow/green solution which, when basified with aqueous NaOH, gave a green solution with a yellow precipitate. The yellow solid was allowed to accumulate overnight and then collected via filtration (1.88 g, 0.008 mol, 43%). ^{1}H NMR (200 MHz, CDCl$_3$): δ 9.17 (d, 1H, J = 3.4, H^3), 8.89 (dt, 1H, J = 8.1, 0.9, H$^{3'}$), 8.79 (ddd, 1H, J = 4.7, 1.8, 1.0, H$^{6'}$), 8.36 (d, 1H, J = 7.2, H^6), 8.07 (dd, 1H, J = 7.2, 3.3, H^5), 7.88 (td, 1H, J = 7.9, 1.9, H$^{4'}$), 7.43 (ddd, 1H, J = 7.6, 4.7 1.2, H$^{5'}$).

4-Bromo-2,2'-bipyridine-N-oxide[108] **6**
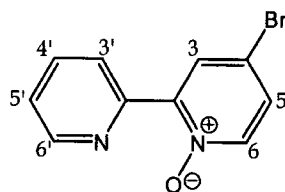
Acetyl bromide (13.8 mL, 0.19 mol) was added to a solution of 4-nitro-2,2'-bipyridine-N-oxide **5** (1.88 g, 8.7 mmol) in glacial acetic acid (23 mL). The solution was heated under reflux for 6 hours. Once cooled to room temperature, the resulting solution and yellow precipitate were poured onto ice and the pH adjusted to 11 with aqueous KOH. The reaction mixture was extracted into chloroform (3 x 100 mL), and the extractions were combined and dried over K$_2$CO$_3$. Removal of solvent under reduced pressure yielded an orange solid (1.84 g), which was found by NMR to be predominantly 4-bromo-2,2'-bipyridine-N-oxide, but some de-oxygenated product was also present. Data refers to the former product. 1H NMR (400 MHz, CDCl3): δ 8.94 (d, 1H, J = 8.2, H$^{6'}$), 8.73 (broad s, 1H, H^6), 8.39 (s, 1H, H^3), 8.14 (dd, 1H, J = 6.8, 4.8, H$^{3'}$), 7.84 (m, 1H, H$^{4'}$), 7.37 (m, 2H, H^5, H$^{5'}$).

4-Bromo-2,2'-bipyridine[108] [bpy-Br] **7**
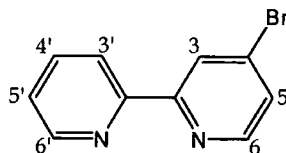
Phosphorous tribromide (5 mL) was added to a solution of 4-bromo-2,2'-bipyridine-N-oxide **6** (1.8 g, 7.8 mmol) in chloroform (38 mL). The resulting yellow solution was heated under reflux for 3 hours, during which time a brown solution with a yellow precipitate was formed. After cooling to room temperature, the reaction mixture was poured onto ice and basicified to pH 10 using aqueous KOH solution. The resulting

white precipitate was extracted into chloroform (3 x 100 mL), and the extractions were combined and dried over K_2CO_3. Removal of solvent under reduced pressure yielded an off-white solid (1.77 g). Purification was achieved via column chromatography (alumina) using gradient elution from 100% hexane to 15% diethyl ether and 85% hexane (1.2 g, 5.1 mmol, 65%). ^{1}H NMR (400 MHz, $CDCl_3$): δ 8.68 (ddd, 1H, J = 4.8, 1.7, 0.9, H$^{6'}$), 8.63 (d, 1H, J = 1.9, H^3), 8.48 (d, 1H, J = 5.3, H^6), 8.39 (dt, 1H, J = 7.9, 0.9, H$^{3'}$), 7.83 (td, 1H, J = 7.8, 1.8, H$^{4'}$), 7.48 (dd, 1H, J = 5.3, 2.0, H^5), 7.34 (ddd, 1H, J = 7.6, 4.8, 1.3, H$^{5'}$). ^{13}C NMR (400 MHz, $CDCl_3$): δ 157.6 (q), 154.9 (q), 150.0 (CH), 149.4 (CH), 137.2 (CH), 134.1 (q), 127.1 (CH), 124.7 (CH), 124.5 (CH), 121.6 (CH). ES$^+$ MS: m/z = 256.8 [M + Na]$^+$. TLC (SiO_2, 2.5% MeOH, 97.5% DCM): R_f = 0.58.

4'-Bromo-(3-carboxyl-3-oxoprop-1-enyl)benzene[22] **8**
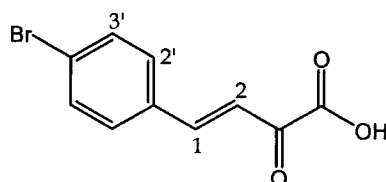
Sodium pyruvate (6.43 g, 0.058 mol) was dissolved in water (50 mL) and added to a solution of 4-bromobenzaldehyde (9.76 g, 0.053 mol) in ethanol (200 mL). Having cooled the mixture to 0°C, aqueous KOH (10.2 g in 100 mL water) was added slowly, giving rise to a cloudy yellow solution. The mixture was stirred at room temperature for 2 hours before acidifying using aqueous hydrochloric acid. The resulting yellow precipitate was collected, washed with cold water and dried under reduced pressure (11.5 g, 0.045 mol, 86%). ^{1}H NMR (400 MHz, $CDCl_3$): δ 8.06 (d, 1H, J = 16.0, H^2), 7.60 (d, 2H, H$^{3'}$), 7.57 (d, 1H, H^1), 7.54 (d, 2H, H$^{2'}$). ^{13}C NMR (400 MHz, $CDCl_3$): δ 182.3 (C=O), 160.2 (q, phenyl), 150.0 (CH, alkene), 132.8 (CH, phenyl), 130.9 (CH, phenyl), 127.3 (q, phenyl), 118.3 (CH, alkene). ES$^+$ MS: m/z = 277.2 [M + Na]$^+$.

1-(2-Oxo-2-pyridin-2-yl-ethyl)-pyridinium iodide[100] **9**
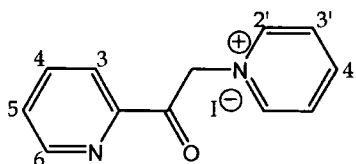
Iodine (20.5 g, 0.08 mol) was dissolved in pyridine (60 mL) and added to a solution of 2-acetylpyridine (9 mL, 0.08 mol) also in pyridine (20 mL). The mixture was stirred and heated at 100°C for 3 hours affording a black solution with grey crystals. After cooling the solution, the crystals were collected via filtration and dissolved in

ethanol/water (18%, 1 L). Charcoal was added to this solution with stirring, allowed to settle and then removed by filtration leaving a clear yellow solution. Once the solution had been concentrated under reduced pressure, a precipitate of cream coloured crystals formed. The crystals were collected and washed with ether before drying under reduced pressure (16.0 g, 0.049 mol, 61%). ^{1}H NMR (200 MHz, d^{6}-DMSO): δ 9.01 (d, 2H, J = 6.0, H$^{2'}$), 8.88 (d, 1H, J = 4.0, H^{6}), 8.73 (t, 1H, J = 7.5, H$^{4'}$), 8.28 (t, 2H, J = 6.5, H$^{3'}$), 8.14 (t, 1H, J = 8.0, H^{4}), 8.08 (d, 1H, J = 7.5, H^{3}), 7.84 (ddd, 1H, J = 7.5, 5.0, 1.0, H^{5}), 6.51 (s, 2H, CH$_2$). ES^{+} MS: m/z = 198.1 [M − I]$^{+}$. IR (KBr disc): 1710 cm^{-1} (ketone, C=O stretch).

4-(4-Bromophenyl)-2,2'-bipyridine[22] [bpy-φ-Br] **10**
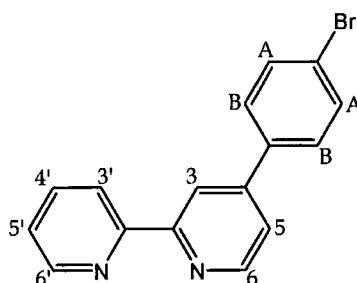
1-(2-Oxo-2-pyridin-2-yl-ethyl)-pyridinium iodide **9** (7.18 g, 0.022 mol), 4-bromo-(3-carboxyl-3-oxoprop-1-enyl)benzene **8** (5.09 g, 0.020 mol) and ammonium acetate (13.3 g, 0.17 mol) were dissolved in water (150 mL) and heated at 100°C for 6 hours. During this time the solution turned from yellow to cream and a cream coloured precipitate formed. After allowing the solution to cool, the precipitate was collected and washed with acetone before drying under reduced pressure (6.13 g). The solid was transferred to a Schlenk tube, which was evacuated and back filled with nitrogen three times. Whilst under nitrogen, the solid was heated strongly until molten, whereupon CO$_2$ gas was evolved. After cooling, the resulting solid was checked by ^{1}H NMR and it was necessary to repeat the thermolysis another two times before complete decarboxylation was achieved. Re-crystallisation from ethanol yielded a white solid (3.61 g, 0.012 mol, 58%). ^{1}H NMR (500 MHz, d^{6}-acetone): δ 8.76 (s, 1H, H^{3}), 8.75 (d, 1H, J = 5.1, H^{6}), 8.71 (d, 1H, J = 4.6, H$^{6'}$), 8.53 (d, 1H, J = 7.9, H$^{3'}$), 7.95 (td, 1H, J = 7.9, 1.5, H$^{4'}$), 7.84 (d, 2H, J = 8.4, H^{B}), 7.76 (d, 2H, J = 8.4, H^{A}), 7.72 (dd, 1H, J = 5.0, 1.7, H^{5}), 7.45 (ddd, 1H, J = 7.6, 4.8, 1.2, H$^{5'}$). ^{13}C NMR (400 MHz, d^{6}-acetone): δ 157.7 (q), 156.7 (q), 150.9 (CH), 150.1 (CH), 148.5 (q), 138.3 (q), 137.8 (CH), 133.2 (CH), 129.8 (CH), 125.0 (CH), 124.0 (q), 122.2 (CH), 121.7 (CH), 118.8 (CH). ES^{+} MS: m/z = 311 [M + H]$^{+}$. TLC (SiO$_2$, 2.5% MeOH, 97.5% DCM): R$_f$ = 0.55.

4-(4-Pyridyl)-2,2'-bipyridine [bpy-py] **11**
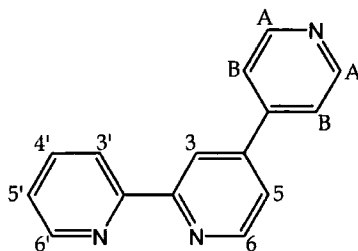
A Schlenk tube was charged with 4-bromo-2,2'-bipyridine **7** (461 mg, 1.96 mmol), pyridine-4-boronic acid (269 mg, 2.19 mmol), aqueous Na_2CO_3 (632 mg in < 1 mL H_2O, 5.96 mmol) and DME (10 mL). The solution was thoroughly degassed via three freeze-pump-thaw cycles and placed under nitrogen. $Pd(PPh_3)_4$ (150 mg, 0.13 mmol) was added to the Schlenk tube under a positive pressure of nitrogen. A reflux condenser was attached to the Schlenk tube and the apparatus was evacuated and back filled with nitrogen. The solution was stirred at 80 – 85°C for 24 hours. After this time, thin layer chromatography (alumina, hexane/diethyl ether, 50:50) revealed the presence of starting material, so additional boronic acid (30 mg) and catalyst (20 mg) were added. The reaction was heated for a further 48 hours. After cooling to room temperature, DME was removed under reduced pressure and the resulting residue was dissolved in DCM and water. The DCM layer was washed with aqueous solutions of KOH (1 M, 3 x 100 mL), dried over K_2CO_3 and evaporated to yield a brown oil (210 mg). Purification was achieved via flash column chromatography (alumina, 100% DCM) to yield a white solid (180 mg, 0.77 mmol, 39%). ^{1}H NMR (500 MHz, $CDCl_3$): δ 8.75 (d, 1H, $J = 5.1$, H^6), 8.72 (dd, 2H, $J = 4.5$, 1.7, H^A), 8.68 (m, 2H, H^3 + H$^{6'}$), 8.43 (d, 1H, $J = 7.9$, H$^{3'}$), 7.82 (td, 1H, $J = 7.8$, 1.8, H$^{4'}$), 7.62 (dd, 2H, $J = 4.5$, 1.7, H^B), 7.51 (dd, 1H, $J = 5.1$, 1.8, H^5), 7.32 (ddd, 1H, $J = 7.5$, 4.7, 1.1, H$^{5'}$). ^{13}C NMR and ^{1}H - ^{13}C HETCOR (500 MHz, $CDCl_3$): δ 157.2 (C), 155.6 (C), 150.7 (CH^A), 150.1 (CH^6), 149.3 (CH$^{6'}$), 146.5 (C), 145.8 (C), 137.1 (CH$^{4'}$), 124.2 (CH$^{5'}$), 121.6 (CH^4), 121.4 (CH^5, CH$^{3'}$), 118.9 (CH^3). ES$^+$ MS: m/z = 234 [M + H]$^+$, 256 [M + Na]$^+$, 297 [M + Cu]$^+$. Data agrees with literature data.[213]

4-(4-(4-Pyridyl)phenyl)-2,2'-bipyridine [bpy-φ-py] **12**
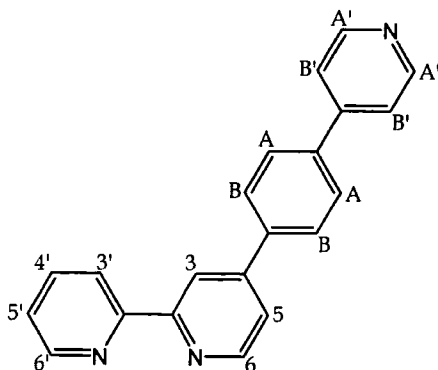
A Schlenk tube was charged with 4-(4-bromophenyl)-2,2'-bipyridine **10** (623 mg, 2.00 mmol), pyridine-4-boronic acid (297 mg, 2.41 mmol), aqueous Na_2CO_3 (645 mg in 2 mL H_2O, 6.09 mmol) and DME (10 mL). The solution was thoroughly degassed via three freeze-pump-thaw cycles and placed under nitrogen. $Pd(PPh_3)_4$ (156 mg, 0.14 mmol) was added under a positive pressure of nitrogen. A reflux condenser was attached and the apparatus was evacuated and back filled with nitrogen. The solution was stirred at room temperature for 30 minutes before heating under reflux for 45 hours. After this time, thin layer chromatography (SiO_2, hexane/diethyl ether, 50:50) revealed the presence of starting material, so additional boronic acid (50 mg) and catalyst (50 mg) were added, and the reaction was heated for a further 7 hours. After cooling to room temperature, DME was removed under reduced pressure and the resulting residue dissolved in DCM and water. The DCM layer was washed with aqueous solutions of KOH (1 M, 3 x 100 mL), dried over K_2CO_3 and evaporated to yield a cream/brown solid (0.52 g). Purification was achieved via column chromatography (silica gel) using gradient elution from 100% DCM to 2.5% methanol and 97.5% DCM (167 mg, 0.54 mmol, 27%). ^{1}H NMR (400 MHz, $CDCl_3$): δ 8.75 (dd, 1H, *J = 4.8, 0.8*, H^6), 8.73 – 8.70 (2 overlapping d, 2H, H^3, H$^{6'}$), 8.69 (dd, 1H, *J = 4.4, 1.6*, H$^{A'}$), 8.46 (dt, 1H, *J = 8.0, 1.0*, H$^{3'}$), 7.89 (d, 2H, *J = 4.8*, H^B), 7.85 (td, 1H, *J = 7.2, 1.6*, H$^{4'}$), 7.76 (d, 2H, *J = 8.8*, H^A), 7.57 (dd, 1H, *J = 5.2, 2.0*, H^5), 7.55 (dd, 2H, *J = 4.6, 1.8*, H$^{B'}$), 7.34 (ddd, 1H, *J = 7.6, 4.8, 1.2*, H$^{5'}$). ^{13}C NMR and ^{1}H – ^{13}C HETCOR (400 MHz, $CDCl_3$): δ 157.0 (C or CH^6), 156.1 (C or CH^6), 150.5 (CH$^{A'}$), 149.9 (C), 149.3 (CH^3 or CH$^{6'}$), 148.5 (C), 147.6 (C), 139.1 (C), 138.9 (C), 137.2 (CH$^{4'}$), 128.1 (CH^B), 127.8 (CH^A), 124.1 (CH$^{5'}$), 121.7, 121.6 and 121.5 (CH$^{3'}$, CH^5, CH$^{B'}$), 119.0 (CH^3 or CH$^{6'}$). ES$^+$ MS: m/z = 310.1 [M + H]$^+$, 332.1 [M + Na]$^+$, 641.2 [2M + Na]$^+$. HR ES$^+$ MS: m/z = 310.13389 measured, 310.13387 calculated for [$C_{21}H_{16}N_3$]$^+$. TLC (SiO_2, 10% MeOH, 90% DCM): R_f = 0.58. A crystal structure was obtained, full details of which are given in appendix I.

2,2'-Bipyridine-4-(4-phenyl)boronic acid [bpy-φ-B(OH)₂] **13** / *4-(4-Neopentylglycolatoboron-phenyl)-2,2'-bipyridine (using conditions reported by Miyaura[140])* [bpy-φ-Bneo] **14**
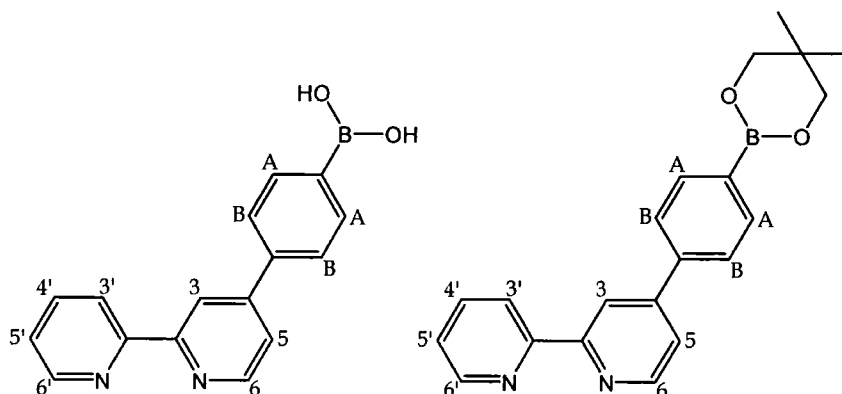
A Schlenk tube was charged with 4-(4-bromophenyl)-2,2'-bipyridine **10** (300 mg, 0.96 mmol), bis(neopentylglycolato)diboron (229 mg, 1.01 mmol), potassium acetate (284 mg, 2.89 mmol) and DMSO (11 mL). The solution was thoroughly degassed via three freeze-pump-thaw cycles and placed under nitrogen. Pd(dppf)Cl₂ (30 mg, 0.04 mmol) was added to the Schlenk tube under a positive pressure of nitrogen. The solution was stirred and heated to 80 – 85°C for 6 hours. The solution was diluted with DCM (30 mL) and washed with copious amounts of water (5 x 100 mL) before drying over Na₂SO₄. Evaporation of solvent under reduced pressure yielded a crude product. The product was dissolved in ethanol with heating and an insoluble white solid was removed via filtration. This gave the desired substituted bipyridine contaminated with some triphenylphosphine oxide and bis(neopentylglycolato)diboron. Some purification was achieved by dissolving the crude product in ethanol at reflux and hot filtration to remove an insoluble white solid. This was found to significantly decrease the amount of B₂neo₂ present in the sample. At this point, NMR integrals were used to estimate the ratio of species present and the product was used without any further purification (estimated yield 60%). [bpy-φ-Bneo] ¹H NMR (400 MHz, CDCl₃): δ 8.75 – 8.67 (m, 3H, H³, H⁶ and H⁶'), 8.44 (d, 1H, *J* = 7.9, H³'), 7.93 (d, 2H, *J* = 7.7, Hᴬ), 7.83 (td, 1H, *J* = 7.7, 1.7, H⁴'), 7.76 (d, 2H, *J* = 7.7, Hᴮ), 7.57 (dd, 1H, *J* = 5.1, 1.6, H⁵), 7.32 (dd, 1H, *J* = 7.4, 4.8, H⁵'), 3.80 (s, 4H, CH₂), 1.04 (s, 6H, CH₃). [bpy-φ-B(OH)₂] ¹H NMR (400 MHz, d₆-DMSO): δ 8.76 (d, 1H, *J* = 5.2, H⁶), 8.74 (d, 1H, *J* = 4.7, H⁶'), 8.69 (d, 1H, *J* = 1.5, H³), 8.44 (d, 1H, *J* = 8.0, H³'), 8.20 (s, 2H, OH), 8.01 – 7.95 (m, 3H, H⁴' and Hᴬ), 7.84 (d, 2H, *J* = 8.2, Hᴮ), 7.81 (dd, 1H, *J* = 5.1, 1.0, H⁵), 7.49 (ddd, 1H, *J* = 7.5, 4.8, 1.0, H⁵'). ES⁺ MS: m/z = 277.2 [bpy-φ-B(OH)₂ + H]⁺, 291.1 [bpy-φ-B(OH)(OMe) + H]⁺, 305.3 [[bpy-φ-B(OMe)₂ + H]⁺, 345.4 [bpy-φ-Bneo + H]⁺. HR ES⁺ MS: m/z = 305.14538 measured, 305.14558 calculated for [C₁₈H₁₃O₂N₂¹¹B]⁺.

6.5 Synthesis of dichloro-bridged metal dimers

Tetrakis(2-phenylpyridine-C,N)bis(μ-chloro)diiridium[69] [Ir(ppy)$_2$Cl]$_2$ **15**
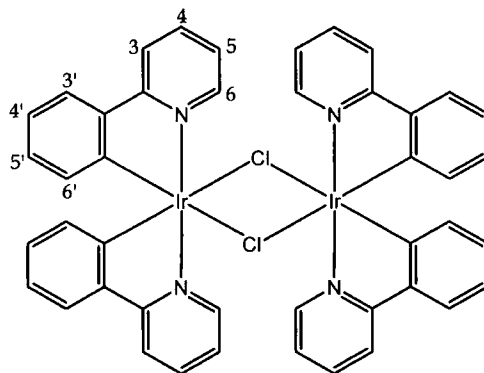
Iridium trichloride hydrate (478 mg, 1.51 mmol) and 2-phenylpyridine (0.46 mL, 497 mg, 3.2 mmol) were heated under reflux in 2-ethoxyethanol (30 mL) and water (10 mL) for 84 hours. The resulting yellow precipitate was collected using a centrifuge, washed with ethanol and dried under reduced pressure (500 mg, 0.47 mmol, 62%). ^{1}H NMR (500 MHz, CDCl$_3$): δ 9.24 (d, 4H, J = 5.7, H^6), 7.87 (d, 4H, J = 8.3, H^3), 7.73 (td, 4H, J = 7.6, 1.4, H^4), 7.48 (d, 4H, J = 7.6, H$^{3'}$), 6.77 (td, 4H, J = 5.7, 1.4, H^5), 6.74 (td, 4H, J = 7.3, 0.8, H$^{4'}$), 6.56 (td, 4H, J = 7.4, 1.3, H$^{5'}$), 5.93 (d, 4H, J = 7.7, H$^{6'}$). ^{13}C NMR (500 MHz, CDCl$_3$): δ 168.7, 151.8, 145.5, 143.8, 136.3 (CH^4), 130.7 (CH$^{6'}$), 129.2 (CH$^{5'}$), 123.8 (CH$^{3'}$), 122.3 (CH^5), 121.5 (CH$^{4'}$), 118.5 (CH^3). ES$^+$ MS: m/z = 501 [C$_{22}$H$_{16}$IrN$_2$]$^+$.

Tetrakis(4-(2-pyridyl)benzaldehyde-C,N)bis(μ-chloro)diiridium[94] [Ir(pba)$_2$Cl]$_2$ **16**
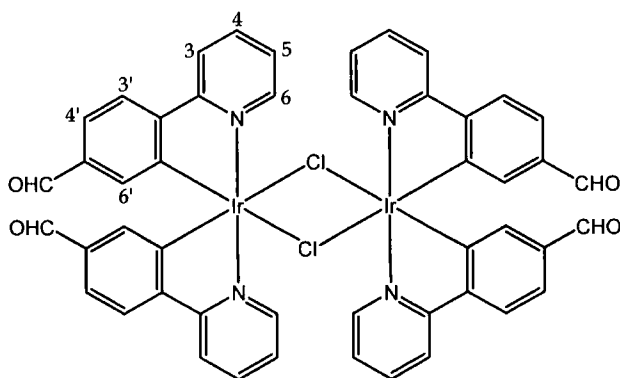
Iridium trichloride trihydrate (532 mg, 1.51 mmol) and 4-(2-pyridyl)benzaldehyde (566 mg, 3.09 mmol) were heated under reflux in water (10 mL) and 2-ethoxyethanol (30 mL) for 24 hours. The resulting orange precipitate was collected using a centrifuge, washed with ethanol (2 x 30 mL) and acetone (1 x 15 mL) and dried under reduced pressure (728 mg, 0.62 mmol, 82%). ^{1}H NMR (500 MHz, CDCl$_3$): δ 9.52 (s, 4H, CHO), 9.26 (d, 4H, J = 5.4, H^6), 8.05 (d, 4H, J = 7.9, H^3), 7.94 (t, 4H, J = 7.7, H^4), 7.67 (d, 4H,

$J = 8.0$, H$^{3'}$), 7.30 (d, 4H, $J = 7.9$, H$^{4'}$), 6.98 (t, 4H, $J = 6.1$, H^5), 6.36 (s, 4H, H$^{6'}$). ES$^+$ MS: m/z = 557 [C$_{24}$H$_{16}$IrN$_2$O$_2$]$^+$, 589 [C$_{24}$H$_{16}$IrN$_2$NaO$_2$]$^+$.

Tetrakis(2-(3,5-difluorophenyl)pyridine-C,N)bis(μ-chloro)diiridium[187] [Ir(ppy-F$_2$)Cl]$_2$ **17**
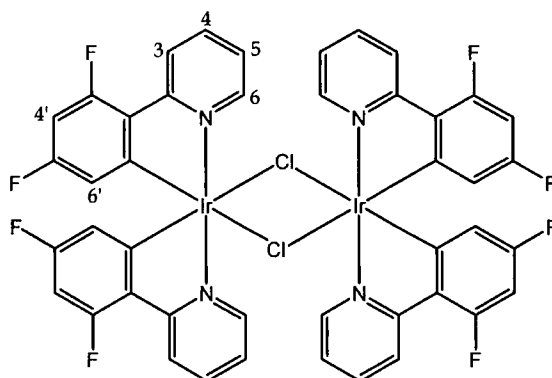
Iridium trichloride hydrate (317 mg, 1.0 mmol) and 2-(4,6-difluorophenyl)pyridine **2** (405 mg, 2.1 mmol) were heated under reflux in 2-ethoxyethanol (20 mL) and water (7 mL) for 72 hours. The resulting bright yellow precipitate was collected using a centrifuge, washed with ethanol and dried under reduced pressure (453 mg, 0.37 mmol, 75%). ^{1}H NMR (400 MHz, CDCl$_3$): δ 9.12 (d, 4H, $J = 5.8$, H^6), 8.31 (d, 4H, $J = 8.8$, H^3), 7.83 (t, 4H, $J = 7.9$, H^4), 6.83 (t, 4H, $J = 6.7$, H^5), 6.34 (ddd, 4H, $J = 12.5, 9.0, 2.2$, H$^{4'}$), 5.29 (dd, 4H, $J = 9.1, 2.4$, H$^{6'}$). ^{19}F NMR (400 MHz, CDCl$_3$): δ -108.1 - -108.2 (m), -110.7 (t, $J = 12.0$). ES$^+$ MS: m/z = 604.7 [C$_{22}$H$_{12}$F$_4$IrN$_2$ + CH$_3$OH]$^+$, 636.6 [C$_{22}$H$_{12}$F$_4$IrN$_2$ + 2CH$_3$OH]$^+$. EI MS: m/z = 1216.1 [C$_{44}$H$_{24}$Cl$_2$F$_8$Ir$_2$N$_4$] (run as solid sample). C, H & N analysis: 42.96% C, 1.96% H and 4.41% N measured, 42.82% C, 2.12% H and 4.54% N calculated for [C$_{44}$H$_{24}$Cl$_2$F$_8$Ir$_2$N$_4$]. H$_2$O.

Tetrakis(2-phenylpyridine-C,N)bis(μ-chloro)dirhodium (based on **15**[69]*)* [Rh(ppy)$_2$Cl]$_2$ **18**
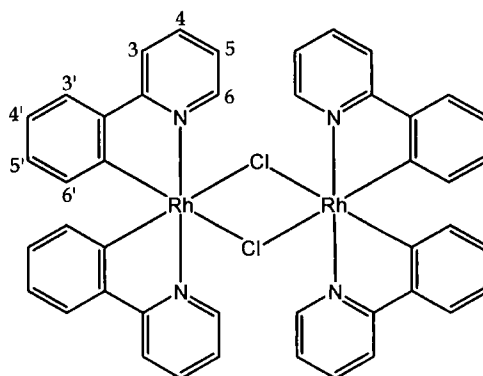
Rhodium trichloride trihydrate (263 mg, 1.0 mmol) and 2-phenylpyridine (0.31 mL, 2.2 mmol) were heated under reflux in 2-ethoxyethanol (21 mL) and water (7 mL) for

138

18 hours. The resulting precipitate was collected using a centrifuge, washed with ethanol and dried under reduced pressure (392 mg, 0.44 mmol, 88%). ^{1}H NMR (500 MHz, CDCl$_3$): δ 9.22 (d, 4H, J = 5.5, H^6), 7.86 (d, 4H, J = 7.8, H^3), 7.81 (td, 4H, J = 7.3, 1.4, H^4), 7.54 (d, 4H, J = 8.1, H$^{3'}$), 6.82 (t, 4H, J = 7.5, H$^{4'}$), 6.78 (td, 4H, J = 6.4, 1.3, H^5), 6.64 (td, 4H, J = 7.6, 1.1, H$^{5'}$), 5.94 (d, 4H, J = 7.9, H$^{6'}$). ES$^+$ MS: m/z = 411.0 [C$_{22}$H$_{16}$N$_2$Rh]$^+$, 857.1 [C$_{44}$H$_{32}$ClN$_4$Rh$_2$]$^+$.

Tetrakis(4-(2-pyridyl)benzaldehyde-C,N)bis(μ-chloro)dirhodium[95] [Rh(pba)$_2$Cl]$_2$ **19**
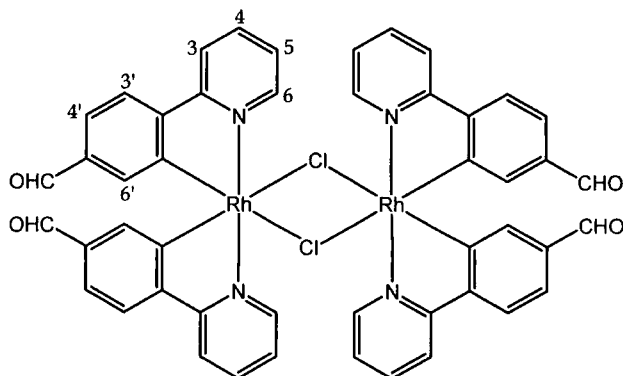
Rhodium trichloride trihydrate (157 mg, 0.6 mmol) and 4-(2-pyridyl)benzaldehyde (436 mg, 2.38 mmol) were heated under reflux in ethanol (15 mL) and water (5 mL) for 24 hours under an atmosphere of nitrogen and in the dark. The resulting yellow-orange precipitate was collected using a centrifuge, washed with ethanol and dried under reduced pressure. It was found that further purification could be achieved via filtration through celite in DCM yielding a yellow solid (259 mg, 0.22 mmol, 74%). ^{1}H NMR (500 MHz, CDCl$_3$): δ 9.52 (s, 4H, CHO), 9.24 (d, 4H, J = 5.3, H^6), 8.07 – 7.98 (m, 8H, H^3 and H^4), 7.74 (d, 4H, J = 7.9, H$^{3'}$), 7.39 (d, 4H, J = 7.9, H$^{4'}$), 6.98 (t, 4H, J = 6.2, H^5), 6.38 (s, 4H, H$^{6'}$). ES$^+$ MS: m/z = 467.0[C$_{24}$H$_{16}$N$_2$O$_2$Rh]$^+$, 499.0 [C$_{24}$H$_{16}$N$_2$O$_2$Rh + CH$_3$OH]$^+$.

Tetrakis(2-(5-fluorophenyl)pyridine-C,N)bis(μ-chloro)diiridium (based on 15[69])

[Ir(ppy-F)₂Cl]₂ **20**
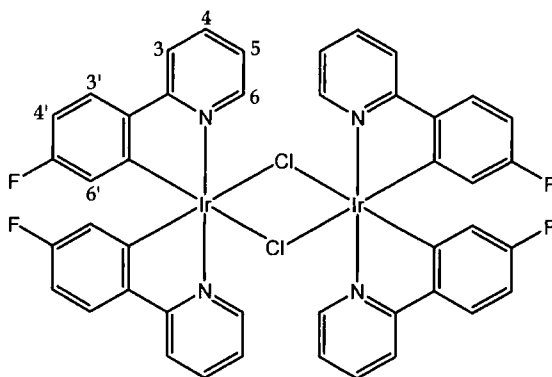
Iridium trichloride hydrate (108 mg, 0.34 mmol) and 2-(4-fluorophenyl)pyridine **1** (130 mg, 0.75 mmol) were heated under reflux in 2-ethoxyethanol (7 mL) and water (2.3 mL) for 48 hours. The resulting precipitate was collected using a centrifuge, washed with ethanol and dried under reduced pressure (120 mg, 0.11 mmol, 62%). ¹H NMR (500 MHz, CDCl₃): δ 9.13 (d, 4H, J = 5.6, H⁶), 7.83 (d, 4H, J = 7.8, H³), 7.77 (t, 4H, J = 7.5, H⁴), 7.50 (dd, 4H, J = 8.5, 5.8, H³'), 6.80 (t, 4H, J = 6.4, H⁵), 6.52 (td, 4H, J = 8.6, 2.2, H⁴'), 5.53 (dd, 4H, J = 9.9, 2.2, H⁶'). ¹³C NMR and ¹H-¹³C HSQC (500 MHz, CDCl₃): δ 167.6 (CH⁶), 163.8 (C), 161.8 (C), 151.5 (C), 147.5 (d, J = 24.5, C), 140.1 (C), 136.9 (CH⁴), 125.5 (d, J_{C-F} = 38.5, CH³'), 122.3 (CH⁵), 118.7 (CH³), 116.8 (d, J_{C-F} = 72.5, CH⁶'), 109.0 (d, J_{C-F} = 93, CH⁴'). ¹⁹F NMR (400 MHz, CDCl₃): δ -112.2. ES⁺ MS: m/z = 537.1 [C₂₂H₁₄F₂IrN₂]⁺. EI MS: m/z = 1144.1 [C₄₄H₂₈Cl₂F₄Ir₂N₄] (run as solid sample). C, H & N analysis: 45.35% C, 2.46% H and 4.66% N measured, 45.48% C, 2.60% H and 4.82% N calculated for [C₄₄H₂₈Cl₂F₄Ir₂N₄]. H₂O.

Tetrakis(2-(5-fluorophenyl)pyridine-C,N)bis(μ-chloro)dirhodium (based on 15[69])

[Rh(ppy-F)₂Cl]₂ **21**
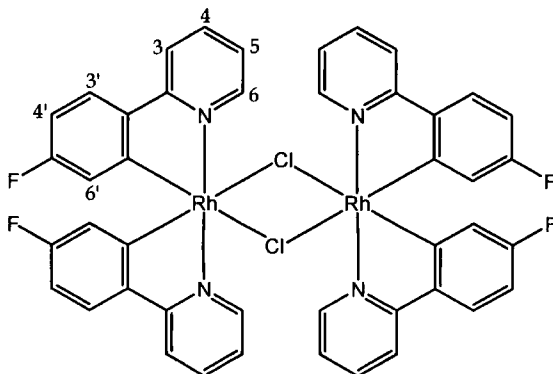
Rhodium trichloride trihydrate (79 mg, 0.3 mmol) and 2-(4-fluorophenyl)pyridine **1**

(114 mg, 0.66 mmol) were heated under reflux in 2-ethoxyethanol (7 mL) and water (2.3 mL) for 65 hours. The resulting precipitate was collected using a centrifuge, washed with ethanol and dried under reduced pressure (122 mg, 0.13 mmol, 84%). ^{1}H NMR (500 MHz, CDCl$_3$): δ 9.11 (d, 4H, J = 5.6, H^6), 7.89 – 7.77 (m, 8H, H^3 and H^4), 7.55 (dd, 4H, J = 8.5, 5.7, H$^{3'}$), 6.80 (t, 4H, J = 6.5, H^5), 6.57 (td, 4H, J = 8.6, 2.3, H$^{4'}$), 5.57 (d, 4H, J = 9.7, H$^{6'}$). ^{19}F NMR (400 MHz, CDCl$_3$): δ -110.5 (m). ES$^+$ MS: m/z = 447.0 [C$_{22}$H$_{14}$F$_2$N$_2$Rh]$^+$, 479.0 [C$_{22}$H$_{14}$F$_2$N$_2$Rh + CH$_3$OH]$^+$. HR EI MS: m/z = 963.9735 measured, 963.9732 calculated for [C$_{44}$H$_{28}$Cl$_2$F$_4$Rh$_2$N$_4$] (run as solid sample).

Tetrakis(2-(3,5-difluorophenyl)pyridine-C,N)bis(μ-chloro)dirhodium (based on 15^{69})
[Rh(ppy-F$_2$)$_2$Cl]$_2$ **22**
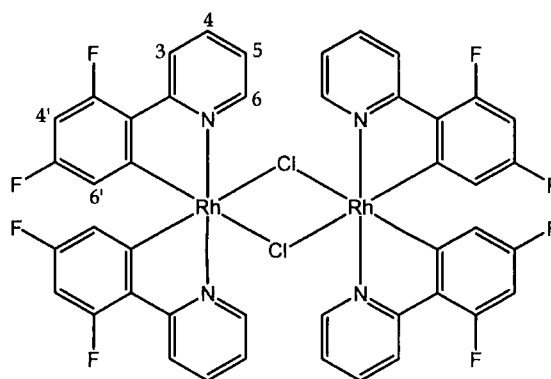
Rhodium trichloride trihydrate (121 mg, 0.46 mmol) and 2-(4,6-difluorophenyl)-pyridine **2** (193 mg, 1.01 mmol) were heated under reflux in water (3.5 mL) and 2-ethoxyethanol (10.5 mL) for 18 hours. The resulting precipitate was collected using a centrifuge, washed with ethanol (2 x 30 mL) and acetone (1 x 15 mL) and dried under reduced pressure (210 mg, 0.20 mmol, 88%). ^{1}H NMR (500 MHz, CDCl$_3$): δ 9.11 (d, 4H, J = 5.6, H^6), 8.27 (d, 4H, J = 8.3, H^3), 7.90 (t, 4H, J = 7.7, H^4), 6.83 (t, 4H, J = 6.6, H^5), 6.37 (ddd, 4H, J = 12.3, 8.9, 2.2, H$^{4'}$), 5.33 (d, 4H, J = 9.0, H$^{6'}$). ^{19}F NMR (200 MHz, CDCl$_3$): δ - 107.9 - -108.1 (m), 110.2 (t, J = 11.6). ES$^+$ MS: m/z = 482.9 [C$_{22}$H$_{12}$F$_4$N$_2$Rh]$^+$, 515.0 [C$_{22}$H$_{12}$F$_4$N$_2$Rh + CH$_3$OH]$^+$, 547.0 [C$_{22}$H$_{12}$F$_4$N$_2$Rh + 2CH$_3$OH]$^+$. HR EI MS: m/z = 1035.9360 measured, 1035.9355 calculated for [C$_{44}$H$_{24}$Cl$_2$F$_8$Rh$_2$N$_4$] (run as solid sample).

Tetrakis(2-(3,4,5-trifluorophenyl)pyridine-C,N)bis(μ-chloro)diiridium (based on 15[69])

[Ir(ppy-F₃)Cl]₂ **23**
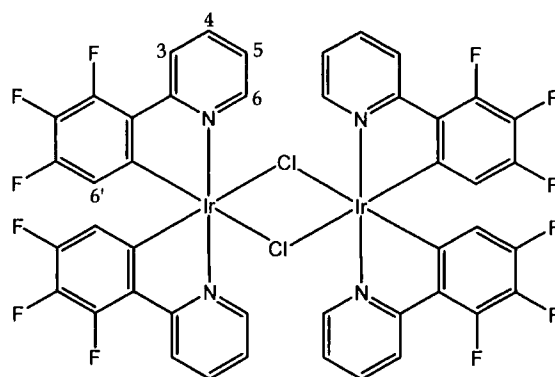
Iridium trichloride hydrate (127 mg, 0.40 mmol) and 2-(4,5,6-trifluorophenyl)pyridine **3** (184 mg, 0.88 mmol) were heated under reflux in 2-ethoxyethanol (8 mL) and water (2.7 mL) for 48 hours. The resulting precipitate was collected using a centrifuge, washed with water (2 x 10 mL) and ethanol (2 x 10 mL) and dried under reduced pressure (197 mg, 0.15 mmol, 76%). ^{1}H NMR (500 MHz, CDCl₃): δ 9.10 (d, 4H, *J = 5.8*, H⁶), 8.32 (d, 4H, *J = 8.3*, H³), 7.89 (td, 4H, *J = 7.8, 1.4*, H⁴), 6.88 (ddd, 4H, *J = 7.4, 5.9, 1.4*, H⁵), 5.27 (t, 4H, *J = 8.4*, H⁶'). ^{13}C NMR: (500 MHz, CDCl₃): δ 165.2 (q), 151.5 (CH⁶), 146.0 – 150.0 (m, 2 C-F), 138.1 (CH⁴), 136.9 (q), 134.9 (m, C-F), 128.2 (q), 123.4 (CH⁵), 123.1 (d, *J$_{C-F}$ = 19.6*, CH³), 112.7 (d, *J$_{C-F}$ = 14.7*, CH⁶'). ^{19}F NMR (400 MHz, CDCl₃): δ -131.8 (m, F³'), -136.9 (dd, *J = 19.0, 10.0*, F⁴'), -169.2 (td, *J = 19.9, 6.8*, F⁵'). ES⁺ MS: m/z = 609.2 [C₂₂H₁₀F₆IrN₂]⁺. EI MS: m/z = 1288.1 [C₄₄H₂₀Cl₂F₁₂Ir₂N₄] (run as solid sample). C, H & N analysis: 40.47% C, 2.09% H and 3.89% N measured, 40.47% C, 1.70% H and 4.29% N calculated for [C₄₄H₂₀Cl₂F₁₂Ir₂N₄]. H₂O.

6.6 Synthesis of monometallic complexes

6.6.1 Synthesis of monometallic complexes via the reaction of dichloro-bridged dimers with 2,2'-bipyridine ligands[78]

(2,2'-Bipyridine)bis(2-phenylpyridine)iridium(III)hexafluorophosphate[5]

[Ir(ppy)₂(bpy)][PF₆] **24**
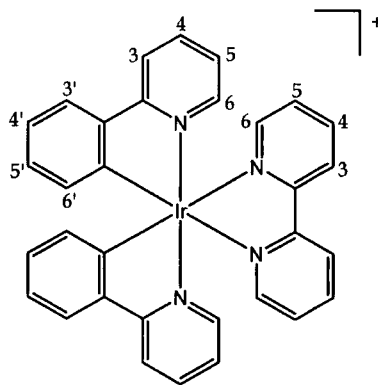
2,2'-Bipyridine (54 mg, 0.35 mmol) was dissolved in DCM (8 mL) and added to a suspension of [Ir(ppy)₂Cl]₂ **15** (163 mg, 0.15 mmol) in methanol (10mL). The solution was stirred at reflux for 90 minutes. Once cooled to room temperature, all solvent was removed under vacuum and the residue redissolved in acetonitrile and water. Filtration of this solution into saturated aqueous KPF₆ gave a yellow/orange precipitate which was collected using a centrifuge and dried under vacuum (227 mg, 0.28 mmol, 93%). ¹H NMR (500 MHz, d⁶-acetone): δ 8.85 (d, 2H, *J* = *8.2*, bpy-H³), 8.30 (td, 2H, *J* = *8.1, 1.5*, bpy-H⁴), 8.24 (d, 2H, *J* = *8.1*, ppy-H³), 8.11 (d, 2H, *J* = *5.4*, bpy-H⁶), 7.96 (td, 2H, *J* = *7.8, 1.5*, ppy-H⁴), 7.90 (d, 2H, *J* = *7.9*, ppy-H³'), 7.83 (d, 2H, *J* = *5.9*, ppy-H⁶), 7.71 (td, 2H, *J* = *6.5, 1.2*, bpy-H⁵), 7.16 (td, 2H, *J* = *6.6, 1.3*, ppy-H⁵), 7.04 (td, 2H, *J* = *7.6, 1.2*, ppy-H⁴'), 6.92 (td, 2H, *J* = *7.5, 1.3*, ppy-H⁵'), 6.35 (d, 2H, *J* = *7.6*, ppy-H⁶'). ES⁺ MS: m/z = 657.1 [M − PF₆]⁺. C, H & N analysis: 47.59% C, 3.39% H and 6.26% N measured, 47.35% C, 3.56% H and 6.59% N calculated for [C₃₂H₂₄F₆IrN₄P]. 1.5 CH₃OH. TLC (Al₂O₃, 5% methanol, 95% DCM): R_f = 0.52.

(2,2'-Bipyridine)bis(2-phenylpyridine)rhodium(III)hexafluorophosphate[5]
[Rh(ppy)₂(bpy)][PF₆] **25**
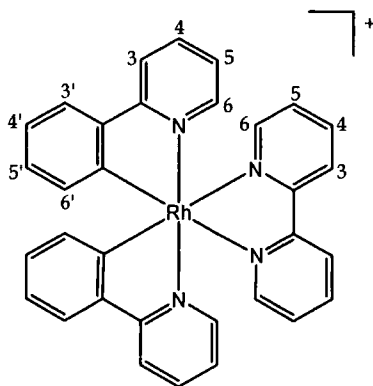
2,2'-Bipyridine (26 mg, 0.17 mmol) was dissolved in DCM (4 mL) and added to a suspension of [Rh(ppy)₂Cl]₂ **18** (67 mg, 0.075 mmol) in methanol (5 mL). The solution was stirred at reflux for 90 minutes. Once cooled to room temperature, all solvent was removed under vacuum and the residue re-dissolved in acetonitrile and water. Filtration of this solution into saturated aqueous KPF₆ gave a pale yellow precipitate which was collected using a centrifuge and dried under vacuum (109 mg, 0.14 mmol, 93%). ¹H NMR (400 MHz, d⁶-acetone): δ 8.81 (d, 2H, J = *8.3*, bpy-H³), 8.30 (td, 2H, J = *7.9, 1.7*, bpy-H⁴), 8.26 (d, 2H, J = *8.1*, ppy-H³), 8.12 (d, 2H, J = *5.2*, bpy-H⁶), 8.03 (td, 2H, J = *7.8, 1.6*, ppy-H⁴), 7.95 (dd, 2H, J = *7.8, 1.3*, ppy-H³'), 7.80 (d, 2H, J = *5.7*, ppy-H⁶), 7.69 (ddd, 2H, J = *7.6, 5.3, 1.0*, bpy-H⁵), 7.21 (ddd, 2H, J = *7.5, 5.7, 1.3*, ppy-H⁵), 7.10 (td, 2H, J = *7.5, 1.1*, ppy-H⁴'), 6.99 (td, 2H, J = *7.5, 1.3*, ppy-H⁵'), 6.37 (d, 2H, J = *7.6*, ppy-H⁶'). ¹³C NMR (500 MHz, d⁶-acetone): δ 168.5 (C), 168.2 (C), 165.8 (C), 155.6 (C), 151.0 (bpy-CH⁶), 144.9 (C), 140.8 (bpy-CH⁴), 139.7 (ppy-CH⁴), 133.5 (ppy-CH⁶'), 131.0 (ppy-CH⁵'), 128.8 (bpy-CH⁵), 125.6 (ppy-CH³'), 125.1 (bpy-CH³), 124.5 (ppy-CH⁵), 124.3 (ppy-CH⁴'), 121.0 (ppy-CH³). ES⁺ MS: m/z = 567.1 [M − PF₆]⁺. HR ES⁺ MS: m/z = 567.10474 measured, 567.10505 calculated [C₃₂H₂₄N₄¹⁰³Rh]⁺. C, H & N analysis: 52.82% C, 3.37% H and 7.70% N measured, 52.62% C, 3.59% H and 7.67% N calculated for [C₃₂H₂₄F₆N₄PRh]. H₂O. TLC (SiO₂, 15% methanol, 85% DCM): R_f = 0.65.

(2,2'-Bipyridine)bis(4-(2-pyridyl)benzaldehyde)rhodium(III)hexafluorophosphate[95]

[Rh(pba)₂(bpy)][PF₆] **26**
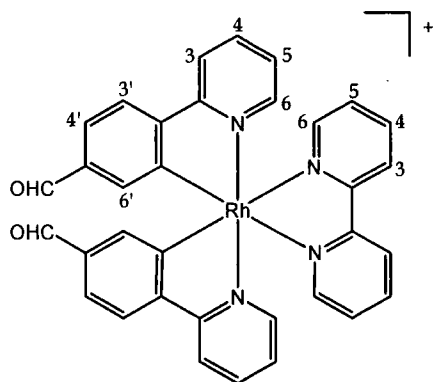
2,2'-Bipyridine (10 mg, 0.066 mmol) was dissolved in DCM (1.6 mL) and added to a suspension of [Rh(pba)₂Cl]₂ **19** (30 mg, 0.03 mmol) in methanol (2.0 mL). The solution was stirred at reflux for 90 minutes. Once cooled to room temperature, all solvent was removed under vacuum and the residue redissolved in acetonitrile and water. Filtration of this solution into saturated aqueous KPF₆ gave a precipitate which was collected using a centrifuge and dried under vacuum (42 mg, 0.094 mmol, 92%). ^{1}H NMR (400 MHz, d⁶-acetone): δ 9.76 (s, 2H, CHO), 8.84 (d, 2H, *J* = *8.2*, bpy-H³), 8.46 (d, 2H, *J* = *7.9*, ppy-H³), 8.34 (td, 2H, *J* = *8.1, 1.6*, bpy-H⁴), 8.24 – 8.15 (m, 6H, ppy-H⁴, ppy-H⁶ and bpy-H⁶), 7.94 (d, 2H, *J* = *5.8*, ppy-H³'), 7.70 (ddd, 2H, *J* = *7.6, 5.2, 1.2*, bpy-H⁵), 7.66 (dd, 2H, *J* = *8.2, 1.7*, ppy-H⁴'), 7.37 (ddd, *J* = *7.7, 5.7, 1.3*, ppy-H⁵), 6.89 (s, 2H, ppy-H⁶'). ES⁺ MS: m/z = 622.8 [M – PF₆]⁺. C, H & N analysis: 52.16% C, 3.24% H and 7.01% N measured, 51.92% C, 3.33% H and 7.12% N calculated for [C₃₄H₂₄F₆N₄O₂PRh]. H₂O. TLC (SiO₂, 15% methanol, 85% DCM): R$_f$ = 0.57.

(2,2'-Bipyridine)bis(2-(5-fluoro)phenylpyridine)iridium(III)hexafluorophosphate

[Ir(ppy-F)₂(bpy)][PF₆] **27**

2,2'-Bipyridine (17 mg, 0.11 mmol) was dissolved in DCM (2.7 mL) and added to a

suspension of [Ir(ppy-F)₂Cl]₂ **20** (57 mg, 0.05 mmol) in methanol (3.3 mL). The solution was heated under reflux for 90 minutes. After cooling to room temperature all solvent was removed under reduced pressure and the residue was re-dissolved in the minimum volume of acetonitrile and water. Filtration of this solution into saturated aqueous KPF_6 gave a yellow precipitate which was collected using a centrifuge and dried under reduced pressure (77 mg, 0.092 mmol, 92%). ¹H NMR (400 MHz, d⁶-acetone): δ 8.87 (d, 2H, *J = 8.0*, bpy-H³), 8.33 (td, 2H, *J = 7.9, 1.6*, bpy-H⁴), 8.24 (d, 2H, *J = 8.3*, ppy-H³), 8.17 (ddd, 2H, *J = 5.5, 1.5, 0.8*, bpy-H⁶), 8.03 – 7.96 (m, 4H, ppy-H³′ and ppy-H⁴), 7.83 (ddd, 2H, *J = 5.8, 1.5, 0.8*, ppy-H⁶), 7.74 (ddd, 2H, *J = 7.7, 5.6, 1.3*, bpy-H⁵), 7.19 (ddd, 2H, *J = 7.5, 5.8, 1.4*, ppy-H⁵), 6.84 (td, 2H, *J = 8.8, 2.5*, ppy-H⁴′), 5.95 (dd, 2H, *J = 9.4, 2.5*, ppy-H⁶′). ¹⁹F NMR (400 MHz, d⁶-acetone): δ -73.0 (d, J_{F-P} = *706*, PF_6), - 111.1 - -111.2 (m, ppy-F). ES⁺ MS: m/z = 693.0 [M – PF_6]⁺. HR ES⁺ MS: m/z = 693.14063 measured, 693.14365 calculated for [$C_{32}H_{22}N_4F_2$¹⁹³Ir]⁺. C, H & N analysis: 45.60% C, 2.75% H and 6.40% N measured, 45.39% C, 2.74% H and 6.62% N calculated for [$C_{32}H_{22}F_8IrN_4P$]. 0.5 H_2O. TLC (SiO_2, 15% methanol, 85% DCM): R$_f$ = 0.55.

(2,2'-Bipyridine)bis(2-(5-fluoro)phenylpyridine)rhodium(III)hexafluorophosphate
[Rh(ppy-F)₂(bpy)][PF₆] **28**
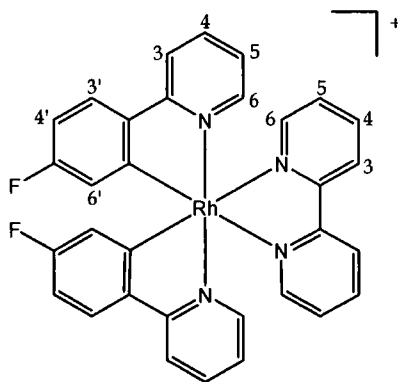
2,2'-Bipyridine (17 mg, 0.11 mmol) was dissolved in DCM (2.7 mL) and added to a suspension of [Rh(ppy-F)₂Cl]₂ **21** (48 mg, 0.05 mmol) in methanol (3.3 mL). The solution was stirred at reflux for 90 minutes. Once cooled to room temperature, all solvent was removed under vacuum and the residue redissolved in acetonitrile and water. Filtration of this solution into saturated aqueous KPF_6 gave a precipitate which was collected using a centrifuge and dried under vacuum (69 mg, 0.092 mmol, 93%). ¹H NMR (400 MHz, d⁶-acetone): δ 8.84 (d, 2H, *J = 8.2*, bpy-H³), 8.34 (td, 2H, *J = 8.0, 1.7*, bpy-H⁴), 8.26 (d, 2H, *J = 8.2*, ppy-H³), 8.19 (d, 2H, *J = 5.3*, bpy-H⁶), 8.10 – 8.03 (m, 4H, ppy-H³′ and ppy-H⁴), 7.80 (d, 2H, *J = 5.8*, ppy-H⁶), 7.73 (ddd, 2H, *J = 7.6, 5.3, 1.2*, bpy-H⁵), 7.24 (ddd, 2H, *J = 7.5, 5.8, 1.3*, ppy-H⁵), 6.89 (td, 2H, *J = 8.9, 2.6*, ppy-H⁴′), 6.00

(ddd, 2H, J = 9.1, 2.5, 1.2, ppy-H$^{6'}$). ^{19}F NMR (400 MHz, d^6-acetone): δ - 73.9 (d, 6F, J_{F-P} = 756, PF$_6$), -110.7 - -110.8 (m, 2F, ppy-F). ES$^+$ MS: m/z = 603.1 [M - PF$_6$]$^+$. HR ES$^+$ MS: m/z = 603.08578 measured, 603.08621 calculated for [C$_{32}$H$_{22}$N$_4$F$_2$^{103}Rh]$^+$. C, H & N analysis: 50.91% C, 2.94% H and 7.42% N measured, 50.74% C, 3.33% H and 7.12% N calculated for [C$_{32}$H$_{24}$F$_6$N$_4$O$_2$Rh]. 0.5 H$_2$O. TLC (SiO$_2$, 15% methanol, 85% DCM): R$_f$ = 0.62.

(2,2'-Bipyridine)bis(2-(3,5-difluorophenyl)pyridine)iridium(III)hexafluorophosphate
[Ir(ppy-F$_2$)$_2$(bpy)][PF$_6$] **29**
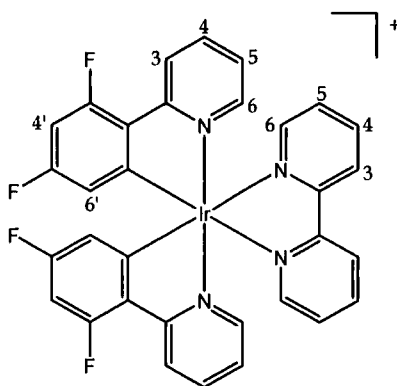
2,2'-Bipyridine (12 mg, 0.077 mmol) was dissolved in DCM (2 mL) and added to a suspension of [Ir(ppy-F$_2$)Cl]$_2$ **17** (43 mg, 0.035 mmol) in methanol (2.5 mL). The solution was stirred at reflux for 90minutes. After cooling to room temperature, all solvent was removed under reduced pressure and the residue was re-dissolved in the minimum volume of acetonitrile and water. Filtration of this solution into a saturated aqueous solution of KPF$_6$ yielded a yellow precipitate which was collected using a centrifuge, washed with water and dried under reduced pressure. Purification was achieved via column chromatography (silica gel) using gradient elution from 100% DCM to 98% DCM to 2% methanol (45 mg, 0.052 mmol, 73%). ^{1}H NMR (400 MHz, d^6-acetone): δ 8.88 (d, 2H, J = 8.5, bpy-H^3), 8.39 (d, 2H, J = 8.4, ppy-H^3), 8.35 (td, 2H, J = 8.1, 1.6, bpy-H^4), 8.22 (d, 2H, J = 5.5, bpy-H^6), 8.06 (td, 2H, J = 8.3, 1.6, ppy-H^4), 7.93 (d, 2H, J = 5.8, ppy-H^6), 7.75 (ddd, 2H, J = 7.7, 5.4, 1.2, bpy-H^5), 7.25 (ddd, 2H, J = 7.5, 5.8, 1.4, ppy-H^5), 6.76 (ddd, 2H, J = 12.7, 9.4, 2.4, ppy-H$^{4'}$), 5.80 (dd, 2H, J = 8.5, 2.4, ppy-H$^{6'}$). ^{19}F NMR (400 MHz, d^6-acetone): δ -72.9 (d, J_{F-P} = 708, PF$_6$), -108.2 - -108.3 (m, ppy-F$_2$), -110.5 (t, J = 11.5, ppy-F$_2$). ES$^+$ MS: m/z = 729.0 [M - PF$_6$]$^+$. HR ES$^+$ MS: m/z = 729.1223 measured, 729.1254 calculated for [C$_{32}$H$_{20}$N$_4$F$_4$^{193}Ir]$^+$. C, H & N analysis: 43.32% C, 2.36% H and 5.94% N measured, 43.10% C, 2.49% H and 6.28% N calculated for [C$_{32}$H$_{20}$F$_{10}$IrN$_4$P] .H$_2$O. TLC (SiO$_2$, 15% methanol, 85% DCM): R$_f$ = 0.45.

(2,2'-Bipyridine)bis(2-(3,5-difluoro)phenylpyridine)rhodium(III)hexafluorophosphate
[Rh(ppy-F₂)₂(bpy)][PF₆] **30**
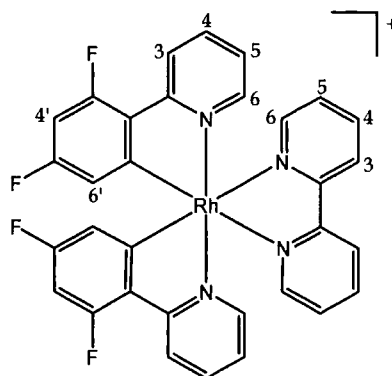
2,2'-Bipyridine (17 mg, 0.11 mmol) was dissolved in DCM (2.7 mL) and added to a suspension of [Rh(ppy-F₂)₂Cl]₂ **22** (52 mg, 0.05 mmol) in methanol (3.3 mL). The solution was stirred at reflux for 90 minutes. Once cooled to room temperature, all solvent was removed under vacuum and the residue redissolved in acetonitrile and water. Filtration of this solution into saturated aqueous KPF₆ gave a precipitate which was collected using a centrifuge and dried under vacuum (74 mg, 0.094 mmol, 94%). ¹H NMR (500 MHz, d⁶-acetone): δ 8.85 (d, 2H, J = *8.2*, bpy-H³), 8.41 – 8.33 (m, 4H, ppy-H³ and bpy-H⁴), 8.25 (d, 2H, J = *5.2*, bpy-H⁶), 8.14 (td, 2H, J = *7.9, 1.1*, ppy-H⁴), 7.89 (d, 2H, J = *5.9*, ppy-H⁶), 7.75 (ddd, 2H, J = *7.6, 5.3, 1.1*, bpy-H⁵), 7.30 (ddd, 2H, J = *7.5, 5.8, 1.2*, ppy-H⁵), 6.83 (ddd, 2H, J = *12.5, 9.3, 2.4*, ppy-H⁴'), 5.85 (d, 2H, J = *8.3*, ppy-H⁶'). ¹⁹F NMR (500 MHz, d⁶-acetone): δ -73.0 (d, 6F, J_{F-P} = *752*, PF₆), -108.0 (m, 1H), -109.8 (m, 1H). ES⁺ MS: m/z = 639.0 [M – PF₆]⁺. HR ES⁺ MS: m/z = 639.06745 measured, 639.06736 calculated for [C₃₂H₂₀N₄F₄¹⁰³Rh]⁺. C, H & N analysis: 47.58% C, 2.52% H and 6.93% N measured, 47.63%% C, 2.81% H and 6.94% N calculated for [C₃₂H₂₀F₁₀N₄PRh]. 1.25 H₂O. TLC (SiO₂, 15% methanol, 85% DCM): R_f = 0.59.

(2,2'-Bipyridine)bis(2-(3,4,5-trifluorophenyl)pyridine)iridium(III)hexafluorophosphate
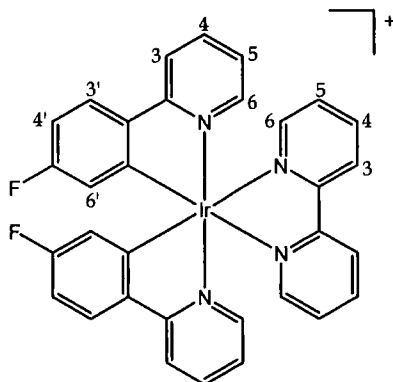[Ir(ppy-F₃)₂(bpy)][PF₆] **31**
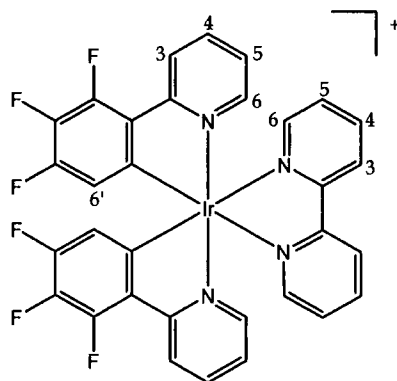
2,2'-Bipyridine (17 mg, 0.11 mmol) was dissolved in DCM (2.7 mL) and added to a suspension of [Ir(ppy-F₃)Cl]₂ **23** (64 mg, 0.05 mmol) in methanol (3.3 mL). The solution was heated under reflux for 90 minutes. After cooling to room temperature all solvent was removed under reduced pressure and the residue was re-dissolved in the minimum volume of acetonitrile and water. Filtration of this solution into saturated aqueous KPF₆ gave a precipitate which was collected using a centrifuge and dried under reduced pressure (74 mg, 0.081 mmol, 81%). ¹H NMR (500 MHz, d⁶-acetone): δ 8.87 (d, 2H, *J* = *8.2*, bpy-H³), 8.41 (d, 2H, *J* = *8.4*, ppy-H³), 8.35 (td, 2H, *J* = *7.9, 1.5*, bpy-H⁴), 8.29 (d, 2H, *J* = *5.5*, bpy-H⁶), 8.10 (t, 2H, *J* = *7.9*, ppy-H⁴), 7.95 (d, 2H, *J* = *5.8*, ppy-H⁶), 7.73 (ddd, 2H, *J* = *7.7, 5.6, 1.3*, bpy-H⁵), 7.30 (ddd, 2H, *J* = *7.5, 5.8, 1.4*, ppy-H⁵), 5.89 (ddd, 2H, *J* = *7.8, 7.2, 1.9*, ppy-H⁶'). ¹³C NMR (500 MHz, d⁶-acetone): δ 164.3 (q), 156.8 (ppy-CH⁶), 153.4 – 149.7 (2 dd, 2C-F), 152.1 (bpy-CH⁶), 150.9 (q), 145.2 (q), 141.2 (bpy-CH⁴), 140.9 (ppy-CH⁴), 136.8 (dt, *J* = *950, 50*, C-F), 129.9 (bpy-CH⁵), 129.4 (q), 126.1 (bpy-CH³), 125.8 (ppy-CH⁵), 124.8 (d, *J* = *56.5*, ppy-CH³),114.8 (d, *J* = *55.5*, ppy-CH⁶'). ¹⁹F NMR: (400 MHz, d⁶-acetone): δ 73.0 (d, *J_{P-F}* = *748*, PF₆), -133.4 (m, F³'), -137.6 (dd, *J* = *18.5, 9.9*, F⁴'), -170.7 (td, *J* = *19.7, 7.1*, F⁵'). ES⁺ MS: m/z = 764.8 [M – PF₆]⁺. HR ES⁺ MS: m/z = 765.10527 measured, 765.10596 calculated for [C₃₂H₁₈N₄F₆¹⁹³Ir]⁺. C, H & N analysis: 42.34% C, 2.01% H and 5.89% N measured, 42.25% C, 1.99% H and 6.16% N calculated for [C₃₂H₁₈F₁₂IrN₄P]. TLC (SiO₂, 15% methanol, 85% DCM): R_f = 0.55.

(4-Bromo-2,2'-bipyridine)bis(2-phenylpyridine)iridium(III)hexafluorophosphate
[Ir(ppy)₂(bpy-Br)][PF₆] **32**
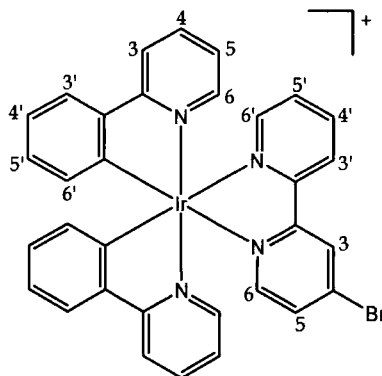
4-Bromo-2,2'-bipyridine **7** (78 mg, 0.33 mmol) was dissolved in DCM (8 mL) and added to a suspension of [Ir(ppy)₂Cl]₂ **15** (163 mg, 0.15 mmol) in methanol (10mL). The solution was stirred at reflux for 90 minutes. Once cooled to room temperature, all solvent was removed under vacuum and the residue redissolved in acetonitrile and water. Filtration of this solution into saturated aqueous KPF₆ gave a yellow/orange precipitate which was collected using a centrifuge and dried under vacuum (264 mg, 0.30 mmol, 98%). ¹H NMR (500 mHz, d⁶-acetone): δ 9.09 (s, 1H, bpy-H³), 8.96 (d, 1H, *J = 8.3*, bpy-H³'), 8.33 (td, 1H, *J = 8.0, 1.2*, bpy-H⁴'), 8.25 (d, 2H, *J = 7.8*, ppy-H³), 8.12 (d, 1H, *J = 5.2*, bpy-H⁶'), 8.01 - 7.92 (m, 4H, ppy-H⁴, bpy-H⁵ and bpy-H⁶), 7.90 (d, 2H, *J = 7.7*, ppy-H³'), 7.83 (d, 1H, *J = 5.6*, ppy-H⁶), 7.75 (t, 1H, *J = 6.3*, bpy-H⁵'), 7.19 - 7.14 (m, 2H, ppy-H⁵), 7.06 - 7.01 (m, 2H, ppy-H⁴'), 6.94 - 6.89 (m, 2H, ppy-H⁵'), 6.33 (d, 2H, *J = 7.8*, ppy-H⁶'). ES⁺ MS: m/z = 734.2 [M - PF₆]⁺. HR ES⁺ MS: m/z = 735.07268 measured, 735.07300 calculated for [C₃₂H₂₃N₄⁷⁹Br¹⁹³Ir]⁺.

(4-Bromo-2,2'-bipyridine)bis(4-(2-pyridyl)benzaldehyde)iridium(III)hexafluorophosphate
[Ir(pba)₂(bpy-Br)][PF₆] **33**
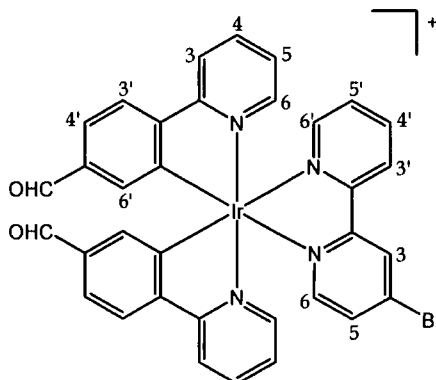
4-Bromo-2,2'-bipyridine **7** (74 mg, 0.315 mmol) was dissolved in DCM (8 mL) and

added to a suspension of [Ir(pba)$_2$Cl]$_2$ **16** (180 mg, 0.152 mmol) in methanol (10 mL). The mixture was heated at reflux for 90 minutes until a clear orange solution was formed. After cooling to room temperature, a saturated solution of NH$_4$PF$_6$ in methanol was added (2 mL). The solvent was removed to give the crude product (215 mg), which was used in subsequent reactions without further purification. ^{1}H NMR (500 MHz, d^6-acetone): δ 9.75 (s, 2H, CHO), 9.14 (s, 1H, bpy-H^3), 9.02 (d, 1H, *J = 8.0*, bpy-H$^{3'}$), 8.45 (d, 2H, *J = 8.0*, ppy-H^3), 8.37 (t, 1H, *J = 8.0*, bpy-H$^{4'}$), 8.18 – 8.07 (m, 6H, ppy-H^4, ppy-H$^{3'}$, bpy-H$^{6'}$, bpy-H^6), 7.98 (t, 2H, *J = 4.5*, ppy-H^6), 7.91 (dd, 1H, *J = 5.5, 1.5*, bpy-H^5), 7.75 (t, 1H, *J = 6.3*, bpy-H$^{5'}$), 7.57 (d, 2H, *J = 8.0*, ppy-H$^{4'}$), 7.33 (2xt, 2H, *J = 6.0*, ppy-H^5), 6.85 (s, 2H, ppy-H$^{6'}$).

(4-Bromo-2,2'-bipyridine)bis(4-(2-pyridyl)benzaldehyde)rhodium(III)hexafluorophosphate [Rh(pba)$_2$(bpy-Br)][PF$_6$] **34**
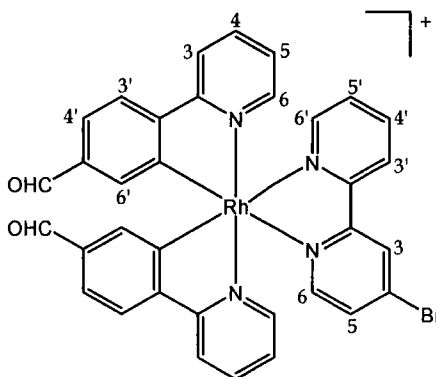
4-Bromo-2,2'-bipyridine **7** (39 mg, 0.17 mmol) was dissolved in DCM (4 mL) and added to a suspension of [Rh(pba)$_2$Cl]$_2$ **19** (75 mg, 0.075 mmol) in methanol (5mL). The solution was stirred at reflux for 90 minutes. Once cooled to room temperature, all solvent was removed under reduced pressure and the residue was redissolved in acetonitrile and water. Filtration of this solution into saturated aqueous KPF$_6$ gave a precipitate which was collected using a centrifuge and dried under reduced pressure (120 mg, 0.142 mmol, 94%). ^{1}H NMR (500 MHz, CD$_3$CN): δ 9.71 (s, 2H, CHO), 8.76 (d, 1H, *J = 1.8*, bpy-H^3), 8.53 (d, 1H, *J = 8.1*, bpy-H$^{3'}$), 8.23 (d, 2H, *J = 8.4*, ppy-H^3), 8.18 (td, 1H, *J = 7.8, 1.6*, bpy-H$^{4'}$), 8.08 – 8.03 (m, 4H, ppy-H$^{3'}$ and ppy-H^4), 8.00 (d, 1H, *J = 5.2*, bpy-H$^{6'}$), 7.79 (d, 1H, *J = 5.7*, bpy-H^6), 7.72 (d, 1H, *J = 5.2*, bpy-H^5), 7.69 – 7.65 (m, 2H, ppy-H^6), 7.62 (dd, 2H, *J = 7.9, 1.6*, ppy-H$^{4'}$), 7.52 (ddd, 1H, *J = 7.7, 5.3, 1.2*, bpy-H$^{5'}$), 7.24 (t, 2H, *J = 6.5*, bpy-H^5), 6.74 (s, 2H, ppy-H$^{6'}$). ES$^+$ MS: m/z = 703.0 [M – PF$_6$]$^+$. HR ES$^+$ MS: m/z = 701.00464 measured, 701.00539 calculated for [C$_{34}$H$_{23}$O$_2$N$_4$^{79}Br^{103}Rh]$^+$.

(4-Bromo-2,2'-bipyridine)bis(2-(5-fluorophenyl)pyridine)iridium(III)hexafluorophosphate
[Ir(ppy-F)₂(bpy-Br)][PF₆] **35**
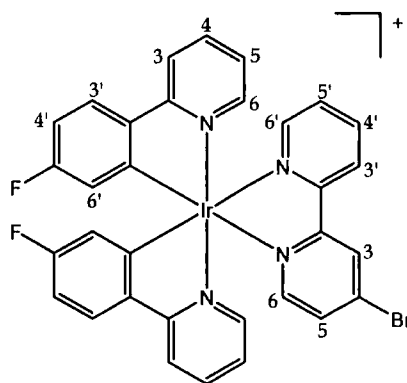
4-Bromo-2,2'-bipyridine **7** (39 mg, 0.17 mmol) was dissolved in DCM (4 mL) and added to a suspension of [Ir(ppy-F)₂Cl]₂ **20** (86 mg, 0.075 mmol) in methanol (5mL). The solution was stirred at reflux for 90 minutes. Once cooled to room temperature, all solvent was removed under reduced pressure and the residue was redissolved in acetonitrile and water. Filtration of this solution into saturated aqueous KPF₆ gave a yellow precipitate which was collected using a centrifuge and dried under reduced pressure (134 mg, 0.146 mmol, 97%). ¹H NMR (500 MHz, d⁶-acetone): δ 9.11 (d, 1H, *J = 1.9*, bph-H³), 8.98 (d, 1H, *J = 8.2*, bpy-H³'), 8.36 (td, 1H, *J = 7.9, 1.6*, bpy-H⁴'), 8.25 (d, 2H, *J = 8.2*, ppy-H³), 8.19 (d, 1H, *J = 5.4*, bpy-H⁶'), 8.03 – 7.94 (m, 6H, ppy-H³', ppy-H⁴, bpy-H⁵ and bpy-H⁶), 7.83 (d, 2H, *J = 5.8*, ppy-H⁶), 7.78 (ddd, 1H, *J = 7.6, 5.5, 1.2*, bpy-H⁵'), 7.22 – 7.16 (m, 2H, ppy-H⁵), 6.84 and 6.83 (2 td, 2H, *J = 9.0, 1.3*, ppy-H⁴'), 5.95 - 5.91 (m, 2H, ppy-H⁶'). ¹⁹F NMR (200 MHz, d⁶-acetone): δ -73.0 (d, *J_{P-F} = 752.6*, PF₆), - 111.0 - -111.2 (m, ppy-F). ES⁺ MS: m/z = 771.1 [M – PF₆]⁺. HR ES⁺ MS: m/z = 769.05164 measured, 769.05182 calculated for [C₃₂H₂₁N₄⁷⁹BrF₂¹⁹¹Ir]⁺.

(4-Bromo-2,2'-bipyridine)bis(2-(3,5-difluorophenyl)pyridine)iridium(III)hexafluorophosphate
[Ir(ppy-F₂)₂(bpy-Br)][PF₆] **36**
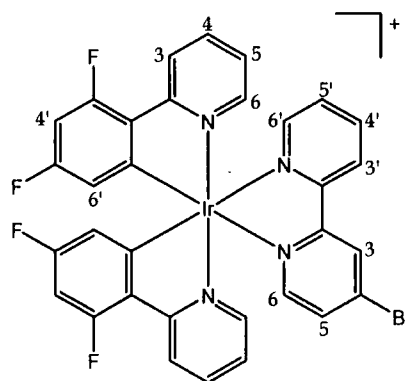
4-Bromo-2,2'-bipyridine 7 (39 mg, 0.17 mmol) was dissolved in DCM (4 mL) and added to a suspension of [Ir(ppy-F$_2$)Cl]$_2$ 17 (91 mg, 0.075 mmol) in methanol (5mL). The solution was stirred at reflux for 2 hours. Once cooled to room temperature, all solvent was removed under reduced pressure and the residue was redissolved in acetonitrile and water. Filtration of this solution into saturated aqueous KPF$_6$ gave a yellow precipitate which was collected using a centrifuge and dried under reduced pressure (112 mg, 0.12 mmol, 78%). ^{1}H NMR (400 MHz, d^6-acetone): δ 9.11 (d, 1H, $J = 1.7$, bpy-H^3), 8.98 (d, 1H, $J = 8.2$, bpy-H$^{3'}$), 8.42 – 8.34 (m, 3H, ppy-H^3 and bpy-H$^{4'}$), 8.24 (d, 1H, $J = 5.3$, bpy-H$^{6'}$), 8.11 – 8.03 (m, 4H, ppy-H^4, bpy-H^5 and bpy-H^6), 7.94 and 7.92 (2 overlapping d, 2H, ppy-H^6), 7.78 (t, 1H, $J = 6.7$, bpy-H$^{5'}$),7.28 – 7.22 (m, 2H, ppy-H^5), 6.79 – 6.73 (m, 2H, ppy-H$^{4'}$), 5.81 – 5.76 (m, 2H, ppy-H$^{6'}$). ^{13}C NMR (500 MHz, d^6-acetone): δ 165.5 – 161.2 (2 overlapping m, 2 C-F), 158.1 (s, C), 155.6 (s, C), 154.9 (d, JC-F = 27, C), 152.4 (s, bpy-CH^5 or bpy-CH^6), 152.1 (s, bpy-CH$^{6'}$), 150.8 (d, $J_{C-F} = 61$, ppy-CH^4), 141.2 (s, bpy-H^4), 140.7 (s, bpy-CH^5 or bpy-CH^6), 137.3 (s, C), 132.9 (s, ppy-CH^6), 130.4 (s, bpy-CH$^{5'}$), 129.5 (s, bpy-CH^3), 128.8 (s, C), 126.6 (s, bpy-CH$^{3'}$), 125.1 (d, $J_{C-F} = 31$, ppy-CH^5), 124.6 (dd, $J_{C-F} = 79$, ppy-CH^3), 117.7 (s, C), 114.6 (m, ppy-CH$^{6'}$), 99.7 (td, $J_{C-F} = 107, 15$, ppy-CH$^{4'}$). ^{19}F NMR (400 MHz, d^6-acetone): δ -72.0, -73.8, -108.1 (m), -110.4 (m). ES$^+$ MS: m/z = 807.0 [M – PF$_6$]$^+$. HR ES$^+$ MS: m/z = 807.03409 measured, 807.03531 calculated for [C$_{32}$H$_{19}$N$_4$^{79}BrF$_4$^{193}Ir]$^+$.

(4-(4-Bromophenyl)-2,2'-bipyridine)bis(2-phenylpyridine)iridium(III)hexafluorophosphate
[Ir(ppy)$_2$(bpy-φ-Br)][PF$_6$] 37

(4-(4-Bromophenyl)-2,2'-bipyridine 10 (102 mg, 0.33 mmol) was dissolved in DCM (8 mL) and added to a suspension of [Ir(ppy)$_2$Cl]$_2$ 15 (163 mg, 0.15 mmol) in methanol (10 mL). The solution was stirred under reflux for 90 minutes. Once cooled to room temperature, all solvent was removed under reduced pressure. The residue was dissolved in acetonitrile and water, filtered and added droppwise to a saturated aqueous solution of KPF$_6$. The resulting yellow/orange precipitate was collected using

a centrifuge and dried under reduced pressure. Purification was achieved via column chromatography (alumina), using gradient elution from 100% DCM to 1% methanol and 99% DCM (197 mg, 0.21 mmol, 69%). ^{1}H NMR (500 MHz, d^6-acetone): δ 9.16 (d, 1H, *J = 1.9*, bpy-H^3), 9.10 (d, 1H, *J = 8.1*, bpy-H$^{3'}$), 8.31 (td, 1H, *J = 8.0, 1.7*, bpy-H$^{4'}$), 8.26 and 8.25 (2 overlapping d, 2H, *J = 7.3*, ppy-H^3), 8.15 – 8.10 (m, 2H, bpy-H^6 and bpy-H$^{6'}$), 8.01 (dd, 1H, *J = 5.7, 2.1*, bpy-H^5), 7.99 – 7.86 (m, 8H, ppy-H^3, ppy-H$^{3'}$, ppy-H^6 and H^B), 7.79 (d, 2H, *J = 8.7*, H^A), 7.73 (ddd, 1H, *J = 7.6, 5.4, 1.2*, bpy-H$^{5'}$), 7.18 and 7.15 (2 overlapping ddd, 2H, *J = 7.5, 5.8, 1.4*, ppy-H^5), 7.06 and 7.04 (2 overlapping ddd, 2H, *J = 7.4, 4.8, 1.1*, ppy-H$^{4'}$), 6.94 and 6.92 (2 overlapping ddd, 2H, *J = 7.4, 4.1, 1.3*, ppy-H$^{5'}$), 6.38 and 6.36 (2 overlapping d, 2H, ppy-H$^{6'}$). ES$^+$ MS: m/z = 811.1 [M – PF$_6$]$^+$. HR ES$^+$ MS: m/z = 811.10622 measured, 811.10430 calculated for [C$_{38}$H$_{27}$N$_4$^{79}Br^{193}Ir]$^+$.

(4-(4-Bromophenyl)-2,2'-bipyridine)bis(4-(2-pyridyl)benzaldehyde)iridium(III)
hexafluorophosphate [Ir(pba)$_2$(bpy-φ-Br)][PF$_6$] **38**
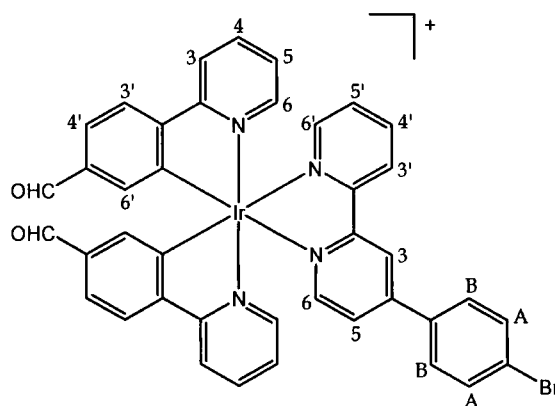
4-(4-Bromophenyl)-2,2'-bipyridine **10** (96 mg, 0.31 mmol) was dissolved in DCM (8 mL) and added to a suspension of [Ir(pba)$_2$Cl]$_2$ **16** (178 mg, 0.15 mmol) in methanol (10 mL). The mixture was heated at reflux for 90 minutes until a clear orange solution was formed. After cooling to room temperature, a saturated solution of NH$_4$PF$_6$ in methanol was added (2 mL). The solvent was removed to give the crude product (254 mg), which was used in subsequent reactions without further purification. ^{1}H NMR (500 MHz, CD$_3$CN): δ 9.73 (d, 2H, *J = 5.2*, CHO), 8.86 (s + d overlap, 2H, bpy-H$^{3'}$, bpy-H^3), 8.22 (m, 3H, ppy-H^3, bpy-H$^{4'}$), 8.04 – 7.93 (m, 6H, ppy-H$^{3'}$, ppy-H^4, bpy-H$^{6'}$, bpy-H^6), 7.84 (d, 2H, *J = 8.1*, H^B), 7.78 – 7.69 (m, 5H, H^A, ppy-H^6, bpy-H^5), 7.56 (m, 2H, ppy-H$^{4'}$), 7.51 (dd, 1H, *J = 13, 5.5*, bpy-H$^{5'}$), 7.20 (t, 2H, *J = 5.8*, ppy-H^5), 6.77 (d, 2H, *J = 5.0*, ppy-H$^{6'}$). ES$^+$ MS: m/z = 867.1 [M – PF$_6$]$^+$.

(4-(4-Bromophenyl)-2,2'-bipyridine)bis(4-(2-pyridyl)benzaldehyde)rhodium(III)
hexafluorophosphate [Rh(pba)₂(bpy-φ-Br)][PF₆] **39**

4-Bromophenyl-2,2'-bipyridine **10** (68 mg, 0.22 mmol) was dissolved in DCM (5.3 mL) and added to a suspension of [Rh(pba)₂Cl]₂ **19** (101 mg, 0.1 mmol) in methanol (6.7 mL). The solution was stirred at reflux for 90 minutes. Once cooled to room temperature, all solvent was removed under reduced pressure and the residue was redissolved in acetonitrile and water. Filtration of this solution into saturated aqueous KPF₆ gave a precipitate which was collected using a centrifuge and dried under vacuum. Purification was achieved via column chromatography (alumina) using gradient elution from 100% DCM to 99% DCM and 1% methanol (137 mg, 0.15 mmol, 74%). ¹H NMR (500 MHz, d⁶-acetone): δ 9.78 and 9.77 (2 s, 2H, CHO), 9.17 (d, 1H, *J* = 1.5, bpy-H³), 9.11 (d, 1H, *J* = 8.2, bpy-H³'), 8.49 and 8.47 (2 overlapping d, 2H, *J* = 7.2, ppy-H³), 8.36 (td, 1H, *J* = 7.7, 1.6, bpy-H⁴'), 8.26 – 8.16 (m, 6H, ppy-H³', ppy-H⁴, bpy-H⁶ and bpy-H⁶'), 8.06 – 7.93 (m, 5H, bpy-H⁵, ppy-H⁶ and H^B), 7.79 (d, 2H, *J* = 8.7, H^A), 7.73 (ddd, 1H, *J* = 7.6, 5.3, 1.0, bpy-H⁵'), 7.68 (ddd, 2H, *J* = 7.9, 5.2, 1.6, ppy-H⁴'), 7.39 and 7.37 (2 overlapping ddd, 2H, *J* = 7.5, 5.7, 1.3, ppy-H⁵), 6.91 and 6.90 (2 s, 2H, ppy-H⁶'). ES⁺ MS: m/z = 779.0 [M – PF₆]⁺. HR ES⁺ MS: m/z = 77.03755 measured, 777.03669 calculated for [C₄₀H₂₇O₂N₄⁷⁹Br¹⁰³Rh]⁺.

(4-(4-Methoxy)phenyl-2,2'-bipyridine)bis(2-phenylpyridine)iridium(III)hexafluorophosphate
[Ir(ppy)₂(bpy-ϕ-OMe)][PF₆] **40**
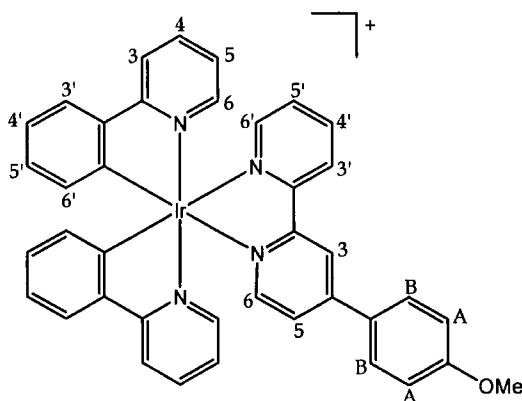
4-(4-Methoxy)phenyl-2,2'-bipyridine (80 mg, 0.31 mmol) was dissolved in DCM (8 mL) and added to a suspension of [Ir(ppy)₂Cl]₂ **15** (162 mg, 0.15 mmol) in methanol (10 mL). The mixture was heated under reflux for 3 hours until a clear orange solution was formed. After cooling to room temperature, the solution was filtered to remove any undissolved solid, and all solvent was removed under reduced pressure. The resulting solid was dissolved in acetonitrile, filtered, and added dropwise to a saturated aqueous solution of KPF₆. The resulting yellow/orange precipitate was collected using a centrifuge and dried under reduced pressure (159 mg, 0.18 mmol, 58%). ¹H NMR (500 MHz, d⁶-acetone): δ 9.09 (s, 1H, bpy-H³'), 9.07 (s, 1H, bpy-H³), 8.20 (td, 1H, J = 7.9, 1.5, bpy-H⁴'), 8.16 (t, 2H, J = 7.3, ppy-H³), 8.03 (d, 1H, J = 5.3, bpy-H⁶'), 7.95 – 7.76 (m, 10H, ppy-H⁶, ppy-H⁴, ppy-H³', bpy-H⁶, bpy-H⁵, H^B), 7.61 (td, 1H, J = 6.3, 1.0, bpy-H⁵'), 7.08 (m, 2H, ppy-H⁵), 7.05 (d, 2H, J = 8.9, H^A), 6.95 (ddd, 2H, J = 7.5, 5.0, 1.0, ppy-H⁴'), 6.84 (ddd, 2H, J = 7.5, 4.0, 1.0, ppy-H⁵'), 6.29 (d, 2H, J = 7.6, ppy-H⁶'), 3.89 (s, 3H, Me). ES⁺ MS: m/z = 762.8 [M – PF₆]⁺. HR ES⁺ MS: m/z = 763.2066 measured, 763.2049 calculated for [C₃₉H₃₀¹⁹³IrN₄O]⁺. C, H & N analysis: 50.67% C, 3.35% H and 5.99% N measured, 50.59% C, 3.48% H and 6.05% N calculated for [C₃₉H₃₀F₆IrN₄OP]. H₂O. TLC (Al₂O₃, 5% methanol, 95% DCM): R_f = 0.68.

(4-(4-Methoxy)phenyl)-2,2'-bipyridine)bis(4-(2-pyridyl)benzaldehyde)iridium(III)
hexafluorophosphate [Ir(pba)₂(bpy-φ-OMe)][PF₆] **41**

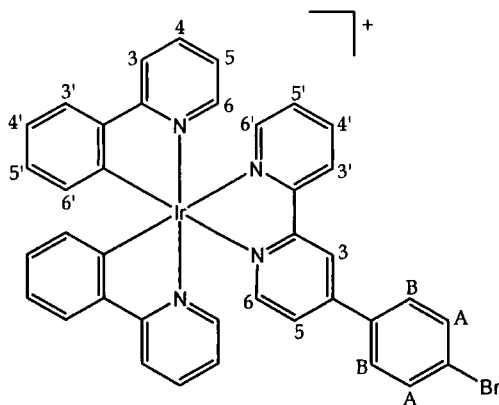4-(4-Methoxy)phenyl-2,2'-bipyridine (84 mg, 0.32 mmol) was dissolved in DCM (8 mL) and added to a suspension of [Ir(pba)₂Cl]₂ **16** (183 mg, 0.15 mmol) in methanol (10 mL). The mixture was heated at reflux for 90 minutes until a clear orange solution was formed. After cooling to room temperature, all solvent was removed under reduced pressure. The resulting solid was dissolved in acetonitrile, filtered and added dropwise to a saturated aqueous solution of KPF₆. The resulting yellow/orange precipitate was collected using a centrifuge and dried under reduced pressure. Purification was achieved via column chromatography (alumina), using gradient elution from 100% DCM to 0.5% methanol and 99.5% DCM (93 mg, 0.097 mmol, 31%).
¹H NMR (500 MHz, d⁶-acetone): δ 9.76 (d, 2H, J = 4.1, CHO), 9.13 (s, 1H, bpy-H³'), 9.11 (s, 1H, bpy-H³), 8.44 (t, 2H, *J = 7.1*, ppy-H³), 8.32 (td, 1H, *J = 7.9, 1.4*, bpy-H⁴'), 8.15 (2xd, 3H, ppy-H³', bpy-H⁶'), 8.12 – 8.05 (m, 4H, ppy-H⁶, ppy-H⁴), 8.02 (d, 1H, *J = 5.5*, bpy-H⁶), 8.00 (d, 2H, *J = 9.0*, Hᴮ), 7.93 (dd, 1H, *J = 5.5, 1.5*, bpy-H⁵), 7.70 (t, 1H, *J = 6.6*, bpy-H⁵'), 7.57 (td, 2H, *J = 7.0, 1.5*, ppy-H⁴'), 7.33 (m, 2H, ppy-H⁵), 7.13 (d, 2H, *J = 8.9*, Hᴬ), 6.91 (s, 2H, ppy-H⁶'), 3.89 (s, 3H, Me). ES⁺ MS: m/z = 818 [M – PF₆]⁺. HR ES⁺ MS: m/z = 819.2028 measured, 819.1947 calculated for [C₄₁H₃₀¹⁹³IrN₄O₃]⁺. C, H & N analysis: 50.16% C, 3.12% H and 5.64% N measured, 50.15% C, 3.28% H and 5.71% N calculated for [C₄₁H₃₀F₆IrN₄O₃P]. H₂O. TLC (Al₂O₃, 5% methanol, 95% DCM): R_f = 0.59.

(4-(4-Pyridyl)-2,2'-bipyridine)bis(2-phenylpyridine)iridium(III)hexafluorophosphate

[Ir(ppy)₂(bpy-py)][PF₆] **42**
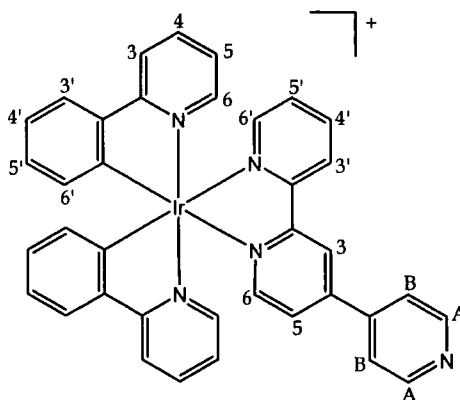
4-(4-Pyridyl)-2,2'-bipyridine **11** (60 mg, 0.26 mmol) was dissolved in DCM (8 mL) and added to a suspension of [Ir(ppy)₂Cl]₂ **15** (137 mg, 0.13 mmol) in methanol (10 mL). The mixture was heated under reflux for 2 hours until a clear yellow solution was formed. After cooling to room temperature, all solvent was removed under reduced pressure. The resulting solid was dissolved in acetonitrile, filtered and added dropwise to a saturated aqueous solution of KPF₆. The resulting yellow/orange precipitate was collected using a centrifuge and dried under reduced pressure. Purification was achieved via column chromatography (alumina), using gradient elution from 100% DCM to 1.5% methanol and 98.5% DCM (51 mg, 0.06 mmol, 22%). ¹H NMR (500 MHz, d⁶-acetone): δ 9.24 (d, 1H, *J* = *1.5*, bpy-H³), 9.12 (d, 1H, *J* = *8.2*, bpy-H³′), 8.80 (d, 2H, *J* = *4.6*, Hᴬ), 8.33 (td, 1H, *J* = *8.0, 1.5*, bpy-H⁴′), 8.26 (t, 2H, *J* = *7.5*, ppy-H³), 8.20 (d, 1H, *J* = *5.8*, bpy-H⁶), 8.14 (d, 1H, *J* = *5.4*, bpy-H⁶′), 8.09 (dd, 1H, *J* = *5.9, 1.8*, bpy-H⁵), 8.00 – 7.87 (m, 8H, Hᴮ, ppy-H⁴, ppy-H³′, ppy-H⁶), 7.74 (t, 1H, *J* = *6.6*, bpy-H⁵′), 7.16 (2 x t, 2H, *J* = *6.6*, ppy-H⁵), 7.05 (dd, 2H, *J* = *14.1, 6.9*, ppy-H⁴′), 6.94 (ddd, 2H, *J* = *12.9, 5.4, 1.0*, ppy-H⁵′), 6.37 (t, 2H, *J* = *8.1*, ppy-H⁶′). ES⁺ MS: m/z = 734.3 [M - PF₆]⁺. HR ES⁺ MS: m/z = 734.18988 measured, 734.18904 calculated for [C₃₇H₂₇¹⁹³IrN₅]⁺. C, H & N analysis: 49.98% C, 3.12% H and 7.83% N measured, 50.05% C, 3.18% H and 7.89% N calculated for [C₃₇H₂₇F₆IrN₅P]. 0.5 H₂O. TLC (Al₂O₃, 5% methanol, 95% DCM): R_f = 0.59.

(4-(4-Pyridyl)-2,2'-bipyridine)bis(4-(2-pyridyl)benzaldehyde)iridium(III)hexafluorophosphate
[Ir(pba)₂(bpy-py)][PF₆] **43**
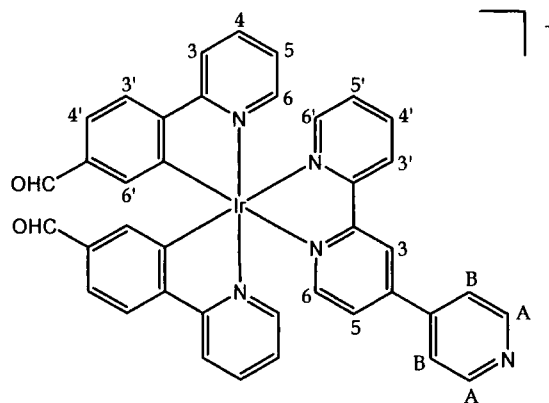
4-(4-Pyridyl)-2,2'-bipyridine **11** (50 mg, 0.21 mmol) was dissolved in DCM (8 mL) and added to a suspension of [Ir(pba)₂Cl]₂ **16** (128 mg, 0.11 mmol) in methanol (10 mL). The mixture was heated under reflux for 4 hours until a clear yellow solution was formed. After cooling to room temperature, all solvent was removed under vacuum. The resulting solid was dissolved in acetonitrile, filtered and added dropwise to a saturated aqueous solution of KPF₆. The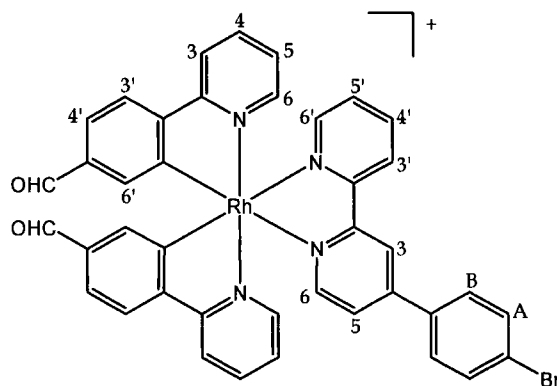 resulting yellow/orange precipitate was collected using a centrifuge and dried under reduced pressure. Purification was achieved via column chromatography (alumina), using gradient elution from 100% DCM to 1% methanol and 99% DCM (37 mg, 0.040 mmol, 19%). ¹H NMR (500 MHz, d⁶-acetone): δ 9.72 (d, 2H, *J* = 3.2, CHO), 8.79 (d, 2H, *J* = 6.0, Hᴬ), 8.75 – 8.71 (m, 2H, bpy-H³', bpy-H³), 8.20 (td, 1H, *J* = 7.9, 1.6, bpy-H⁴'), 8.11 (d, 2H, *J* = 8.4, ppy-H³), 8.05 (d, 1H, *J* = 5.6, bpy-H⁶ or bpy-H⁵), 7.99 (d, 1H, *J* = 5.6, bpy-H⁶'), 7.95 – 7.89 (m, 4H, ppy-H⁴, ppy-H³'), 7.70 – 7.61 (m, 5H, ppy-H⁶, Hᴮ and bpy-H⁶ or bpy-H⁵), 7.58 – 7.55 (m, 2H, ppy-H⁴'), 7.50 (td, 1H, *J* = 6.4, 1.0, bpy-H⁵'), 7.21 – 7.16 (m, 2H, ppy-H⁵), 6.74 (dd, 2H, *J* = 9.9, 1.4, ppy-H⁶'). ES⁺ MS: m/z = 790.3 [M – PF₆]⁺. HR ES⁺ MS: m/z = 790.17880 measured, 790.17887 calculated for [C₃₉H₂₇¹⁹³IrN₅O₂]⁺. TLC (Al₂O₃, 5% methanol, 95% DCM): R_f = 0.38.

(4-(4-(4-Pyridyl)phenyl)-2,2'-bipyridine)bis(2-phenylpyridine)iridium(III)hexafluorophosphate
[Ir(ppy)$_2$(bpy-ϕ-py)][PF$_6$] **44**

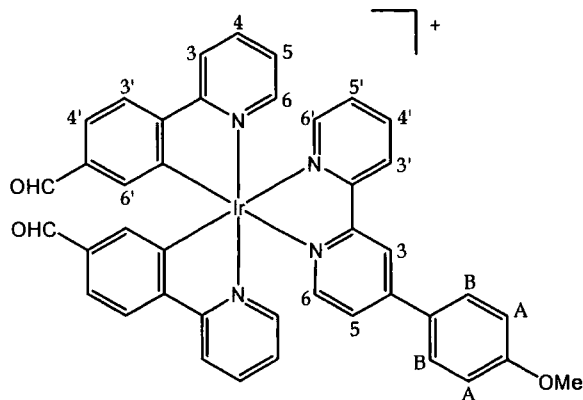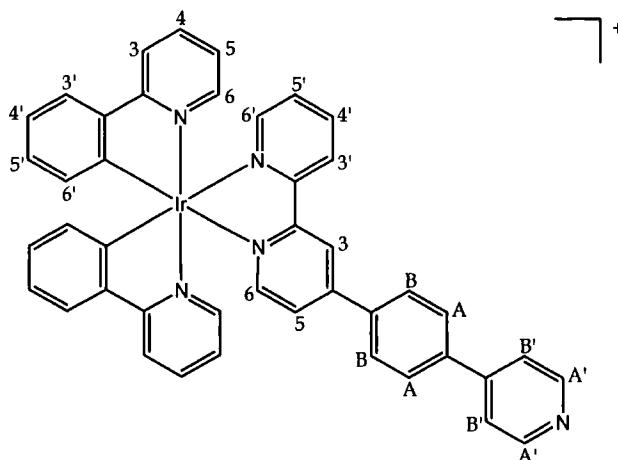4-(4-(4-Pyridyl)phenyl)-2,2'-bipyridine **12** (69 mg, 0.22 mmol) was dissolved in DCM (8 mL) and added to a suspension of [Ir(ppy)$_2$Cl]$_2$ **15** (95 mg, 0.089 mmol) in methanol (10 mL). The mixture was heated under reflux for 90 minutes, until a clear yellow solution was formed. After cooling to room temperature, all solvent was removed under reduced pressure. The resulting solid was dissolved in acetonitrile and added dropwise to a saturated aqueous solution of KPF$_6$. The resulting yellow/orange precipitate was collected using a centrifuge and dried under reduced pressure. Purification was achieved via column chromatography (alumina), using gradient elution from 100% DCM to 1% methanol and 99% DCM (36 mg, 0.038 mmol, 21%). ^{1}H NMR (500 MHz, d^6-acetone): δ 9.24 (s, 1H, bpy-H^3), 9.15 (d, 1H, *J* = *8.3*, bpy-H$^{3'}$), 8.69 (d, 2H, *J* = *5.7*, H$^{A'}$), 8.34 (td, 1H, *J* = *7.9, 1.5*, bpy-H$^{4'}$), 8.27 (t, 2H, *J* = *8.3*, ppy-H^3), 8.20 – 8.13 (m, 4H, bpy-H$^{6'}$, bpy-H^6, H^B), 8.10 (dd, 1H, *J* = *5.8, 1.8*, bpy-H^5), 8.04 (d, 2H, *J* = *8.4*, H^A), 8.01 – 7.87 (m, 6H, ppy-H^6, ppy-H^4, ppy-H$^{3'}$), 7.78 – 7.73 (m, 3H, bpy-H$^{5'}$, H$^{B'}$), 7.21 – 7.14 (m, 2H, ppy-H^5), 7.06 (q, 2H, *J* = *7.42*, ppy-H$^{4'}$), 6.94 (q, 2H, *J* = *6.3*, ppy-H$^{5'}$), 6.38 (t, 2H, *J* = *7.2*, ppy-H$^{6'}$). ES$^+$ MS: m/z = 810.3 [M – PF$_6$]$^+$. HR ES$^+$ MS: m/z = 810.22132 measured, 810.22034 calculated for [C$_{43}$H$_{31}$^{193}IrN$_5$]$^+$. TLC (Al$_2$O$_3$, 5% methanol, 95% DCM): R$_f$ = 0.63.

6.6.2 Elaborating monometallic complexes via chemistry on the complex

(4-(4-Hydroxy)phenyl-2,2'-bipyridine)bis(2-phenylpyridine)iridium(III)hexafluorophosphate (based on work by Ward et al[6]) [Ir(ppy)₂(bpy-∅-OH)](PF)₆ **45**
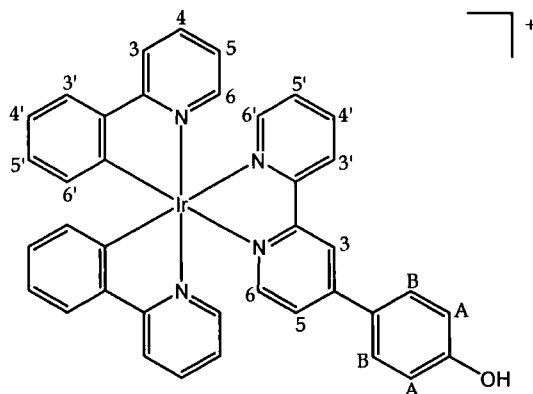
[Ir(ppy)₂(bpy-φ-OMe)][PF₆] **40** (50 mg, 0.055 mmol) was dissolved in DCM (15 mL) and placed under nitrogen. Boron tribromide (0.40 mL of 1.0 M solution in DCM, equivalent to 0.40 mmol) was carefully added to this solution whilst cooling in ice, and the resulting mixture stirred at room temperature for 3 hours. After this time water (20 mL) was added to quench any unreacted boron tribromide and the DCM layer was separated, washed with water (2 x 20 mL), dried over magnesium sulphate and evaporated to dryness. The yellow solid was then dissolved in acetonitrile and water, filtered and added dropwise to a saturated aqueous solution of KPF₆. The resulting precipitate was collected via filtration and dried under reduced pressure (37 mg, 0.041 mmol, 75%). ¹H NMR (500 MHz, d⁶-acetone): δ 9.14 (s, 1H, OH), 9.08 (d, 1H, *J = 8.2*, bpy-H³'), 9.05 (d, 1H, *J = 1.7*, bpy-H³), 8.30 (td, 1H, *J = 7.8, 1.5*, bpy-H⁴'), 8.25 (t, 2H, *J = 7.0*, ppy-H³), 8.12 (dd, 1H, *J = 5.5, 0.9*, bpy-H⁶'), 8.01 – 7.86 (m, 10H, ppy-H⁶, ppy-H⁴, ppy-H³', bpy-H⁶, bpy-H⁵, Hᴮ), 7.70 (t, 1H, *J = 5.5*, bpy-H⁵'), 7.17 (t, 2H, *J = 6.6*, ppy-H⁵), 7.04 (m, 4H, ppy-H⁴', Hᴬ), 6.93 (m, 2H, ppy-H⁵'), 6.37 (d, 2H, *J = 7.7*, ppy-H⁶'). ES⁺MS: m/z = 748.3 [M – PF₆]⁺. HR ES⁺ MS: m/z = 749.18836 measured, 749.18871 calculated for [C₃₈H₂₈¹⁹³IrN₄O]⁺. C, H & N analysis: 49.44% C, 3.31% H and 5.80% N measured, 49.56% C, 3.39% H and 6.08% N calculated for [C₃₈H₂₈F₆IrN₄OP]. 1.5 H₂O. TLC (Al₂O₃, 5% methanol, 95% DCM): R_f = 0.38.

(2,2'-Bipyridine)bis(2-(4-bromophenyl)pyridine)iridium(III)hexafluorophosphate (based on work by Coudret et al[177]) [Ir(ppy-Br)₂(bpy)][PF₆] **46**
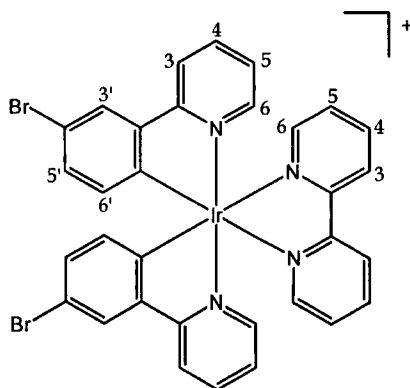
N-Bromosuccinimide (58 mg, 0.33 mmol) in acetonitrile (2 mL) was added to a solution of [Ir(ppy)₂(bpy)][PF₆] **24** (101 mg, 0.13 mmol) also in acetonitrile (10 mL). After stirring at room temperature for 18h, the solution was concentrated under vacuum and added dropwise to a saturated aqueous solution of KPF₆. The resulting precipitate was collected and washed with water (113 mg). However, ¹H NMR revealed that there was still a trace of either non-brominated or singly brominated iridium complex, so the residue was redissolved in acetonitrile (5 mL) and a further amount of N-bromosuccinimide (10 mg) was added. After a further 18h the reaction was worked up as before, yielding exclusively the di-brominated iridium complex (104 mg, 0.11 mmol, 86%). ¹H NMR (500 MHz, d6-acetone): δ 8.87 (d, 2H, *J* = *8.1*, bpy-H³), 8.37 (d, 2H, *J* = *8.2*, ppy-H³), 8.33 (td, 2H, *J* = *7.9, 1.5*, bpy-H⁴), 8.18 (d, 2H, *J* = *5.5*, bpy-H⁶), 8.07 (d, 2H, *J* = *2.1*, ppy-H³'), 8.02 (td, 2H, *J* = *7.9, 1.4*, ppy-H⁴), 7.87 (d, 2H, *J* = *5.8*, ppy-H⁶), 7.75 (td, 2H, *J* = *6.5, 1.0*, bpy-H⁵), 7.23 (td, 2H, *J* = *6.6, 1.2*, ppy-H⁵), 7.07 (dd, 2H, *J* = *8.1, 2.0*, ppy-H⁵'), 6.25 (d, 2H, *J* = *8.1*, ppy-H⁶'). ES⁺ MS: m/z = 814.7 [M – PF₆]⁺. HR ES⁺ MS: m/z = 816.97878 measured, 816.97942 calculated for [C₃₂H₂₂N₄⁸¹Br₂¹⁹³Ir]⁺.

(2,2'-Bipyridine)bis(2-(4-bromo-5-fluoro)phenylpyridine)iridium(III)hexafluorophosphate (based on work by Coudret et al[177]) [Ir(ppy-F,Br)₂(bpy)][PF₆] **47**
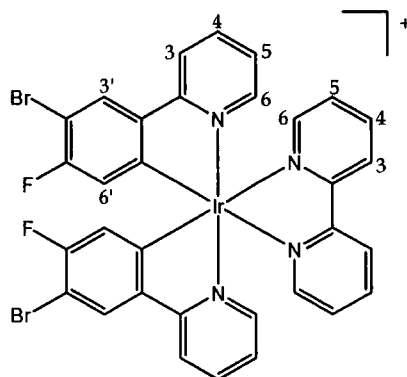
N-Bromosuccinimide (9 mg, 0.053 mmol) in acetonitrile (1 mL) was added to a solution of [Ir(ppy-F)₂(bpy)][PF₆] **27** (20 mg, 0.024 mmol) also in acetonitrile (1 mL). The mixture was heated to 50°C with stirring for 94 h. At this point, ^{1}H NMR revealed that there was still a trace of either non-brominated or singly brominated iridium complex, so the solution was heated at 50°C for a further 24 h after an additional equivalent of N-bromosuccinimide (4 mg) was added. After removing all solvent under reduced pressure, the residue was redissolved in acetonitrile and water and added dropwise to a saturated aqueous solution of KPF₆. The resulting solid was collected using a centrifuge, wash with water and dried under reduced pressure (20 mg, 0.020 mmol, 84%). ^{1}H NMR (500 MHz, d⁶-acetone): δ 8.88 (d, 2H, J = 8.2, bpy-H³), 8.39 – 8.32 (m, 4H, ppy-H³ and bpy-H⁴), 8.26 (d, 2H, J = 5.6, bpy-H⁶), 8.24 (d, 2H, J = 6.7, ppy-H³'), 8.04 (td, 2H, J = 7.8, 1.4, ppy-H⁴), 7.87 (d, 2H, J = 5.8, ppy-H⁶), 7.75 (ddd, 2H, J = 7.6, 5.4, 1.1, bpy-H⁵), 7.25 (ddd, 2H, J = 7.3, 5.9, 1.2, ppy-H⁵), 6.03 (d, 2H, J = 9.3, ppy-H⁶'). ^{19}F NMR (200 MHz, d⁶-acetone): δ 73.1 (d, J_{F-P} = 704, PF₆), -107.0 (dd, J = 9.3, 6.2, ppy-F). ES⁺ MS: m/z = 851.0 [M – PF₆]⁺. HR ES⁺ MS: m/z = 848.96644 measured, 848.96467 calculated for [C₃₂H₂₀N₄⁷⁹Br₂F₂¹⁹³Ir]⁺.

(4-(4-Dimethylaminophenyl)-2,2'-bipyridine)bis(4-(2-pyridyl)benzaldehyde)iridium(III)
hexafluorophosphate [Ir(pba)₂(bpy-φ-NMe₂)][PF₆] **50**
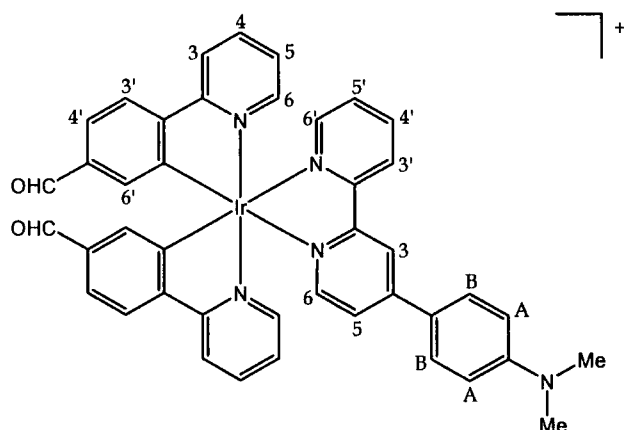
A Schlenk tube was charged with [Ir(pba)₂(bpy-Br)][PF₆] **33** (350 mg, 0.26 mmol), dimethylaminophenyl-4-boronic acid (95 mg, 0.58 mmol), aqueous Na₂CO₃ (88 mg, 0.83 mmol in 1 mL H₂O) and DMSO (10 mL). The mixture was thoroughly degassed via four freeze-pump-thaw cycles and placed under nitrogen. Pd(PPh₃)₄ (30 mg, 0.03 mmol) was added to the Schlenk tube under a positive pressure of nitrogen and the solution stirred and heated to 80 – 85°C for 24 hours. Once cooled, the DMSO solution was filtered and added dropwise to a saturated aqueous solution of KPF₆. The resulting precipitate was collected using a centrifuge, washed with water and dried under reduced pressure. Purification was achieved via column chromatography (alumina), using gradient elution from 100% DCM to 0.5% methanol and 99.5% DCM (127 mg, 0.13 mmol, 50%). ¹H NMR (500 MHz, d⁶-acetone): δ 9.77 (s, 2H, CHO), 9.10 (d, 1H, *J* = *8.2*, bpy-H³'), 9.03 (s, 1H, bpy-H³), 8.44 (t, 2H, *J* = *6.5*, ppy-H³), 8.31 (t, 1H, *J* = *7.6*, bpy-H⁴'), 8.18 – 7.99 (m, 7H, ppy-H⁶, ppy-H⁴, ppy-H³', bpy-H⁶'), 7.95 – 7.85 (m, 4H, bpy-H⁶, bpy-H⁵, Hᴮ), 7.69 (t, 1H, *J* = *6.5*, bpy-H⁵'), 7.58 (t, 2H, *J* = *6.2*, ppy-H⁴'), 7.34 (d, 2H, *J* = *5.8*, ppy-H⁵), 6.90 (s, 2H, ppy-H⁶'), 6.87 (d, 2H, *J* = *8.5*, Hᴬ), 3.07 (s, 6H, Me). ES⁺ MS: m/z = 832.3 [M – PF₆]⁺. HR ES⁺ MS: m/z = 832.2254 measured, 832.2258 calculated for [C₄₂H₃₃¹⁹³IrN₅O₂]⁺. C, H & N analysis: 51.15% C, 3.40% H and 6.24% N measured, 50.87% C, 3.90% H and 6.78% N calculated for [C₄₂H₃₃F₆IrN₅O₂P]. 1.75 H₂O. TLC (Al₂O₃, 5% methanol, 95% DCM): R_f = 0.56.

(4-(4-(4-Dimethylaminophenyl)phenyl)-2,2'-bipyridine)bis(4-(2-pyridyl)benzaldehyde)
iridium(III)hexafluorophosphate [Ir(pba)₂(bpy-φ-φ-NMe₂)][PF₆] **51**
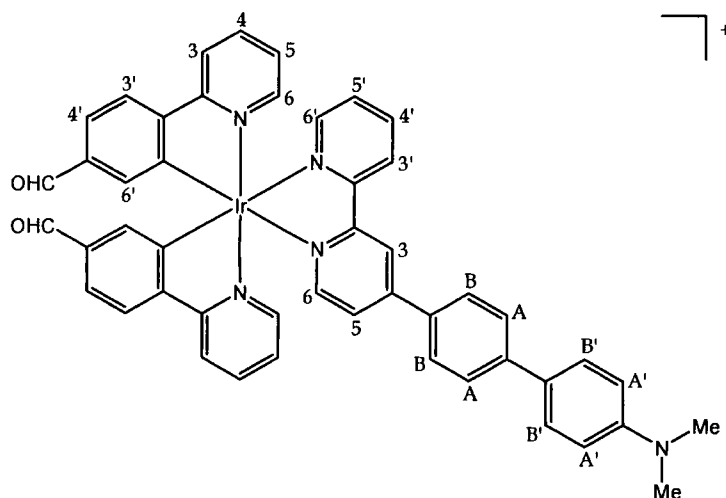
A Schlenk tube was charged with [Ir(pba)₂(bpy-φ-Br)][PF₆] **38** (121 mg, 0.12 mmol), dimethylaminophenyl-4-boronic acid (42 mg, 0.25 mmol), aqueous Na₂CO₃ (39 mg, 0.37 mmol in 1 mL H₂O) and DMSO (6 mL). The mixture was thoroughly degassed via three freeze-pump-thaw cycles and placed under nitrogen. Pd(PPh₃)₄ (10 mg, 0.009 mmol) was added to the Schlenk tube under a positive pressure of nitrogen and the solution stirred and heated to 80 – 85°C for 24 hours. Once cooled, the DMSO solution was added dropwise to a saturated aqueous solution of KPF₆. The resulting precipitate was collected using a centrifuge, washed with water and dried under reduced pressure. Purification was achieved via column chromatography (alumina column), using gradient elution from 100% DCM to 1% methanol and 99% DCM (35 mg, 0.033 mmol, 28%). ¹H NMR (500 MHz, CD₃CN): δ 9.72 (d, 2H, *J* = 2.3, CHO), 8.79 (s, 1H, bpy-H³), 8.74 (d, 1H, *J* = 8.2, bpy-H³'), 8.23 (t, 2H, *J* = 7.7, ppy-H³), 8.17 (t, 1H, *J* = 7.8, bpy-H⁴'), 8.04 – 7.88 (m, 8H, ppy-H³', ppy-H⁴, bpy-H⁶', Hᴮ, bpy-H⁶), 7.82 - 7.71 (m, 5H, ppy-H⁶, bpy-H⁵, Hᴬ), 7.61 (d, 2H, *J* = 8.8, Hᴮ'), 7.55 (t, 2H, *J* = 6.5, ppy-H⁴'), 7.51 (t, 1H, *J* = 6.5, bpy-H⁵'), 7.20 (dd, *J* = 12.7, 6.4, ppy-H⁵), 6.82 (d, 2H, *J* = 8.7, Hᴬ'), 6.78 (s, 2H, ppy-H⁶'), 2.97 (s, 6H, Me). ES⁺ MS: m/z = 908.4 [M – PF₆]⁺. HR ES⁺ MS: m/z = 908.2571 measured, 908.2571 calculated for [C₄₈H₃₇¹⁹³IrN₅O₂]⁺. C, H & N analysis: 52.43% C, 3.35% H and 6.17% N measured, 52.50% C, 3.86% H and 6.38% N calculated for [C₄₈H₃₇F₆IrN₅O₂P]. 2.5 H₂O. TLC (Al₂O₃, 5% methanol, 95% DCM): R_f = 0.41.

(4-Phenyl-2,2'-bipyridine)bis(2-phenylpyridine)iridium(III)hexafluorophosphate
[Ir(ppy)₂(bpy-ph)][PF]₆ **52**
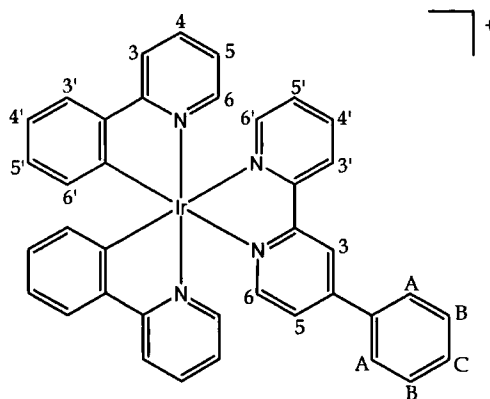
A Schlenk tube was charged with [Ir(ppy)₂(bpy-Br)][PF₆] **32** (88 mg, 0.10 mmol), benzeneboronic acid (27 mg, 0.22 mmol), Na₂CO₃ (64 mg in 400 μL H₂O, 0.6 mmol) and DMSO (8 mL). The solution was thoroughly degassed via 3 freeze-pump-thaw cycles before adding Pd(PPh₃)₄ (14 mg, 0.012 mmol) under a positive pressure of nitrogen. The solution was stirred at 80 - 85°C for 24 h. After this time, the DMSO solution was diluted with acetonitrile (5 mL) and centrifuged to remove an insoluble black solid. Filtration into a saturated aqueous solution of KPF₆ yielded a yellow precipitate which was collected using a centrifuge (86 mg). Purification was achieved via column chromatography (silica gel) using gradient elution from 100% DCM to 98.5% DCM and 1.5% methanol. Evaporation of solvent gave the desired product which was dried under reduced pressure (70 mg, 0.08 mmol, 80%). ¹H NMR (500 MHz, d⁶-acetone): δ 9.13 (s, 1H, bpy-H³), 9.12 (d, 1H, *J* = 8.2, bpy-H³'), 8.32 (t, 1H, *J* = 7.8, bpy-H⁴'), 8.26 and 8.25 (2 overlapping d, 2H, *J* = 7.4, ppy-H³), 8.14 and 8.11 (2 overlapping d, 2H, bpy-H⁵ and bpy-H⁶'), 8.03 - 7.86 (m, 9H, ppy-H⁴, ppy-H⁶, ppy-H³', bpy-H⁶ and Hᴬ), 7.73 (t, 1H, *J* = 6.5, bpy-H⁵'), 7.63 - 7.58 (m, 3H, Hᴮ and Hᶜ), 7.18 and 7.16 (2 overlapping t, 2H, *J* = 7.0, ppy-H⁵), 7.05 and 7.04 (2 overlapping t, 2H, *J* = 7.0, ppy-H⁴), 6.94 - 6.93 (2 overlapping t, 2H, *J* = 7.3, ppy-H⁵'), 6.38 and 6.37 (2 overlapping d, 2H, ppy-H⁶'). ¹H NMR (400 MHz, CD₃CN): δ 8.74 (s, 1H, bpy-H³), 8.70 (d, 1H, *J* = 8.3, bpy-H³'), 8.15 (td, 1H, *J* = 7.8, 1.6, bpy-H⁴'), 8.09 and 8.07 (2 overlapping d, 2H, ppy-H³), 8.02 (d, 1H, *J* = 5.3, bpy-H⁶'), 7.97 (d, 1H, *J* = 5.8, bpy-H⁶), 7.90 - 7.78 (m, 6H, ppy-H⁴, ppy-H⁶ and Hᴬ), 7.75 (dd, 1H, *J* = 5.8, 1.7, bpy-H⁵), 7.67 and 7.65 (2 overlapping d, 2H, *J* = 6.4, ppy-H³'), 7.61 - 7.56 (m, 3H, Hᴮ and Hᶜ), 7.52 (t, 1H, *J* = 6.4, bpy-H⁵'), 7.10 - 7.00 (m, 4H, ppy-H⁴' and ppy-H⁵), 6.96 - 6.90 (2 overlapping dd, 2H, ppy-H⁵'), 6.30 (d, 2H, *J* = 7.6, ppy-H⁶'). ES⁺ MS: m/z = 733.3 [M - PF₆]⁺. HR ES⁺ MS: m/z = 733.1957 measured, 733.1943 calculated for [C₃₈H₂₈¹⁹³IrN₄]⁺. C, H & N analysis: 51.16% C, 3.21% H and 6.15% N measured, 50.95% C, 3.38% H and 6.25% N calculated for

[$C_{38}H_{28}F_6IrN_4P$]. H_2O. TLC (Al_2O_3, 5% methanol, 95% DCM): R_f = 0.62.

(4-Phenyl-2,2'-bipyridine)bis(2-(5-fluorophenyl)pyridine)iridium(III)hexafluorophosphate
[Ir(ppy-F)$_2$(bpy-ph)][PF$_6$] **53**
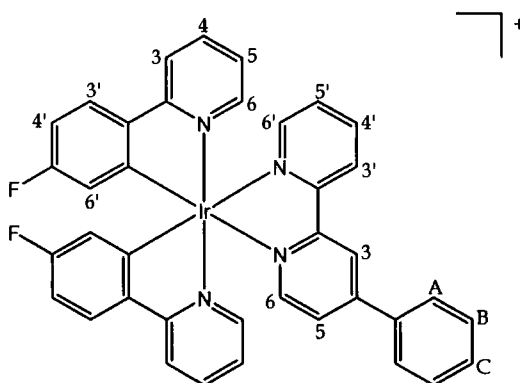
A Schlenk tube was charged with [Ir(ppy-F)$_2$(bpy-Br)][PF$_6$] **35** (80 mg, 0.087 mmol), benzene boronic acid (13 mg, 0.11 mmol), Na_2CO_3 (28 mg in 250 µL H_2O, 0.26 mmol) and DMSO (8 mL). The solution was thoroughly degassed via 3 freeze-pump-thaw cycles before adding Pd(PPh$_3$)$_4$ (6 mg, 0.005 mmol) under a positive pressure of nitrogen. The solution was stirred at 80 - 85°C for 48 h. After this time, the DMSO solution was diluted with acetonitrile (5 mL) and filtered into a saturated aqueous solution of KPF$_6$. The resulting precipitate was collected using a centrifuge. Purification was achieved via column chromatography (silica gel) using gradient elution from 100% DCM to 98.5% DCM and 1.5% methanol. Evaopration of solvent gave the desired product which was dried under reduced pressure (62 mg, 0.068 mmol, 78%). ^1H NMR (500 MHz, d^6-acetone): δ 9.15 (d, 1H, *J = 1.7*, bpy-H^3), 9.14 (d, 1H, *J = 8.2*, bpy-H$^{3'}$), 8.35 (td, 1H, *J = 7.6, 1.4*, bpy-H$^{4'}$), 8.27 and 8.25 (2 d, 2H, *J = 7.4*, ppy-H^3), 8.19 (d, 1H, *J = 5.0*, bpy-H$^{6'}$), 8.17 (d, 1H, *J = 6.0*, bpy-H^6), 8.06 - 7.97 (m, 7H, ppy-H$^{3'}$, ppy-H^4, bpy-H^5 and H^B), 7.88 and 7.93 (2 d, *J = 5.7*, ppy-H^6), 7.76 (ddd, 1H, *J = 7.6, 5.4, 1.0*, bpy-H$^{5'}$), 7.64 - 7.57 (m, 3H, H^A and H^C), 7.23 - 7.17 (m, 2H, ppy-H^5), 6.85 and 6.84 (2 overlapping ddd, 2H, ppy-H$^{4'}$), 5.98 and 5.96 (2 dd, *J = 4.1, 2.6*, ppy-H$^{6'}$). ^{13}C NMR (500 MHz, d^6-acetone): δ 167.5, 165.6, 163.6, 157.4, 156.9, 154.5 (d, *J$_{C-F}$ =133.5*, C-F), 152.2 (bpy-CH^6 or bpy-CH$^{6'}$), 151.8 (bpy-CH^6 or bpy-CH$^{6'}$), 150.2, 141.4, 140.7, 140.0 (ppy-CH$^{3'}$, ppy-CH^4, bpy-CH^5 or CH^b), 136.5, 131.7 (CH^a or CH^c), 130.4 (CH^a or CH^c), 129.7 (bpy-CH$^{5'}$), 128.4 (ppy-CH$^{3'}$, ppy-CH^4, bpy-CH^5 or CH^b), 128.2 (ppy-CH$^{3'}$, ppy-CH^4, bpy-CH^5 or CH^b), 126.8 (ppy-CH$^{3'}$, ppy-CH^4, bpy-CH^5 or CH^b), 126.2 (bpy-H$^{3'}$), 124.6 (ppy-CH^5), 123.3 (bpy-CH^3), 121.0 (ppy-CH^3), 118.3 (dd, *J = 72.5, 10*, ppy-CH$^{6'}$), 110.5 (d, *J = 91.5*, ppy-CH$^{4'}$). ^{19}F NMR (400 MHz, d^6-acetone): δ -73.0 (d, *J$_{P-F}$ = 752*, PF$_6$), -111.1 - -111.2 (m, C-F). ES$^+$ MS: m/z = 769.3 [M − PF$_6$]$^+$. HR ES$^+$ MS: m/z = 767.17235 measured, 767.17261 calculated for [$C_{38}H_{26}N_4F_2{}^{191}Ir$]$^+$.

C, H & N analysis: 49.72% C, 2.90% H and 5.92% N measured, 49.95% C, 2.87% H and 6.13% N calculated for [C$_{38}$H$_{26}$F$_8$IrN$_4$P]. TLC (SiO$_2$, 15% methanol, 85% DCM): R$_f$ = 0.61.

(4-Phenyl-2,2'-bipyridine)bis(2-(3,5-difluorophenyl)pyridine)iridium(III)hexafluorophosphate
[Ir(ppy-F$_2$)$_2$(bpy-ph)][PF$_6$] **54**
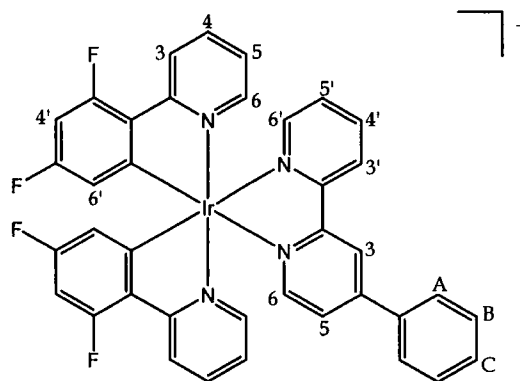
A Schlenk tube was charged with [Ir(ppy-F$_2$)$_2$(bpy-Br)][PF$_6$] **36** (90 mg, 0.094 mmol), benzene boronic acid (25 mg, 0.21 mmol), Na$_2$CO$_3$ (60 mg in 400 μL H$_2$O, 0.57 mmol) and DMSO (8 mL). The solution was thoroughly degassed via three freeze-pump-thaw cycles before adding Pd(PPh$_3$)$_4$ (13 mg, 0.011 mmol) under a positive pressure of nitrogen. The solution was stirred at 80 - 85°C for 24 h. After this time, the DMSO solution was diluted with acetonitrile (5 mL) and centrifuged to remove an insoluble black solid. Filtration into a saturated aqueous solution of KPF$_6$ yielded a yellow precipitate which was collected using a centrifuge (81 mg). Purification was achieved via column chromatography (silica gel) using gradient elution from 100% DCM to 98.5% DCM and 1.5% methanol. Evaporation of solvent gave the desired product which was dried under reduced pressure (65 mg, 0.068 mmol, 72%). ^{1}H NMR (500 MHz, d^6-acetone): δ 9.18 - 9.13 (m, 2H, bpy-H^3 and bpy-H$^{3'}$), 8.44 - 8.35 (m, 3H, bpy-H$^{4'}$ and ppy-H^3), 8.26 - 8.21 (m, 2H, bpy-H^5 and bpy-H$^{6'}$), 8.10 - 7.95 (m, 7H, ppy-H^4, ppy-H^6, bpy-H^6 and H^A), 7.77 (t, 1H, *J* = 6.6, bpy-H$^{5'}$), 7.64 - 7.58 (m, 3H, H^B and H^C), 7.27 and 7.25 (2 overlapping t, 2H, *J* = 7.2, ppy-H^5), 6.83 - 6.72 (m, 2H, ppy-H$^{4'}$), 5.83 and 5.81 (2 overlapping d, 2H, *J* = 5.3, ppy-H$^{6'}$). ^{1}H NMR (400 MHz, CD$_3$CN): δ 8.75 (d, 1H, *J* = 1.9, bpy-H^3), 8.71 (d, 1H, *J* = 8.2, bpy-H$^{3'}$), 8.37 - 8.29 (m, 2H, ppy-H^3), 8.19 (td, 1H, J = 7.9, 1.5, bpy-H$^{4'}$), 8.04 (d, 1H, *J* = 5.3, bpy-H$^{6'}$), 8.00 (d, 1H, *J* = 5.8, bpy-H^6), 7.95 - 7.85 (m, 4H, ppy-H^4, H^A), 7.77 (dd, 1H, *J* = 5.8, 1.9, bpy-H^5), 7.68 and 7.66 (2 overlapping d, 2H, ppy-H^6), 7.63 - 7.50 (m, 4H, bpy-H$^{5'}$, H^B and H^C), 7.13 - 7.05 (m, 2H, ppy-H^5), 6.76 - 6.67 (m, 2H, ppy-H$^{4'}$), 5.76 (2 overlapping d, 2H, ppy-H$^{6'}$). ^{19}F NMR (400 MHz, d^6-acetone): δ -72.93 (d, 6H, *J$_{P-F}$* = 705.9, PF$_6$), -108.14 - -108.27 (m, 2H, ppy-F^5), -110.45 (t, 2H, *J* = 11.6, ppy-F^3). ES$^+$ MS: m/z = 805.4

[M – PF$_6$]$^+$.   HR ES$^+$ MS: m/z = 805.1534 measured, 805.1567 calculated for [C$_{38}$H$_{24}$F$_4$^{193}IrN$_4$]$^+$.   C, H & N analysis: 48.02% C, 2.64% H and 5.59% N measured, 48.05% C, 2.55% H and 5.90% N calculated for [C$_{38}$H$_{24}$F$_{10}$IrN$_4$P].   TLC (SiO$_2$, 15% methanol, 85% DCM): R$_f$ = 0.67.

(4-Phenyl-2,2'-bipyridine)bis(4-(2-pyridyl)benzaldehyde)rhodium(III)hexafluorophosphate [Rh(pba)$_2$(bpy-ph)][PF$_6$] **55**
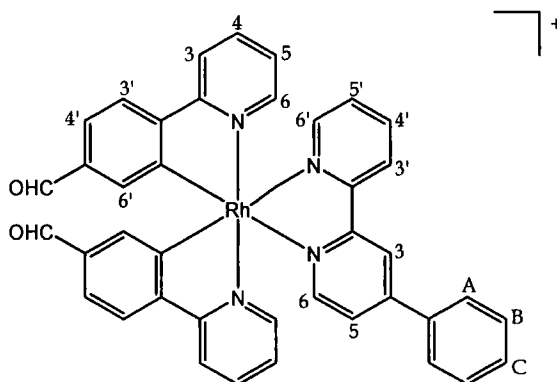
A Schlenk tube was charged with [Rh(pba)$_2$(bpy-Br)][PF$_6$] **34** (85 mg, 0.10 mmol), benzene boronic acid (15 mg, 0.12 mmol), Na$_2$CO$_3$ (32 mg in 250 µL H$_2$O, 0.30 mmol) and DMSO (8 mL).   The solution was thoroughly degassed via 3 freeze-pump-thaw cycles before adding Pd(PPh$_3$)$_4$ (7 mg, 0.006 mmol) under a positive pressure of nitrogen.   The solution was stirred at 80 - 85°C for 48 h.   After this time, the DMSO solution was diluted with acetonitrile (4 mL) and filtered into a saturated aqueous solution of KPF$_6$.   The resulting pale yellow precipitate was collected using a centrifuge.   Purification was achieved via column chromatography (silica gel) using gradient elution from 100% DCM to 98% DCM and 2% methanol.   Evaporation of solvent gave the desired product which was dried under reduced pressure (71 mg, 0.084 mmol, 84%). ^{1}H NMR (500 MHz, CD$_3$CN): δ 9.73 and 9.72 (2 s, 2H, CHO), 8.76 (d, 1H, *J* = *1.5*, bpy-H^3), 8.72 (d, 1H, *J* = *8.2*, bpy-H$^{3'}$), 8.25 and 8.24 (2 d, 2H, *J* = *7.2*, ppy-H^3), 8.19 (td, 1H, *J* = *7.8, 1.7*, bpy-H$^{4'}$), 8.09 - 8.02 (m, 5H, ppy-H$^{3'}$, ppy-H^4 and bpy-H$^{6'}$), 7.99 (d, 1H, *J* = *5.5*, bpy-H^6), 7.89 - 7.86 (m, 2H, H^A), 7.77 - 7.71 (m, 3H, ppy-H^6 and bpy-H^5), 7.65 - 7.61 (2 overlapping dd, 2H, ppy-H$^{4'}$), 7.61 - 7.57 (m, 3H, H^B and H^C), 7.52 (ddd, 1H, *J* = *7.6, 5.3, 1.1*, bpy-H$^{5'}$), 7.25 and 7.24 (2 td, 2H, *J* = *5.8, 1.3*, ppy-H^5), 6.79 (s, 2H, ppy-H$^{6'}$).   ES$^+$ MS: m/z = 700.2 [M – PF$_6$]$^+$.   HR ES$^+$ MS: m/z = 699.12715 measured, 699.12618 calculated for [C$_{40}$H$_{28}$N$_4$O$_2$^{103}Rh]$^+$.   C, H & N analysis: 56.34% C, 3.46% H and 6.28% N measured, 56.29% C, 3.42% H and 6.56% N calculated for [C$_{40}$H$_{28}$F$_6$N$_4$O$_2$PRh]. 0.5 H$_2$O.   TLC (SiO$_2$, 15% methanol, 85% DCM): R$_f$ = 0.62.

(2,2'-Bipyridine)bis(2-((4-phenyl)-phenyl)pyridine)iridium(III)hexafluorophosphate
[Ir(ppy-ph)₂(bpy)][PF₆] **56**
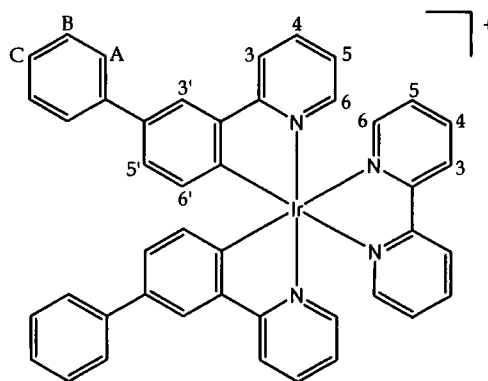
A Schlenk tube was charged with [Ir(ppy-Br)₂(bpy)][PF₆] **46** (48 mg, 0.05 mmol), benzene boronic acid (24 mg, 0.20 mmol), Na₂CO₃ (64 mg in 400 µL H₂O, 0.60 mmol) and DMSO (8 mL). The solution was thoroughly degassed via 3 freeze-pump-thaw cycles before adding Pd(PPh₃)₄ (14 mg, 0.012 mmol) under a positive pressure of nitrogen. The solution was stirred at 80 – 85 °C for 20 h. After this time, the DMSO solution was diluted with acetonitrile (5 mL) and centrifuged to remove an insoluble black solid. Filtration into a saturated aqueous solution of KPF₆ yielded a precipitate which was collected using a centrifuge (59 mg). Purification was achieved via column chromatography (silica gel) using gradient elution from 100% DCM to 97% DCM and 3% methanol. Evaopration of solvent gave the desired product which was dried under reduced pressure (40 mg, 0.042 mmol, 84%). ¹H NMR (400 MHz, d⁶-acetone): δ 8.88 (d, 2H, J = *8.3*, bpy-H³), 8.50 (d, 2H, J = *7.9*, ppy-H³), 8.32, td, 2H, J = *7.8, 1.6*, bpy-H⁴), 8.26 - 8.21 (m, 4H, ppy-H³' and bpy-H⁶), 8.02 (td, 2H, J = *7.9, 1.5*, ppy-H⁴), 7.91 (d, 2H, J = *5.7*, ppy-H⁶), 7.73 (ddd, 2H, J = *7.6, 5.4, 1.2*, bpy-H⁵), 7.70 (d, 4H, J = *7.7*, H^B), 7.43 (t, 4H, J = *7.6*, H^A), 7.31 (t, 2H, J = *7.6*, H^C), 7.27 (dd, 2H, J = *8.0, 2.1*, ppy-H⁵'), 7.22 (ddd, 2H, J = *7.5, 5.8, 1.4*, ppy-H⁵), 6.50 (d, 2H, J = *7.9*, ppy-H⁶'). ES⁺ MS: m/z = 809.4 [M - PF₆]⁺. HR ES⁺ MS: m/z = 809.2242 measured, 809.2256 calculated for [C₄₄H₃₂N₄¹⁹³Ir]⁺. TLC (SiO₂, 15% methanol, 85% DCM): R_f = 0.56.

6.6.3 Synthesis of boronic acid substituted monometallic complexes

(4-(4-Phenylboronic acid)-2,2'-bipyridine)bis(2,2'bipyridine)ruthenium(II)hexafluorophosphate (based on route described by Meyer at al[191] and subsequent conditions reported by Hammarström et al[192]) [Ru(bpy)₂(bpy-φ-B(OH)₂)][PF₆]₂ **57**
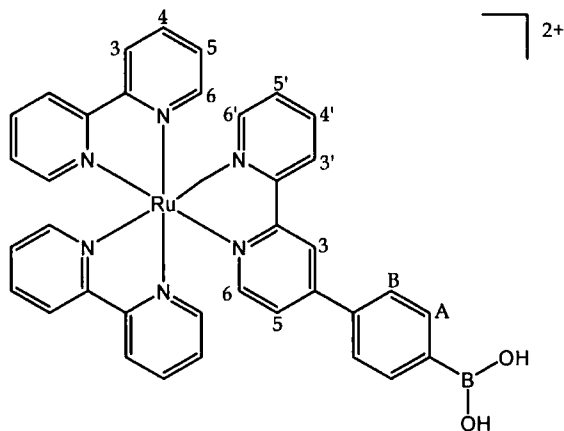
A dry round bottom flask was back-filled with nitrogen and charged with cis-bis(2,2'-bipyridine)dichlororuthenium(II)dihydrate (302 mg, 0.58 mmol), silver tetrafluoroborate (225 mg, 1.16 mmol) and acetone (40 mL, distilled). The mixture was stirred in the dark under nitrogen for 20 hours. After filtration of the solution through celite to remove solid silver chloride, the filtrate was concentrated under reduced pressure and degassed using a flow of nitrogen for 1 hour. Bpy-φ-neo **14** (200 mg, 0.58 mmol) was dissolved in acetone (10 mL, distilled) and added to the initial solution, which was stirred at room temperature under nitrogen for 45 hours. After this time, solvent was removed under reduced pressure and the residue was redissolved in acetonitrile (5 mL). Addition to water (25 mL) produced an insoluble solid which was removed via filtration. Upon the addition of saturated aqueous potassium hexafluorophosphate (5 mL) a red oily solid was precipitated, which was collected using a centrifuge, washed with water and dried. Purification was achieved via column chromatography (silica gel) using gradient elution from 100% CH₃CN to 80% CH₃CN, 19.8% H₂O, 0.2% KNO₃ (313 mg, 0.32 mmol, 55%). ¹H NMR (400 MHz, CD₃CN): δ 8.76 (d, 1H, *J* = 1.6, bpy-φ-H³), 8.69 (d, 1H, *J* = 8.2, bpy-φ-H³'), 8.52 (dd, 4H, *J* = 8.0, 4.8, bpy-H³), 8.11 – 8.03 (m, 5H, bpy-H⁴ and bpy-φ-H⁴'), 7.96 (d, 2H, *J* = 7.9, H^B), 7.87 (d, 2H, *J* = 7.9, H^A), 7.83 – 7.73 (m, 6H, bpy-H⁶, bpy-φ-H⁶ and bpy-φ-H⁶'), 7.67 (dd, 1H, *J* = 6.1, 2.0, bpy-φ-H⁵), 7.46 – 7.37 (m, 5H, bpy-H⁵ and bpy-φ-H⁵'), 6.19 (s, 2H, OH). ES⁺ MS: m/z = 345.1 [(bpy)₂Ru(bpy-φ-B(OH)₂)]²⁺/2 and 352.1 [(bpy)₂Ru(bpy-φ-B(OH)(OMe))]²⁺/2. HR ES⁺ MS: m/z = 348.58513 measured, 348.58514 calculated for [C₃₇H₃₁O₂N₆¹⁰B⁹⁶Ru]²⁺/2.

(4-Phenyl-2,2'-bipyridine)bis(2,2'-bipyridine)ruthenium(II)hexafluorophosphate
[Ru(bpy)₂(bpy-ph)][PF₆]₂ **58**

$[Ru(bpy)_2(bpy\text{-}ph)][PF_6]_2$ **58**
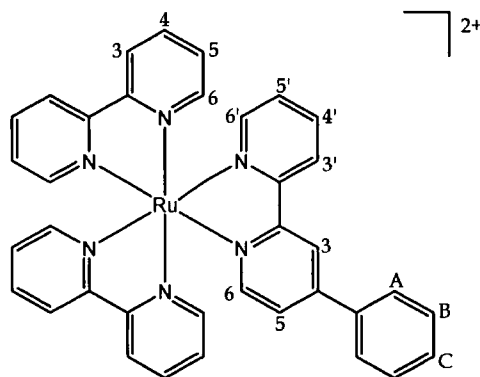
Isolated during column chromatography of [Ru(bpy)₂(bpy-φ-B(OH)₂)][PF₆]₂ **57** (silica gel, 90% CH₃CN, 9.8% H₂O and 0.2% KNO₃). ¹H NMR (500 MHz, CD₃CN): δ 8.74 (d, 1H, *J* = *1.6*, bpy-φ-H³), 8.68 (d, 1H, *J* = *8.3*, bpy-φ-H³'), 8.51 (t, 4H, *J* = *7.1*, bpy-H³), 8.11 - 8.02 (m, 5H, bpy-H⁴ and bpy-φ-H⁴'), 7.87 (d, 2H, *J* = 7.4, Hᴬ), 7.82 – 7.71 (m, 6H, bpy-H⁶, bpy-φ-H⁶ and bpy-φ-H⁶'), 7.64 (dd, 1H, *J* = *6.0, 1.9*, bpy-φ-H⁵), 7.62 – 7.54 (m, 3H, Hᴮ and Hᶜ), 7.44 – 7.38 (m, 5H, bpy-H⁵ and bpy-φ-H⁵'). ES⁺MS: m/z = 323.1 [M - 2PF₆]²⁺/2, 646.2 [M - 2PF₆ + e⁻]⁺, 791.1 [M - PF₆]⁺. HR ES⁺MS: m/z = 791.1018 measured, 791.1061 calculated for [C₃₆H₂₈N₆F₆P¹⁰²Ru]⁺. TLC (SiO₂, 2% KNO₃ (aq), 18% H₂O, 80% CH₃CN): Rf = 0.50.

(4-(4-Phenylboronic acid)-2,2'-bipyridine)bis(2-phenylpyridine)iridium(III)
hexafluorophosphate [Ir(ppy)₂(bpy-φ-B(OH)₂)][PF₆] **59**
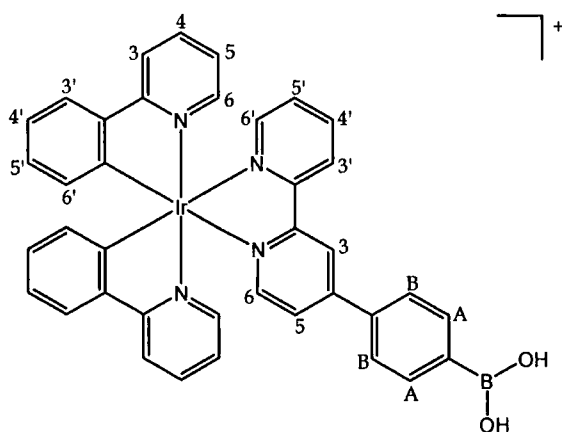
Bpy-φ-Bneo **14** (0.22 mmol) was dissolved in DCM (5.5 mL) and added to a suspension of [Ir(ppy)₂Cl]₂ **15** (107 mg, 0.10 mmol) in methanol (7mL). The solution was stirred at reflux for 90 minutes. Once cooled to room temperature, all solvent was removed under reduced pressure and the residue was re-dissolved in the minimum volume of

172

acetonitrile and water. Filtration of this solution into saturated aqueous KPF_6 gave a precipitate which was collected using a centrifuge and dried under reduced pressure (184 mg). The product was used without any further purification. ^{1}H NMR (500 MHz, d^6-acetone): δ 9.14 (d, 1H, $J = 1.6$, bpy-H^3), 9.11 (d, 1H, $J = 8.3$, bpy-H$^{3'}$), 8.31 (td, 1H, $J = 7.9$, 1.3, bpy-H$^{4'}$), 8.28 – 8.23 (2 overlapping d, 2H, ppy-H^3), 8.15 – 8.10 (m, 2H, bpy-H^6 and bpy-H$^{6'}$), 8.02 (td, 1H, $J = 5.5$, 1.7, bpy-H^5), 8.00 – 7.85 (m, 10H, ppy-H$^{3'}$, ppy-H^4, ppy-H^6, H^A and H^B), 7.72 (t, 1H, $J = 6.5$, bpy-H$^{5'}$), 7.43 (s, OH), 7.20 – 7.14 (m, 2H, ppy-H^5), 7.08 – 7.02 (m, 2H, ppy-H$^{4'}$), 6.97 – 6.90 (m, 2H, ppy-H$^{5'}$), 6.38 and 6.37 (2 d, 2H, ppy-H$^{6'}$). ES$^+$ MS: m/z = 777.24 [M – PF$_6$]$^+$. HR ES$^+$ MS: m/z = 777.20029 measured, 777.20075 calculated for [C$_{38}$H$_{29}$O$_2$N$_4$^{11}B^{193}Ir]$^+$.

(4-(4-Phenylboronic acid)-2,2'-bipyridine)bis(2-(5-fluorophenyl)pyridine)iridium(III)
hexafluorophosphate [Ir(ppy-F)$_2$(bpy-φ-B(OH)$_2$)][PF$_6$] **60**
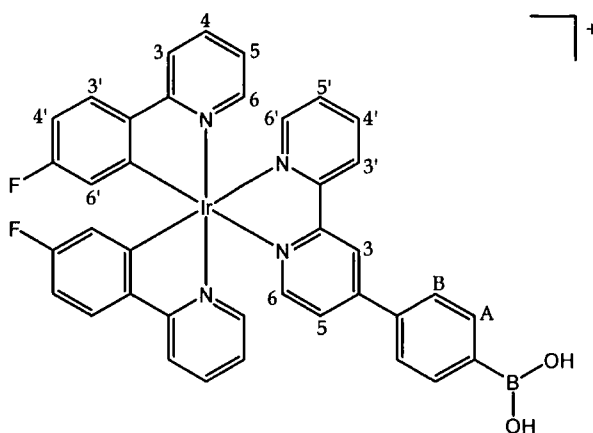
Bpy-φ-Bneo **14** (0.22 mmol) was dissolved in DCM (5.3 mL) and added to a suspension of [Ir(ppy-F)$_2$Cl]$_2$ **20** (77 mg, 0.10 mmol) in methanol (6.7 mL). The solution was stirred at reflux for 90 minutes. Once cooled to room temperature, all solvent was removed under reduced pressure and the residue was re-dissolved in the minimum volume of acetonitrile and water. Filtration of this solution into saturated aqueous KPF_6 gave a precipitate which was collected using a centrifuge and dried under reduced pressure (173 mg). The product was reacted on without any further purification. ^{1}H NMR (500 MHz, CD$_3$CN): δ 8.81 (d, 1H, $J = 1.7$, bpy-H^3), 8.76 (d, 1H, $J = 8.3$, bpy-H$^{3'}$), 8.22 (td, 1H, $J = 7.8$, 1.4, bpy-H$^{4'}$), 8.13 – 7.88 (m, 12H, ppyH^3, ppy-H$^{3'}$, bpy-H^6, bpy-H$^{6'}$, H^A, H^B and ppy-H^4 or ppy-H^6), 7.82 (td, 1H, $J = 6.1$, 1.8, bpy-H^5), 7.69 – 7.64 (m, 2H, ppy-H^4 or ppy-H^6), 7.59 (t, 1H, $J = 6.5$, bpy-H$^{5'}$), 7.13 – 7.07 (m, 2H, ppy-H^5), 6.92 – 6.86 (m, 2H, ppy-H$^{4'}$), 6.27 (s, OH), 5.97 – 5.93 (2 overlapping d, ppy-H$^{6'}$). ^{19}F NMR (400 MHz, CD$_3$CN): δ -73.3 (d, $J_{P-F} = 748$, PF$_6$), -111.4 – -111.5 (m, C-F). ES$^+$ MS: m/z = 813.3 [M - PF$_6$]$^+$. HR ES$^+$ MS: m/z = 810.18313 measured, 810.18320 calculated for
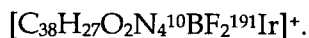
$[C_{38}H_{27}O_2N_4{}^{10}BF_2{}^{191}Ir]^+$.

(4-(4-Phenylboronic acid)-2,2'-bipyridine)bis(2-(3,5-difluorophenyl)pyridine)iridium(III) hexafluorophosphate $[Ir(ppy-F_2)_2(bpy-\phi-B(OH)_2)][PF_6]$ **61**
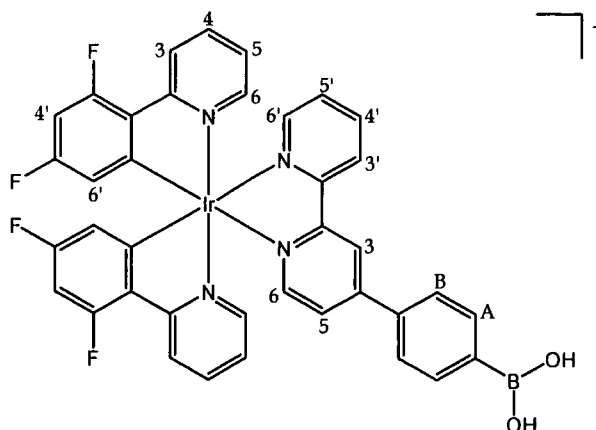
Bpy-ϕ-Bneo **14** (0.16 mmol) was dissolved in DCM (4 mL) and added to a suspension of $[Ir(ppy-F_2)Cl]_2$ **17** (92 mg, 0.076 mmol) in methanol (5mL). The solution was stirred at reflux for 90 minutes. Once cooled to room temperature, all solvent was removed under reduced pressure and the residue was re-dissolved in the minimum volume of acetonitrile and water. Filtration of this solution into saturated aqueous KPF_6 gave a yellow/green precipitate which was collected using a centrifuge and dried under reduced pressure (152 mg). Previous purification attempts using silica gel and DCM/MeOH solvent system had caused the product to deboronate. However, some degree of purification was achieved for 50 mg of the crude sample via column chromatography (silica column), using gradient elution from 100% CH_3CN to 94% CH_3CN, 5.9% H_2O and 0.1% KNO_3. After evaporation of solvent, the desired product was separated from excess KNO_3 by selective dissolution into hot acetonitrile containing a drop of water. This solution was concentrated and filtered into saturated aqueous KPF_6 to precipitate the product as the PF_6 salt, which was collected using the centrifuge and washed with water (20 mg, 38% yield based on crude mass). ^1H NMR (400 MHz, d^6-acetone): δ 9.20 - 9.14 (m, 2H, bpy-H^3 and bpy-$H^{3'}$), 8.45 - 8.34 (m, 3H, bpy-$H^{4'}$ and ppy-H^3), 8.29 - 8.21 (m, 2H, bpy-H^5 and bpy-$H^{6'}$), 8.13 - 7.91 (m, 9H, ppy-H^4, ppy-H^6, bpy-H^6, H^A and H^B), 7.78 (t, 1H, J = 6.4, bpy-$H^{5'}$), 7.42 (s, 2H, OH), 7.27 and 7.25 (2 overlapping t, 2H, J = 5.9, ppy-H^5), 6.83 - 6.74 (m, 2H, ppy-$H^{4'}$), 5.85 - 5.80 (m, 2H, ppy-$H^{6'}$). ^{19}F NMR (200 MHz, d^6-acetone): δ -72.96 (d, 6H, J_{P-F} = 707.8, PF_6), -108.06 - -108.38 (m, 2H, ppy-$F^{5'}$), -110.45 (t, 2H, J = 11.8, ppy-$F^{3'}$). ES$^+$ MS: m/z = 863.1 $[(ppyF_2)_2Ir(bpy-\phi-B(OH)(OMe)]^+$ and 877.1 $[(ppyF_2)_2Ir(bpy-\phi-B(OMe)_2]^+$. HR ES$^+$ MS: m/z = 860.18021 measured, 860.18001 calculated for $[C_{39}H_{27}O_2N_4{}^{10}BF_4{}^{191}Ir]^+$; 874.19554

measured, 874.19566 calculated for $[C_{40}H_{29}O_2N_4{}^{10}BF_4{}^{191}Ir]^+$.

(4-(4-Phenylboronic acid)-2,2'-bipyridine)bis(4-(2-pyridyl)benzaldehyde)rhodium(III)
hexafluorophosphate [Rh(pba)₂(bpy-ɸ-B(OH)₂)][PF₆] **62**
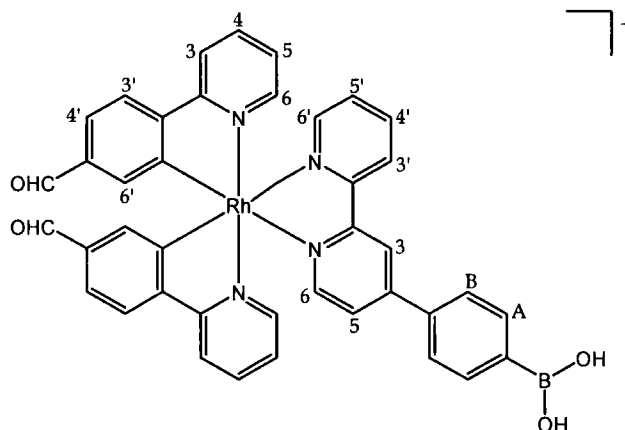
Bpy-ɸ-Bneo **14** (0.11 mmol) was dissolved in DCM (2.7 mL) and added to a suspension of [Rh(pba)₂Cl]₂ **19** (50 mg, 0.05 mmol) in methanol (3.4 mL). The solution was stirred at reflux for 90 minutes. Once cooled to room temperature, all solvent was removed under reduced pressure and the residue was re-dissolved in the minimum volume of acetonitrile and water. Filtration of this solution into saturated aqueous KPF₆ gave a precipitate which was collected using a centrifuge and dried under reduced pressure (75 mg). The product was reacted on without any further purification. ¹H NMR (400 MHz, CD₃CN): δ 9.73 and 9.72 (2 s, 2H, CHO), 8.78 (d, 1H, *J* = *1.4*, bpy-H³), 8.71 (d, 1H, *J* = *8.3*, bpy-H³'), 8.26 and 8.24 (2 overlapping d, 2H, ppy-H³), 8.19 (td, 1H, *J* = *8.0, 1.6*, bpy-H⁴'), 8.10 – 7.98 (m, 6H, ppy-H³', ppy-H⁴, bpy-H⁶ and bpy-H⁶'), 7.96 (d, 2H, *J* = *8.5*, Hᴮ), 7.86 (d, 2H, *J* = *8.5*, Hᴬ), 7.77 – 7.70 (m, 3H, bpy-H⁵ and ppy-H⁶), 7.65 – 7.61 (2 overlapping dd, 2H, ppy-H⁴'), 7.51 (ddd, 1H, *J* = *7.6, 5.4, 1.0*, bpy-H⁵'), 7.27 – 7.21 (m, 2H, ppy-H⁵), 6.78 (s, 2H, ppy-H⁶'), 6.21 (s, OH). ES⁺ MS: m/z = 743.3 [(pba)₂Rh(bpy-ɸ-B(OH)₂]⁺, 757.3 [(pba)₂Rh(bpy-ɸ-B(OH)(OMe)]⁺, 811.3 [(pba)₂Rh(bpy-ɸ-Bneo]⁺. HR ES⁺ MS: m/z = 810.19944 measured, 810.19937 calculated for $[C_{45}H_{37}O_4N_4{}^{10}B^{103}Rh]^+$.

6.6.4 Synthesis of 2,2':6',2"-terpyridine containing monometallic complexes

(2,2':6',2"-Terpyridine)iridium(III)trichloride[194] [Ir(tpy)Cl₃] **63**
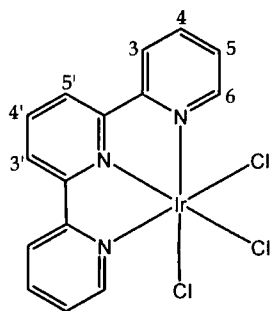
A solution of 2,2':6',2"-terpyridine (234 mg, 1.00 mmol) and iridium trichloride trihydrate (354 mg, 1.00 mmol) in ethylene glycol (13 mL) was heated to 160 °C for 15 minutes. After cooling to room temperature, the resulting precipitate was collected using a centrifuge and washed with ethanol (3 x 10 mL), water (3 x 10 mL), ethanol again (1 x 10 mL) and finally with diethyl ether (3 x 10 mL). The final product was dried under reduced pressure (290 mg, 0.55 mmol, 54%). ^{1}H NMR (500 MHz, CD₃CN): δ 9.23 (dd, 2H, J = 5.0, 0.7, H⁶), 8.78 (d, 2H, J = 8.2, H³), 8.74 (d, 2H, J = 8.0, H³' and H⁵'), 8.34 – 8.20 (m, 3H, H⁴ and H⁴'), 7.98 (dd, 2H, J = 6.0, 0.5, H⁵).

(2,2':6',2"-Terpyridine)ruthenium(III)trichloride[195] [Ru(tpy)Cl₃] **64**
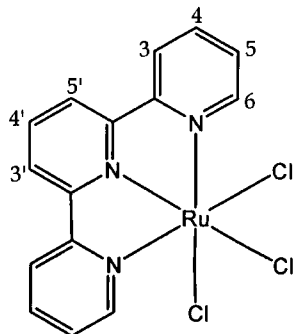
A solution of 2,2':2',6"-terpyridine (134 mg, 0.57 mmol) and ruthenium trichloride trihydrate (150 mg, 0.57 mmol) in ethanol (20 mL) was heated to reflux for 4 h. After cooling to room temperature the resulting solid was collected using a centrifuge and washed with toluene (3 x 10 mL), ethanol (3 x 10 mL) and diethyl ether (3 x 10 mL). The product was reacted on without any further purication (231 mg, 0.52 mmol, 91%).

(2,2':6',2''-terpyridine)(4-(4-bromo)phenyl)-2,2':6',2''-terpyridine)iridium(III)
hexafluorophosphate[142] [Ir(tpy)(tpy-φ-Br)][PF$_6$]$_3$ **65**
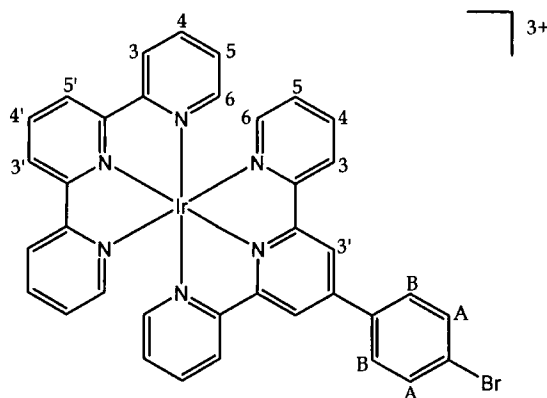
A solution of [Ir(tpy)Cl$_3$] **63** (202 mg, 0.38 mmol) and 4'-(4-bromophenyl)-2,2':6',2''-terpyridine (148 mg, 0.38 mmol) in ethylene glycol (12 mL) was heated strongly at 220 °C for 15 minutes yielding a clear dark red solution. After cooling to room temperature the solution was diluted with water (40 mL). Addition of a solution of saturated aqueous KPF$_6$ (10 mL) produced a precipitate which was collected using a centrifuge, washed with water and dried under reduced pressure. Purification was achieved via column chromatograohy (silica gel) using gradient elution from 100% CH$_3$CN to 53% CH$_3$CN, 45% H$_2$O and 2% KNO$_3$. After evaporation of solvent, the desired product was separated from excess KNO$_3$ by selective dissolution into hot acetonitrile containing a drop of water. This solution was concentrated and filtered into saturated aqueous KPF$_6$ to precipitate the product as the PF$_6$ salt, which was collected using the centrifuge and washed with water (149 mg, 0.12 mmol, 32%). ^{1}H NMR (400 MHz, CD$_3$CN): δ 9.05 (s, 2H, tpy-φ-Br-H$^{3'}$), 8.85 (d, 2H, $J = 8.2$, tpy-H$^{3'}$), 8.77 (t, 1H, $J = 8.2$, tpy-H$^{4'}$), 8.69 (d, 2H, $J = 8.2$, tpy-φ-Br-H^3), 8.58 (d, 2H, $J = 8.2$, tpy-H^3), 8.26 – 8.17 (m, 4H, tpy-H^4 and tpy-φ-Br-H^4), 8.11 (d, 2H, $J = 8.3$, H^B), 7.99 (d, 2H, $J = 8.3$, H^A), 7.66 (d, 2H, $J = 5.5$, tpy-H^6 or tpy-φ-Br-H^6), 7.58 (d, 2H, $J = 5.5$, tpy-H^6 or tpy-φ-Br-H^6), 7.51 – 7.44 (m, 4H, tpy-H^5 and tpy-φ-Br-H^5). ES$^+$ MS: m/z = 271.0 [M - 3PF$_6$]$^{3+}$/3, 479.0 [M - 2PF$_6$]$^{2+}$/2, 1102.9 [M - PF$_6$]$^+$.

(2,2':6',2"-terpyridine)(4-(4-bromophenyl)-2,2':6',2"-terpyridine)ruthenium(II)
hexafluorophosphate [Ru(tpy)(tpy-φ-Br)][PF₆]₂ **66**
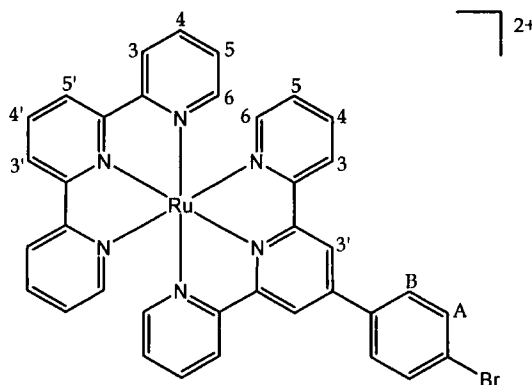
[Ru(tpy)Cl₃] **64** (148 mg, 0.34 mmol) and silver triflate (259 mg, 1.01 mmol) were dissolved in a mixture of acetone (145 mL) and ethanol (35 mL) and heated to 80°C under an atmosphere of nitrogen in the dark for 3 h. After cooling to room temperature, the purple solution was filtered through celite to remove solid silver chloride. Acetone was removed from the solution under reduced pressure and 4'-(4-bromophenyl)-2,2':2',6"-terpyridine (130 mg, 0.34 mmol) and ethanol (115 mL) were added before heating the solution to 80°C under an atmosphere nitrogen and in the dark for a further 3.5 h. After cooling to room temperature, all solvent was removed and the residue was re-dissolved in acetonitrile. Filtration of this solution into a saturated aqueous solution of KPF₆ yielded a dark red precipitate which was collected using a centrifuge and washed with water. Purification was achieved via column chromatography (silica gel) using gradient elution from 100% CH₃CN to 90% CH₃CN, 9.9% H₂O and 0.1% KNO₃. After evaporation of solvent, the desired product was separated from excess KNO₃ by selective dissolution into hot acetonitrile containing a drop of water. This solution was concentrated and filtered into saturated aqueous KPF₆ to precipitate the product as the PF₆ salt, which was collected using the centrifuge and washed with water (140 mg, 0.14 mmol, 41%). ¹H NMR (500MHz, d⁶-acetone): δ 9.46 (s, 2H, tpy-φ-Br-H³'), 9.10 (d, 2H, *J = 8.1,* tpy-H³'), 9.04 (d, 2H, *J = 8.1,* tpy-φ-Br-H³), 8.83 (d, 2H, *J = 8.1,* tpy-H³), 8.60 (t, 1H, *J = 8.1,* tpy-H⁴'), 8.30 (d, 2H, *J = 8.5,* Hᴮ), 8.13 – 8.06 (m, 4H, tpy-H⁴ and tpy-φ-Br-H⁴), 7.94 (d, 2H, *J = 8.5,* Hᴬ), 7.80 (d, 2H, *J = 5.6,* tpy-H⁶), 7.74 (d, 2H, *J = 5.6,* tpy-φ-Br-H⁶), 7.38 – 7.30 (m, 4H, tpy-H⁵ and tpy-φ-Br-H⁵). ES⁺ MS: m/z = 362.0 [M – 2PF₆]²⁺ / 2, 869.1 [M – PF₆]⁺.

6.7 Synthesis of multimetallic systems

[(ppy)₂Ir(bpy-φ-bpy)Ru(bpy)₂][PF₆]₃ [Ir-φ-Ru] **67**
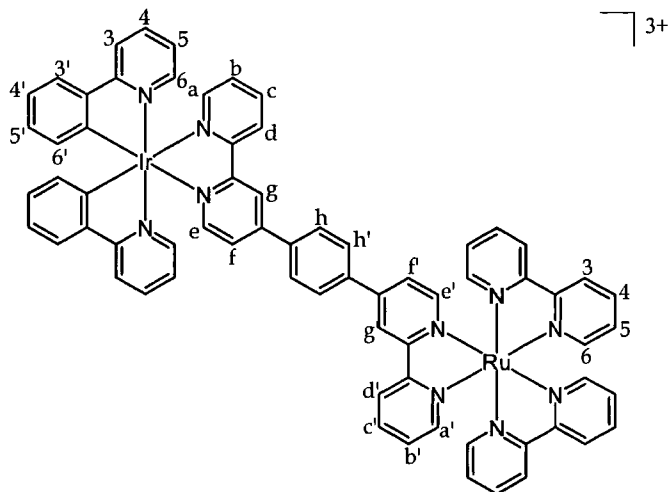
A Schlenk tube was charged with [Ir(ppy)₂(bpy-Br)][PF₆] **32** (42 mg, 0.047 mmol), [Ru(bpy)₂(bpy-φ-B(OH)₂)][PF₆]₂ **57** (55 mg, 0.056 mmol), Na₂CO₃ (15 mg in 100 μL water, 0.14 mmol) and DMSO (5 mL). The solution was thoroughly degassed via 3 freeze-pump-thaw cycles before adding Pd(PPh₃)₄ (10 mg, 0.009 mmol) under a positive pressure of nitrogen. The solution was stirred at 80 - 85°C for 96 h, with an additional amount of catalyst (10 mg) added after 72 h. The DMSO was diluted with acetonitrile (3 mL) and filtered into saturated aqueous solution of KPF₆. The orange precipitate was collected using a centrifuge and transferred in acetonitrile (144 mg). Purification was achieved via column chromatography (silica column), gradient elution from 100% acetonitrile to 88% - 86% acetonitrile, 11.9% - 13.8% water and 0.1% - 0.2% KNO₃. After evaporation of solvent, the product was separated from excess KNO₃ by selective dissolution into hot acetonitrile containing a drop of water. This solution was concentrated and filtered into saturated aqueous KPF₆ to precipitate the product as the PF₆ salt, which was collected using the centrifuge and washed with water (51 mg, 0.03 mmol, 62%). ¹H NMR (500MHz, CD₃CN): δ 8.81 + 8.79 (2 overlapping d, 2H, *J = 1.7*, Hᵍ and Hᵍ′), 8.74 + 8.70 (2 overlapping d, 2H, *J = 8.2*, Hᵈ and Hᵈ′), 8.52 (t, 4H, *J = 7.1*, bpy-H³), 8.17 (td, 1H, *J = 8.0, 1.7*, Hᶜ), 8.12 - 8.00 (m, 13H, Hᵃ, Hᶜ′, Hʰ, Hʰ′, bpy-H⁴, ppy-H³ and Hᵉ or Hᵉ′), 7.90 - 7.64 (m, 14H, Hᵃ′, Hᶠ, Hᶠ′, bpy-H⁶, ppy-H³′, ppy-H⁴, ppy-H⁶ and Hᵉ or Hᵉ′), 7.55 (ddd, 1H, *J = 7.7, 5.5, 1.1*, Hᵇ), 7.46 - 7.37 (m, 5H, Hᵇ′ and bpy-H⁵), 7.11 - 7.01 (m, 4H, ppy-H⁴′ and ppy-H⁵), 6.95 + 6.94 (2 overlapping td, 2H, ppy-H⁵′), 6.32 + 6.30 (2 overlapping d, 2H, ppy-H⁶′). ES⁺ MS: m/z = 433.8 [M - 3PF₆]³⁺/3, 723.1 [M - PF₆]²⁺/2. HR ES⁺ MS: m/z = 433.7631 measured, 433.7625 calculated for [C₆₈H₅₀N₁₀¹⁹³Ir¹⁰²Ru]³⁺/3, 723.1278 measured, 723.1262 calculated for [C₆₈H₅₀N₁₀F₆¹⁹³IrP¹⁰²Ru]²⁺/2. TLC (SiO₂, 2% KNO₃ (aq), 18% H₂O, 80% CH₃CN):

$R_f = 0.60$.

[(ppy)₂Ir(bpy-φ-φ-bpy)Ru(bpy)₂][PF₆]₃ [Ir-φ-φ-Ru] **68**
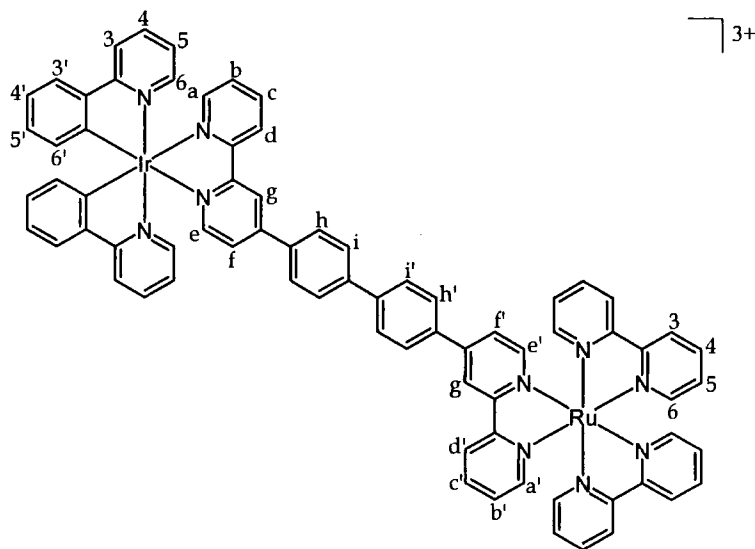
A Schlenk tube was charged with [Ir(ppy)₂(bpy-φ-Br)][PF₆] **37** (72 mg, 0.075 mmol), [Ru(bpy)₂(bpy-φ-B(OH)₂)][PF₆]₂ **57** (84 mg, 0.086 mmol), Na₂CO₃ (26 mg in 100 μL water, 0.25 mmol) and DMSO (8 mL). The solution was thoroughly degassed via 3 freeze-pump-thaw cycles before adding Pd(PPh₃)₄ (10 mg, 0.009 mmol) under a positive pressure of nitrogen. The solution was stirred at 80 - 85°C for 96 h. After this time, the DMSO solution was diluted with acetonitrile (5 mL) and filtered into saturated aqueous solution of KPF₆. The orange precipitate was collected using a centrifuge and transferred in acetonitrile (144 mg). Purification was achieved via column chromatography (silica gel) using gradient elution from 100% acetonitrile to 86% acetonitrile, 13.7% water and 0.3% KNO₃. After evaporation of solvent, the desired product was separated from excess KNO₃ by selective dissolution into hot acetonitrile containing a drop of water. This solution was concentrated and filtered into saturated aqueous KPF₆ to precipitate the product as the PF₆ salt, which was collected using the centrifuge and washed with water (90 mg, 0.05 mmol, 66%). ¹H NMR (500 MHz, CD₃CN): δ 8.82 - 8.78 (m, 2H, Hᵍ and Hᵍ'), 8.76 - 8.69 (m, 2H, Hᵈ and Hᵈ'), 8.52 (t, 4H, *J* = *7.8*, bpy-H³), 8.17 (td, 1H, *J* = *8.0, 1.4*, Hᶜ), 8.12 - 7.95 (m, 17H, ppy-H³, Hᵃ, Hᵉ, Hʰ, Hʰ', Hⁱ, Hⁱ', Hᶜ' and bpy-H⁴), 7.90 - 7.65 (m, 11H, ppy-H³', ppy-H⁴, Hᶠ, Hᵃ', Hᵉ' and bpy-H⁶), 7.71 (dd, 1H, *J* = *6.0, 1.9*, Hᶠ'), 7.68 and 7.67 (2 overlapping d, 2H, ppy-H⁶), 7.54 (t, 1H, *J* = *6.5*, Hᵇ), 7.45 - 7.38 (m, 5H, Hᵇ' and bpy-H⁵), 7.10 - 7.03 (m, 4H, ppy-H⁵ and ppy-H⁴'), 6.95 and 6.94 (2 overlapping t, 2H, *J* = *7.4*, ppy-H⁵'), 6.32 and 6.31 (2 overlapping d, 2H, ppy-H⁶'). ES⁺ MS: m/z = 459.1 [(M - 3PF₆)³⁺/3]. HR ES⁺ MS: m/z = 459.1060 measured, 459.1063 calculated for [C₇₄H₅₄N₁₀¹⁹³Ir¹⁰²Ru]³⁺/3. C, H & N

analysis: 46.72% C, 2.92% H, 7.45% N measured, 46.74% C, 3.39% H, 7.37% N calculated for [C74H54F18N10P3IrRu]. 5 H2O. TLC (SiO2, 2% KNO3 (aq), 18% H2O, 80% CH3CN): Rf = 0.61.

[(bpy)Ir[(ppy-φ-bpy)Ru(bpy)2]2][PF6]5 [[Ru-φ]2-Ir] 69
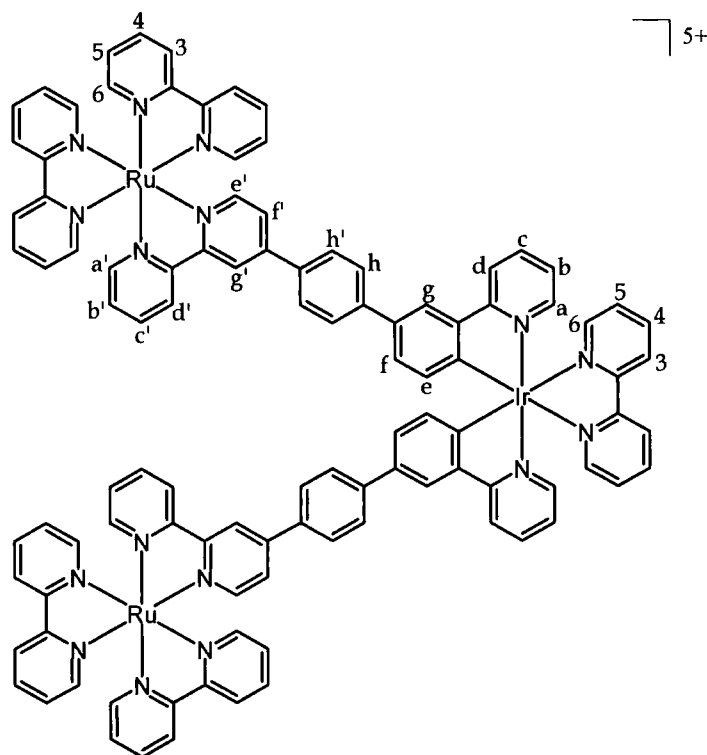
A Schlenk tube was charged with [Ir(ppy-Br)2(bpy)][PF6] **46** (51 mg, 0.05 mmol), [Ru(bpy)2(bpy-φ-B(OH)2)][PF6]2 **57** (113 mg, 0.11 mmol), Na2CO3 (34 mg in 200 μL H2O, 0.32 mmol) and DMSO (10 mL). The solution was thoroughly degassed via 3 freeze-pump-thaw cycles before adding Pd(PPh3)4 (8 mg, 0.006 mmol) under a positive pressure of nitrogen. The solution was stirred at 80 - 85°C for 90 h, with additional catalyst (8 mg) being added after 65 h. The DMSO solution was diluted with acetonitrile (5 mL) and filtered into a saturated aqueous solution of KPF6. The resulting orange precipitate was collected using a centrifuge and transferred in acetonitrile (167 mg). Purification was achieved via column chromatography (silica gel) using gradient elution from 100% acetonitrile to 78% acetonitrile, 21.5% water and 0.5% KNO3. After evaporation of solvent, the desired product was separated from excess KNO3 by selective dissolution into hot acetonitrile containing a drop of water. This solution was concentrated and filtered into saturated aqueous KPF6 to precipitate the product as the PF6 salt, which was collected using the centrifuge and washed with water (42 mg, 0.016 mmol, 31%). ¹H NMR (500 MHz, CD3CN): δ 8.78 (s, 2H, Hg'), 8.70 (d, 2H, *J* = 8.3, Hd'), 8.57 (d, 2H, *J* = 8.0, Ir-bpy-H³), 8.55 - 8.48 (m, 8H, Ru-bpy-H³), 8.30

(d, 2H, *J = 8.0*, H^d), 8.20 (s, 2H, H^g), 8.19 – 8.15 (m, 2H, Ir-bpy-H^4), 8.12 – 8.01 (m, 12H, H$^{c'}$, Ir-bpy-H^6 and Ru-bpy-H^4), 8.00 – 7.88 (m, 10H, H^c, H^h and H$^{h'}$), 7.84 – 7.66 (m, 16H, H^a, H$^{a'}$, H$^{e'}$, H^f and Ru-bpy-H^6), 7.54 (t, 2H, *J = 6.1*, Ir-bpy-H^5), 7.46 – 7.37 (m, 10H, H$^{b'}$ and Ru-bpy-H^5), 7.34 (d, 2H, *J = 7.5*, H^f), 7.12 (t, 2H, *J = 6.4*, H^b), 6.46 (d, 2H, *J = 7.9*, H^e). ES$^+$ MS: m/z = 389.2 [M – 5PF$_6$]$^{5+}$/5, 522.7 [M – 4PF$_6$]$^{4+}$/4, 648.6 [M – 5PF$_6$ + 2e$^-$]$^{3+}$/3. HR ES$^+$ MS: m/z = 522.5945 measured, 522.5944 calculated for [C$_{104}$H$_{76}$N$_{16}$F$_6$^{193}IrP^{102}Ru]$^{4+}$/4. C, H & N analysis: 44.83% C, 2.80% H and 7.82% N measured, 45.13% C, 3.17% H and 8.10% N calculated for [C$_{104}$H$_{76}$F$_{30}$IrN$_{16}$P$_5$Ru]. 5.5 H$_2$O. TLC (SiO$_2$, 2% KNO$_3$ (aq), 18% H$_2$O, 80% CH$_3$CN): R$_f$ = 0.34.

[(bpy)Ir[(ppy-ϕ-bpy)Ru(ppy-F$_2$)$_2$]$_2$][PF$_6$]$_3$ [[Ir^{F2}-ϕ]$_2$-Ir] 70
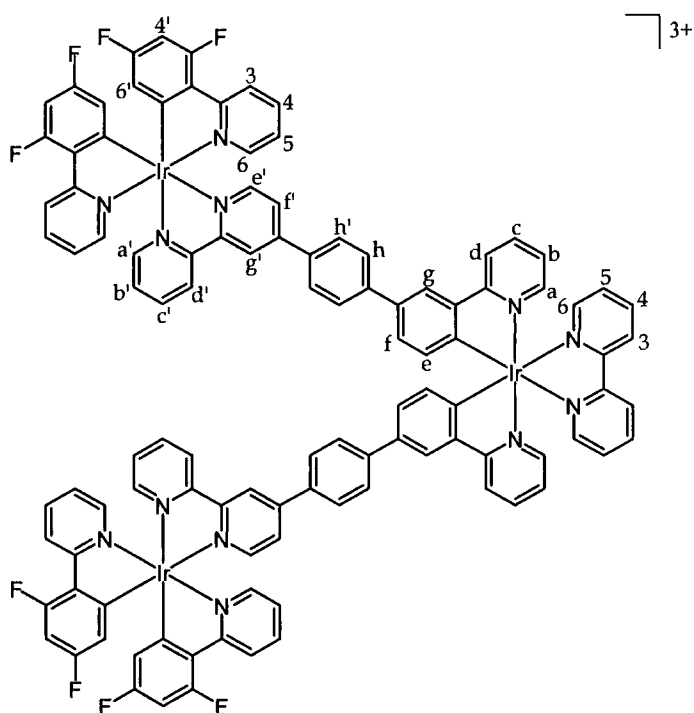
A Schlenk tube was charged with [Ir(ppy-Br)$_2$(bpy)][PF$_6$] **46** (40 mg, 0.042 mmol), [Ir(ppy-F$_2$)$_2$(bpy-ϕ-B(OH)$_2$)][PF$_6$] **61** (124 mg, 0.125 mmol), Na$_2$CO$_3$ (27 mg in 200 µL H$_2$O, 0.25 mmol) and DMSO (10 mL). The solution was thoroughly degassed via 3 freeze-pump-thaw cycles before adding Pd(PPh$_3$)$_4$ (6 mg, 0.005 mmol) under a positive pressure of nitrogen. The solution was stirred at 80 - 85°C for 48 h. After this time, the DMSO solution was diluted with acetonitrile (6 mL) and filtered into saturated aqueous solution of KPF$_6$. The precipitate was collected using a centrifuge, washed with water and transferred in acetonitrile. Purification was achieved via column chromatography (silica gel) using gradient elution from 100% acetonitrile to 94% acetonitrile, 5.9% water and 0.1% KNO$_3$. After evaporation of solvent, the desired

product was separated from excess KNO$_3$ by selective dissolution into hot acetonitrile containing a drop of water. This solution was concentrated and filtered into saturated aqueous KPF$_6$ to precipitate the product as the PF$_6$ salt, which was collected using the centrifuge and washed with water. This product was re-columned (silica gel) using gradient elution from 100% DCM to 90% DCM and 10% methanol (23 mg, 0.009 mmol, 20%). ^{1}H NMR (500 MHz, d^6-acetone): δ 9.22 (d, 2H, $J = 1.4$, H$^{g'}$), 9.16 (d, 2H, $J = 8.2$, H$^{d'}$), 8.90 (d, 2H, $J = 8.3$, bpy-H^3), 8.54 (d, 2H, $J = 8.2$, H^d), 8.44 – 8.32 (m, 10H, H$^{c'}$, H^g, bpy-H^4 and ppy-H^3), 8.25 + 8.24 (2 overlapping d, 4H, H$^{a'}$ and bpy-H^6), 8.20 (d, 2H, $J = 5.9$, H$^{e'}$), 8.15 – 7.94 (m, 22H, H^a, H^c, H^f, H^h, H$^{h'}$, ppy-H^4 and ppy-H^6), 7.78 + 7.75 (2 overlapping t, 4H, $J = 6.4$, H$^{b'}$ and bpy-H^5), 7.40 (dd, 2H, $J = 8.0, 1.7$, H^f), 7.30 – 7.21 (m, 6H, H^b and ppy-H^5), 6.84 – 6.74 (m, 4H, ppy-H$^{4'}$), 6.56 (d, 2H, $J = 8.0$, H^e), 5.83 + 5.81 (2 overlapping dd, 4H, ppy-H$^{6'}$). ES$^+$ MS: m/z = 753.9 [M – 3PF$_6$]$^{3+}$/3, 1203.9 [M - 2PF$_6$]$^{2+}$/2. HR ES$^+$ MS: m/z = 752.47908 measured, 752.47879 calculated for [C$_{108}$H$_{68}$N$_{12}$F$_8$^{191}Ir$_3$]$^{3+}$/3, 1201.20010 measured, 1201.20056 calculated for [C$_{108}$H$_{68}$N$_{12}$F$_{14}$^{191}Ir$_3$P]$^{2+}$/2. TLC (SiO$_2$, 2% KNO$_3$(aq), 18% H$_2$O, 80% CH$_3$CN): R$_f$ = 0.60.

[(tpy)Ir(tpy-φ-φ-bpy)Ru(bpy)$_2$][PF$_6$]$_5$ [^{tpy}Ir-φ-φ-Ru^{bpy}] **71**
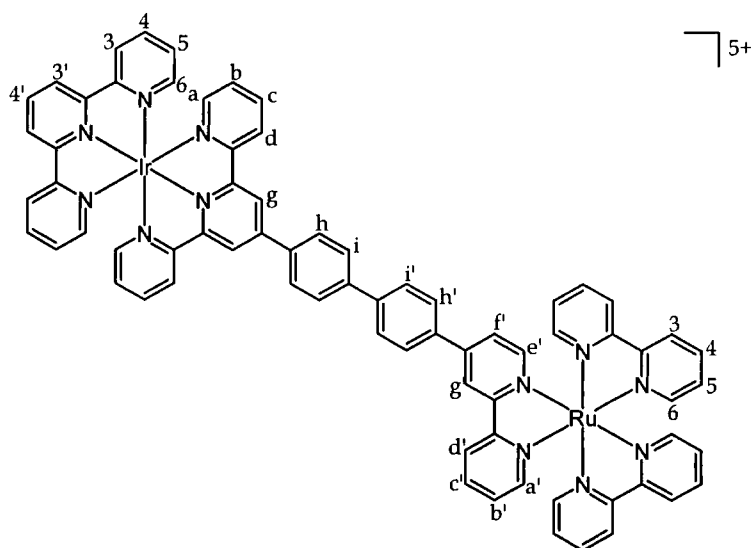
A Schlenk tube was charged with [Ir(tpy)(tpy-φ-Br)][PF$_6$]$_3$ **65** (73 mg, 0.058 mmol), [Ru(bpy)$_2$(bpy-φ-B(OH)$_2$)][PF$_6$]$_2$ **57** (75 mg, 0.077 mmol), Na$_2$CO$_3$ (19 mg in 100 μL water, 0.17 mmol) and DMSO (10 mL). The solution was thoroughly degassed via 3 freeze-pump-thaw cycles before adding Pd(PPh$_3$)$_4$ (4 mg, 0.004 mmol) under a positive pressure of nitrogen. The solution was stirred at 80 - 85°C for 75h. After this time, the DMSO solution was diluted with acetonitrile (8 mL) and filtered into saturated aqueous solution of KPF$_6$. The precipitate was collected using a centrifuge and transferred in acetonitrile (117 mg). Purification was achieved via column

chromatography (silica gel) using gradient elution from 100% acetonitrile to 62% acetonitrile, 36% water and 2% KNO_3. After evaporation of solvent, the desired product was separated from excess KNO_3 by selective dissolution into hot acetonitrile containing a drop of water. This solution was concentrated and filtered into saturated aqueous KPF_6 to precipitate the product as the PF_6 salt, which was collected using the centrifuge and washed with water (17 mg, 0.008 mmol, 14%). ^{1}H NMR (500 MHz, CD_3CN): δ 9.14 (s, 2H, H^g), 8.89 – 8.83 (m, 3H, H$^{g'}$ and tpy-H$^{3'}$), 8.80 – 8.72 (m, 4H, H$^{d'}$, H^d and tpy-H$^{4'}$), 8.60 (d, 2H, J = 8.3, tpy-H^3), 8.54 and 8.52 (2 overlapping d, 4H, J = 8.8, bpy-H^3), 8.37 (d, 2H, J = 8.1, H^h), 8.27 – 8.17 (m, 6H, H^c, H^i and tpy-H^4), 8.14 – 8.05 (m, 9H, H$^{c'}$, H$^{i'}$, H$^{h'}$ and bpy-H^4), 7.86 – 7.73 (m, 7H, H$^{a'}$, H$^{e'}$, H^f and bpy-H^6), 7.71 (d, 2H, J = 5.6, H^a or tpy-H^6), 7.60 (d, 2H, J = 5.6, H^a or tpy-H^6), 7.53 – 7.47 (m, 4H, H^b and tpy-H^5), 7.47 – 7.40 (m, 5H, H$^{b'}$ and bpy-H^5). ES$^+$ MS: m/z = 275.9 [M – 5PF$_6$]$^{5+}$/5, 344.6 [M – 5PF$_6$ – H$^+$]$^{4+}$/4, 459.4 [M – 5PF$_6$ – 2H$^+$]$^{3+}$/3, 556.4 [M – 3PF$_6$]$^{3+}$/3. HR ES$^+$ MS: m/z = 344.5758 measured, 344.5751 calculated for [C$_{72}$H$_{51}$N$_{12}$^{102}Ru^{193}Ir]$^{4+}$/4.

[(tpy)Ru(tpy-φ-φ-bpy)Ir(ppy)₂][PF₆]₃ [tpyRu-φ-φ-IrPPy] **72**
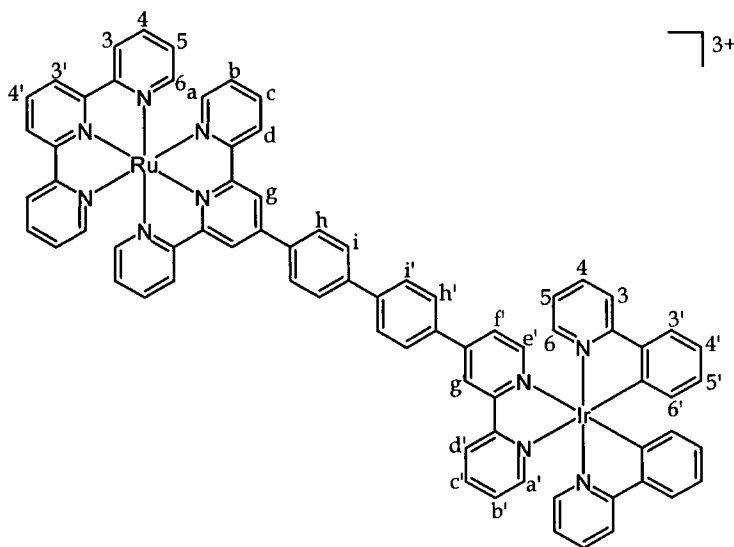
A Schlenk tube was charged with [Ru(tpy)(tpy-φ-Br)][PF₆]₂ **66** (51 mg, 0.050 mmol), [Ir(ppy)₂(bpy-φ-B(OH)₂)][PF₆] **59** (92 mg, 0.10 mmol), Na₂CO₃ (16 mg in 200 μL water, 0.15 mmol) and DMSO (10 mL). The solution was thoroughly degassed via 3 freeze-pump-thaw cycles before adding Pd(PPh₃)₄ (4 mg, 0.003 mmol) under a positive pressure of nitrogen. The solution was stirred at 80 - 85°C for 22 h. After this time, the DMSO solution was diluted with acetonitrile (6 mL) and filtered into saturated aqueous solution of KPF₆. The precipitate was collected using a centrifuge and transferred in acetonitrile (128 mg). Purification was achieved via column chromatography (silica gel) using gradient elution from 100% acetonitrile to 88%

acetonitrile, 11.8% water and 0.2% KNO₃. After evaporation of solvent, the desired product was separated from excess KNO₃ by selective dissolution into hot acetonitrile containing a drop of water. This solution was concentrated and filtered into saturated aqueous KPF₆ to precipitate the product as the PF₆ salt, which was collected using the centrifuge and washed with water (42 mg, 0.02 mmol, 46%). ^{1}H NMR (500 MHz, CD₃CN): δ 9.06 (s, 2H, H^f and H^g), 8.85 (d, 1H, J = 1.5, H$^{g'}$), 8.79 – 8.74 (m, 3H, H$^{d'}$ and tpy-H$^{3'}$), 8.67 (d, 2H, J = 8.1, H^d), 8.50 (d, 2H, J = 8.2, tpy-H^3), 8.42 (t, 1H, J = 8.2, tpy-H$^{4'}$), 8.35 (d, 2H, J = 8.5, H^h), 8.19 (td, 1H, J = 7.8, 1.5, H^c), 8.16 – 8.01 (m, 10H, ppy-H^3, H$^{a'}$, H$^{e'}$, H$^{h'}$, H^i and H$^{i'}$), 7.98 – 7.82 (m, 9H, H^c, H^f, tpy-H^4, ppy-H^4 and ppy-H$^{3'}$ or ppy-H^6), 7.73 – 7.67 (m, 2H, ppy-H$^{3'}$ or ppy-H^6), 7.56 (t, 1H, J = 6.5, H$^{b'}$), 7.43 (d, 2H, J = 5.6, H^a or tpy-H^6), 7.36 (d, 2H, J = 5.6, H^a or tpy-H^6), 7.21 – 7.15 (m, 4H, H^b and tpy-H^5), 7.11 – 7.05 (m, 4H, ppy-H$^{4'}$ and ppy-H^5), 6.99 – 6.93 (m, 2H, ppy-H$^{5'}$), 6.34 and 6.32 (2 overlapping d, 2H, ppy-H$^{6'}$). ES$^+$ MS: m/z = 458.4 [(M – 3PF₆)$^{3+}$/3], 760.1 [(M – 2PF₆)$^{2+}$/2]. HR ES$^+$ MS: m/z = 458.43586 measured, 458.43443 calculated for [C₇₄H₅₂N₁₀^{193}Ir^{102}Ru]$^{3+}$/3, 760.13808 measured, 760.13401 calculated for [C₇₄H₅₂N₁₀F₆^{193}IrP^{102}Ru]$^{2+}$/2. C, H & N analysis: 47.16% C, 2.84% H and 7.19% N measured, 47.47% C, 3.18% H and 7.48% N calculated for [C₇₄H₅₂F₁₈IrN₁₀P₃Ru]. 3.5 H₂O. TLC (SiO₂, 2% KNO₃ (aq), 18% H₂O, 80% CH₃CN): R$_f$ = 0.55.

[(ppy-Br)₂Ir(bpy-φ-bpy)Ru(bpy)₂][PF₆]₃ [Ir^{Br2}-φ-Ru] **73**
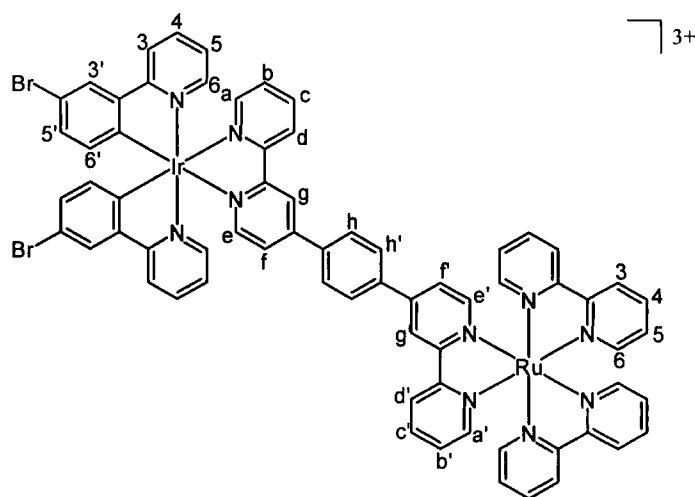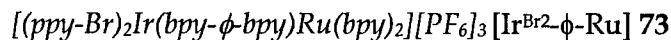
A solution of [(ppy)₂Ir(bpy-φ-bpy)Ru(bpy)₂][PF₆]₃ **67** (20 mg, 0.012 mmol) and N-bromosuccinimide (5 mg, 0.025 mmol) in CH₃CN (5 mL) was stirred at room temperature overnight. Having concentrated the solution under reduced pressure (~ 1 mL), it was added dropwise to a saturated aqueous solution of KPF₆. The resulting precipitate was collected using a centrifuge and washed with water (16 mg,

0.009 mmol, 75%). ^{1}H NMR (500 MHz, CD$_3$CN): δ 8.82 – 8.78 (m, 2H, H^g and H$^{g'}$), 8.74 + 8.71 (2 overlapping d, 2H, J = 8.0, H^d and H$^{d'}$), 8.52 (t, 4H, J = 7.2, bpy-H^3), 8.19 (t, 1H, J = 7.9, H^c), 8.14 – 7.98 (m, 15H, H^a, H$^{c'}$, H^h, H$^{h'}$, bpy-H^4, ppy-H^3, ppy-H$^{3'}$ and H^e or H$^{e'}$), 7.90 (t, 2H, J = 7.9, ppy-H^4), 7.85 – 7.69 (m, 8H, H$^{a'}$, H^f, H$^{f'}$, bpy-H^6 and H^e or H$^{e'}$), 7.67 + 7.65 (2 overlapping d, 2H, ppy-H^6), 7.56 (t, 1H, J = 6.6, H^b), 7.47 – 7.36 (m, 5H, H$^{b'}$ and bpy-H^5), 7.14 – 7.04 (m, 4H, ppy-H^5 and ppy-H$^{5'}$), 6.21 – 6.17 (2 overlapping d, 2H, ppy-H$^{6'}$). ES$^+$ MS: m/z = 486.3 [M – 3PF$_6$]$^{3+}$/3, 801.9 [M – 2PF$_6$]$^{2+}$/2. HR ES$^+$ MS: m/z = 485.03561 measured, 485.03544 calculated for [C$_{68}$H$_{48}$N$_{10}$^{79}Br$_2$^{191}Ir^{102}Ru]$^{3+}$/3, 801.03604 measured, 801.03669 calculated for [C$_{68}$H$_{48}$N$_{10}$^{79}Br$_2$F$_6$^{193}IrP^{102}Ru]$^{2+}$/2.

[(ppy-Br)$_2$Ir(bpy-φ-φ-bpy)Ru(bpy)$_2$][PF$_6$]$_3$ [Ir^{Br2}-φ-φ-Ru] **74**
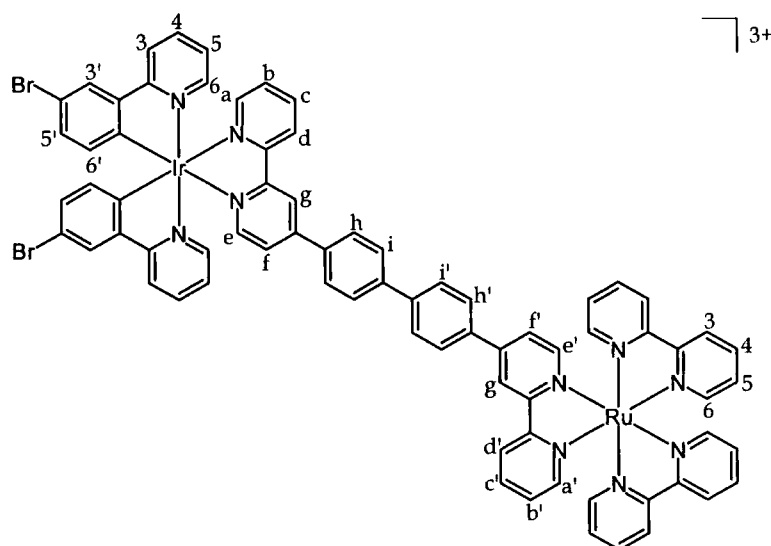
A solution of [(ppy)$_2$Ir(bpy-φ-φ-bpy)Ru(bpy)$_2$][PF$_6$]$_3$ **68** (18mg, 0.010 mmol) and N-bromosuccinimide (4mg, 0.022 mmol) in CH$_3$CN (4mL) was stirred at room temperature overnight. Having concentrated the solution under reduced pressure, it was added dropwise to an aqueous solution of saturated KPF$_6$. The resulting precipitate was collected using a centrifuge and washed with water (21mg, quantitative yield). ^{1}H NMR (400 MHz, CD$_3$CN): δ 8.81 and 8.80 (2 overlapping d, 2H, H^g and H$^{g'}$), 8.75 and 8.72 (2 overlapping d, 2H, H^d and H$^{d'}$), 8.52 (t, 4H, J = 6.8, bpy-H^3), 8.19 (td, 1H, J = 7.9, 1.5, H^c), 8.15 – 7.95 (m, 19H, ppy-H^3, ppy-H$^{3'}$, H^a, H^e, H^h, H$^{h'}$, H^i, H$^{i'}$, H$^{c'}$ and bpy-H^4), 7.90 and 7.85 (2 overlapping td, 2H, J = 7.9, 1.4, ppy-H^4), 7.85 – 7.74 (m, 7H, H^f, H$^{a'}$, H$^{e'}$, and bpy-H^6), 7.71 (dd, 1H, J = 6.0, 1.8, H^f), 7.68 and 7.66 (2 overlapping d, 2H, J = 6.7, ppy-H^6), 7.55 (ddd, 1H, J = 7.6, 5.4, 1.0, H^b), 7.46 – 7.39 (m, 5H, H$^{b'}$ and bpy-H^5), 7.15 – 7.02 (m, 4H, ppy-H^5 and ppy-H$^{5'}$), 6.22 - 6.17 (2 overlapping d, 2H, ppy-H$^{6'}$). ES$^+$ MS: m/z = 511.8 [M – 3PF$_6$]$^{3+}$/3. HR ES$^+$ MS: m/z = 511.0464 measured, 511.0472

calculated for [C$_{74}$H$_{52}$N$_{10}$^{79}Br$_2$^{102}Ru^{193}Ir]$^{3+}$/3.

[[(ppy)₂Ir(bpy-φ-ppy)]₂Ir(bpy-φ-φ-bpy)Ru(bpy)₂][PF₆]₅ [[Ir-φ]₂-Ir-φ-φ-Ru] 75

A Schlenk tube was charged with [(ppy-Br)₂Ir(bpy-φ-φ-bpy)Ru(bpy)₂][PF₆]₃ **74** (70 mg, 0.035 mmol), [Ir(ppy)₂(bpy-φ-B(OH)₂)][PF₆] **59** (75 mg, 0.078 mmol), Na₂CO₃ (22 mg in 200 µL water, 0.21 mmol) and DMSO (8 mL). The solution was thoroughly degassed via 3 freeze-pump-thaw cycles before adding Pd(PPh₃)₄ (5 mg, 0.004 mmol) under a positive pressure of nitrogen. The solution was stirred at 80 - 85°C for 44 h. After this time, the DMSO solution was diluted with acetonitrile (5 mL) and filtered into saturated aqueous solution of KPF₆. The precipitate was collected using a centrifuge. Purification was achieved via column chromatography (silica gel) using gradient elution from 100% acetonitrile to 88% acetonitrile, 11.8% water and 0.2% KNO₃. After evaporation of solvent, the desired product was separated from excess KNO₃ by selective dissolution into hot acetonitrile containing a drop of water. This solution was concentrated and filtered into saturated aqueous KPF₆ to precipitate the product as the PF₆ salt, which was collected using the centrifuge and washed with water (64 mg, 0.018 mmol, 51%). ¹H NMR (500 MHz, CD₃CN): δ 8.88 - 8.70 (m, 8H, H^D, H^G, H^d, H^g, H$^{d'}$ and H$^{g'}$), 8.53 and 8.52 (2 d, 4H, *J* = 7.5, bpy-H³), 8.33 and 8.31 (2 d, 2H, H$^{D'}$), 8.26 - 7.90 (m, 38H, ppy-H³, bpy-H⁴, H^A, H^a, H^C, H$^{C'}$, H^c, H$^{c'}$, H^F, H^f, H$^{G'}$, H^H, H^h, H$^{H'}$, H$^{h'}$, H^i and H$^{i'}$), 7.89 - 7.74 (m, 19H, ppy-H³', ppy-H⁴, bpy-H⁶, H$^{A'}$, H$^{a'}$, H^E, H^e, H$^{e'}$), 7.72 (dd, 1H, *J* = 6.1, 1.9, H^f), 7.68 and 7.67 (2 d, 4H, *J* = 5.7, ppy-H⁶), 7.58 (t, 1H, *J* = 6.5, H^b), 7.53 (t, 2H, *J* = 6.5, H^B), 7.46 - 7.40 (m, 5H, bpy-H⁵ and H$^{b'}$), 7.37 and 7.36 (2 dd, 2H,

J = 7.8, 1.9, H^F'), 7.16 and 7.15 (2 overlapping td, 2H, H^B'), 7.09 – 7.02 (m, 8H, ppy-H^4' and ppy-H^5), 6.94 (2 overlapping ddd, 4H, ppy-H^5'), 6.50 and 6.49 (2 d, 2H, *J* = 7.7, H^E'), 6.31 (d, 4H, *J* = 7.7, ppy-H^6'). ES$^+$ MS: m/z = 567.7 [M – 5PF$_6$]$^{5+}$/5, 745.6 [M – 4PF$_6$]$^{4+}$/4, 1042.67 [M – 3PF$_6$]$^{3+}$/3. HR ES$^+$ MS: m/z = 565.53334 measured, 565.53429 calculated for [C$_{150}$H$_{106}$N$_{18}$^{191}Ir$_3$^{96}Ru]$^{5+}$/5. TLC (SiO$_2$, 2% KNO$_3$ (aq), 18% H$_2$O, 80% CH$_3$CN): R$_f$ = 0.58.

[[(ppy-F)₂Ir(bpy-φ-ppy)]₂Ir(bpy-φ-φ-bpy)Ru(bpy)₂][PF₆]₅ [[Ir^F-φ]₂-Ir-φ-φ-Ru] 76

A Schlenk tube was charged with [(ppy-Br)₂Ir(bpy-φ-φ-bpy)Ru(bpy)₂][PF₆]₃ **74** (108 mg, 0.054 mmol), [Ir(ppy-F)₂(bpy-φ-B(OH)₂)][PF₆] **60** (123 mg, 0.12 mmol), Na₂CO₃ (35 mg in 250 µL water, 0.33 mmol) and DMSO (12 mL). The solution was thoroughly degassed via 3 freeze-pump-thaw cycles before adding Pd(PPh₃)₄ (8 mg, 0.007 mmol) under a positive pressure of nitrogen. The solution was stirred at 80 - 85°C for 24 h. After this time, the DMSO solution was diluted with acetonitrile (8 mL) and filtered into saturated aqueous solution of KPF₆. The precipitate was collected using a centrifuge and washed with water. Purification was achieved via column chromatography (silica gel) using gradient elution from 100% acetonitrile to 88% acetonitrile, 11.8% water and 0.2% KNO₃. After evaporation of solvent, the desired product was separated from excess KNO₃ by selective dissolution into hot acetonitrile containing a drop of water. This solution was concentrated and filtered into saturated aqueous KPF₆ to precipitate the product as the PF₆ salt, which was collected using the centrifuge and washed with water (80 mg, 0.0022 mmol, 41%). ¹H NMR (500 MHz,

CD3CN): δ 8.88 – 8.69 (m, 8H, H^d, H^g, H$^{d'}$, H$^{g'}$, H^D and H^G), 8.53 and 8.51 (2 d, 4H, J = 7.2, bpy-H^3), 8.33 and 8.31 (2 d, 2H, J = 7.7, H$^{D'}$), 8.25 – 8.15 (m, 5H, H^C, H$^{G'}$ and H^c), 8.14 – 7.80 (m, 45H, ppyF-H^3, ppyF-H$^{3'}$, ppyF-H^4, bpy-H^4, H^A, H^a, H$^{C'}$, H$^{c'}$, H^E, H^e, H$^{e'}$, H^F, H^f, H^i, H$^{i'}$, H^H, H$^{H'}$, H^h, H$^{h'}$), 7.80 – 7.73 (m, 7H, H$^{A'}$, H$^{a'}$ and bpy-H^6), 7.71 (dd, 1H, J = 6.0, 2.0, H^f), 7.64 and 7.62 (2 d, 4H, J = 6.6, ppyF-H^6), 7.59 – 7.53 (m, 3H, H^B and H^b), 7.46 – 7.39 (m, 5H, bpy-H^5 and H$^{b'}$), 7.38 – 7.34 (m, 2H, H$^{F'}$), 7.16 and 7.14 (2 td, 2H, J = 6.0, 1.6, H$^{B'}$), 7.09 – 7.03 (2 overlapping td, 4H, ppyF-H^5), 6.88 – 6.82 (m, 4H, ppyF-H$^{4'}$), 6.50 and 6.48 (2 d, 2H, J = 7.9, H$^{E'}$), 5.93 – 5.89 (m, 4H, ppyF-H$^{6'}$). ^{19}F NMR (400 MHz, CD3CN): δ -73.3 (d, J_{P-F} = 748, PF$_6$), -111.4 - -111.5 (m, C-F). ES$^+$ MS: m/z = 582.1 [M – 5PF$_6$]$^{5+}$/5, 763.9 [M - 4PF$_6$]$^{4+}$/4. HR ES$^+$ MS: m/z = 579.92691 measured, 579.92675 calculated for [C$_{150}$H$_{102}$N$_{18}$F$_4$^{191}Ir$_3$^{96}Ru]$^{5+}$/5. TLC (SiO$_2$, 2% KNO$_3$ (aq), 18% H$_2$O, 80% CH$_3$CN): R$_f$ = 0.58.

[[(ppy-F₂)₂Ir(bpy-φ-ppy)]₂Ir(bpy-φ-φ-bpy)Ru(bpy)₂][PF₆]₅ [Ir^{F2}-φ]₂-Ir-φ-φ-Ru **77**
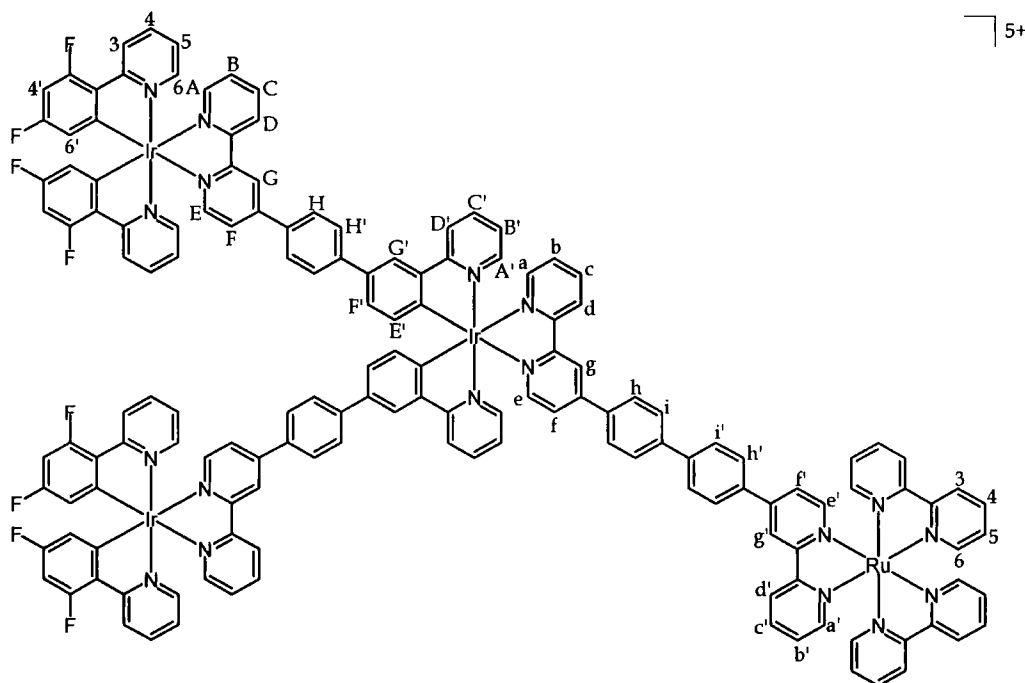
A Schlenk tube was charged with [(ppy-Br)$_2$Ir(bpy-φ-φ-bpy)Ru(bpy)$_2$][PF$_6$]$_3$ **74** (17 mg, 0.0086 mmol), [Ir(ppy-F$_2$)$_2$(bpy-φ-B(OH)$_2$)][PF$_6$] **61** (25 mg, 0.025 mmol), Na$_2$CO$_3$ (5 mg in 100 µL water, 0.050 mmol) and DMSO (5 mL). The solution was thoroughly degassed via 3 freeze-pump-thaw cycles before adding Pd(PPh$_3$)$_4$ (2 mg, 0.0017 mmol) under a positive pressure of nitrogen. The solution was stirred at 80 - 85°C for 72 h. After this time, the DMSO solution was diluted with acetonitrile (3 mL) and filtered into saturated aqueous solution of KPF$_6$. The precipitate was collected using a centrifuge (35 mg). Purification was achieved via column chromatography (silica gel)

using gradient elution from 100% acetonitrile to 88% acetonitrile, 11.8% water and 0.2% KNO$_3$. After evaporation of solvent, the desired product was separated from excess KNO$_3$ by selective dissolution into hot acetonitrile containing a drop of water. This solution was concentrated and filtered into saturated aqueous KPF$_6$ to precipitate the product as the PF$_6$ salt, which was collected using the centrifuge and washed with water (13 mg, 0.0035 mmol, 41%). ^{1}H NMR (500 MHz, CD$_3$CN): δ 8.87 – 8.69 (m, 8H, H^D, H^G, H^d, H^g, H$^{d'}$and H$^{g'}$), 8.52 (t, 4H, J = 7.4, bpy-H^3), 8.37 – 8.30 (m, 4H, ppyF-H^3), 8.25 – 8.17 (m, 4H, H^C and H$^{D'}$), 8.15 – 7.89 (m, 35H, ppyF-H^4, H^A, H^E, H^H, H$^{C'}$, H$^{G'}$, H$^{H'}$, H^a, H^c, H^e, H^h, H^i, H$^{c'}$, H$^{h'}$, H$^{i'}$ and bpy-H^4), 7.87 – 7.64 (m, 15H, ppyF-H^6, H$^{a'}$, H$^{A'}$, H$^{e'}$, H^f, H^F and bpy-H^6), 7.60 – 7.54 (m, 3H, H^b and H^B), 7.45 – 7.34 (m, 7H, H$^{b'}$, H$^{F'}$ and bpy-H^5), 7.19 – 7.06 (m, 7H, ppyF-H^5, H$^{B'}$ and H$^{f'}$), 6.77 – 6.68 (m, 4H, ppyF-H$^{4'}$), 6.50 and 6.49 (2 overlapping d, 2H, H^E), 5.76 (d, 4H, J = 8.5, ppyF-H$^{6'}$). ^{19}F NMR (200 MHz, CD$_3$CN): δ -73.28 (d, 30H, J_{P-F} = 707.3, PF$_6$), -108.54 – -108.76 (m, 4H, ppy-F$^{5'}$), -110.51 (t, 4H, J = 11.3, ppy-F$^{3'}$). ES$^+$ MS: m/z = 596.2 [M - 5PF$_6$]$^{5+}$/5, 745.3 [M – 5PF$_6$ + e-]$^{4+}$/4, 781.7 [M - 4PF$_6$]$^{4+}$/4, 1091.0 [M – 3PF$_6$]$^{3+}$/3. HR ES$^+$ MS: m/z = 782.1417 measured, 782.1411 calculated [C$_{150}$H$_{98}$N$_{18}$F$_{14}$^{193}Ir$_3$P^{102}Ru]$^{4+}$/4. C, H & N analysis: 48.67% C, 2.91% H, 6.74% N measured, 48.60% C, 2.66% H, 6.80% N calculated for [C$_{150}$H$_{98}$N$_{18}$F$_{38}$^{193}Ir$_3$P$_5$^{102}Ru]. TLC (SiO$_2$, 2% KNO$_3$ (aq), 18% H$_2$O, 80% CH$_3$CN): R$_f$ = 0.58.

[[(pba)$_2$Rh(bpy-ϕ-ppy)]$_2$Ir(bpy-ϕ-bpy)Ru(bpy)$_2$][PF$_6$]$_5$ [[Rh-ϕ]$_2$-Ir-ϕ-Ru] **78**
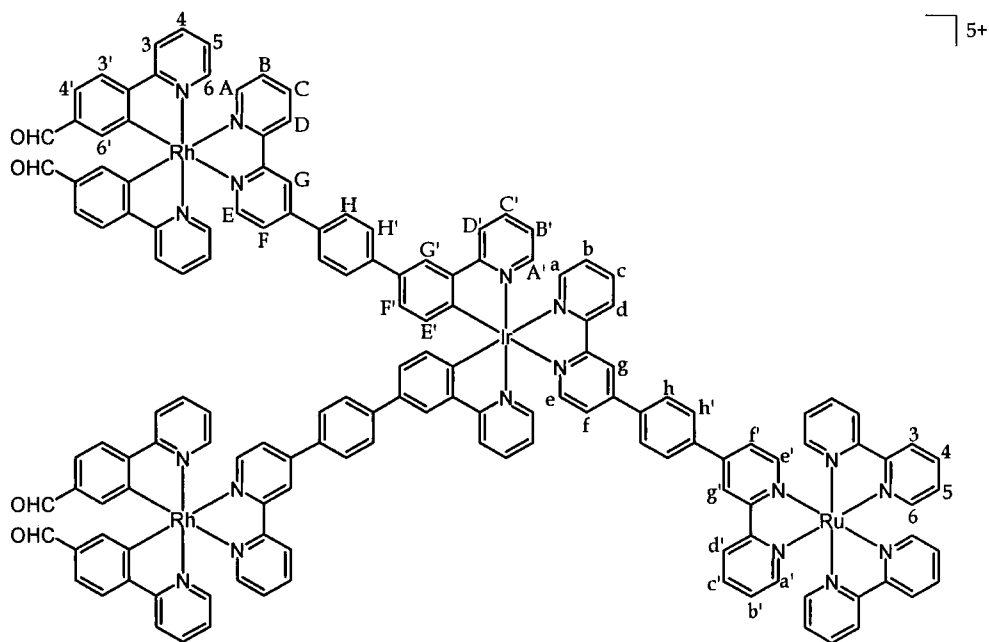
A Schlenk tube was charged with [(ppy-Br)$_2$Ir(bpy-ϕ-bpy)Ru(bpy)$_2$][PF$_6$]$_3$ **73** (18 mg, 0.0095 mmol), [Rh(pba)$_2$(bpy-ϕ-B(OH)$_2$)][PF$_6$] **62** (21 mg, 0.024 mmol), Na$_2$CO$_3$ (6 mg in

100 μL water, 0.057 mmol) and DMSO (8 mL). The solution was thoroughly degassed via 3 freeze-pump-thaw cycles before adding Pd(PPh$_3$)$_4$ (2 mg, 0.0017 mmol) under a positive pressure of nitrogen. The solution was stirred at 80 - 85°C for 20 h. After this time, the DMSO solution was diluted with acetonitrile (4 mL) and filtered into saturated aqueous solution of KPF$_6$. The precipitate was collected using a centrifuge (35 mg). Purification was achieved via column chromatography (silica gel) using gradient elution from 100% acetonitrile to 84% acetonitrile, 15.8% water and 0.2% KNO$_3$. After evaporation of solvent, the desired product was separated from excess KNO$_3$ by selective dissolution into hot acetonitrile containing a drop of water. This solution was concentrated and filtered into saturated aqueous KPF$_6$ to precipitate the product as the PF$_6$ salt, which was collected using the centrifuge and washed with water (12 mg, 0.0035 mmol, 37%). ^{1}H NMR (500 MHz, CD$_3$CN): δ 9.74 (2 s, 4H, CHO), 8.87 - 8.69 (m, 8H, H^D, H^G, H^d, H^g, H$^{d'}$ and H$^{g'}$), 8.53 and 8.51 (2 d, 4H, J = 7.8, bpy-H^3), 8.33 and 8.31 (2 d, 2H, J = 7.4, H$^{D'}$), 8.28 - 8.17 (m, 9H, ppyCHO-H^3, H^c, H^C and H$^{G'}$), 8.14 - 8.02 (m, 21H, bpy-H^4, ppyCHO-H$^{3'}$, ppyCHO-H^4, H^A, H^a, H$^{c'}$, H^e, H^h and H$^{h'}$), 8.01 - 7.89 (m, 12H, H$^{C'}$, H^e, H^H, H$^{H'}$), 7.85 (dd, 1H, J = 5.9, 1.7, H^f), 7.83 - 7.70 (m, 15H, ppyCHO-H^6, bpy-H^6, H$^{A'}$, H$^{a'}$, H$^{e'}$, H^f and H^F), 7.65 and 7.64 (2 dd, 4H, J = 8.0, 1.6, ppyCHO-H$^{4'}$), 7.58 (ddd, 1H, J = 7.4, 5.7, 1.0, H^b), 7.53 (ddd, 2H, J = 7.6, 5.5, 0.9, H^B), 7.46 - 7.39 (m, 5H, bpy-H^5 and H$^{b'}$), 7.37 and 7.35 (2 overlapping dd, 4H, H^F), 7.26 and 7.24 (2 overlapping td, 4H, ppyCHO-H^5), 7.15 and 7.14 (2 overlapping td, 2H, H$^{B'}$), 6.79 (s, 4H, ppyCHO-H$^{6'}$), 6.50 and 6.48 (2 d, 2H, J = 7.5, H$^{E'}$). ES$^+$ MS: m/z = 539.2 [M - 5PF$_6$]$^{5+}$/5, 710.2 [M – 4PF$_6$]$^{4+}$/4, 995.3 [M – 3PF$_6$]$^{3+}$/3. HR ES$^+$ MS: m/z = 537.50193 measured, 537.50192 calculated for [C$_{148}$H$_{102}$O$_4$N$_{18}$^{191}Ir^{103}Rh$_2$^{96}Ru]$^{5+}$/5. TLC (SiO$_2$, 2% KNO$_3$ (aq), 18% H$_2$O, 80% CH$_3$CN): R$_f$ = 0.55.

[[(ppy-Br)₂Ir(bpy-φ-ppy)]₂Ir(bpy-φ-φ-bpy)Ru(bpy)₂][PF₆]₅ **[Ir^Br2-φ]₂-Ir-φ-φ-Ru 79**
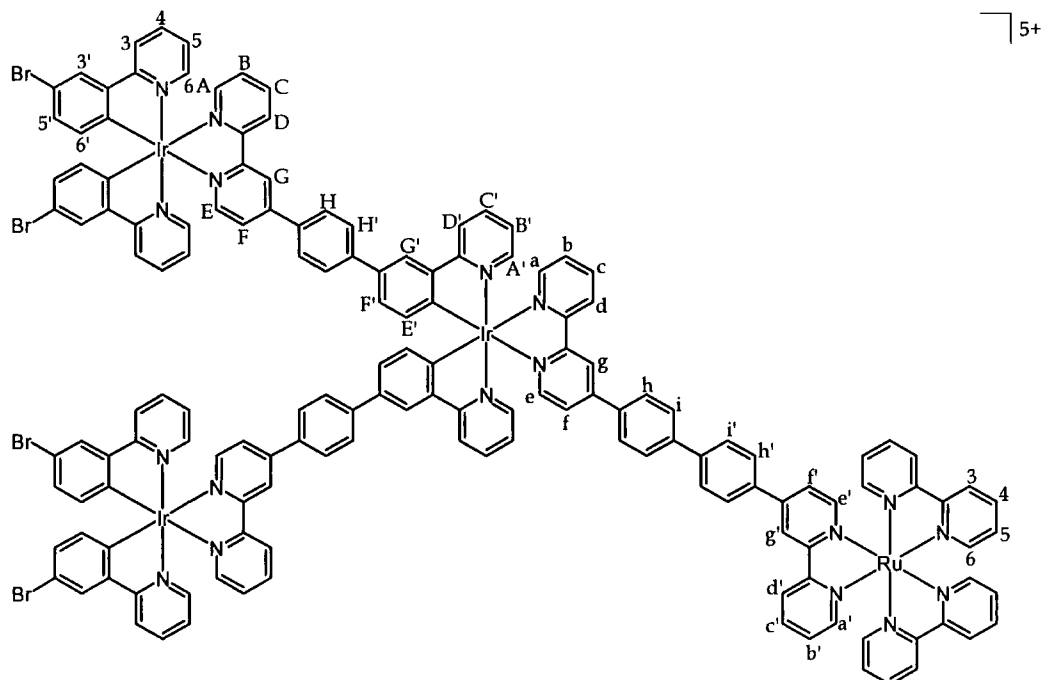
A solution of [[(ppy)₂Ir(bpy-φ-ppy)]₂Ir(bpy-φ-φ-bpy)Ru(bpy)₂][PF₆]₅ **75** (31 mg, 0.009 mmol) and N-bromosuccinimide (7 mg, 0.04 mmol) in CH₃CN (4 mL) was stirred at room temperature for 38 h. Having concentrated the solution under reduced pressure (~ 1 mL), it was added dropwise to a saturated aqueous solution of KPF₆. The resulting precipitate was collected using a centrifuge and washed with water (36 mg, 0.009 mmol, 100%). ¹H NMR (500 MHz, CD₃CN): δ 8.88 – 8.69 (m, 8H, H^D, H^G, H^d, H^g, H^d′ and H^g′), 8.53 and 8.51 (2 d, 4H, *J = 7.5*, bpy-H³), 8.33 and 8.31 (2 d, 2H, *J = 8.6*, H^D′), 8.25 – 7.85 (m, 46H, ppy-H³, ppy-H³′, ppy-H⁴, bpy-H⁴, H^A, H^a, H^C, H^C′, H^c, H^c′, H^F, H^f, H^G′, H^H, H^h, H^H′, H^h′, H^i and H^i′), 7.84 – 7.74 (m, 11H, bpy-H⁶, H^A′, H^a′, H^E, H^e, H^e′), 7.71 (dd, 1H, *J = 6.1, 1.9*, H^f′), 7.67 and 7.65 (2 d, 4H, *J = 6.3*, ppy-H⁶), 7.59 – 7.51 (m, 3H, H^B and H^b), 7.45-7.39 (m, 5H, bpy-H⁵ and H^b′), 7.37 – 7.33 (m, 2H, H^F′), 7.16 and 7.15 (2 overlapping td, 2H, H^B′), 7.12 – 7.03 (m, 8H, ppy-H⁵ and ppy-H⁵′), 6.50 and 6.49 (2 d, 2H, *J = 7.5*, H^E′), 6.18 (d, 4H, *J = 8.2*, ppy-H⁶′). ES⁺ MS: m/z = 630.8 [M – 5PF₆]⁵⁺/5. HR ES⁺ MS: m/z = 630.26342 measured, 630.26345 calculated for [C₁₅₀H₁₀₂N₁₈⁷⁹Br₄¹⁹³Ir₃¹⁰²Ru]⁵⁺/5.

[[[(ppy-F₂)₂Ir(bpy-φ-ppy)]₂Ir(bpy-φ-ppy)]₂Ir(bpy-φ-φ-bpy)Ru(bpy)₂][PF₆]₉

[[[Ir^F2-φ]₂-Ir-φ]₂-Ir-φ-φ-Ru] **80**

9+
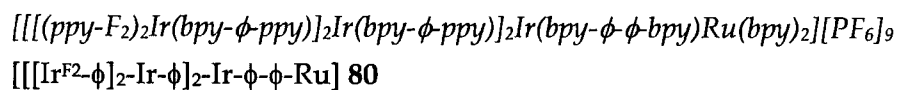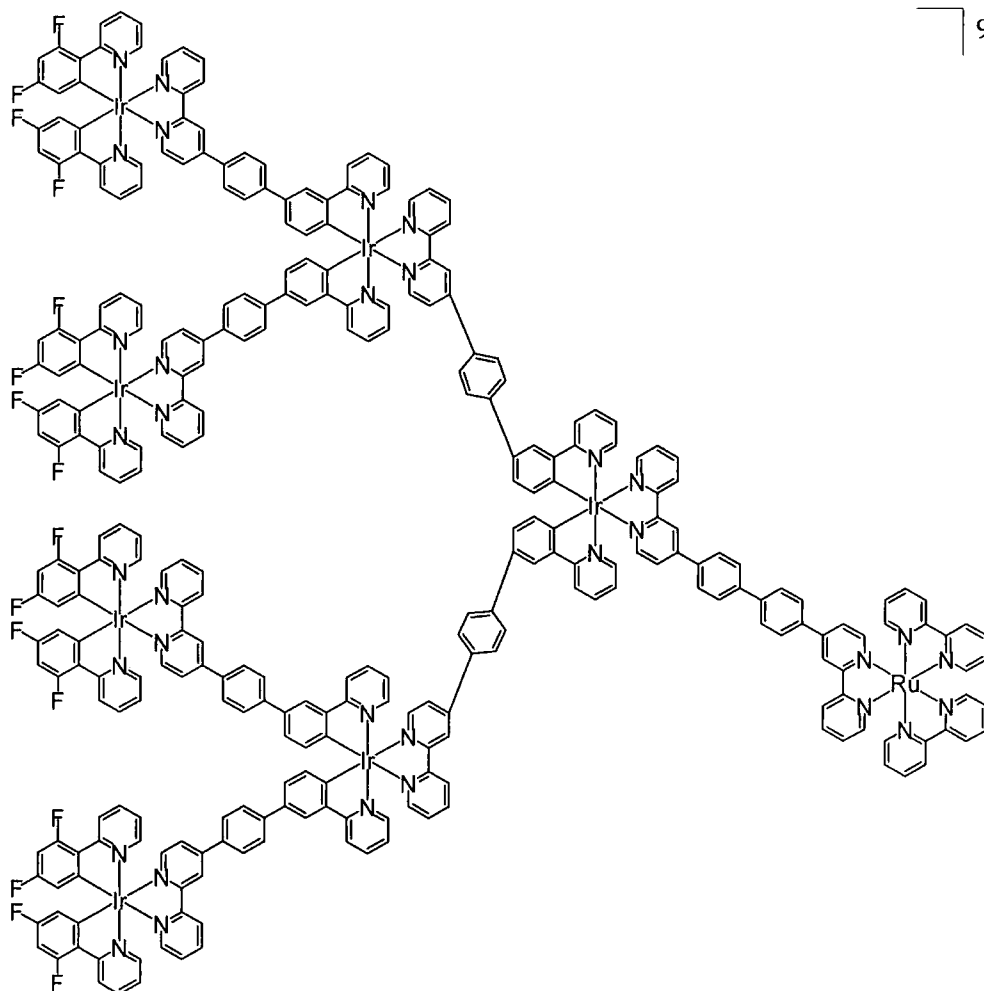
A Schlenk tube was charged with [[(ppy-Br)₂Ir(bpy-φ-ppy)]₂Ir(bpy-φ-φ-bpy)Ru(bpy)₂][PF₆]₅ **79** (35 mg, 0.009 mmol), [Ir(ppy-F₂)₂(bpy-φ-B(OH)₂)][PF₆] **61** (42 mg, 0.041 mmol), Na₂CO₃ (12 mg in 100 µL water, 0.11 mmol) and DMSO (8 mL). The solution was thoroughly degassed via 3 freeze-pump-thaw cycles before adding Pd(PPh₃)₄ (3 mg, 0.002 mmol) under a positive pressure of nitrogen. The solution was stirred at 80 - 85°C for 22 h. After this time, the DMSO solution was diluted with acetonitrile (5 mL) and filtered into saturated aqueous solution of KPF₆. The precipitate was collected using a centrifuge. Purification was achieved via column chromatography (silica gel) using gradient elution from 100% acetonitrile to 80% acetonitrile, 19.5% water and 0.5% KNO₃. After evaporation of solvent, the desired product was separated from excess KNO₃ by selective dissolution into hot acetonitrile containing a drop of water. This solution was concentrated and filtered into saturated aqueous KPF₆ to precipitate the product as the PF₆ salt, which was collected using the centrifuge and washed with water (28 mg, 0.0038 mmol, 42%). ¹H NMR (500 MHz,

193

CD$_3$CN): δ 8.87 – 8.69 (m, 16H, H^3 and H$^{3'}$ on all bpy-∅ units), 8.53 + 8.51 (2 d, 4H, bpy-H^3), 8.38 – 8.28 (m, 14H), 8.25 – 8.17 (m, 14H, includes ppy-H$^{3'}$), 8.14 (m, 63H, includes ppyF-H^4 and ppy-H^4), 7.87 – 7.65 (m, 28H, includes ppyF-H^6 and ppy-H^6), 7.60 – 7.54 (m, 7H), 7.46 – 7.32 (m, 11H, includes ppy-H$^{5'}$), 7.19 – 7.04 (m, 15H, includes ppyF-H^5 and ppy-H^5), 6.76 – 6.68 (m, 8H, ppyF-H$^{4'}$), 6.52 – 6.46 (m, 6H, ppy-H$^{6'}$), 5.76 (d, 8H, $J = 8.3$, ppyF-H$^{6'}$). ^{19}F NMR (200 MHz, CD$_3$CN): δ -73.3 (d, $J_{P-F} = 751$, PF$_6$), -108.6 – -108.7 (m, ppy-F$^{5'}$), -110.5 – -110.6 (m, ppy-F$^{3'}$). ES$^+$ MS: m/z = 672.4 [M – 9PF$_6$]$^{9+}$/9, 774.5 [M – 8PF$_6$]$^{8+}$/8, 905.6 [M – 7PF$_6$]$^{7+}$/7, 1080.9 [M – 6PF$_6$]$^{6+}$/6. HR ES$^+$ MS: m/z = 672.3603 measured, 672.3603 calculated for [C$_{302}$H$_{194}$N$_{34}$F$_{16}$^{193}Ir$_7$^{101}Ru]$^{9+}$/9, 774.4009 measured, 774.4008 calculated for [C$_{302}$H$_{194}$N$_{34}$F$_{22}$P^{193}Ir$_7$^{100}Ru]$^{8+}$/8, 905.4529 measured, 905.4530 calculated for [C$_{302}$H$_{194}$N$_{34}$F$_{28}$P$_2$^{193}Ir$_7$^{101}Ru]$^{7+}$/7. TLC (SiO$_2$, 2% KNO$_3$ (aq), 18% H$_2$O, 80% CH$_3$CN): R$_f$ = 0.58.

CHAPTER 7

REFERENCES

7 References

1.   F. P. Dwyer, H. A. Goodwin and E. C. Gyarfas, *Aust. J. Chem.*, 1963, **16**, 42.

2.   F. P. Dwyer, H. A. Goodwin and E. C. Gyarfas, *Aust. J. Chem.*, 1963, **16**, 544.

3.   A. Juris, V. Balzani, F. Barigelletti, S. Campagna, P. Belser and A. von Zelewsky, *Coord. Chem. Rev.*, 1988, **84**, 85.

4.   I. M. Dixon, J.-P. Collin, J.-P. Sauvage, L. Flamigni, S. Encinas and F. Barigelletti, *Chem. Soc. Rev.*, 2000, **29**, 385.

5.   Y. Ohsawa, S. Sprouse, K. A. King, K. DeArmond, K. W. Hanck and R. J. Watts, *J. Phys. Chem.*, 1987, **91**, 1047.

6.   M. A. Hayes, C. Meckel, E. Schatz and M. D. Ward, *J. Chem. Soc., Dalton Trans.*, 1992, 703.

7.   V. Balzani, S. Campagna, G. Denti, A. Juris, S. Serroni and M. Venturi, *Acc. Chem. Res.*, 1998, **31**, 26.

8.   M. Kasha, *Discussions of the Faraday Society*, 1950, **9**, 14.

9.   V. Balzani, A. Juris, M. Venturi, S. Campagna and S. Serroni, *Chem. Rev.*, 1996, **96**, 759.

10.   A. J. Lees, *Chem. Rev.*, 1987, **87**, 711.

11.   R. J. Watts, *J. Chem. Educ.*, 1983, **60**, 834.

12.   D. P. Rillema and D. S. Jones, *J. Chem. Soc., Chem. Commun.*, 1979, 849.

13.   J. P. Paris and W. W. Brandt, *J. Am. Chem. Soc.*, 1959, **81**, 5001.

14.   F. E. Lytle and D. M. Hercules, *J. Am. Chem. Soc.*, 1969, **91**, 253.

15.   G. A. Crosby, W. G. Perkins and D. M. Klassen, *J. Chem. Phys.*, 1965, **43**, 1498.

16.   N. H. Damrauer, T. R. Boussie, M. Devenney and J. K. McCusker, *J. Am. Chem. Soc.*, 1997, **119**, 8253.

17.   J. A. Treadway, B. Loeb, R. Lopez, P. A. Anderson, F. R. Keene and T. J. Meyer, *Inorg. Chem.*, 1996, **35**, 2242.

18.   A. Harriman, M. Hissler, A. Khatyr and R. Ziessel, *Chem. Commun.*, 1999, 735.

19.   D. S. Tyson, J. Bialecki and F. N. Castellano, *Chem. Commun.*, 2000, 2355.

20.   D. S. Tyson, K. B. Henbest, J. Bialecki and F. N. Castellano, *J. Phys. Chem. A*, 2001, **105**, 8154.

21.   J. G. Vos, *Polyhedron*, 1992, **11**, 2285.

22.   M. Montalti, S. Wadhwa, W. Y. Kin, R. A. Kipp and R. H. Schmehl, *Inorg. Chem.*, 2000, **39**, 76.

23.   S. Encinas, A. Farran Morales, F. Barigelletti, A. M. Barthram, C. M. White, S. M. Couchman, J. C. Jeffery, M. D. Ward, D. C. Grills and M. W. George, *J. Chem. Soc., Dalton Trans.*, 2001, 3312.

24.   L. De Cola, L. Prodi, N. Zaccheroni and B. König, *Inorg. Chim. Acta*, 2002, **336**, 1.

25.   F. Liu, K. Wang, G. Bai, Y. Zhang and L. Gao, *Inorg. Chem.*, 2004, **43**, 1799.

26.   I. M. M. de Carvalho, I. C. N. Diogenes, I. d. S. Moreira and M. H. Gehlen, *J. Photochem. Photobiol. A: Chemistry*, 2005, **171**, 107.

27.   A. M. W. Cargill Thompson, M. C. C. Smailes, J. C. Jeffery and M. D. Ward, *J. Chem. Soc., Dalton Trans.*, 1997, 737.

28.   C. Metcalfe and J. A. Thomas, *Chem. Soc. Rev.*, 2003, **32**, 215.

29.   A. Friedman, J.-C. Chambron, J.-P. Sauvage, N. Turro and J. K. Barton, *J. Am. Chem. Soc.*, 1990, **112**, 4960.

30.   C. Metcalfe, H. Adams, I. Haq and J. A. Thomas, *Chem. Commun.*, 2003, 1152.

31.   C. Metcalfe, I. Haq and J. A. Thomas, *Inorg. Chem.*, 2004, **43**, 317.

32.   C. Rawle, P. Moore and N. W. Alcock, *J. Chem. Soc., Chem. Commun.*, 1992, 684.

33.   P. D. Beer, O. Kocian, R. J. Mortimer and C. Ridgway, *J. Chem. Soc., Dalton Trans.*, 1993, 2629.

34.   B. D. Muegge and M. M. Richter, *Anal. Chem.*, 2002, **74**, 547.

35.   P. D. Beer, F. Szemes, P. Passaniti and M. Maestri, *Inorg. Chem.*, 2004, **43**, 3965.

36.   T. Lazarides, T. A. Miller, J. C. Jeffery, T. K. Ronson, H. Adams and M. D. Ward, *Dalton Trans.*, 2005, 528.

37.   J. D. Slinker, D. Bernards, P. L. Houston, H. D. Abruna, S. Bernhard and G. G. Malliaras, *Chem. Commun.*, 2003, 2392.

38.   E. Holder, B. M. W. Langeveld and U. S. Schubert, *Adv. Mater.*, 2005, **17**, 1109.

39. J.-K. Lee, D. S. Yoo, E. S. Handy and M. F. Rubner, *App. Phys. Lett.*, 1996, **69**, 1686.

40. E. S. Handy, A. J. Pal and M. F. Rubner, *J. Am. Chem. Soc.*, 1999, **121**, 3525.

41. K. M. Maness, R. H. Terrill, T. J. Meyer, R. W. Murray and R. M. Wightman, *J. Am. Chem. Soc.*, 1996, **118**, 10609.

42. J. K. Lee, D. S. Yoo, E. S. Handy and M. F. Rubner, *Chem. Mater.*, 1997, **9**, 1710.

43. C. M. Elliott, F. Pichot, C. J. Bloom and L. S. Rider, *J. Am. Chem. Soc.*, 1998, **120**, 6781.

44. A. P. Wu, D. S. Yoo, J. K. Lee and M. F. Rubner, *J. Am. Chem. Soc.*, 1999, **121**, 4883.

45. C. H. Lyons, E. D. Abbas, J. K. Lee and M. F. Rubner, *J. Am. Chem. Soc.*, 1998, **120**, 12100.

46. H. Rudmann and M. F. Rubner, *J. App. Phys.*, 2001, **90**, 4338.

47. H. Rudmann, S. Shimada and M. F. Rubner, *J. Am. Chem. Soc.*, 2002, **124**, 4918.

48. K. Kalyanasundaram and M. Grätzel, *Coord. Chem. Rev.*, 1998, **77**, 347.

49. A. Hagfeldt and M. Grätzel, *Acc. Chem. Res.*, 2000, **33**, 269.

50. M. Grätzel, *Nature*, 2001, **414**, 338.

51. M. Grätzel, *Journal of Photochemistry and Photobiology C: Photochemistry Reviews*, 2003, **4**, 145.

52. L. Spiccia, G. B. Deacon and C. M. Kepert, *Coord. Chem. Rev.*, 2004, **248**, 1329.

53. B. O'Regan and M. Grätzel, *Nature*, 1991, **353**, 737.

54. K. Nazeeruddin, A. Kay, I. Rodicio, R. Humphry-Baker, E. Muller, P. Liska, N. Vlachopoulos and M. Grätzel, *J. Am. Chem. Soc.*, 1993, **115**, 6382.

55. G. Benkö, J. Kallioinen, J. E. I. Korppi-Tommola, A. Yartsev and V. Sundström, *J. Am. Chem. Soc.*, 2002, **124**, 489.

56. M. K. Nazeeruddin, P. Péchy, T. Renouard, S. M. Zakeeruddin, R. Humphry-Baker, P. Comte, P. Liska, L. Cevey, E. Costa, V. Shklover, L. Spiccia, G. B. Deacon, C. A. Bignozzi and M. Grätzel, *J. Am. Chem. Soc.*, 2001, **123**, 1613.

57.   T. Renouard, R.-A. Fallahpour, M. K. Nazeeruddin, R. Humphry-Baker, S. I.
        Gorelsky, A. B. P. Lever and M. Grätzel, *Inorg. Chem.*, 2002, **41**, 367.

58.   P. Wang, S. M. Zakeeruddin, J. E. Moser, R. Humphry-Baker, P. Comte, V.
        Aranyos, A. Hagfeldt, K. Nazeeruddin and M. Grätzel, *Adv. Mater.*, 2004, **16**,
        1806.

59.   C. Klein, K. Nazeeruddin, P. Liska, D. Di Censo, N. Hirata, E. Palomares, J. R.
        Durrant and M. Grätzel, *Inorg. Chem.*, 2005, **44**, 178.

60.   B. Martin and G. M. Waind, *J. Chem. Soc.*, 1958, 4284.

61.   J. N. Demas, E. W. Harrris, C. M. Flynn Jr. and D. Diemente, *J. Am. Chem. Soc.*,
        1975, **97**, 3838.

62.   J. L. Kahl, K. W. Hanck and K. DeArmond, *J. Phys. Chem.*, 1978, **82**, 540.

63.   A. Slama-Schwok, D. Avnir and M. Ottolenghi, *J. Am. Chem. Soc.*, 1991, **113**,
        3984.

64.   R. J. Watts, J. S. Harrington and J. Van Houten, *J. Am. Chem. Soc.*, 1977, **99**, 2179.

65.   R. D. Gillard, R. J. Lancashire and P. A. Williams, *J. Chem. Soc., Dalton Trans.*,
        1979, 190.

66.   W. A. Wickramasinghe, P. H. Bird and N. Serpone, *J. Chem. Soc., Chem.
        Commun.*, 1981, 1284.

67.   P. J. Spellane and R. J. Watts, *Inorg. Chem.*, 1983, **22**, 4060.

68.   P. S. Braterman, G. A. Heath, A. J. MacKenzie, B. C. Noble, R. D. Peacock and L.
        J. Yellowlees, *Inorg. Chem.*, 1984, **23**, 3425.

69.   S. Sprouse, K. A. King, P. J. Spellane and R. J. Watts, *J. Am. Chem. Soc.*, 1984, **106**,
        6647.

70.   U. Mader, T. Jenny and A. von Zelewsky, *Helv. Chim. Acta*, 1986, **69**, 1085.

71.   K. A. King, P. J. Spellane and R. J. Watts, *J. Am. Chem. Soc.*, 1985, **107**, 1431.

72.   K. A. King and R. J. Watts, *J. Am. Chem. Soc.*, 1987, **109**, 1589.

73.   K. Ichimura, T. Kobayashi, K. A. King and R. J. Watts, *J. Phys. Chem.*, 1987, **91**,
        6104.

74.   A. P. Wilde and R. J. Watts, *J. Phys. Chem.*, 1991, **95**, 622.

75. A. P. Wilde, K. A. King and R. J. Watts, *J. Phys. Chem.*, 1991, **95**, 629.

76. M. Nonoyama, *J. Organomet. Chem.*, 1974, **82**, 271.

77. F. O. Garces, K. Dedeian, N. L. Keder and R. J. Watts, *Acta Crystallogr. Sect. C Cryst. Struct. Commun.*, 1993, **C49**, 1117.

78. F. Neve, A. Crispini, S. Campagna and S. Serroni, *Inorg. Chem.*, 1999, **38**, 2250.

79. M. Maestri, D. Sandrini, V. Balzani, U. Maeder and A. von Zelewsky, *Inorg. Chem.*, 1987, **26**, 1323.

80. M. G. Colombo, A. Zilian and H. U. Güdel, *J. Am. Chem. Soc.*, 1990, **112**, 4581.

81. J. D. Slinker, A. A. Gorodetsky, M. S. Lowry, J. Wang, S. Parker, R. Rohl, S. Bernhard and G. G. Malliaras, *J. Am. Chem. Soc.*, 2004, **126**, 2763.

82. F. O. Garces, K. A. King and R. J. Watts, *Inorg. Chem.*, 1988, **27**, 3464.

83. D. Sandrini, M. Maestri, V. Balzani, U. Maeder and A. von Zelewsky, *Inorg. Chem.*, 1988, **27**, 2640.

84. F. Neve, A. Crispini, F. Loiseau and S. Campagna, *J. Chem. Soc., Dalton Trans.*, 2000, 1399.

85. F. Neve and A. Crispini, *Eur. J. Inorg. Chem.*, 2000, 1039.

86. M. Lepeltier, T. K.-M. Lee, K. K.-W. Lo, L. Toupet, H. Le Bozec and V. Guerchais, *Eur. J. Inorg. Chem.*, 2005, 110.

87. F. Neve, M. La Deda, A. Crispini, A. Bellusci, F. Puntoriero and S. Campagna, *Organometallics*, 2004, **23**, 5856.

88. E. A. Plummer, J. W. Hofstraat and L. De Cola, *Dalton Trans.*, 2003, 2080.

89. P. Didier, I. Ortmans, A. Kirsch-De Mesmaeker and R. J. Watts, *Inorg. Chem.*, 1993, **32**, 5239.

90. P. Coppo, E. A. Plummer and L. De Cola, *Chem. Commun.*, 2004, 1774.

91. P. Coppo, M. Duati, V. N. Kozhevnikov, J. W. Hofstraat and L. De Cola, *Angew. Chem. Int. Ed.*, 2005, **44**, 1806.

92. K. K.-W. Lo, D. C.-M. Ng and C.-K. Chung, *Organometallics*, 2001, **20**, 4999.

93. K. K.-W. Lo, C.-K. Chung, T. K.-W. Lee, L.-H. Lui, K. H.-K. Tsang and N. Zhu, *Inorg. Chem.*, 2003, **42**, 6886.

94.   K. K.-W. Lo, C.-K. Chung and N. Zhu, *Chem. Eur. J.*, 2003, **9**, 475.

95.   K. K.-W. Lo, C.-K. Li, K.-W. Lau and N. Zhu, *Dalton Trans.*, 2003, 4682.

96.   K. K.-W. Lo, J. S.-W. Chan, C.-K. Chung, V. W.-H. Tsang and N. Zhu, *Inorg. Chim. Acta*, 2004, **357**, 3109.

97.   K. K.-W. Lo, J. S.-W. Chan, L.-H. Lui and C.-K. Chung, *Organometallics*, 2004, **23**, 3108.

98.   A. E. Tschitschibabin, *J. Prackt. Chem. (2)*, 1924, **107**, 122.

99.   F. Kröhnke and W. Zecher, *Angew. Chem. Int. Ed.*, 1962, **1**, 626.

100.   F. Kröhnke, *Synthesis*, 1976, 1.

101.   E. P. Linton, *J. Am. Chem. Soc.*, 1940, **62**, 1945.

102.   E. Ochiai, *J. Org. Chem.*, 1953, **18**, 534.

103.   G. Maerker and F. H. Case, *J. Am. Chem. Soc.*, 1958, **80**, 2745.

104.   R. A. Jones, B. D. Roney, W. H. F. Sasse and K. O. Wade, *J. Chem. Soc. B*, 1967, **2**, 106.

105.   J. C. Craig and K. K. Purushothaman, *J. Org. Chem.*, 1970, **35**, 1721.

106.   D. Wenkert and R. B. Woodward, *J. Org. Chem.*, 1983, **48**, 283.

107.   G. R. Newkome, W. E. Puckett, G. E. Kiefer, V. K. Gupta, Y. Xia, M. Coreil and M. A. Hackney, *J. Org. Chem.*, 1982, **47**, 4116.

108.   J. B. R. Regnouf de Vains, A. L. Papet and A. Marsura, *J. Heterocyclic Chem.*, 1994, **31**, 1069.

109.   T. Mizuno, M. Takeuchi, I. Hamachi, K. Nakashima and S. Shinkai, *J. Chem. Soc., Perkin Trans. 2*, 1998, 2281.

110.   P. E. Fanta, *Chem. Rev.*, 1946, **38**, 139.

111.   P. E. Fanta, *Chem. Rev.*, 1964, **64**, 613.

112.   P. E. Fanta, *Synthesis*, 1974, 9.

113.   E. Negishi, *J. Organomet. Chem.*, 2002, **653**, 34.

114.   E. Negishi, A. O. King and N. Okukado, *J. Org. Chem.*, 1977, **42**, 1821.

115.   S. A. Savage, A. P. Smith and C. L. Fraser, *J. Org. Chem.*, 1998, **63**, 10048.

116.   Y.-Q. Fang, M. I. J. Polson and G. S. Hanan, *Inorg. Chem.*, 2003, **42**, 5.

117.   D. Milstein and J. K. Stille, *J. Am. Chem. Soc.*, 1979, **101**, 4992.

118.   J. K. Stille, *Angew. Chem. Int. Ed.*, 1986, **25**, 508.

119.   D. J. Cardenas and J.-P. Sauvage, *Synlett*, 1996, 916.

120.   G. R. Pabst, O. C. Pfuller and J. Sauer, *Tetrahedron*, 1999, **55**, 8045.

121.   J. Sauer, D. K. Heldmann and G. R. Pabst, *Eur. J. Org. Chem.*, 1999, 313.

122.   G. R. Pabst, O. C. Pfuller and J. Sauer, *Tetrahedron*, 1999, **55**, 5047.

123.   G. R. Pabst and J. Sauer, *Tetrahedron*, 1999, **55**, 5067.

124.   K. Sonogashira, Y. Tohda and N. Hagihara, *Tetrahedron Lett.*, 1975, **16**, 4467.

125.   V. Grosshenny and R. Ziessel, *Tetrahedron Lett.*, 1992, **33**, 8075.

126.   F. M. Romero and R. Ziessel, *Tetrahedron Lett.*, 1994, **35**, 9203.

127.   V. Grosshenny, F. M. Romero and R. Ziessel, *J. Org. Chem.*, 1997, **62**, 1491.

128.   D. Tzalis and Y. Tor, *Tetrahedron Lett.*, 1995, **36**, 6017.

129.   R. Ziessel and C. Stroh, *Tetrahedron Lett.*, 2004, **45**, 4051.

130.   N. Miyaura and A. Suzuki, *Chem. Rev.*, 1995, **95**, 2457.

131.   J. Hassan, M. Sévignon, C. Gozzi, E. Schulz and M. Lemaire, *Chem. Rev.*, 2002, **102**, 1359.

132.   W. J. Thompson, J. H. Jones, P. A. Lyle and J. E. Thies, *J. Org. Chem.*, 1988, **53**, 2052.

133.   O. Lohse, P. Thevenin and E. Waldvogel, *Synlett*, 1999, 45.

134.   W. Goodall and J. A. G. Williams, *Chem. Commun.*, 2001, 2514.

135.   W. Goodall, K. Wild, K. J. Arm and J. A. G. Williams, *J. Chem. Soc., Perkin Trans. 2*, 2002, 1669.

136.   D. Tzalis and Y. Tor, *Chem. Commun.*, 1996, 1043.

137.   Y. Tor, *Synlett*, 2002, **7**, 1043.

138.   D. J. Hurley and Y. Tor, *J. Am. Chem. Soc.*, 1998, **120**, 2194.

139.   D. J. Hurley and Y. Tor, *J. Am. Chem. Soc.*, 2002, **124**, 3749.

140.   T. Ishiyama, M. Murata and N. Miyaura, *J. Org. Chem.*, 1995, **60**, 7508.

141.   C. J. Aspley and J. A. G. Williams, *New J. Chem.*, 2001, **25**, 1136.

142.   W. Leslie, A. S. Batsanov, J. A. K. Howard and J. A. G. Williams, *Dalton Trans.*, 2004, 623.

143.   G. Denti, S. Campagna, L. Sabatino, S. Serroni, M. Ciano and V. Balzani, *Inorg. Chem.*, 1990, **29**, 4750.

144.   S. Campagna, G. Denti, S. Serroni, M. Ciano and V. Balzani, *Inorg. Chem.*, 1991, **30**, 3728.

145.   F. Puntoriero, S. Serroni, M. Galletta, A. Juris, A. Licciardello, C. Chiorboli, S. Campagna and F. Scandola, *ChemPhysChem*, 2005, **6**, 129.

146.   G. Denti, S. Campagna, L. Sabatino, S. Serroni, M. Ciano and V. Balzani, *Inorg. Chim. Acta*, 1990, **176**, 175.

147.   S. Campagna, G. Denti, S. Serroni, M. Ciano, A. Juris and V. Balzani, *Inorg. Chem.*, 1992, **31**, 2982.

148.   K. J. Brewer, W. R. Murphy Jr., S. R. Spurlin and J. D. Petersen, *Inorg. Chem.*, 1986, **25**, 882.

149.   W. R. Murphy Jr., K. J. Brewer, G. Gettliffe and J. D. Petersen, *Inorg. Chem.*, 1989, **28**, 81.

150.   S. Campagna, G. Denti, L. Sabatino, S. Serroni, M. Ciano and V. Balzani, *J. Chem. Soc., Chem. Commun.*, 1989, 1500.

151.   S. Serroni, G. Denti, S. Campagna, M. Ciano and V. Balzani, *J. Chem. Soc., Chem. Commun.*, 1991, 944.

152.   G. Denti, S. Campagna, S. Serroni, M. Ciano and V. Balzani, *J. Am. Chem. Soc.*, 1992, **114**, 2944.

153.   G. Denti, S. Serroni, S. Campagna, V. Ricevuto and V. Balzani, *Inorg. Chim. Acta*, 1991, **182**, 127.

154.   S. Serroni and G. Denti, *Inorg. Chem.*, 1992, **31**, 4251.

155.   G. Denti, S. Serroni, S. Campagna, V. Ricevuto, A. Juris, M. Ciano and V. Balzani, *Inorg. Chim. Acta*, 1992, **198-200**, 507.

156.   S. Serroni, G. Denti, S. Campagna, A. Juris, M. Ciano and V. Balzani, *Angew. Chem. Int. Ed.*, 1992, **31**, 1493.

157. S. Serroni, A. Juris, M. Venturi, S. Campagna, I. R. Resino, G. Denti, A. Credi and V. Balzani, *J. Mater. Chem.*, 1997, **7**, 1227.

158. S. Serroni, A. Juris, S. Campagna, M. Venturi, G. Denti and V. Balzani, *J. Am. Chem. Soc.*, 1994, **116**, 9086.

159. S. Baitalik, B. Dutta and K. Nag, *Polyhedron*, 2004, **23**, 913.

160. J. H. van Diemen, R. Hage, J. G. Haasnoot, H. E. B. Lempers, J. Reedijk, J. G. Vos, L. De Cola, F. Barigelletti and V. Balzani, *Inorg. Chem.*, 1992, **31**, 3518.

161. I. Ortmans, P. Didier and A. Kirsch-De Mesmaeker, *Inorg. Chem.*, 1995, **34**, 3695.

162. M. Furue, M. Hirata, S. Kinoshita, T. Kushida and M. Kamachi, *Chem. Lett.*, 1990, 2065.

163. M. T. Indelli, C. A. Bignozzi, A. Harriman, J. R. Schoonover and F. Scandola, *J. Am. Chem. Soc.*, 1994, **116**, 3768.

164. S. Encinas, A. M. Barthram, M. D. Ward, F. Barigelletti and S. Campagna, *Chem. Commun.*, 2001, 277.

165. S. Van Wallendael and D. P. Rillema, *Coord. Chem. Rev.*, 1991, **111**, 297.

166. A. Harriman, M. Hissler, R. Ziessel, A. De Cian and J. Fisher, *J. Chem. Soc., Dalton Trans.*, 1995, 4067.

167. S. Baitalik, X.-Y. Wang and R. H. Schmehl, *J. Am. Chem. Soc.*, 2004, **126**, 16304.

168. F. Neve, A. Crispini, S. Serroni, F. Loiseau and S. Campagna, *Inorg. Chem.*, 2001, **40**, 1093.

169. J. Leveque, B. Elias, C. Moucheron and A. Kirsch-De Mesmaeker, *Inorg. Chem.*, 2005, **44**, 393.

170. E. C. Constable, *Chem. Commun.*, 1997, 1073.

171. E. C. Constable and P. Harverson, *Chem. Commun.*, 1996, 33.

172. S. J. Dunne and E. C. Constable, *Inorg. Chem. Commun.*, 1998, **1**, 167.

173. K. O. Johansson, J. A. Lotoski, C. C. Tong and G. S. Hanan, *Chem. Commun.*, 2000, 819.

174. Y. Tor, *C. R. Chimie*, 2003, **6**, 755.

175. D. Tzalis and Y. Tor, *J. Am. Chem. Soc.*, 1997, **119**, 852.

176. P. J. Connors Jr, D. Tzalis, A. L. Dunnick and Y. Tor, *Inorg. Chem.*, 1998, **37**, 1121.

177. C. Coudret, S. Fraysse and J.-P. Launay, *Chem. Commun.*, 1998, 663.

178. S. Fraysse, C. Coudret and J.-P. Launay, *J. Am. Chem. Soc.*, 2003, **125**, 5880.

179. P. K. Ng, X. Gong, W. T. Wong and W. K. Chan, *Macromol. Rapid Commun.*, 1997, **18**, 1009.

180. W. Frank, T. Pautzsch and E. Klemm, *Macromol. Chem. Phys.*, 2001, **202**, 2535.

181. S. Chodorowski-Kimmes, M. Beley, J.-P. Collin and J.-P. Sauvage, *Tetrahedron Lett.*, 1996, **37**, 2963.

182. C. Patoux, J.-P. Launay, M. Beley, S. Chodorowski-Kimmes, J.-P. Collin, S. James and J.-P. Sauvage, *J. Am. Chem. Soc.*, 1998, **120**, 3717.

183. F. Lafolet, S. Welter, Z. Popovic and L. De Cola, *J. Mater. Chem.*, 2005, **15**, 2820.

184. P. Gros, A. Doudouh and Y. Fort, *Tetrahedron Lett.*, 2004, **45**, 6239.

185. W. Wang, A. Baba, R. H. Schmehl and J. T. Mague, *Acta Crystallogr. Sect. C Cryst. Struct. Commun.*, 1996, **52**, 658.

186. S. Altobello, C. A. Bignozzi, S. Caramori, G. Larramona, S. Quici, G. Marzanni and R. Lakhmiri, *J. Photochem. Photobiol. A: Chemistry*, 2004, **166**, 91.

187. A. B. Tamayo, B. D. Alleyne, P. I. Djurovich, S. Lamansky, I. Tsyba, N. N. Ho, R. Bau and M. E. Thompson, *J. Am. Chem. Soc.*, 2003, **125**, 7377.

188. M. Nonoyama, *Bull. Chem. Soc. Jpn.*, 1974, **47**, 767.

189. S. Campagna, S. Serroni, S. Bodige and F. M. MacDonnell, *Inorg. Chem.*, 1999, **38**, 692.

190. F. C. Fischer and E. Havinga, *Rec. Trav. Chim. Pays-Bas.*, 1974, **93**, 21.

191. B. P. Sullivan, D. J. Salmon and T. J. Meyer, *Inorg. Chem.*, 1978, **17**, 3334.

192. K. E. Berg, A. Tran, M. K. Raymond, M. Abrahamsson, J. Wolny, S. Redon, M. Andersson, L. Sun, S. Styring, L. Hammarstrom, H. Toftlund and B. Akermark, *Eur. J. Inorg. Chem.*, 2001, 1019.

193. J.-P. Sauvage, J.-P. Collin, J.-C. Chambron, S. Guillerez, C. Coudret, V. Balzani, F. Barigelletti, L. De Cola and L. Flamigni, *Chem. Rev.*, 1994, **94**, 993.

194.	J.-P. Collin, I. M. Dixon, J.-P. Sauvage, J. A. G. Williams, F. Barigelletti and L. Flamigni, *J. Am. Chem. Soc.*, 1999, **121**, 5009.

195.	J.-P. Collin, S. Guillerez, J.-P. Sauvage, F. Barigelletti, L. De Cola, L. Flamigni and V. Balzani, *Inorg. Chem.*, 1991, **30**, 4230.

196.	K. Dedeian, P. I. Djurovich, F. O. Garces, G. Carlson and R. J. Watts, *Inorg. Chem.*, 1991, **30**, 1685.

197.	A. P. de Silva, H. Q. N. Gunaratne, T. Gunnlaugsson, A. J. M. Huxley, C. P. McCoy, J. T. Rademacher and T. E. Rice, *Chem. Rev.*, 1997, **97**, 1515.

198.	A. P. de Silva, D. B. Fox, A. J. M. Huxley and T. S. Moody, *Coord. Chem. Rev.*, 2000, **205**, 41.

199.	A. P. de Silva and R. A. D. D. Rupasinghe, *J. Chem. Soc., Chem. Commun.*, 1985, 1669.

200.	B. K. Selinger, *Aust. J. Chem.*, 1977, **30**, 2087.

201.	M. Licini and J. A. G. Williams, *Chem. Commun.*, 1999, 1943.

202.	S. J. Farley, D. L. Rochester, A. L. Thompson, J. A. K. Howard and J. A. G. Williams, *Inorg. Chem.*, 2005, in press.

203.	W. Leslie, R. A. Poole, P. R. Murray, L. J. Yellowlees, A. Beeby and J. A. G. Williams, *Polyhedron*, 2004, **23**, 2769.

204.	Y. Ohsawa, K. W. Hanck and M. DeArmond, *J. Electroanal. Chem.*, 1984, **175**, 229.

205.	M. J. Cook, A. P. Lewis, G. S. G. McAuliffe, V. Skarda, A. J. Thomson, A. J. Glasper and D. J. Robbins, *J. Chem. Soc., Perkin Trans. 2*, 1984, 1293.

206.	W. H. Elfring Jr. and G. A. Crosby, *J. Am. Chem. Soc.*, 1981, **103**, 2683.

207.	M. Beley, J.-P. Collin, J.-P. Sauvage, H. Sugihara, F. Heisel and A. Miehé, *J. Chem. Soc., Dalton Trans.*, 1991, 3157.

208.	L. M. Vogler, B. Scott and K. J. Brewer, *Inorg. Chem.*, 1993, **32**, 898.

209.	M. Cavazzini, P. Pastorelli, S. Quici, F. Loiseau and S. Campagna, *Chem. Commun.*, 2005, 5266.

210.	SHELXTL v. 5.1, Bruker Analytical X-Ray Instruments Inc., Madison, WI, 1999.

211.	K. Nakamaru, *Bull. Chem. Soc. Jpn.*, 1982, **55**, 2697.

212. Gaussian98 Revision A.9, M. J. Frisch, G. W. Trucks, H. B. Schlegel, G. E. Scuseria, M. A. Robb, J. R. Cheeseman, V. G. Zakrzewski, J. A. Montgomery Jr., R. E. Stratmann, J. C. Burant, S. Dapprich, J. M. Millam, A. D. Daniels, K. N. Kudin, M. C. Strain, O. Farkas, J. Tomasi, V. Barone, M. Cossi, R. Cammi, B. Mennucci, C. Pomelli, C. Adamo, S. Clifford, J. Ochterski, G. A. Petersson, P. Y. Ayala, Q. Cui, K. Morokuma, D. K. Malick, A. D. Rabuck, K. Raghavachari, J. B. Foresman, J. Cioslowski, J. V. Ortiz, A. G. Baboul, B. B. Stefanov, G. Liu, A. Liashenko, P. Piskovz, I. Komaromi, R. Gomperts, R. L. Martin, D. J. Fox, T. Keith, M. A. Al-Laham, C. Y. Peng, A. Nanayakkara, M. Challacombe, P. M. W. Gill, B. Johnson, W. Chen, M. N. Wong, J. L. Andres, C. Gonzalez, M. Head-Gordon, E. S. Replogle and J. A. Pople, Gaussian Inc., Pittsburgh, PA, 1998.

213. L. Persaud and G. Barbiero, *Can. J. Chem.*, 1991, **69**, 315.

APPENDICES

Appendix I: Crystal Structure Data for bpy-φ-py 12

Table 1. Crystal data and structure refinement for 03srv085.

Identification code	03srv085
Empirical formula	C22 H16 Cl3 N3
Formula weight	428.73
Temperature	120(2) K
Wavelength	0.71073 Å
Crystal system	Monoclinic
Space group	P2(1)/c
Unit cell dimensions	a = 5.7089(2) Å $\alpha = 90°$.
	b = 37.1368(12) Å $\beta = 105.0740(10)°$.
	c = 9.7250(3) Å $\gamma = 90°$.
Volume	1990.85(11) Å^3
Z	4
Density (calculated)	1.430 Mg/m^3
Absorption coefficient	0.473 mm^{-1}
F(000)	880
Crystal size	0.16 x 0.14 x 0.06 mm^3
Theta range for data collection	2.72 to 26.74°.
Index ranges	-7<=h<=7, -47<=k<=41, -12<=l<=12
Reflections collected	14074
Independent reflections	3922 [R(int) = 0.0539]
Completeness to theta = 26.74°	92.6 %
Absorption correction	Integration
Max. and min. transmission	0.9722 and 0.9281
Refinement method	Full-matrix least-squares on F^2
Data / restraints / parameters	3922 / 21 / 340
Goodness-of-fit on F^2	1.215
Final R indices [I>2sigma(I)]	R1 = 0.0863, wR2 = 0.1480
R indices (all data)	R1 = 0.1222, wR2 = 0.1608
Extinction coefficient	0
Largest diff. peak and hole	0.285 and -0.404 e.Å^{-3}

Table 2. Atomic coordinates (x 10^4) and equivalent isotropic displacement parameters (Å^2x 10^3) for 03srv085. U(eq) is defined as one third of the trace of the orthogonalized U^{ij} tensor.

	x	y	z	U(eq)
N(1)	11090(6)	4271(1)	-696(4)	38(1)
N(2)	-1685(5)	2079(1)	1267(3)	25(1)
N(3)	1536(6)	1555(1)	-780(3)	29(1)
C(1)	9439(8)	4329(1)	38(5)	39(1)
C(2)	7835(7)	4074(1)	249(4)	30(1)
C(3)	7890(6)	3729(1)	-299(4)	22(1)
C(4)	9545(7)	3667(1)	-1104(4)	27(1)
C(5)	11069(7)	3943(1)	-1267(4)	32(1)
C(6)	6248(6)	3440(1)	-45(3)	20(1)
C(7)	5569(6)	3428(1)	1230(4)	22(1)
C(8)	4052(7)	3162(1)	1491(4)	22(1)
C(9)	3139(6)	2898(1)	477(3)	19(1)
C(10)	3836(6)	2907(1)	-808(3)	20(1)
C(11)	5354(6)	3174(1)	-1057(4)	22(1)
C(12)	1488(6)	2614(1)	748(3)	20(1)
C(13)	-190(6)	2687(1)	1537(3)	23(1)
C(14)	-1677(7)	2413(1)	1770(4)	24(1)
C(15)	-80(6)	2006(1)	498(3)	21(1)
C(16)	1522(6)	2264(1)	238(3)	21(1)
C(17)	-88(6)	1633(1)	-39(3)	24(1)
C(18)	-1715(8)	1374(1)	187(4)	32(1)
C(19)	-1582(9)	1029(1)	-299(4)	39(1)
C(20)	95(8)	948(1)	-1033(4)	34(1)
C(21)	1592(8)	1221(1)	-1261(5)	35(1)
C(1S)	-6329(7)	196(1)	2672(5)	41(1)
Cl(1)	-4472(6)	-173(1)	3350(4)	33(1)
Cl(2)	-4932(5)	510(1)	1767(3)	46(1)
Cl(3)	-9184(12)	68(2)	1663(9)	132(3)
Cl(1A)	-4723(19)	-199(3)	3117(12)	135(5)
Cl(2A)	-5537(10)	356(2)	1178(6)	96(2)
Cl(3A)	-9302(9)	55(2)	1908(8)	53(2)

Table 3.   Bond lengths [Å] and angles [°] for 03srv085.

|			
N(1)-C(1)	1.339(5)	C(19)-H(19)	0.92(4)
N(1)-C(5)	1.341(5)	C(20)-C(21)	1.379(6)
N(2)-C(14)	1.331(5)	C(20)-H(20)	0.93(4)
N(2)-C(15)	1.353(4)	C(21)-H(21)	1.02(4)
N(3)-C(21)	1.331(5)	C(1S)-Cl(1A)	1.723(9)
N(3)-C(17)	1.345(4)	C(1S)-Cl(2A)	1.735(6)
C(1)-C(2)	1.369(6)	C(1S)-Cl(3)	1.736(7)
C(1)-H(1)	0.94(4)	C(1S)-Cl(3A)	1.746(6)
C(2)-C(3)	1.391(5)	C(1S)-Cl(1)	1.753(5)
C(2)-H(2)	0.98(4)	C(1S)-Cl(2)	1.771(4)
C(3)-C(4)	1.393(5)	C(1S)-H(1S)	0.98
C(3)-C(6)	1.487(5)	C(1S)-H(1SA)	0.98
C(4)-C(5)	1.378(5)	C(1)-N(1)-C(5)	115.7(4)
C(4)-H(4)	0.92(3)	C(14)-N(2)-C(15)	116.9(3)
C(5)-H(5)	0.93(4)	C(21)-N(3)-C(17)	118.1(3)
C(6)-C(7)	1.393(5)	N(1)-C(1)-C(2)	124.1(4)
C(6)-C(11)	1.393(5)	N(1)-C(1)-H(1)	111(2)
C(7)-C(8)	1.379(5)	C(2)-C(1)-H(1)	125(2)
C(7)-H(7)	0.97(3)	C(1)-C(2)-C(3)	119.8(4)
C(8)-C(9)	1.393(5)	C(1)-C(2)-H(2)	120(2)
C(8)-H(8)	0.90(3)	C(3)-C(2)-H(2)	120(2)
C(9)-C(10)	1.407(4)	C(2)-C(3)-C(4)	116.9(3)
C(9)-C(12)	1.481(5)	C(2)-C(3)-C(6)	121.5(3)
C(10)-C(11)	1.381(5)	C(4)-C(3)-C(6)	121.6(3)
C(10)-H(10)	0.99(3)	C(5)-C(4)-C(3)	119.0(4)
C(11)-H(11)	0.90(4)	C(5)-C(4)-H(4)	120(2)
C(12)-C(16)	1.394(5)	C(3)-C(4)-H(4)	121(2)
C(12)-C(13)	1.400(5)	N(1)-C(5)-C(4)	124.4(4)
C(13)-C(14)	1.381(5)	N(1)-C(5)-H(5)	115(2)
C(13)-H(13)	0.92(4)	C(4)-C(5)-H(5)	120(2)
C(14)-H(14)	0.98(4)	C(7)-C(6)-C(11)	118.0(3)
C(15)-C(16)	1.393(5)	C(7)-C(6)-C(3)	120.4(3)
C(15)-C(17)	1.481(5)	C(11)-C(6)-C(3)	121.6(3)
C(16)-H(16)	0.92(3)	C(8)-C(7)-C(6)	121.4(3)
C(17)-C(18)	1.392(5)	C(8)-C(7)-H(7)	118.9(19)
C(18)-C(19)	1.373(6)	C(6)-C(7)-H(7)	119.7(19)
C(18)-H(18)	0.91(4)	C(7)-C(8)-C(9)	120.7(3)
C(19)-C(20)	1.369(6)	C(7)-C(8)-H(8)	121(2)

C(9)-C(8)-H(8)	118(2)	C(19)-C(20)-C(21)	118.0(4)
C(8)-C(9)-C(10)	118.1(3)	C(19)-C(20)-H(20)	122(3)
C(8)-C(9)-C(12)	120.9(3)	C(21)-C(20)-H(20)	120(3)
C(10)-C(9)-C(12)	121.0(3)	N(3)-C(21)-C(20)	123.8(4)
C(11)-C(10)-C(9)	120.5(3)	N(3)-C(21)-H(21)	115(2)
C(11)-C(10)-H(10)	119.5(18)	C(20)-C(21)-H(21)	121(2)
C(9)-C(10)-H(10)	120.0(18)	Cl(1A)-C(1S)-Cl(2A)	105.3(5)
C(10)-C(11)-C(6)	121.2(3)	Cl(1A)-C(1S)-Cl(3)	105.6(5)
C(10)-C(11)-H(11)	119(2)	Cl(2A)-C(1S)-Cl(3)	91.7(4)
C(6)-C(11)-H(11)	120(2)	Cl(1A)-C(1S)-Cl(3A)	104.3(5)
C(16)-C(12)-C(13)	116.7(3)	Cl(2A)-C(1S)-Cl(3A)	100.5(4)
C(16)-C(12)-C(9)	122.1(3)	Cl(3)-C(1S)-Cl(3A)	8.8(6)
C(13)-C(12)-C(9)	121.3(3)	Cl(1A)-C(1S)-Cl(1)	8.3(5)
C(14)-C(13)-C(12)	119.1(3)	Cl(2A)-C(1S)-Cl(1)	108.6(3)
C(14)-C(13)-H(13)	122(2)	Cl(3)-C(1S)-Cl(1)	112.7(4)
C(12)-C(13)-H(13)	119(2)	Cl(3A)-C(1S)-Cl(1)	110.6(3)
N(2)-C(14)-C(13)	124.6(3)	Cl(1A)-C(1S)-Cl(2)	113.9(4)
N(2)-C(14)-H(14)	118(2)	Cl(2A)-C(1S)-Cl(2)	27.1(2)
C(13)-C(14)-H(14)	117(2)	Cl(3)-C(1S)-Cl(2)	112.1(4)
N(2)-C(15)-C(16)	122.2(3)	Cl(3A)-C(1S)-Cl(2)	119.9(4)
N(2)-C(15)-C(17)	116.3(3)	Cl(1)-C(1S)-Cl(2)	113.3(2)
C(16)-C(15)-C(17)	121.5(3)	Cl(1A)-C(1S)-H(1S)	113
C(15)-C(16)-C(12)	120.4(3)	Cl(2A)-C(1S)-H(1S)	130.8
C(15)-C(16)-H(16)	117.3(19)	Cl(3)-C(1S)-H(1S)	106
C(12)-C(16)-H(16)	122.2(19)	Cl(3A)-C(1S)-H(1S)	98.9
N(3)-C(17)-C(18)	121.2(4)	Cl(1)-C(1S)-H(1S)	106
N(3)-C(17)-C(15)	116.7(3)	Cl(2)-C(1S)-H(1S)	106
C(18)-C(17)-C(15)	122.1(3)	Cl(1A)-C(1S)-H(1SA)	115
C(19)-C(18)-C(17)	119.3(4)	Cl(2A)-C(1S)-H(1SA)	115
C(19)-C(18)-H(18)	123(2)	Cl(3)-C(1S)-H(1SA)	120.9
C(17)-C(18)-H(18)	118(2)	Cl(3A)-C(1S)-H(1SA)	115
C(20)-C(19)-C(18)	119.6(4)	Cl(1)-C(1S)-H(1SA)	107
C(20)-C(19)-H(19)	121(2)	Cl(2)-C(1S)-H(1SA)	88.8
C(18)-C(19)-H(19)	119(2)	H(1S)-C(1S)-H(1SA)	18.9

Table 4. Anisotropic displacement parameters $(\text{Å}^2 \times 10^3)$ for 03srv085. The anisotropic displacement factor exponent takes the form: $-2\pi^2[\, h^2\, a^{*2} U^{11} + ... + 2\, h\, k\, a^*\, b^*\, U^{12}\,]$

	U^{11}	U^{22}	U^{33}	U^{23}	U^{13}	U^{12}
N(1)	29(2)	34(2)	45(2)	8(2)	2(2)	-10(2)
N(2)	20(2)	37(2)	17(2)	5(1)	5(1)	-2(1)
N(3)	29(2)	25(2)	35(2)	-2(1)	11(2)	-4(1)
C(1)	37(3)	30(3)	49(3)	-4(2)	10(2)	-9(2)
C(2)	29(2)	27(2)	36(2)	-4(2)	9(2)	-5(2)
C(3)	17(2)	30(2)	18(2)	3(2)	0(2)	-1(2)
C(4)	22(2)	30(2)	27(2)	2(2)	1(2)	-3(2)
C(5)	20(2)	41(3)	34(2)	7(2)	6(2)	-4(2)
C(6)	21(2)	20(2)	18(2)	0(1)	3(1)	0(2)
C(7)	23(2)	26(2)	16(2)	-4(2)	2(2)	-1(2)
C(8)	26(2)	29(2)	12(2)	2(1)	5(2)	4(2)
C(9)	18(2)	22(2)	14(2)	3(1)	0(1)	3(2)
C(10)	18(2)	26(2)	14(2)	-3(2)	1(1)	-2(2)
C(11)	21(2)	29(2)	17(2)	0(2)	8(2)	0(2)
C(12)	16(2)	29(2)	14(2)	3(1)	2(1)	0(2)
C(13)	22(2)	31(2)	14(2)	2(2)	3(2)	4(2)
C(14)	20(2)	38(2)	17(2)	6(2)	9(2)	2(2)
C(15)	21(2)	28(2)	12(2)	6(1)	1(1)	0(2)
C(16)	17(2)	32(2)	13(2)	0(1)	5(2)	0(2)
C(17)	25(2)	30(2)	14(2)	4(2)	2(2)	-4(2)
C(18)	37(3)	39(3)	21(2)	3(2)	8(2)	-12(2)
C(19)	50(3)	34(3)	29(2)	8(2)	6(2)	-21(2)
C(20)	40(3)	24(2)	33(2)	0(2)	1(2)	-3(2)
C(21)	30(2)	29(2)	45(3)	-5(2)	10(2)	-1(2)
C(1S)	41(3)	37(3)	48(3)	14(2)	19(2)	9(2)
Cl(1)	28(1)	28(2)	44(1)	16(1)	14(1)	18(1)
Cl(2)	45(2)	51(2)	46(2)	24(1)	20(1)	4(1)
Cl(3)	91(4)	85(4)	191(7)	30(3)	-14(4)	-8(3)
Cl(1A)	147(9)	95(7)	186(10)	57(6)	85(7)	41(6)
Cl(2A)	67(3)	146(6)	75(4)	66(3)	21(3)	-4(3)
Cl(3A)	24(2)	25(3)	93(3)	-30(2)	-19(2)	7(2)

Table 5. Hydrogen coordinates (x 10^4) and isotropic displacement parameters (Å^2x 10 ^{3}) for 03srv085.

	x	y	z	U(eq)
H(1)	9550(70)	4565(11)	390(40)	32(11)
H(2)	6670(70)	4133(10)	790(40)	34(11)
H(4)	9660(60)	3445(10)	-1510(30)	17(9)
H(5)	12230(70)	3904(9)	-1760(40)	23(10)
H(7)	6170(60)	3608(9)	1950(40)	17(9)
H(8)	3700(60)	3147(8)	2340(30)	10(8)
H(10)	3240(60)	2720(8)	-1540(30)	8(8)
H(11)	5750(60)	3179(9)	-1890(40)	24(10)
H(13)	-220(60)	2912(10)	1920(40)	21(10)
H(14)	-2770(70)	2467(10)	2370(40)	31(10)
H(16)	2630(60)	2191(8)	-250(30)	10(8)
H(18)	-2860(70)	1444(9)	630(40)	26(10)
H(19)	-2640(70)	857(10)	-130(40)	26(10)
H(20)	260(70)	718(11)	-1360(40)	40(12)
H(21)	2910(80)	1173(11)	-1780(50)	51(13)
H(1S)	-6592	324	3502	49
H(1SA)	-6144	370	3451	49
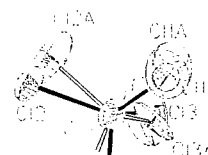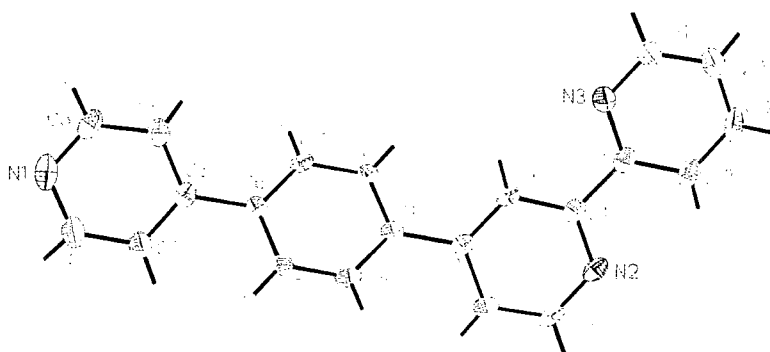
Appendix II: Conferences Attended and Publications

Conferences Attended

- UK Macrocycles and Supramolecular Chemistry Meeting, University of Newcastle, 5-6th January 2005. Poster presentation and RSC first prize winner: *'New Cross Coupling Methodology for the Synthesis of Photoactive Metal Complexes and Multimetallic Assemblies.'*

- RSC Photochemistry Group Young Researchers Meeting, Rutherford-Appleton Laboratories, 15th December 2004. Oral presentation: *'Intermetallic Energy Transfer in Multimetallic Complexes Prepared Using a Novel Cross-Coupling Approach.'*

- UK Macrocycles and Supramolecular Chemistry Meeting, University of York, 18-19th December 2002. Poster presentation: *'Luminescent Sensors Based on Metal Complexes.'*

Publications

- 'Synthesis and pH-sensitive luminescence of bis-terpyridyl iridium(III) complexes incorporating pendent pyridyl groups.' Kathryn J. Arm, Wendy Leslie and J. A. Gareth Williams, *Inorg. Chim. Acta.*, in press.

- 'Boronic acid-substituted metal complexes: versatile building blocks for the synthesis of multimetallic assemblies.' Kathryn J. Arm and J. A. Gareth Williams, *Chem. Commun.*, 2005, 230. Also featured in Chemistry World, February 2005 (page 14) as a 'hot topic'.

- 'The synthesis of 4'-aryl substituted terpyridines by Suzuki cross-coupling reactions: substituent effects on ligand fluorescence.' W. Goodall, K. Wild, K. J. Arm and J. A. G. Williams, *J. Chem. Soc., Perkin Trans. 2*, 2002, 1669.